



NKS-316
ISBN 978-87-7893-395-9

Effective Models for Simulation of Thermal Stratification and Mixing Induced by Steam Injection into a Large Pool of Water

Hua Li, Walter Villanueva, Pavel Kudinov

Division of Nuclear Power Safety, Royal Institute of Technology (KTH)
Stockholm, Sweden

October 2014

Abstract

Steam condensation in a large pool of water creates both a source of heat and a source of momentum. Complex interplay between these two sources leads to either thermal stratification or mixing. Development of thermal stratification in a pressure suppression pool (PSP) of a boiling water reactor (BWR), increases temperature of the free surface reducing the steam condensation capacity of the pool and increasing containment pressure. It is important to know how fast a stratified pool can be mixed. Modelling of direct contact condensation on the steam-water interface remains a computational challenge. Therefore Effective Heat Source (EHS) and Effective Momentum Source (EMS) models have been proposed to model thermal stratification and mixing in case of steam injection through a vertical pipe submerged in a pool under two condensation regimes: complete condensation inside the pipe and chugging. Computational efficiency and sufficiently accuracy of the models are achieved by resolving only integral effect of small scale steam condensation phenomena on the large scale flow structures and temperature distributions in the pool. The models are implemented in GOTHIC® software. In previous NKS reports, validation of EHS and EMS models against POOLEX STB and PPOOLEX STR tests have been presented.

In this report, we focus on the validation of the EHS/EMS models against recent PPOOLEX MIX tests. Excellent agreement in the development of thermal stratification and mixing in the pool between the experiment and simulation has been achieved. For completeness, an updated discussion of some of the previous STB and STR tests have been included with parametric sensitivity analysis. Improvement of EHS/EMS models are discussed. Effective momentum can be determined based on the frequency and amplitude of oscillations in the blowdown pipe. We demonstrate that existing analytical models (e.g. by Nariai) that can be used for prediction of the frequency and amplitude were developed using data from small scale experiments and have rather large uncertainty when applied to large scale PPOOLEX tests. A scaling approach is proposed to generalize available data on amplitude and frequency of oscillations during chugging at different scales.

Key words

Thermal Stratification, Mixing, Pressure Suppression Pool, Containment, Thermal Hydraulic, GOTHIC, Light Water Reactor

NKS-316
ISBN 978-87-7893-395-9
Electronic report, October 2014
NKS Secretariat
P.O. Box 49
DK - 4000 Roskilde, Denmark
Phone +45 4677 4041
www.nks.org
e-mail nks@nks.org



Effective Models for Simulation of Thermal Stratification and Mixing Induced by Steam Injection into a Large Pool of Water

**Final Report from the NKS-R ENPOOL activity
(Contract: NKS_R_2011_90)**

Hua Li, Walter Villanueva, Pavel Kudinov

Division of Nuclear Power Safety (NPS), Royal Institute of Technology (KTH),
Stockholm

June, 2014
Stockholm

CONTENTS

CONTENTS	3
EXECUTIVE SUMMARY	5
1 INTRODUCTION	7
1.1 MOTIVATION.....	7
1.2 STATE OF THE ART REVIEW	8
1.3 GOAL AND APPROACH.....	13
2 DEVELOPMENT OF EFFECTIVE MODELS	15
2.1 EFFECTIVE HEAT SOURCE (EHS) MODEL.....	15
2.2 EFFECTIVE MOMENTUM SOURCE (EMS) MODEL	16
2.2.1 <i>Synthetic jet model for prediction of the effective momentum source</i>	17
3 POOLEX/PPOOLEX EXPERIMENTS	22
3.1 EXPERIMENTAL FACILITY	22
3.2 POOLEX EXPERIMENTS	24
3.2.1 <i>STB 20</i>	24
3.2.2 <i>STB-21</i>	26
3.3 PPOOLEX EXPERIMENTS	27
3.3.1 <i>STR tests</i>	27
3.3.2 <i>MIX tests</i>	28
4 VALIDATION OF EFFECTIVE MODELS AGAINST POOLEX TESTS	30
4.1 VALIDATION OF EFFECTIVE HEAT SOURCE (EHS) MODEL AGAINST POOLEX STB-20 TEST... 30	
4.1.1 <i>GOTHIC modeling and assumptions</i>	30
1. Lumped Parameter Simulation	30
2. 2D simulation with EHS model	33
4.1.1.1 Sensitivity to Boundary Conditions.....	33
4.1.1.2 Sensitivity to Grid Resolution Study	38
4.1.1.3 Sensitivity Study to Gas Space and Free Surface Modeling	43
4.1.1.4 Effect of numerical finite difference scheme.....	45
4.1.2 <i>Analysis of results</i>	46
4.2 VALIDATION OF EHS AND EMS (EFFECTIVE MOMENTUM SOURCE) MODELS AGAINST POOLEX STB-21 TEST	48
4.2.1 <i>Estimation of Effective Momentum</i>	50
4.2.2 <i>EHS-EMS models validation and parametric studies</i>	53
4.2.3 <i>Validation of EMS model based on analytical estimation of amplitude and frequency</i> .. 55	
5 VALIDATION OF EFFECTIVE MODELS AGAINST PPOOLEX TESTS	57
5.1 VALIDATION OF EFFECTIVE HEAT SOURCE (EHS) MODEL AGAINST PPOOLEX STR-03 TEST. 57	
5.1.1 <i>GOTHIC modeling and assumptions</i>	58
5.1.2 <i>Analysis of results</i>	62
5.2 VALIDATION OF EHS AND EMS MODELS AGAINST PPOOLEX MIX-01 TO MIX-06 TESTS 63	
5.2.1 <i>EHS/EMS validation against MIX-01 test</i>	65
5.2.2 <i>EHS/EMS validation against MIX-02 test</i>	71
5.2.3 <i>EHS/EMS validation against MIX-03 test</i>	78
5.2.4 <i>EHS/EMS validation against MIX-04 test</i>	85
5.2.5 <i>EHS/EMS validation against MIX-05 test</i>	92
5.2.6 <i>EHS/EMS validation against MIX-06 test</i>	99
5.3 VALIDATION OF EHS AND EMS MODELS AGAINST PPOOLEX MIX-07 TO MIX-12 TESTS ... 106	
5.3.1 <i>EHS/EMS validation against MIX-07 test</i>	107
5.3.2 <i>EHS/EMS validation against MIX-08 test</i>	113
5.3.3 <i>EHS/EMS validation against MIX-09 test</i>	119
5.3.4 <i>EHS/EMS validation against MIX-10 test</i>	126
5.3.5 <i>EHS/EMS validation against MIX-11 test</i>	132
5.3.6 <i>EHS/EMS validation against MIX-12 test</i>	138

6	SCALING APPROACH FOR GENERALIZATION OF EXPERIMENTAL DATA ON AMPLITUDE AND FREQUENCY OF OSCILLATIONS	145
6.1	AVAILABLE EXPERIMENTAL DATA AND RELEVANT SCALING PARAMETERS.....	145
6.2	OSCILLATIONS CHARACTERISTICS IN CHUGGING PHENOMENA	150
6.2.1	<i>Amplitude of oscillations</i>	150
6.2.2	<i>Frequency of oscillations</i>	153
7	CONCLUSIONS	157
	ACKNOWLEDGEMENT	159
	DISCLAIMER	160
	APPENDIX	161
	ANALYTICAL MODEL OF AYA AND NARIAI FOR PREDICTION OF AMPLITUDE AND FREQUENCY OF OSCILLATIONS DURING CHUGGING.....	161
	REFERENCES	163

Executive Summary

Steam venting and condensation in a large pool of water creates both a source of heat and a source of momentum. Complex interplay between these two sources leads to either thermal stratification or mixing. If heat source dominates, development of thermal stratification in a pressure suppression pool (PSP) of a boiling water reactor (BWR), increases temperature of the free surface which reduces the steam condensation capacity of the pool and can lead to significant pressure increase in the containment. If mixing is dominant it is important to know how fast a stratified pool can be mixed to restore the steam condensation capacity and reduce containment pressure. Advanced modeling and simulation of direct contact condensation in large systems remains a challenge as evident in commercial and research codes mainly due to long transients and small time-steps to resolve direct contact condensation on the free surface of steam-water interface.

The Effective Heat Source (EHS) and Effective Momentum Source (EMS) models have been proposed to simulate thermal stratification and mixing during a steam injection into a large pool of water. The EHS/EMS models are developed for steam injection through a vertical pipe submerged in a pool under two condensation regimes: complete condensation inside the pipe and chugging. The models are (i) computationally efficient, since small scale phenomena of steam injection and direct contact condensation are not resolved explicitly, and (ii) sufficiently accurate, since the integral effect of these phenomena on the large scale flow structure and temperature distribution in the pool is taken into account. These effective models are implemented in GOTHIC[®] software and validated against POOLEX and PPOOLEX tests.

In previous NKS reports, validation of EHS and EMS models against POOLEX STB and PPOOLEX STR tests have been presented. In this report, we focus on the recent PPOOLEX MIX tests. For completeness, a more organized (e.g., parametric sensitivity analysis) and updated discussion of some of the previous STB and STR tests have been included. In general, this report presents the work on improvement of EHS/EMS models for the blowdown pipes in order to reduce uncertainties and improve accuracy in predictions. The work is motivated by the results of PPOOLEX STR and MIX tests series which suggest that stratification characteristics in the upper layer of the pool can be affected by (i) regime of condensation inside the blowdown pipe, and (ii) possible steam efflux from the pipe and condensation in the pool. In addition, the original models developed by Nariai for prediction of condensation oscillations have rather large uncertainty when applied to large scale (e.g. PPOOLEX STR) tests. Specific goals of this work are: (i) to develop for the EMS detailed maps for frequency and amplitude of oscillations on the blowdown pipe. (ii) to validate the model for prediction of frequency and amplitude of oscillations against the recently completed PPOOLEX-MIX tests. Existing analytical models for prediction of the frequency and amplitude were developed using data from small scale experiments at limited range of parameters. Proper extension of the models to larger scale experiments and prototypic plant conditions is necessary. A scaling approach is proposed to generalize available data on amplitude and frequency of oscillations during chugging. The approach can be used for prediction of the amplitude in frequency at different scales. Validation of the EHS/EMS models also has been carried out against recent PPOOLEX MIX tests. Excellent agreement in averaged pool temperature and water level in the pool between the

experiment and simulation has been achieved. The development of thermal stratification and mixing of the pool are also well captured in the simulation.

1 Introduction

1.1 Motivation

A pressure suppression pool is an important part of a BWR reactor containment safety design. It serves as a heat sink and steam condenser to prevent containment pressure buildup during loss of coolant accident (LOCA) or during safety relief valve (SRV) opening in normal operations. Steam released from the reactor vessel is vented through the blowdown pipes (in case of LOCA) or through spargers (in case of SRV operation) and condenses in the pressure suppression water pool. The temperature of the pool gradually increases as a result of condensation. This leads to a reduction of the pool's pressure suppression capacity. Efficiency of the pool pressure suppression function is contingent upon the temperature of the pool surface, which determines the steam partial pressure in the wetwell gas space. An increase of the pool's surface temperature due to stratification can lead to a significant increase in containment pressure [1]. Steam condensation stops when water at the level of the steam injection point and above reaches saturation temperature. The pool temperature is also important for Emergency Core Cooling System (ECCS) which takes water from the pool and pumps it into the vessel to remove decay heat. ECCS pumps will be shut down to prevent cavitation if Net Positive Suction Head (NPSH) will drop below certain limit. The NPSH is also determined by water temperature in the pool. Cooling of the pool is implemented in order to keep water temperature low. However, cooling might be inefficient if stratification of the pool persists. Therefore the pool has to be mixed to increase pool's pressure suppression capacity, reduce containment pressure and provide reliable ECCS operation. While pool mixing systems are also a part of the design, they are active non-safety graded systems which can fail. The main motivation of this study is clarification at which conditions steam injection itself can be regarded in safety analysis as a factor which can enhance pool mixing.

Steam injection in a pool of water is a source of both heat and momentum. A competition between heat and momentum defines the pool state whether it is thermally mixed or stratified. The heat source induces the development of thermal stratification. The configuration of the stratified layers generally depends on the spatial distribution of the heat source and history of transient heat transfer in the pool (heating and cooling phases). In a BWR pressure suppression pool operation, thermal stratification development is caused by a heat source (such as a blowdown pipe or a sparger) immersed into the pool at a certain depth. There are two typical transient stratification configurations (as shown in Figure 1), (i) a stratified layer with continuous increase of water temperature from the bottom of the heat source while a constant temperature of cold water T_c below the heat source (Figure 1a), and (ii) an isothermal top layer at temperature T_h separated from the bottom layer of cold water by relatively thin thermocline layer where temperature is changing rapidly from T_c to T_h (Figure 1b). Such different configuration can exhibit different resistance to mixing.

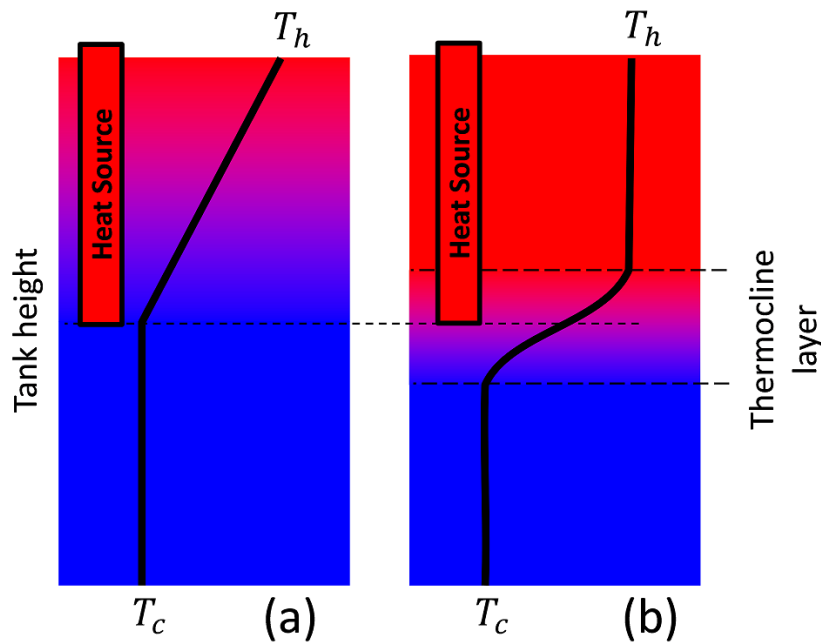


Figure 1: Typical configurations of thermal stratification in a tank (a) stratified layer; (b) thermocline layer. Note: T_h – temperature of hot liquid; T_c – temperature of cold liquid.

The momentum induced by steam condensation is capable to create large scale circulation which can mix the pool. However, mixing of a stratified pool takes some time which generally depends on the momentum rate. The time which is necessary to achieve mixing determines how fast the suppression pool's capacity can be restored. Thus, the characteristic mixing time scale is considered as an important parameter of the pool's operation.

1.2 State of the art review

The competition between the sources of heat and momentum is determined by the steam condensation regime. Condensation regimes of steam injection into a subcooled water pool at different conditions were studied intensively in the past [2, 3, 4, 5, 6, 7]. Figure 2 depicts a 2D condensation regime map with dependencies on the steam mass flux and pool bulk temperature [2]. Recently, Petrovic de With et al, [7] have compiled a 3D condensation regime diagram. The injector diameter was introduced as a third dimension in addition to the traditional water subcooling and steam mass fluxes. The 3D diagram is based on the data produced over three decades in different experiments with injector diameters up to 5 cm.

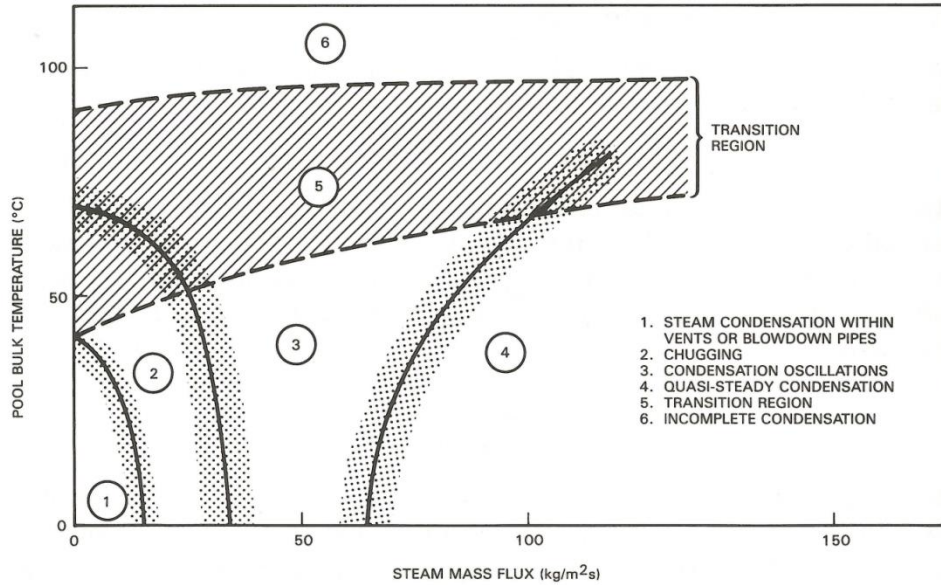


Figure 2: Regime map of steam condensation [2].

A chugging regime [2, 8] can result in large amplitude oscillations of the steam-liquid interface. The momentum source created by such oscillations can enhance mixing [1]. Aya and Nariai [9, 10] studied chugging oscillations using a small scale experiment with a blowdown pipe of 18 mm in diameter and 1 m in height. The steam mass flow rate was in the range of 0.74 ~ 35 g/s. It was also shown that the analytical model proposed by Aya and Nariai is capable to reproduce the experimentally obtained frequency and amplitude of the oscillations.

Stratification and mixing phenomena in a large pool of water with a heat source have been studied experimentally and analytically. A strong stratification above a heat source submerged in a water pool was observed in different tests [11, 12, 13, 14, 15, 16, 17, 18, 19, 20]. Heat transfer into the layer below the heat and momentum source was found to be limited by thermal conduction. The region below the source of heat remains inactive as a heat sink.

An experimental study of thermal stratification and mixing in relatively large pools was carried out in the PUMA facility [19]. It has been shown that the degree of thermal stratification in the suppression pool is strongly affected by the vent opening submergence depth, pool initial pressure, noncondensable gas flow rate, and steam injection rate, and is less sensitive to the initial water temperature. Unfortunately, information provided in [19] is not sufficient to perform independent validation of codes and models against the PUMA data.

Similar experimental programs called POOLEX (POOL Experiment) and PPOOLEX (Pressurized POOLEX) [11, 12, 13, 14] have been performed at Lappeenranta University of Technology (LUT, Finland). The POOLEX facility is an open cylindrical stainless steel tank with an outer diameter of 2.4 m and a water pool depth of about 2.95 m. Steam is injected through a submerged vertical blowdown pipe that has about 200 mm in inner diameter and is located close to the center of the tank. Heating and cooling phases were studied in the POOLEX tests.

It is instructive to note that flow regime domains observed in the POOLEX/PPOOLEX test agree rather well with the data from [2]. Apparent influence of chugging on mixing in the pool was observed in the POOLEX experiment [11]. The steam flow rate in the POOLEX STB-20 and STB-21 was kept below certain limit to prevent mixing in the pool by steam flow pulsations. In the STB-20 test, for example, the steam mass flow rate was kept in the range of 25-55 g/s to make sure that steam condenses inside the blowdown pipe. In the STB-21 test, thermal stratification in the pool is formed with steam injection at small mass flow rate similar to the STB-20. Then the steam mass flow rate was increased up to 210 g/s which resulted to an erosion of the thermal stratification layers and a uniform temperature (isothermal) distribution in the pool was observed. After a period of mixing, the steam mass flow rate was decreased at the level of 35 g/s and thermal stratification started to develop again. In both experiments the duration of the heating phase was about 4 hours while the cooling phase took about 48 hours.

The POOLEX was later modified to become PPOOLEX (see Figure 3), which has both a drywell ($\sim 13.3 \text{ m}^3$) and a wetwell ($\sim 17.8 \text{ m}^3$). First, steam is injected through a horizontal inlet plenum, then into the drywell, and finally discharges into the wetwell through a vertical blowdown pipe which is installed close to the central axis of the tank. A series of STR and MIX tests [12, 13, 14] have been performed in PPOOLEX to investigate thermal stratification and mixing. In the MIX-01 test (see Figure 4b), for example, there is a clearing phase which took about 500 s followed by development of thermal stratification for about 2200 s. An increase in steam mass flow rate resulted in thermal mixing that took about 300 s and remained thermally mixed until the end of the test. In the STR-02 test, as shown in Figure 4c, a thermocline layer is observed in the water pool where the upper part is nearly isothermal with temperature increase up to $90 \text{ }^\circ\text{C}$ while the temperature in the lower part remains uniform around $20 \text{ }^\circ\text{C}$.

The availability of the detailed data from the POOLEX/PPOOLEX tests was instrumental for the development and validation of the approaches described in this work.

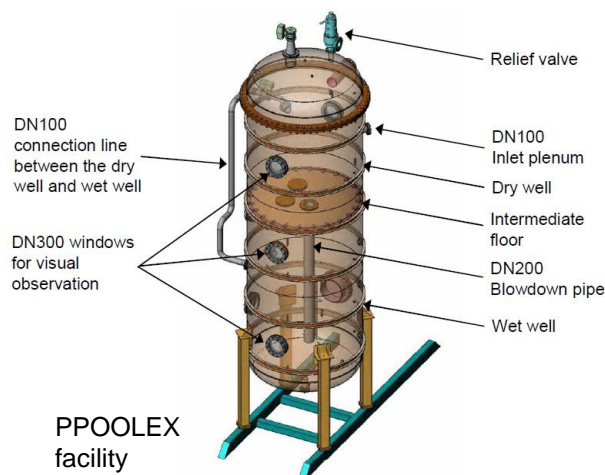
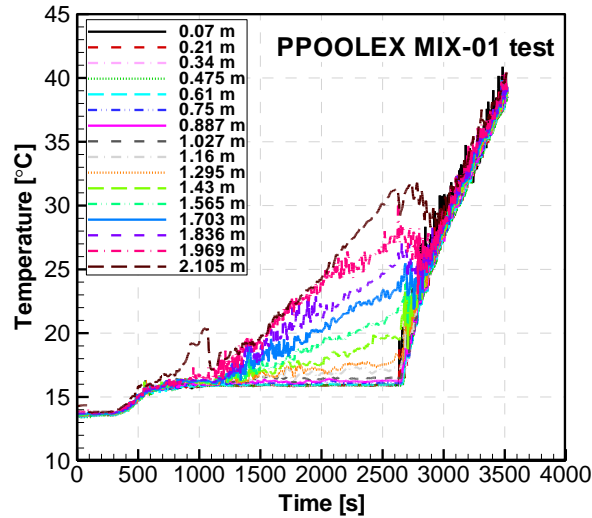
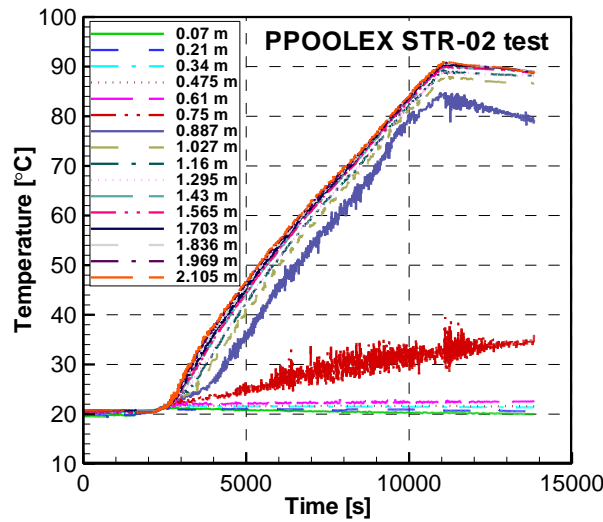


Figure 3: PPOOLEX experiment facility [12].



a)



b)

Figure 4: PPOOLEX tests of (a) thermal stratification development during the MIX-01 test [14], and (b) existence of a thermocline layer during the STR-02 test [12].

CFD modeling of POOLEX/PPOOLEX tests have been carried out by VTT, a technical research center in Finland. The direct contact condensation in short transients is directly simulated with different heat transfer correlations and interfacial surface area between the liquid and the vapor. The results showed that the condensation rate is very sensitive to the correlations. The oscillation frequencies of the steam water interface in the blowdown pipe were much smaller than in the experiments [21, 22, 23].

Scaling approaches for prediction of thermal stratification and mixing in pools and in large interconnected enclosures were developed and applied by Peterson and co-workers at UC Berkeley [1, 24, 25, 26, 27, 28, 29]. A 1D simulation code BMIX/BMIX++ was also developed to simulate stratification development in stably stratified conditions [27]. It was validated against a number of experiments [26, 27, 28, 29]. However, BMIX++ does not predict a transient where initially stratified pool is gradually mixed, and thus it cannot help to infer about the time scale for such mixing processes.

Gamble et al. [1] studied post-accident long-term containment performance in case of passive SBWR containment and found that surface temperature of the pressure suppression pool is an important factor in determining the overall long-term containment pressure. Analytical models were developed and implemented into a 1D system simulation code, TRACG, and used to model thermal stratification behavior in a scaled test facility [1]. The main idea of the proposed model was based on analysis of the effect of injected momentum in each computational cell. Good agreement with the scaled experimental test data was reported. However such models are design specific and their validity in application to other designs and steam injection conditions is not clear.

Condensation and mixing phenomena during loss of coolant accident in a scaled down pressure suppression pool of simplified boiling water reactor were also studied by Norman et al. [20]. The results of their experiments were compared with the 1D thermal hydraulic code TRACE predictions and showed deficiency in the code capabilities to predict thermal stratification in the pool. Specifically, complete mixing was predicted using TRACE while thermal stratification was observed in the experiments.

An experimental investigation of steam condensation and CFD analysis of thermal stratification and mixing in subcooled water of the In-containment Refueling Water Storage Tank (IRWST) of Advanced Power Reactor 1400 (APR1400) were performed by Song et al. [30], Kang and Song [31] and Moon et al. [32]. The IRWST is a BWR SP technology adopted in a PWR design to reduce the containment failure risk by condensing steam in a subcooled pool. A lumped volume condensation region model [31] was used to provide boundary conditions for temperature and velocity of the condensed steam and the entrained water in the CFD simulations. Their approach is similar to the model proposed earlier by Austin and Baisley [33]. However, these works address the case of steam injection through small holes (order of a centimeter in diameter) in a sparger as opposed to a blowdown pipe (about few hundred centimeters in diameter) that is considered in this report. In addition, CFD codes, even with the condensation region model, are still too demanding for computational resources to be used for parameter sensitivity analysis in long transients (order of few days physical time).

The state of the art in understanding, data and modeling capabilities relevant to suppression pool stratification and mixing phenomena can be summarized as follows:

- Numerous experimental studies were performed in the past on stratification and mixing in a pool, but only few are large scale tests with steam injection. Tests with steam injection have been carried out mostly with small diameter pipes in order to clarify steam condensation regime and not in conjunction with mixing and stratification phenomena. Not all experimental data is readily available for model development and code validation. The POOLEX/PPOOLEX is a unique series of tests at relatively large scale which provides the most complete set of data on transient stratification and mixing caused by steam injection, which is necessary for code development and validation.
- System thermal-hydraulic 1D codes are unsuccessful in prediction of stratification development unless expressly developed and calibrated models and closures are provided. Lumped-parameter and 1D models based on scaling approaches were developed and successfully used for modeling of thermal stratification development. Unfortunately, the applicability of these methods is

limited to stably stratified or well mixed conditions. The time scale of transient stratified layer erosion has not been addressed with these models.

- Direct application of fine resolution CFD (RANS, LES, DNS) methods is not practical due to large uncertainty and excessive computing power in modeling of 3D high-Rayleigh-number natural convection flows in a large pool [34], and most importantly, direct contact condensation on the steam-water interface [35].

1.3 Goal and approach

The objective of the present work is to propose reliable and computationally efficient methods that can predict transient mixing and stratification phenomena induced by steam injection into a large pool. These methods are necessary for safety analysis of the pressure suppression pool's operations in different accident scenarios.

The main challenge of this work is how to take into account in a robust and computationally efficient manner the direct contact condensation (DCC) phenomena of steam injection into a subcooled pool that are important for development of stratification or mixing in the pool.

First, we stipulate that the goal of the analysis is prediction of the stratification and mixing, and not DCC phenomena. Second, we recognize that the characteristic time and space scales of DCC phenomena are much smaller than the characteristic time and space scales of development of thermal stratification and global circulation and mixing in the pool. Third, we postulate that the individual details of small scale high frequency oscillations are lost due to the scale separation and only integral “*net effects*” of the DCC phenomena are important for mixing and stratification in a large pool. We describe these effects in terms of the heat and momentum sources induced by steam injection. In this work, we develop the “Effective Heat Source” (EHS) model to provide the effect of steam injection on pool heat transfer as a distributed along pipe surface heat source; and the “Effective Momentum Source” (EMS) model to provide the effect of steam-water interface dynamic on the large scale circulation in the pool as a local source of momentum [36, 37, 38, 39].

Thus instead of “direct” CFD-type modeling of DCC phenomena, we propose to use the effective models [see also 40, 41] which can introduce the effect of DCC through appropriate boundary conditions implemented in 3D modeling of transient thermal stratification and mixing. It is instructive to note that such approach is close to the ideas proposed by Austin and Baisley [33] and later developed by Kang and Song [31] for horizontal steam injection at high velocities through relatively small nozzles of the spargers. In our work we address vertical injection of steam through large blowdown pipes at relatively low velocities. Also instead of CFD, we use as a computational vehicle in our analysis a thermal hydraulic code called GOTHIC[®], which was developed for containment analysis with the possibility to resolve 3D flow structures and has been extensively validated including stratification and mixing phenomena in large gas volumes [42, 43, 44]. GOTHIC provides a middle-ground approach between a lumped parameter approach and CFD. In each cell of a 3D grid, GOTHIC uses closures and correlations for simulation of heat, mass, and momentum transfer at subgrid scales using local cell parameters as an input. With such an approach the computational efficiency can be dramatically improved in comparison with standard

CFD methods due to the much less strict demands for necessary grid resolution. For example, there is no need in GOTHIC to resolve near wall boundary layers, because heat and mass transfer is resolved by subgrid scale models based on boundary layer theories or experimental correlations. At the same time, 3D resolution of the flow field in GOTHIC is an advantage for the study of phenomena such as mixing and stratification, and it provides much greater flexibility than in 0D and 1D models. A schematic of the EHS and EMS models is shown in Figure 5. One thermal conductor in GOTHIC is used to supply the equivalent heat flux through the pipe wall. One pump is used in GOTHIC to impose effective momentum into the water pool.

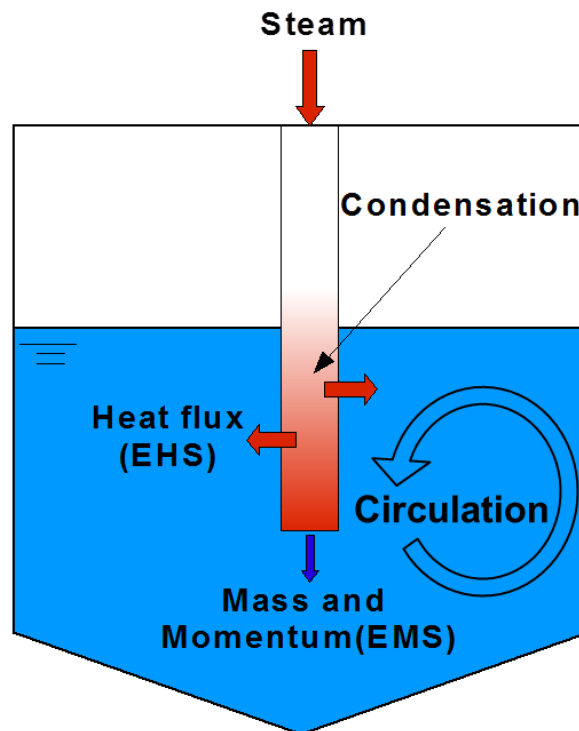


Figure 5: Schematic of Effective Heat Source (EHS) and Effective Momentum Source (EMS) models.

In previous NKS reports [36, 37, 38, 39], the EHS/EMS models are implemented and validated against POOLEX/PPOOLEX experiments [11, 14]. A more organized (e.g., parametric sensitivity analysis) and updated discussion of the two POOLEX tests, STB-20 and STB-21, and PPOOLEX STR-03 tests have been included here. However, the focus of this work is on the recent PPOOLEX MIX tests, specifically (i) validation of EHS and EMS models, and (ii) approach to generalize the available experimental data on the amplitude and frequency of oscillations.

2 Development of effective models

2.1 Effective Heat Source (EHS) model

The EHS model provides integral heat source caused by steam injection. Its purpose is to conserve mass and thermal energy of injected steam. In Figure 6, the schematic of the EHS model is shown. It is assumed that only hot saturated water flows out of the blowdown pipe. This is the case also in reality when all steam condenses inside the blowdown pipe. Such approach correctly preserves the mass balance in the system even if some fraction of injected steam is condensed outside the pipe outlet.

A time averaged mass flow ($\dot{\bar{M}}_{steam}$) and enthalpy (\bar{h}_{steam}) of the steam define the total effective heat source

$$\begin{aligned} H_{eff_total}(t) &= \dot{\bar{M}}_{steam}(t) \cdot \bar{h}_{steam}(t) \\ &= \frac{1}{\Delta t} \int_{t-\Delta t}^t \dot{M}_{steam}(\tau) \cdot h_{steam}(\tau) d\tau \quad \text{Eq. 1} \end{aligned}$$

while the spatial distribution of the effective heat source is determined as follows

$$Q_{eff_total}(\mathbf{t}) = \int_S Q_{eff}(\mathbf{x}, t) dS \quad \text{Eq. 2}$$

$$Q_{eff}(\mathbf{x}, t) = \frac{1}{\Delta t} \int_{t-\Delta t}^t Q(\mathbf{x}, \tau) d\tau, \quad \text{Eq. 3}$$

where $Q_{eff}(\mathbf{x}, t)$ denotes the spatial (\mathbf{x}) distribution (flux) of effective (time averaged) heat source at time moment t ; Δt is the time averaging interval which is considerably larger than the characteristic time scale of DCC oscillations; $Q(\mathbf{x}, \tau)$ is the local instantaneous heat flux through S which denotes the surface of the pipe wall and pipe outlet.

The schematic illustration of the steam condensation inside the blowdown pipe is shown in Figure 6. Steam directed through the blowdown pipe can condense on the walls and on the free water surface which results in local heat fluxes on the walls and on the free surface close to the outlet. The spatial distribution of the effective heat source depends on the steam flow rate and condensation regime. For example, if the steam mass flow rate and temperature of the surrounding pool are relatively low, the condensation and thus effective heat source can be more-or-less uniformly distributed along the submerged surface of the blowdown pipe. With significantly higher steam mass flow rates or closer to saturation pool temperature in the upper layer, steam condensation inside the blowdown pipe is limited and most of condensation will occur in the vicinity of the blowdown pipe outlet. While detailed modeling of such phenomena is possible in the GOTHIC code, it is beyond the scope of current work. In order to demonstrate the feasibility of the proposed approach we consider two limiting cases in the EHS model with respect to the distribution of a total heat flux Q_{eff_total} : (i) the total effective heat rate is distributed uniformly along the pipe walls $Q_{eff-wall} = Q_{eff_total}$, or (ii) the total effective heat rate is applied at the pipe outlet free surface, $Q_{eff-free\ surface} = Q_{eff_total}$. In reality, intermediate states are possible with arbitrary re-distribution of

the total heat flux between the pipe wall and outlet. However, as we will show later, one of the limiting cases provides sufficiently accurate results for the POOLEX/PPOOLEX experiments where typical steam flow rates during the thermal stratification phase are between 50-60 g/s, with respective heat rate between 112-134 kW while steam flow rates during the mixing phase are between 200-425 g/s, with respective heat rate between 446-948 kW.

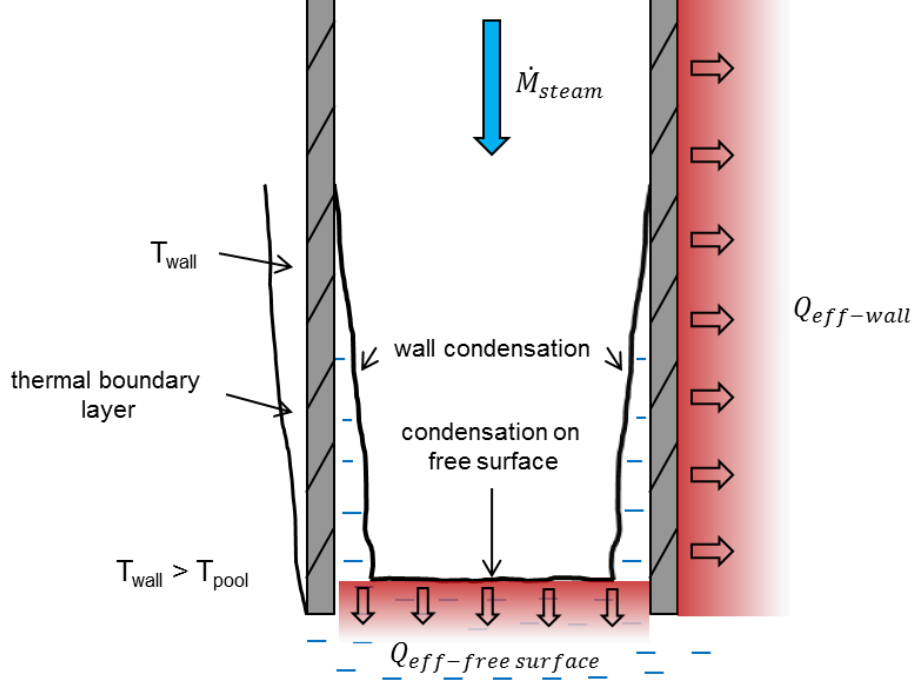


Figure 6: Condensation inside the blowdown pipe during steam injection.

2.2 Effective Momentum Source (EMS) model

The EMS model provides time averaged momentum source induced by steam injection. This momentum creates large scale circulation in the pool which can lead to erosion of thermally stratified layer and mixing of the pool. The effective momentum source is calculated by

$$\mathbf{M}_{eff}(t) = \frac{1}{\Delta t} \int_{t-\Delta t}^t \mathbf{M}(\tau) d\tau \quad \text{Eq. 4}$$

It is instructive to note that steam condensation can induce different time averaged (effective) momentum rates at the same mass flow rate of steam depending on the condensation regime. Thus the goal of the EMS model is to establish a connection between steam injection parameters, pool conditions, and resulting momentum injected into the pool.

For a given diameter of the blowdown pipe the condensation regime depends on the injected steam flux and pool bulk temperature (see Figure 2). In the POOLEX/PPOOLEX experiments, the condensation regime typically starts from condensation within the pipe (region 1) then goes to chugging (region 2) as the steam flow rates are increased and in some tests it goes further to the transition regime (region 5) as the pool bulk temperature increases. According to the observed pool mixing rate in PPOOLEX tests [13, 14], the effective momentum source during condensation within

the pipe regime is negligible compared to the effective momentum during chugging. The effective momentum in the chugging regime is also higher than that in the transition regime, although the steam mass flow rate can be higher in the transition regime.

The reason is that steam injected into a subcooled pool creates different patterns of fluid oscillations in different regimes. For instance, in the chugging regime, large amplitude periodic oscillations of the free surface inside the pipe are caused by the periodic process of (i) steam injection, (ii) expansion of the steam bubble around the pipe outlet, (iii) volumetric condensation inside of the over-expanded steam followed by, (iv) sudden bubble collapse and suction of water inside the blowdown pipe. No steam bubble plume is injected into the pool above the pipe outlet. As shown in Figure 7, the fluid motion inside the pipe during each cycle of the chugging can be separated into two parts: water injection in downward direction, and then suction of water in upward direction during steam condensation phase. Both phases of such quasi-periodic motion introduce a momentum source that affects large scale circulation flow in the pool.

In this work we consider a specific case when the momentum is generated mostly by the oscillatory flow in the blowdown pipe. The other case, when steam and possibly non-condensable gases escaping the pipe can contribute to generation of momentum in the pool due to the buoyancy force, is beyond the scope of this work.

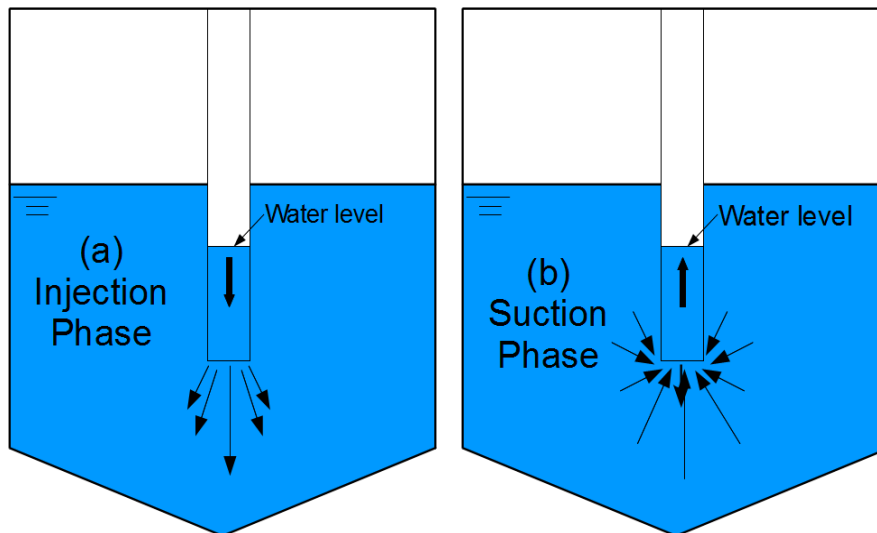


Figure 7: Separate effect during chugging regime when steam is injected through vertical pipe, (a) injection phase and (b) suction phase.

2.2.1 Synthetic jet model for prediction of the effective momentum source

The “synthetic jet” term was introduced to denote fluid motion which can be generated by oscillatory flow through an orifice with zero time averaged mass flow [45]. The vibrations of a diaphragm inside an enclosed volume with single orifice are usually used in order to create a synthetic jet (Figure 8a). It has been shown that the injection phase of the oscillatory flow creates a train of vortices which has enough thrust to propagate and is not destroyed during the suction phase (see Figure 8b). The resulting (synthetic) jet is responsible for the far-field quasi-steady flow. In an axisymmetric case, a criterion

for jet formation [46, 47] is given as $L/(2\pi d) > 0.16$ where L is called the stroke length and d is the diameter of the orifice. Early experiments by Smith and Glezer [48] have shown that a low Reynolds number synthetic jet has many characteristics that resemble continuous higher Reynolds number jets. Mallinson, et al. [49] has also shown that the far-field behavior of round synthetic jets is closer to that of conventional (turbulent) round jets, i.e., the centerline velocity decays like $1/x$.

For a single harmonic oscillation, the velocity scale based on the momentum flux [50] is given as,

$$U_0 = \sqrt{2}fL \quad \text{Eq. 5}$$

where f is the frequency of oscillation and L is the amplitude of oscillation. The momentum rate is then given as,

$$M = \pi\rho U_0^2 d^2 / 4 \quad \text{Eq. 6}$$

where ρ is the liquid density and d is the diameter of blowdown pipe.

In this work we use similarities between basic physics of synthetic jets and flow created by the free surface oscillations in the blowdown pipe in order to propose a model for effective momentum. Indeed, in case of condensation oscillations, the velocity of periodic oscillations is usually much larger than the velocity determined by the mass flow of steam, while in the synthetic jet case, the mass flow through the orifice is exactly zero. Similarly to the synthetic jet, the large scale circulation in the pool does not follow the high frequency oscillations of the water level in the pipe, that is, the flow pattern in the pool is not oscillatory.

Our hypothesis, which is validated in the work of this report, is that the effective momentum source in case of steam injection into subcooled water can be predicted using the synthetic jet model, i.e. based on Eq. 5 and Eq. 6. Such characteristics as frequency and stroke lengths (or amplitude) of the oscillations should be known in order to do that.

The amplitude and frequency of the water-level oscillations in the pipe can be obtained experimentally, e.g. by temperature measurements on the pipe's inner surface or by a level meter. Figure 9a shows a sample 5 second time window of TC measurements inside the blowdown pipe during chugging in PPOOLEX MIX-01 test. The corresponding water level positions inside the pipe are shown in Figure 9b. To calculate the effective momentum given the TC measurements inside the blowdown pipe, the following steps are implemented.

1. Convert the TC measurements to water level positions (see Figure 9 as an example).
2. Calculate the velocities $u = \frac{dz}{dt}$, where z is the water level position.
3. Calculate the moving time-averaged velocities

$$\bar{U}(t) = \sqrt{\frac{1}{\Delta t} \int_{t-\Delta t}^t u^2(\tau) d\tau} \quad \text{Eq. 7}$$

with an averaging time scale $\Delta t = 100$ s.

4. Calculate the effective (jet) velocity $U_0(t) = \frac{2}{\pi} \cdot \bar{U}(t)$. This relation can be shown simply by taking a single harmonic signal $z(t) = L \cdot \sin(2\pi ft)$ where $f = 1/T$ and use Equations 5 and 7.
5. Calculate the effective momentum rate M_{eff} given by Equation 6.

For the 5 s time window given in Figure 9b, the time-averaged velocities are around 0.65 m/s and the momentum rates are around 14.6 kg·m/s².

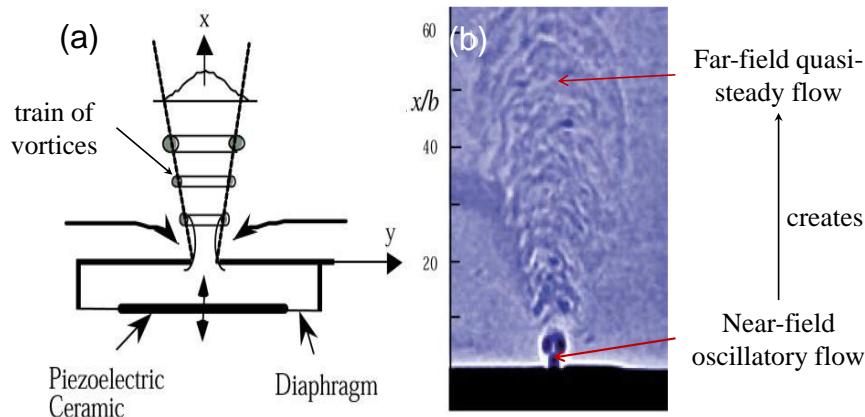


Figure 8: (a) Schematic of a synthetic jet actuator and (b) Schlieren image of a rectangular synthetic jet [48].

The ultimate goal of the EMS model is to calculate the effective momentum M_{eff} (see Figure 10), given the steam mass flux, pool bulk temperature, and design specific parameters. The first step is to determine the condensation regime. The 2D condensation regime map of Lahey and Moody [2] is found to be sufficient for large scale diameters of the pipe (~200 mm). Next, given the condensation regime and design specific parameters, the frequency and amplitude of oscillations in the pipe (if they occur) should be obtained from the experiment or predicted using such models as the Aya and Nariai model [51]. However, scalability of the Aya and Nariai model for large injection diameters is still an issue and is currently being investigated (see Appendix). The last step is the calculation of the effective momentum that is based on synthetic jet theory. In the synthetic jet theory, the amplitude and frequency of oscillations inside the pipe are directly proportional to the velocity scale and hence the effective momentum.

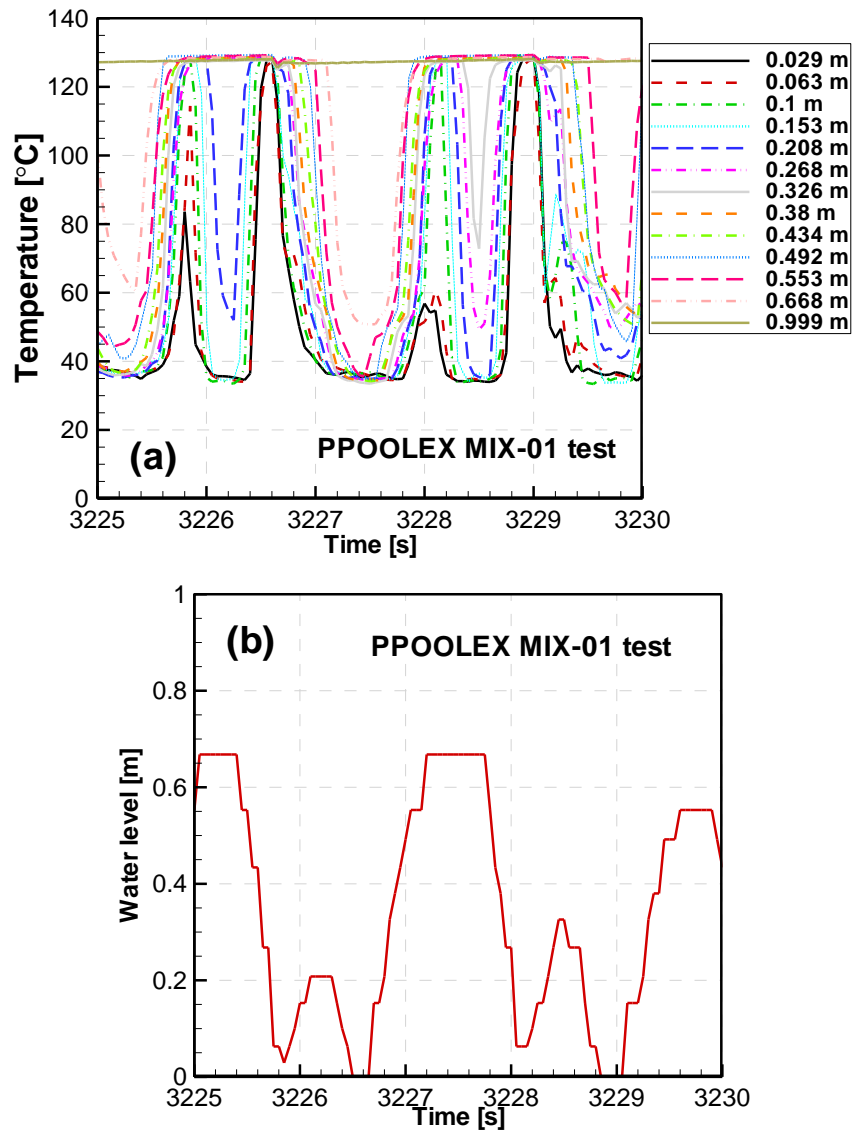


Figure 9: (a) TC measurements inside the blowdown pipe and corresponding (b) water level positions for a 5 s time window and superimposed smoothed data with a moving average filter. Frequency and amplitude of oscillations can be based on the water level positions inside the pipe. The outlet of the pipe is at 0 m [14].

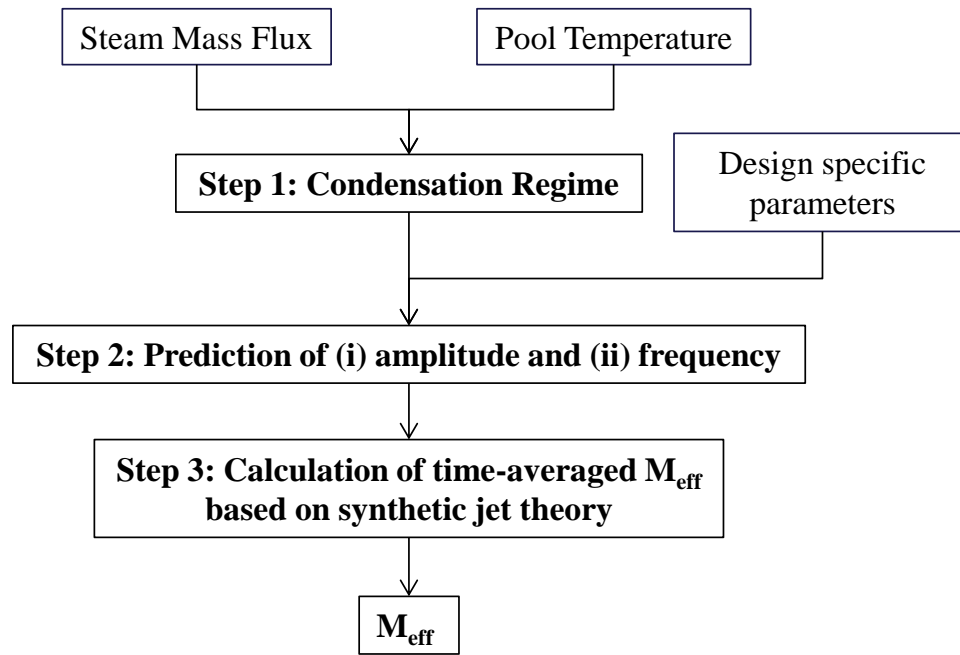


Figure 10: Calculation diagram for the effective momentum M_{eff} with input of steam mass flux, pool temperature, and design specific parameters.

3 POOLEX/PPOOLEX Experiments

3.1 *Experimental facility*

A series of experiments on steam condensation, thermal stratification, and mixing in a large water pool have been performed at Lappeenranta University of Technology (Finland) with POOLEX (POOL EXperiment) and later modified PPOOLEX (Pressurized POOLEX) facility [11, 12, 13, 14]. The POOLEX/PPOOLEX series are among the few experiments on water pool mixing/stratification at such large scales, and the availability of data was very instrumental for the validation of EHS/EMS models [11, 12, 13, 14].

The POOLEX facility is an open cylindrical stainless steel tank with an outer diameter of 2.4 m and a water pool depth of 2.95 m (see Figure 11a). The bottom is conical and the walls are not insulated during the tests. Steam is injected through a submerged vertical blowdown pipe that has a 214 mm inner diameter and is located close to the center of the tank. Three vertical trains of thermocouples (with 16 thermocouples in each train) were installed in the tank to monitor water temperature during the test. Temperature inside the blowdown pipe was monitored with 3 thermocouples (TCs). These TCs can be used to estimate the level of water inside the pipe. The room temperature in the lab is also measured during the experiments since the facility is an open tank.

The POOLEX facility was later modified to become PPOOLEX. It has both a drywell and a wetwell (see Figure 11b) and is considered to be realistically closer to a containment of BWRs than POOLEX. First, steam is injected through a horizontal inlet plenum, then into the drywell, and finally it discharges into the wetwell through a vertical blowdown pipe which is installed close to the central axis of the tank. A vacuum valve is installed between the drywell and the wetwell in order to balance the pressure between the compartments once the steam discharge is stopped. A single train of 16 TCs was installed in the wetwell at different elevations to measure the temperature distribution in the pool.

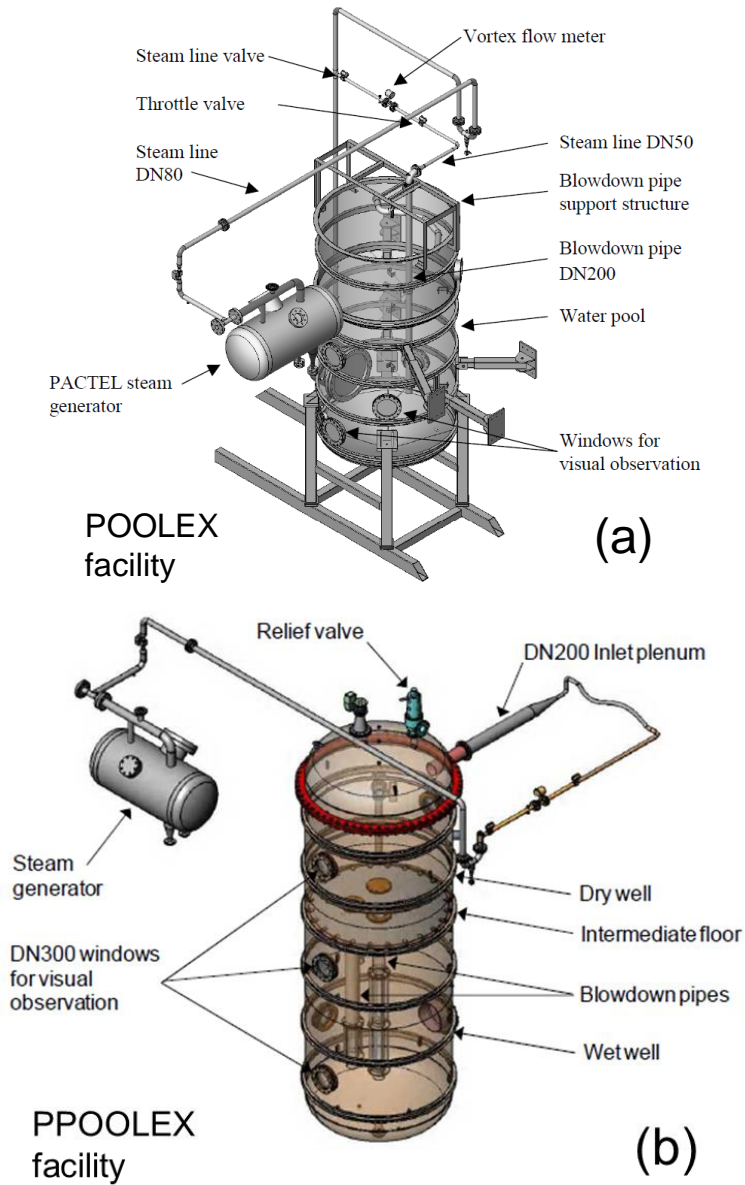


Figure 11: (a) POOLEX and (b) PPOOLEX experimental facility [11, 13].

3.2 POOLEX experiments

Heating (by steam injection through the blowdown pipe) and cooling (after stop of steam injection) phases were studied in the POOLEX tests. There are two tests, STB-20 and STB-21, performed in POOLEX for study of thermal stratification and mixing [11]. In both experiments the duration of the heating phase was about 4 hours while the cooling phase was about 48 hours.

3.2.1 STB 20

In the STB-20 test, the steam mass flow rate was kept in the range of 25-55 g/s to make sure that steam condenses inside the blowdown pipe, as shown by F1 in Figure 12.

The temperature history in the water during the steam injection is shown in Figure 13a. As expected, strong stratification above the outlet of the blowdown pipe, measured by T106-T114, was observed in the test, whereas the part below the pipe, measured by T101-T105, remained cold. The maximum temperature difference between T114 at the top, and T101 at the bottom reached more than 35 °C at the end of the heating phase. In the cooling phase without the steam injection, the temperature decreases faster at the top layer than at the bottom layer, as shown in Figure 13b.

The experimental data measured in the heating phase of STB-20 is expected to be used for validation of the EHS model, since the momentum out of the pipe is negligible. It is appropriate to assume all the latent heat released due to steam condensation inside the pipe is transferred through the pipe wall.

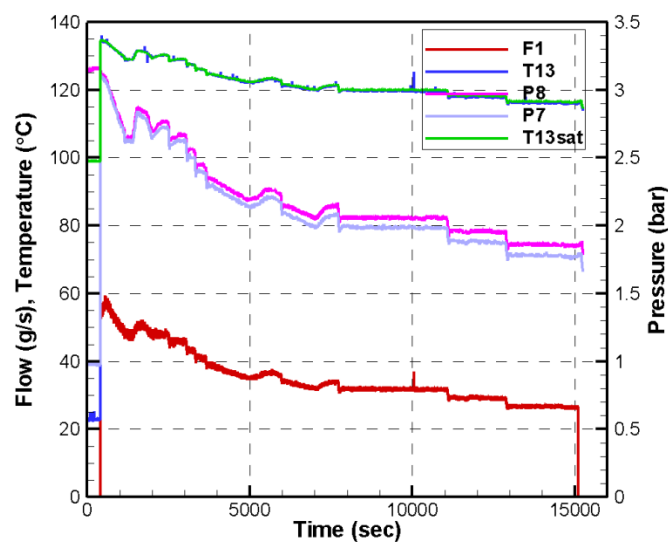
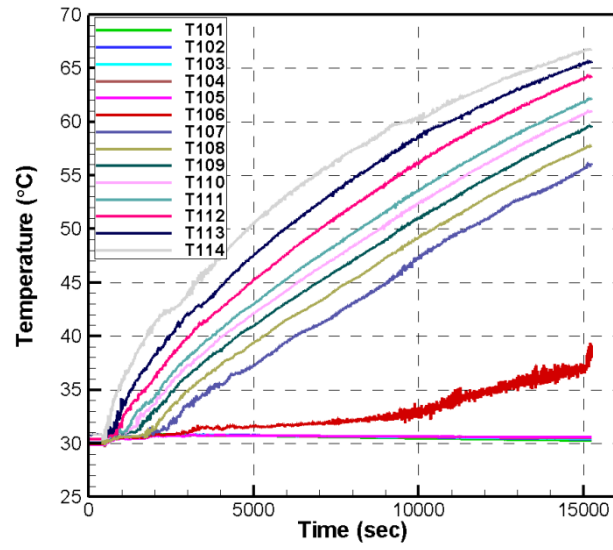
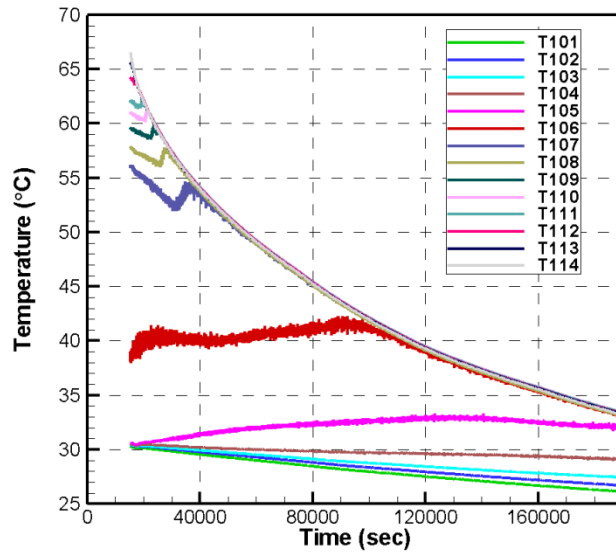


Figure 12: The measured injected steam conditions in STB-20 [11].



a)



b)

Figure 13: The measured data in STB-20, a) temperature history for heating phase with steam injection; b) temperature history for cooling phase [11].

3.2.2 STB-21

In the STB-21 test, thermal stratification in the pool was formed with steam injection at a small mass flow rate similar to the STB-20 case, as shown in Figure 14a. The steam mass flow rate was decreased from 75 g/s to about 40 g/s gradually until all steam condensed inside the pipe. Then the steam mass flow rate was increased up to 210 g/s which resulted to an erosion of the thermal stratification layers and a uniform temperature (isothermal) distribution in the pool was observed. After a period of mixing, the steam mass flow rate was decreased to the level of 35 g/s and thermal stratification started to develop again.

Figure 14b shows the temperature measured in the blowdown pipe. The temperature changes represent the motion of water level inside the blowdown pipe. In the period with temperature oscillation, the water surface inside the pipe moves up and down periodically. Between 3000 s to 4000 s, relatively high temperatures with small changes were measured by the thermocouples which means the water level remains stable. The pool temperature measurements are shown in Figure 14c. The mixing phases, thermal stratification phases and the transitions between them were captured. Mixing is observed in the pool in the early stage due to high steam mass flow rates. Then stratification develops around 2000 s with decreasing steam flow rates. The second mixing phase started about 4200 s and complete mixing was obtained at 4900 s. The second stratification phase started around 6800 s.

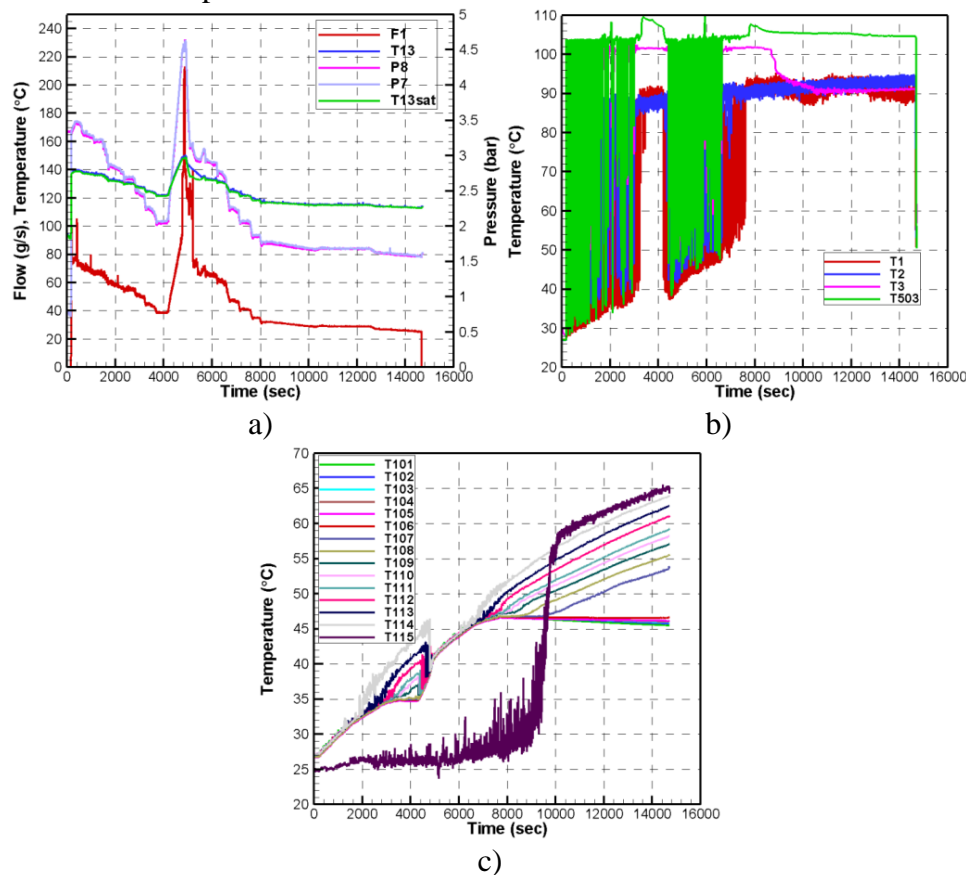


Figure 14: The measured data in STB-21, a) Steam conditions; b) temperature in the blowdown pipe; c) temperature history during steam injection [11].

3.3 PPOOLEX experiments

A series of STR and MIX tests have been performed in PPOOLEX to investigate thermal stratification and mixing. For STR tests series, there are 11 tests, with different boundary and initial conditions [12, 13]. For example, in STR-01 test the pool had initially high uniform temperature and was cooled down without steam injection. The STR-02, STR-03 and STR-04 tests concerns the development of thermal stratification in the water pool. In STR-05 and STR-06 tests, complete mixing was achieved followed by development of thermal stratification. For STR-07 to STR-11 tests, the main purpose was to completely mix a thermally stratified layer in the water pool. The TC measurements also changed in the tests. In the STR-01 to STR-08 tests, only three thermocouples were installed in the blowdown pipe with a 0.9 m interval and a measurements frequency of 1 Hz. In the STR-09 to STR-11 tests, four more thermocouples were installed in the blowdown pipe and the minimum interval of the thermocouples was 0.225 m. The frequency for data acquisition in the tests STR-09 to STR-11 is 10 Hz. In the MIX tests, a total of 17 TCs were installed inside the blowdown pipe (as compared to only 3 TCs in the STR tests) with 20 Hz frequency of measurements, and the temperature readings were used to estimate the level of water inside the pipe especially during the chugging regime.

3.3.1 STR tests

In the STR-02, STR-03 and STR-04 tests, the steam mass flow rates were controlled to have all steam condenses inside the pipe with the water level close to the pipe exit. A thermocline was observed in STR-02 and STR-03 tests while thermal stratification was observed in STR-04 test.

Figure 15a shows the steam mass flow rates in STR-03. The steam mass flow rate increases from 0.06 kg/s to 0.1 kg/s and decreases slowly to 0.06 kg/s again at 10000 seconds. After that it is maintained around 0.06 kg/s until the end of the steam injection around 14500 seconds.

Figure 15b shows the temperature history in STR-03 tests. The thermocouple of T507 shows temperature increase to around 60 °C and then remain constant until the end of the transient.

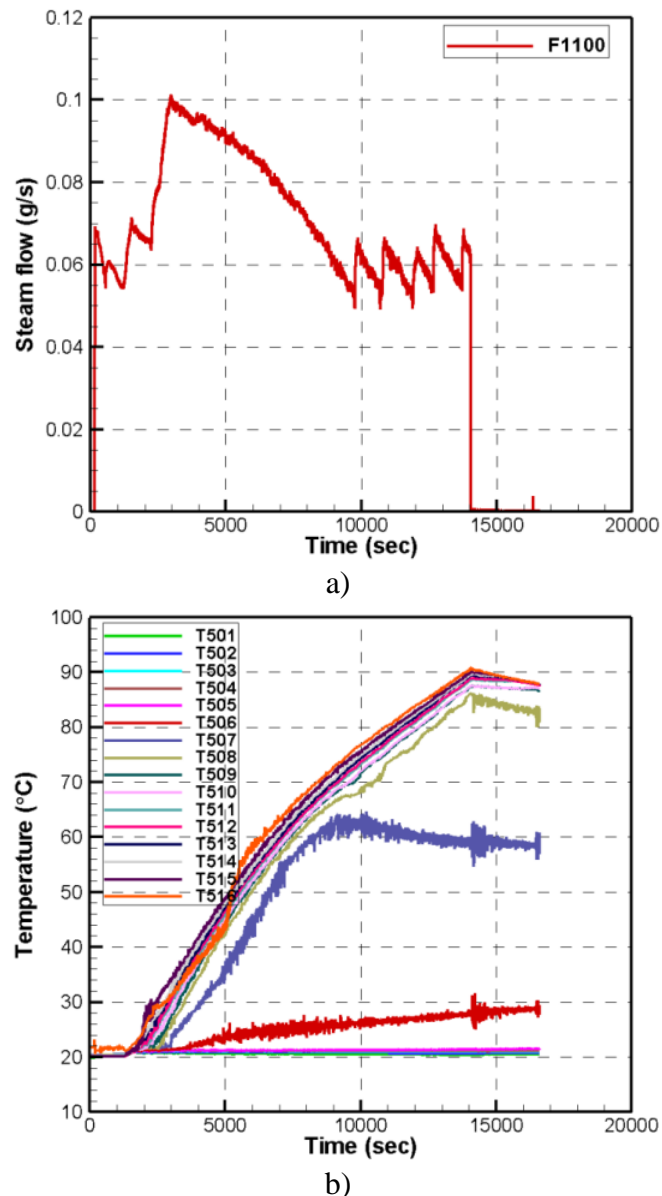


Figure 15: The data in test STR-03, a) steam mass flow rate; b) temperature history [11].

The goal of STR-07 to STR-11 tests is to investigate the process from thermal stratification to mixing. Generally, a small steam mass flow rate is imposed to develop thermal stratification, and then the mass flow rate is increased to introduce a large momentum, in order to break up the stratification and can result in a well-mixed pool. However, none of tests achieved complete mixing after the thermal stratification phase.

3.3.2 MIX tests

There are 6 tests in total in the MIX tests series. During the tests the drywell wall was insulated while the wetwell was not insulated. In all MIX tests, the clearing phase took about 500 s followed by development of thermal stratification. Then the steam mass flow rate was increased to break up the stratified layers. The steam mass flow rate was almost same in all MIX tests during the thermal stratification phase but varied during the mixing phase. In MIX-01, MIX-02, MIX-03 and MIX-04 tests, the pool remained

thermally mixed until the end of the test. In MIX-05 and MIX-06 tests, a second thermal stratification phase was observed after complete mixing (see Figure 16).

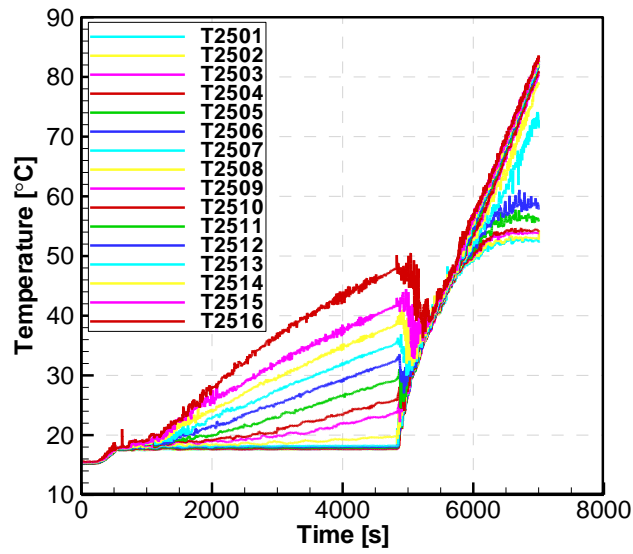


Figure 16: The temperature history in the pool in MIX-05 tests [14].

4 Validation of effective models against POOLEX tests

4.1 Validation of Effective Heat Source (EHS) model against POOLEX STB-20 test

4.1.1 GOTHIC modeling and assumptions

In the POOLEX STB-20 test [11], practically all steam condenses inside the blowdown pipe and the steam-water interface stays close to the pipe outlet. And since the mass flow rate in the STB-20 test is considered small, it is then assumed that the momentum induced by the condensate flowing out of the pipe outlet is negligible. In addition, the mass added into the pool due to steam injection is neglected in the modeling since the water inventory in the pool has only increased about 4 % during the entire heating phase. Thus, the EHS model is only used to simulate STB-20 while both EHS and EMS models are used in STB-21 since the effective momentum there is significant.

1. Lumped Parameter Simulation

POOLEX facility has an open tank and heat losses from the tank to ambient atmosphere are not directly measured in the POOLEX experiments. Thus, a lumped parameter model in GOTHIC is used to calculate the missing experimental data on heat fluxes through the vessel walls and on the pool free surface. Then we use these data as unsteady boundary conditions for the distributed parameter model in the simulations of thermal stratification.

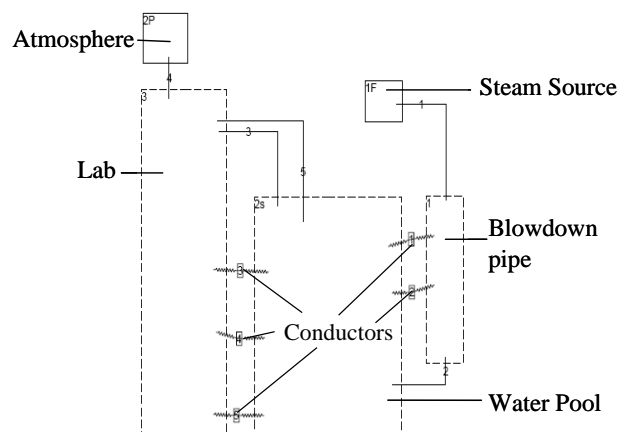


Figure 17: GOTHIC lumped parameter input model.

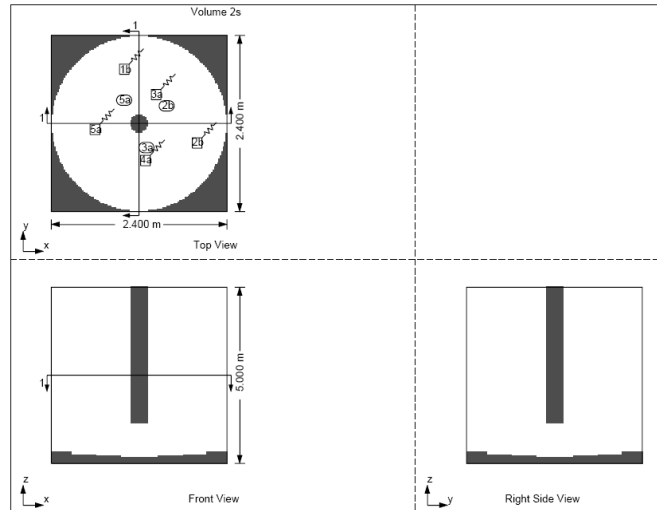


Figure 18: POOLEX tank geometry representation in GOTHIC model.

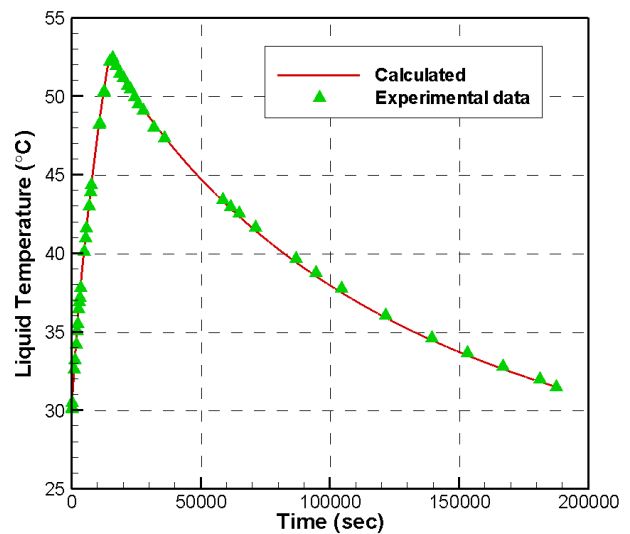
The lumped parameter model developed for simulation of POOLEX experiment is shown in Figure 17. First, the steam source is represented by the flow boundary condition (marked 1F). The experimental data, i.e., steam temperature, pressure, and flow rate is used as time dependent flow boundary condition for 1F. Next, the atmosphere is modeled by a pressure boundary condition (2P) with constant pressure (1 bar) and temperature (20 °C). The blowdown pipe, water pool, and the lab, are represented by volumes 1, 2s, and 3, respectively. The heat transfer between the blowdown pipe and the vapor phase is simulated by thermal conductor 1 while the heat transfer between the blowdown pipe and the liquid phase is simulated by thermal conductor 2. Similarly, the heat transfer between the vessel walls and the lab atmosphere are represented by thermal conductors 3, 4 and 5. The vapor part of the vessel sidewall is represented by conductors 3 while the liquid part is represented by conductor 4. Lastly, the bottom wall of the vessel is represented by conductor 5. The heat transfer coefficients for all heat conductors are calculated by default GOTHIC models for natural convection on vertical (conductors 1, 2, 3, 4) and horizontal (conductor 5) surfaces.

A blockage is used to represent the geometry of the pool in GOTHIC [52]. An example of the tank geometry representation, obtained by partial blockage in GOTHIC rectangular cell is shown in Figure 18. It is notable that such blockage is only for visualization. GOTHIC will not calculate the free volume of tank based on the size of the blockage. The tank is still treated as lumped volume with given free volume by user, since there is no gridline made in the volume. In distributed parameter model (see next section), the same blockage used to represent vessel geometry is taken into account during the calculation of free volume in the tank.

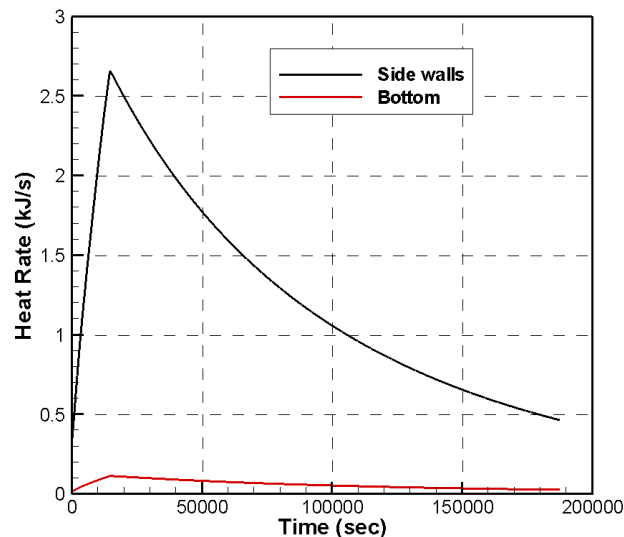
The POOLEX facility lab has a ventilation system but is not modeled in the present work because the parameters of this system are uncertain. Instead, an effect of ventilation system is introduced by a large (10^7 m^3) volume of the lab. The temperature of the lab atmosphere in the experiment and in the calculations is about 24°C. In addition, the natural circulation above the pool surface is taken into account (according to the recommendations of GOTHIC manual [52]) by two parallel flow paths (marked 3 and 5 in Figure 17). Intensity of natural circulation in such model depends on (i) the difference between the vertical positions of the parallel flow paths' outlets, and on (ii)

the loss coefficients assumed for the flow paths. The elevations of the flow paths' outlets and loss coefficients in the flow paths are adjusted to match the experimental data for the average temperature in the pool measured in the STB-20 test.

In the STB-20 experiment, steam injection was initiated at 400 s since the start of the data recording by the data acquisition system. This was done in order to provide measurements of initial conditions in the pool. In GOTHIC calculations we are not considering the first 400 s without steam injection. The simulation is started directly at the moment when steam injection starts in experiment, which means that heating (steam injection) phase lasts for 14 600 s. The whole transient physical time is 187 600 s (~52 hours).



a)



b)

Figure 19: Lumped parameter model results:

a) averaged water temperature in the tank; b) heat fluxes to the vessel walls.

Comparison of experimental and simulation results for averaged pool water temperature are shown in Figure 19a. Good agreement between experimental and simulation data for both heating and cooling phases of the STB-20 test are obtained.

As mentioned previously, the main goal of the lumped parameter model calculations is to obtain proper boundary conditions for the distributed parameter model simulation. In Figure 19b we show the heat losses from the tank to the lab through the side and bottom walls of the tank. It can be observed that the heat loss through the bottom wall of the tank is much smaller than that through the side walls.

The CPU time for calculation of STB-20 whole transient, including heating and cooling phases (187 600 s of physical time), with lumped parameter model is about 250 seconds on a PC Pentium IV with 2.8 GHz processor.

2. 2D simulation with EHS model

4.1.1.1 Sensitivity to Boundary Conditions

Heat fluxes on the pool free surface and through the vessel walls were calculated with lumped parameter model presented in Section 1. In lumped model uniform pool temperature is assumed. In reality the higher level layer in the tank is hotter during the development of thermal stratification, which means the heat loss through the tank walls at different parts calculated by lumped parameter model is over and under predicted.

Potential influence of boundary conditions on development of thermal stratification is studied in this section. In the simulations, cylindrical water tank was treated as 2D axisymmetric volume. Only liquid part is simulated. The liquid volume is divided into 12×30 meshes in horizontal and in vertical directions respectively.

Three different kinds of thermal boundary conditions are used to simulate heat transfer through the tank walls, as shown in Figure 20. In all cases the heat loss from free surface is modeled by virtual thermal conductor made of steel wall with thickness of 0.01 cm. It is also assumed that all enthalpy of injected steam is transferred to the liquid part through submerged pipe surface and there is no mass influx into the pool. Heat fluxes used as boundary conditions on the pipe wall are presented in Figure 21a, and heat loss from free surface is shown in Figure 21b.

We denote as boundary conditions 1 (BC1) the case (Figure 20a) when transient heat losses are uniformly distributed along vertical and bottom vessel walls and are obtained from GOTHIC lumped parameter simulation (Section 1). In case of boundary conditions 2 (BC2), the thermal conductor which represents vessel side wall is connected with the lab (Figure 20b). In this case, the heat transfer between the side wall and the lab is simulated by a built-in heat transfer models in GOTHIC. Boundary conditions 3 (BC3) correspond to the case (Figure 20c) when heat loss through the bottom and side walls of the vessel to the lab are calculated by built-in model in GOTHIC. In order to span the thermal conductor into the sub-volumes the conical bottom is been changed to a flat plate.

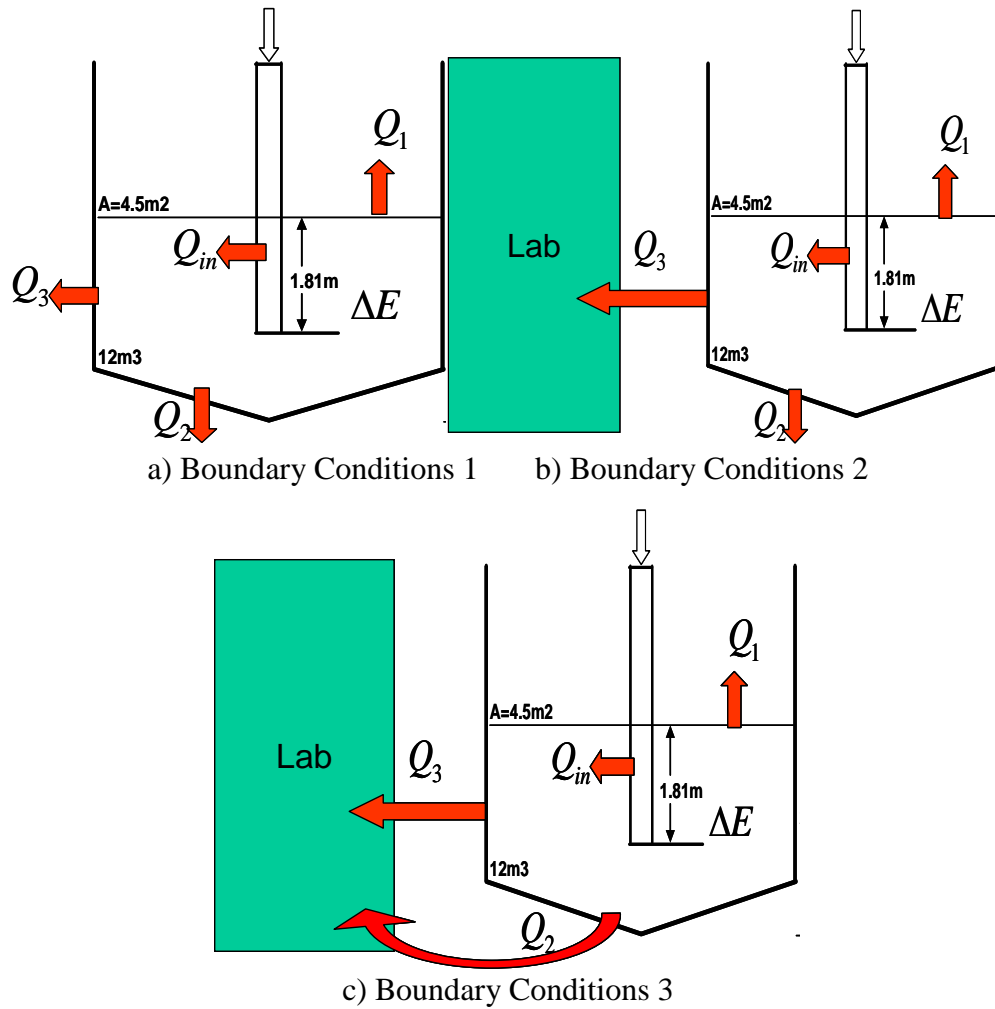
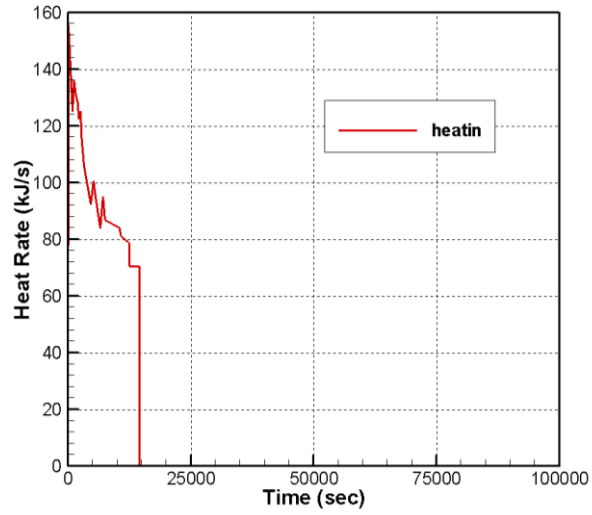
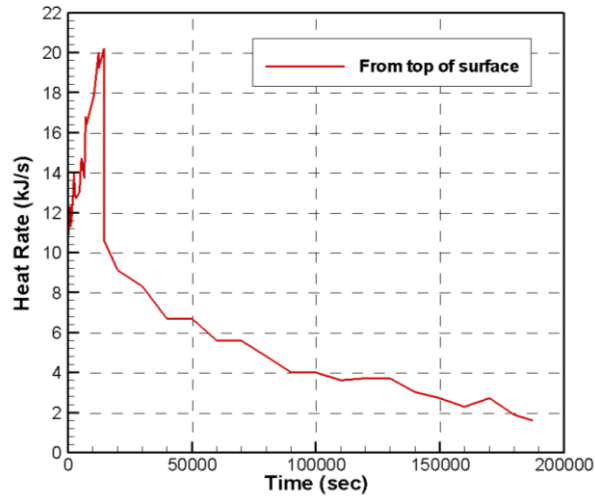


Figure 20: Schematics of boundary conditions BC1, BC2 and BC3.

The transient time for simulation is in total 187600 seconds (~52 hours). The computational time for simulations with different boundary condition is about 5 hours on a PC Pentium IV with 2.8 GHz processor. In Figure 22, we can see that the average liquid temperature is almost the same with different boundary conditions. It implies that the heat loss calculated with subdivided volume and with lumped parameter volume has almost identical effect in all considered cases.



a)



b)

Figure 21: Heat rate: a) through the pipe wall; and b) on free surface.

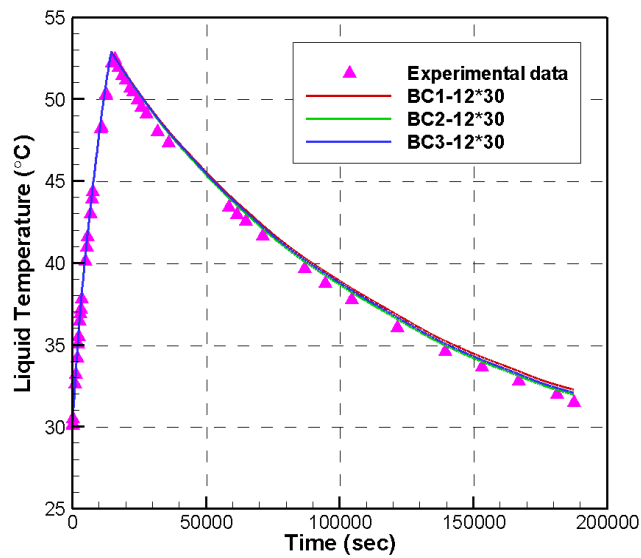


Figure 22: Averaged liquid temperature with different boundary condition.

The predicted temporal evolution of spatial temperature distribution in the pool is shown in Figure 23. Both heating and cooling phases of the experiment are presented. Development of hot layer on top during the heating phase and formation of isothermal layer in cooling phase are clearly visible even on the relatively coarse grid with 12×30 cells.

Figure 24 shows the temperature distribution predicted with different boundary conditions. There is a slight difference in the temperature distribution below the pipe outlet (Figure 24a). In that part, simulation with boundary condition 1 (BC1) has predicted slightly (less than 1°C) lower temperature than that with the other boundary conditions for cooling phase. The reason is that the imposed heat flux using for BC1 has been obtained from lumped parameter simulation in which uniform temperature has been used. The real heat loss through the bottom wall should be smaller than that predicted with BC1 because liquid at the bottom layer is colder compared to the average liquid temperature used in BC1.

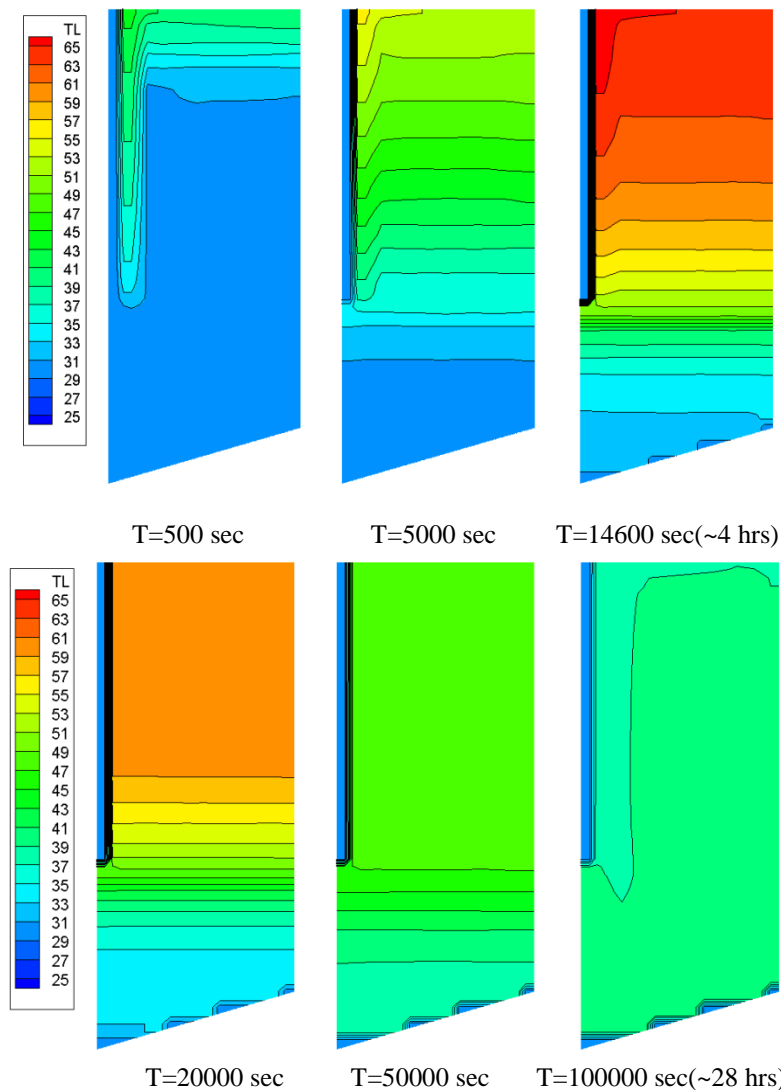
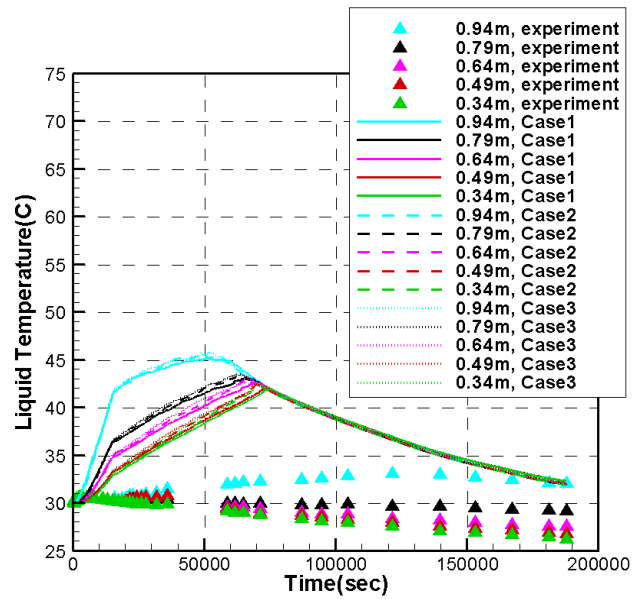
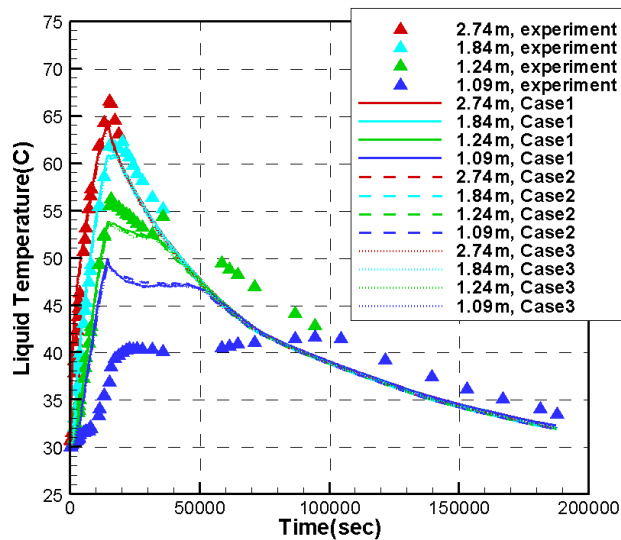


Figure 23: Temperature distribution in the pool calculated with BC1 and grid with 12×30 cells.



a) Part below the pipe outlet



b) Part above the pipe outlet

Figure 24: Temperature distribution in the simulation with different boundary conditions and comparison to experiment.

Simulations with built-in model in GOTHIC for thermal conductors are closer to reality. Since heat loss from side wall and bottom wall is quite small compared to the heat loss from the top free surface, the resulting difference due to the boundary conditions on the side and bottom walls is insignificant. The flat bottom can also be used to simplify the modeling for complex bottom geometry. Figure 24 also shows that using the flat bottom instead of the conic bottom in the boundary condition 3, has no significant effect on the simulation results.

Considerable over-prediction of temperature in the bottom layer is probably due to coarse grid resolution in the simulation. Effect of grid resolution is systematically addressed in the following section.

4.1.1.2 Sensitivity to Grid Resolution Study

In the previous section, 2D simulation in GOTHIC with grid 12×30 has been performed with different boundary condition and compared to experimental data. Although most of the simulation results show thermal stratification development and good agreement with measurement, still some deviations from experimental data has been observed in the bottom layer of tank. A probable reason is the excessive numerical diffusion in the simulations on coarse grids. In order to investigate influence of numerical diffusion on simulation of thermal stratification, four grids with sequentially doubled space resolutions are used in GOTHIC for 2D simulations. The coarse grid resolution is 12×30 with mesh size 0.1 m. Other tested grid resolutions are 24×59 with mesh size 0.05 m and 48×118 with mesh size 0.025 m. The finest grid resolution is 48×236 , since a grid with 96×236 is too computationally expensive to run.

Since the simulation results is found to be insensitive to boundary conditions (see previous section), only the boundary condition 1 (BC1) with four fixed heat fluxes has been used for the grid sensitivity study.

From Figure 25, we can see the results with different grids scheme. Figure 25a shows the temperature distribution in the bottom part, i.e. below the pipe outlet. Results with grid 48×118 and grid 48×236 overlap each other in this part. This is an indication that grid resolution in horizontal direction has no big influence on the temperature distribution at the bottom of the tank. Results obtained with grid 48×118 and 48×236 are in much better agreement with the experimental data if compared to that obtained with other grids. The calculated temperature in the position of 0.64 m is close to the measured value. The temperature in the position of 0.94 m is over-predicted on the grid 48×236 by ~ 3 °C in comparison with the experiment. Such results confirm that the numerical error due to coarse grid in the bottom can be considerable in simulation of the thermal stratification development. Reasonably fine grid can help in reduction of numerical diffusion during simulation.

Figure 25b shows that some of the simulation results obtained on fine grid over-predict temperature gradient in the upper layer compared to the experimental data. The figure also shows temperature distribution above the pipe outlet. The temperature at 1.09 m, which is almost in the same plane with the pipe outlet, is higher with coarser grids than in the experimental data, and it is lower with grid 48×236 . The calculated temperatures at 2.74 m with fine grids 48×118 and 48×236 are higher than in the experimental data, while coarser grid gives better agreement with the experimental data.

Another possible reason for the difference between simulation with finer grid and the experiment is that the momentum introduced by injected steam is ignored in the simulation. Although the steam has been totally condensed within pipe, the hot condensate coming from outlet of pipe can still introduce momentum in the liquid pool. This momentum is not taken into account to reduce possible computational expenses related to the resolution of free surface of liquid. On the other hand, there is a short

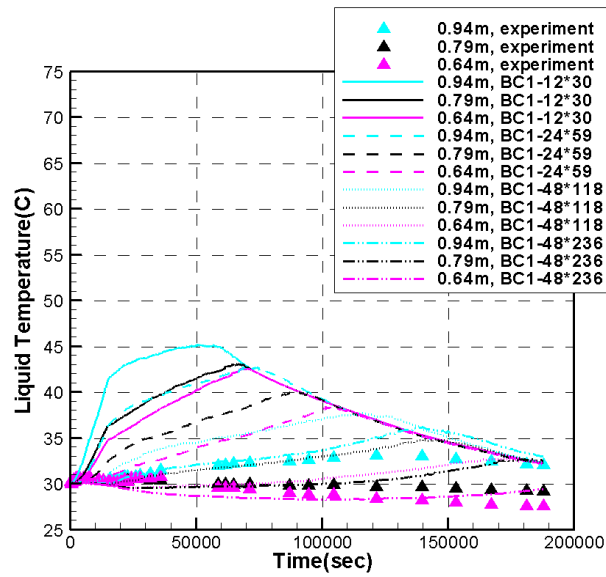
period of venting and chugging in the blowdown pipe at the beginning of the experiment and this could also introduce some initial momentum in the pool. Such momentum could result in partial mixing and decreases the top layer temperature while increases the middle layer temperature.

Same phenomenon can be observed in Figure 26, in which liquid temperature along height of pool is shown. Simulation results obtained with the finest grid 48×236 for the bottom layer of the pool are in a good agreement with the experiment at all three time moments $t = 14000$, 30000 , and 100000 seconds.

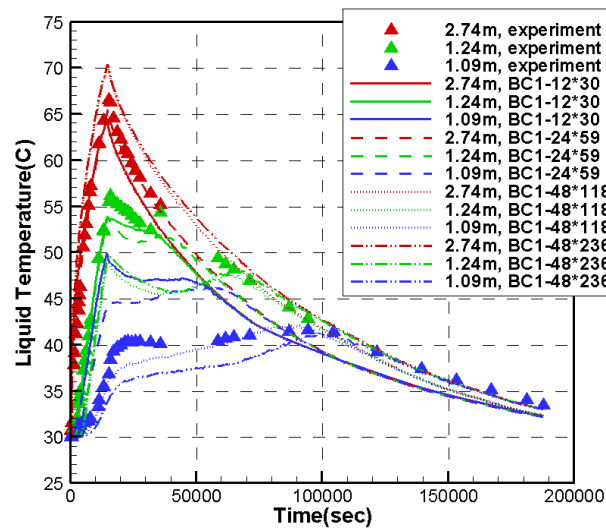
At 14000 second (about 4 hours), the temperature distribution obtained with grid 24×59 agree with the measured data in the part above the pipe outlet, while simulation with grid 48×118 and 48×236 over-predict temperature of this layer. Also in the figure, a thin unstably stratified layer at the free surface is visible. The layer is formed by the hot liquid that rises along the pipe wall and spreads over the pool free surface which is cooled from the top. Comparison of GOTHIC prediction with experimental data on temperature distribution suggests that GOTHIC seems to be capable in predicting convective overturning in the unstably stratified layer using $k-\varepsilon$ turbulence model with sufficient grid resolution (48×118 in Figure 26a, Figure 26b).

At time 30000 seconds (about 8 hours), a similar behavior can be found and the grid 24×59 still shows good capability to predict temperature distribution in the upper layer. At time 100000 seconds (about 28 hours), the temperature distribution obtained with fine grids 48×118 and 48×236 agree with the measured data well both in the upper part and the bottom part. The computational time for grid 48×236 is about 17 days, while it takes about 5 hours with the coarsest grid.

Spatial distribution of the temperature obtained with different grids is shown in Figure 27 and Figure 28. Considerable improvement of the solution quality on refined grid can be observed at later stages of the transient cooling (> 20000 seconds).



a) Pool layer below the pipe outlet



b) Pool layer above the pipe outlet

Figure 25: Temperature distribution obtained with different grid resolutions.

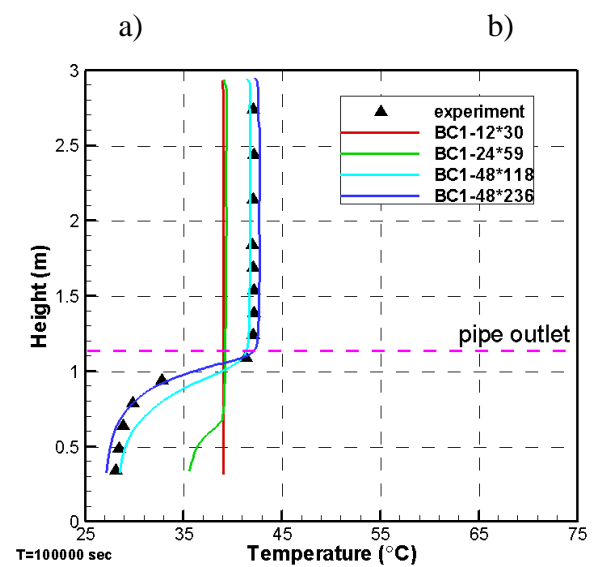
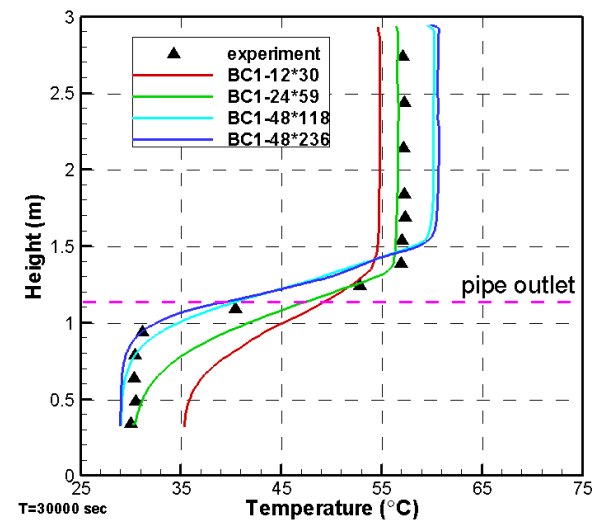
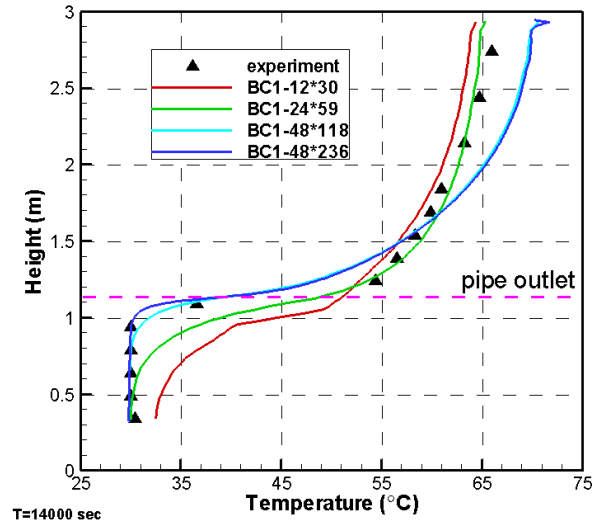


Figure 26: Liquid temperature along elevation at different transient time.

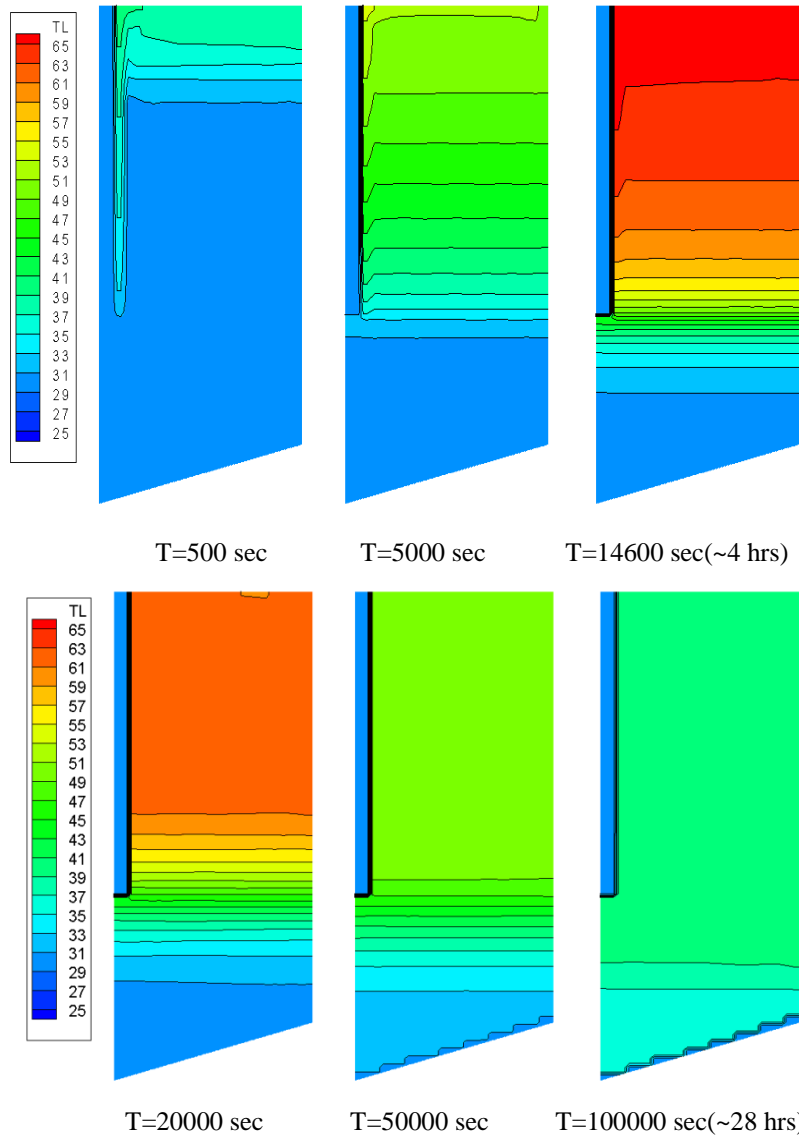


Figure 27: Temperature distribution in the pool grid of 24x59.

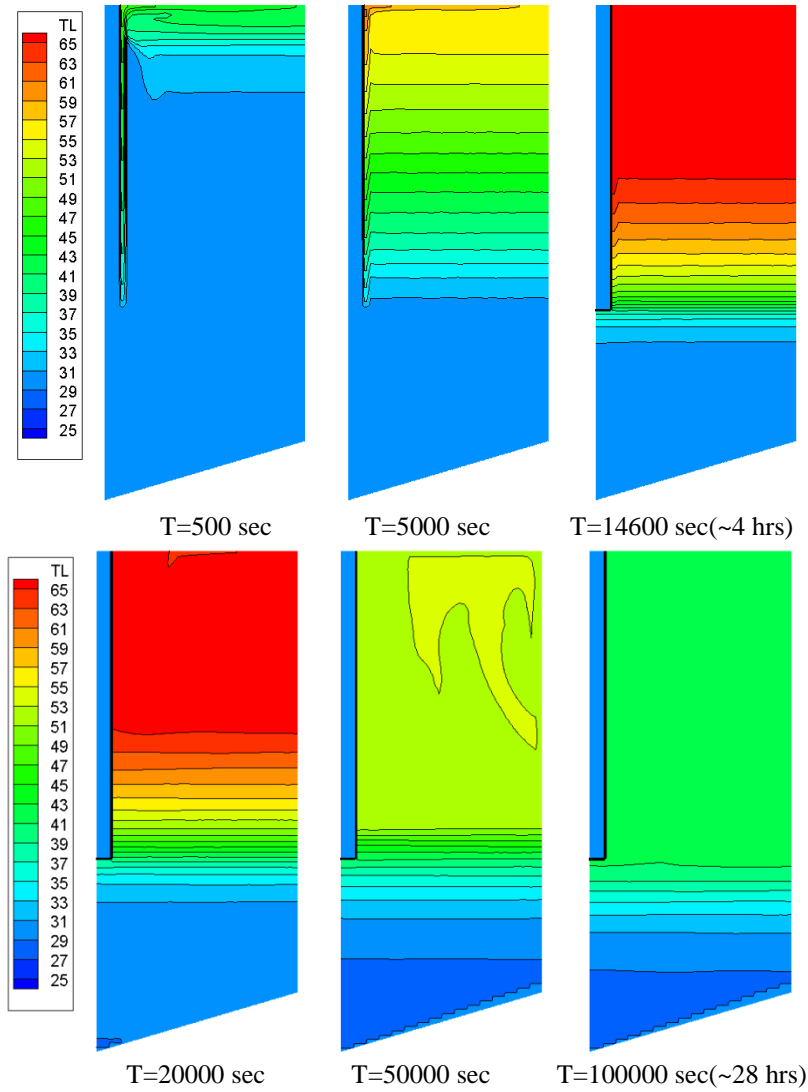


Figure 28: Temperature distribution in the pool grid of 48x118.

4.1.1.3 Sensitivity Study to Gas Space and Free Surface Modeling

The gas space of the tank has not been taken into account in previous simulation study. If water level increment is not negligible (e.g. as in the STB-21 test) then the gas space and free surface should be considered in modeling.

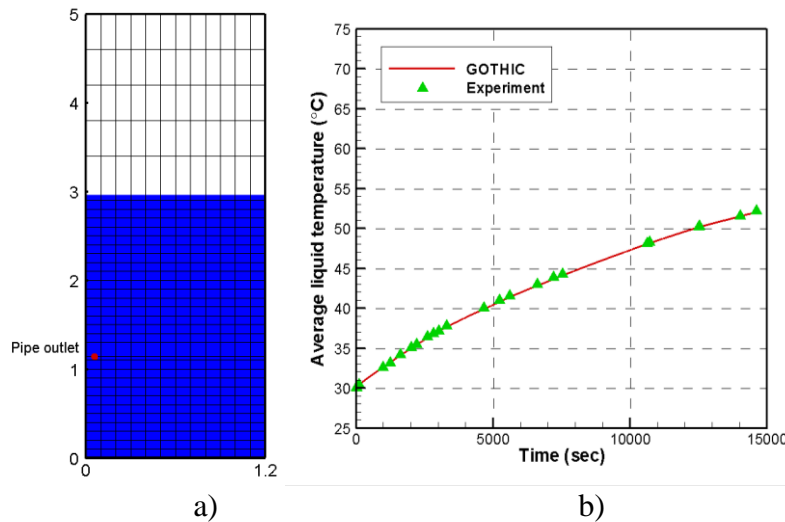


Figure 29: GOTHIC simulations: a) mesh with liquid and gas space; b) comparison of experimental and predicted averaged liquid temperature in STB-20.

Grid configuration with gas space is shown in Figure 29. The water pool geometry is modeled as 2D axisymmetric. The coarsest grid used in the analysis has 29 cells in the vertical direction for the liquid part, 1 cell for the liquid-gas interface, 4 cells for the gas space, and 12 cells in the horizontal direction. The mesh cell size in the liquid part is 0.1m×0.1m, 0.5m×0.1m for the cell with interface, and 0.4m×0.1m in the gas space of the tank (Figure 29a). Heat conduction through the blowdown pipe wall and through the tank walls is modeled with the GOTHIC models for thermal conductors. In addition, a large size lumped volume that is connected to a pressure boundary conditions simulates the lab atmosphere. Finally, a 3D connector is used to model flow and heat transfer between the lab and the pool in the open tank.

Results presented in Figure 29b suggest that GOTHIC can predict heat losses from the open tank and thus averaged liquid temperature in the POOLEX experiments. The average temperature predicted by GOTHIC models with and without gas space is practically identical.

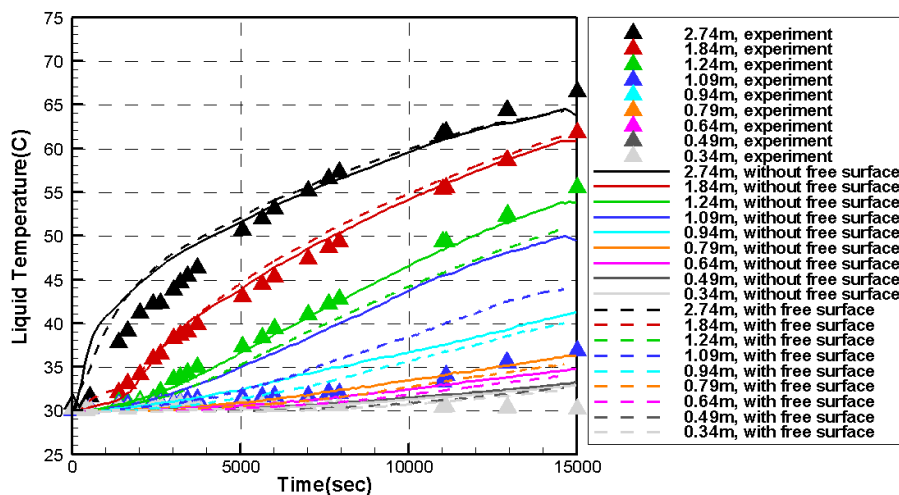


Figure 30: Temperature history in simulation with heat source and with/without pool free surface.

Figure 30 shows good agreement between experimental data for time dependent vertical temperature distribution in the STB-20 and results predicted by the GOTHIC with EHS model and with and without considering the gas space in the tank. Temperature of the very top layer of the pool is slightly overestimated (Figure 30), which can be attributed to the slight underestimation of the momentum in the effective heat source approach.

4.1.1.4 Effect of numerical finite difference scheme

The EHS model scheme for study the effect of numerical approximation is shown in Figure 31a. A large size lumped volume (marked '1') corresponds to the lab which models the lab's temperature with a ventilation system. In addition, this lumped volume 1 is connected to a pressure boundary (marked '1P') to keep the pressure constant in the lab. One 3D connector models the open orifice between the lab and the water tank. The heat losses through the side wall and bottom of the water tank are modeled by two thermal conductors, '2s' and '3s', respectively. The GOTHIC built-in heat transfer models are chosen for the thermal conductors.

The water tank is modeled as a 2D axisymmetric volume (Volume '2s'). GOTHIC supports only Cartesian coordinate system so in order to make a cylindrical geometry for volume 2s, the porosities of volume and surface area of all cells are adjusted. The spaces occupied by pipe and bottom conical section are modeled by blockage and with assumption that the bottom is flat. It is also assumed that the blowdown pipe is located at the center of the tank as opposed to a 0.3 m distance between the center and the pipe.

Both a first order upwind differencing scheme and a second order upwind difference scheme are tested. There are 3 mesh grids used for the water tank to determine the influence of grid resolution for each numerical scheme. The coarsest grid has 12 cells in the horizontal direction and a total of 34 cells in the vertical direction, that is, 29 cells in the liquid part, 1 cell for the liquid-gas interface and 4 cells in the gas space. The mesh cell sizes are, 0.1m×0.1m for the liquid part, 0.5m×0.1m for the cell with the liquid-gas interface, and 0.4m×0.1m for the gas space of the tank. The middle grid has 24 cells in the horizontal direction and a total of 60 cells in the vertical direction with distribution of cells similar to the coarsest grid except adding 26 cells to the liquid part. The finest grid has 48 cells in the horizontal direction and a total of 114 cells in the vertical direction with distribution of cells similar to the coarsest grid except adding 80 cells to the liquid part, as shown in Figure 31b.

The standard k-e turbulence model is used for the pool volume. An adaptive time-step option is implemented with minimum and maximum time-steps of 10^{-4} s and 1 s, respectively.

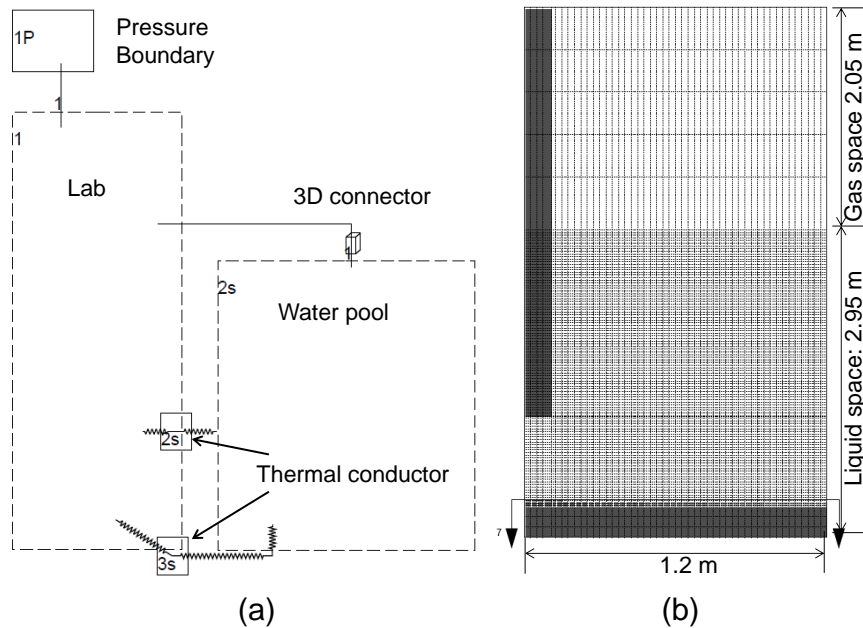


Figure 31: (a) EHS model scheme using GOTHIC of POOLEX STB experiment, and (b) 2D mesh with 48×114 for the pool.

4.1.2 Analysis of results

The comparison between experimental and predicted liquid average temperature is shown in Figure 32. In the STB-20 test, the initial temperature is around $30\text{ }^{\circ}\text{C}$ and increases up to $52.4\text{ }^{\circ}\text{C}$ during the heating phase. All the simulations predicted the average temperature excellently especially during the first half of the heating phase. The coarsest grid has a difference of only about $1\text{ }^{\circ}\text{C}$ near the end of the heating phase of the experiment while the finer grids have even smaller difference against the experiment. It can be fairly stated here that the heat balance during the heating phase is not sensitive to grid resolution.

Figure 33 shows the snapshot of temperature profiles in the pool with the EHS model using 3 different grids, 12×34 , 24×60 , and 48×114 cells, at $t = 14000\text{ s}$ compared against STB-20 experimental data. As expected all the simulation cases predicted the cold bottom layer ($30\text{ }^{\circ}\text{C}$) in the experiment since no effective momentum has been imposed in the modeling. High gradient in temperature is observed in the vicinity of the level of the pipe outlet which is captured by the simulations. Then the temperature increases more slowly to about $66\text{ }^{\circ}\text{C}$ in the experiments than in the simulations. The finest grid captures better the temperature of the upper layer with the maximum temperature at the top at about $65\text{ }^{\circ}\text{C}$ compared to about $64\text{ }^{\circ}\text{C}$ with the coarser grids.

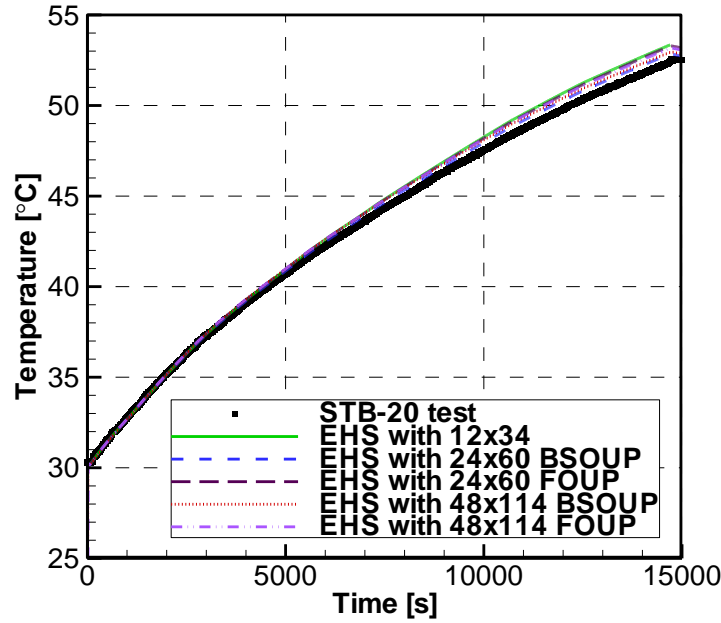


Figure 32: Average liquid temperature calculated with different grid resolution compared to STB-20 experimental data.

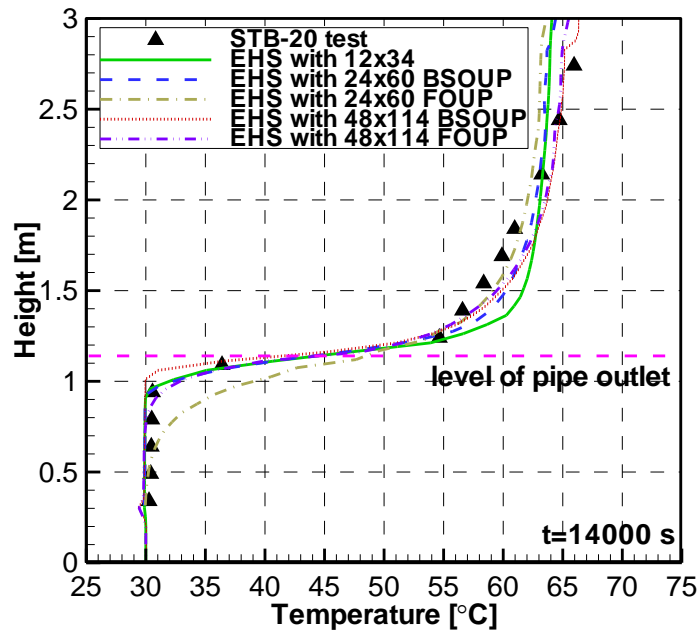


Figure 33: Snapshot of temperature profiles predicted by EHS using different grids from a radius of 0.6 m from the center (midline) as a function of height at time $t = 14000$ s in comparison with STB-20 experimental data.

EHS simulation results showing the temperature distribution in the tank at different times $t = 500$, 10000 , and 14000 s can be seen in Figure 34. In Figure 34a at 500 s, the heat source starts to heat up the water surrounding the blowdown pipe creating a buoyant plume that goes upward and circulates and also heats up part of the gas space. At a later time $t = 10000$ s (Figure 34b), the bottom layer remains cold and heating of the upper layer including the gas space intensifies with maximum temperature reaching about 62 °C. Further at $t = 14000$ s (Figure 34c), the build-up of thermal stratification layers is more pronounced and the maximum temperature even increases to about 70 °C.

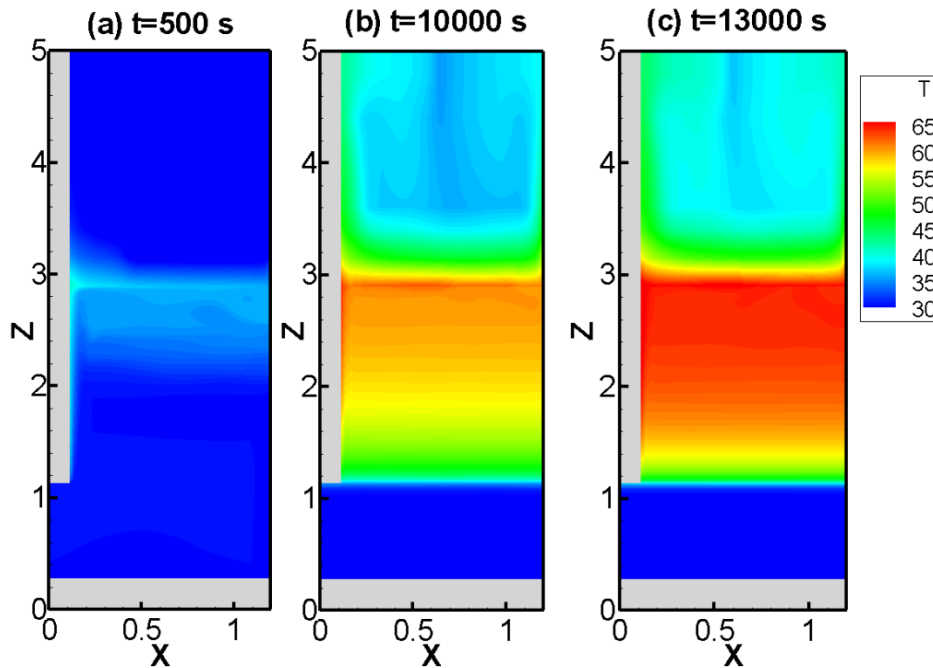


Figure 34: Temperature distribution at different times $t = 500, 10000,$ and 14000 s with EHS simulation of STB-20 test using 48×114 cells.

The calculation time for the 14700 s transient took about ~ 10 min with 12×34 cells on 1 core in an i5 3.2GHz desktop with BSOUP and direct pressure solution while it took about ~ 2 h with 24×60 cells on the same desktop and the same numerical methods. For the 48×114 cells with BSOUP, it took about ~ 14 h on 4 cores in an i7 3.4GHz desktop with conjugate gradient method.

4.2 Validation of EHS and EMS (Effective Momentum Source) models against POOLEX STB-21 test

An important criterion in the erosion of a thermally stratified pool by steam injection is the time needed to reach an isothermal pool. Not surprisingly, this time scale of mixing is also important in the operation of pressure suppression pools. Thus, predictive capabilities of proposed models should be assessed not only for averaged temperatures and thermal behaviour of certain layers but also for the time scale of mixing.

In the STB-21 experimental test, oscillations are observed in the blowdown pipe, when steam is injected into the pool. The condensation regime for this oscillation is determined as chugging, based on the condensation map and the injection condition, i.e., steam mass flux and pool temperature. In the POOLEX facility, three thermocouples (denoted by T1, T2, and T3) are installed inside the blowdown pipe, as shown in Figure 35a. The space interval between them is 0.9 m. Figure 35b shows the measured temperatures in the blowdown pipe in the STB-21 test exhibiting the oscillations of the water level at certain time windows. These thermocouple (TC) readings are used to determine the amplitude and frequency of oscillations of the water level at different time periods.

Figure 36a shows the vertical temperature distribution measured in the test STB-21 of POOLEX experiment while Figure 36b shows the corresponding steam flow rate from the steam generator. The general behavior of the STB-21 test can be divided into 6 phases. In phase A, mixing is observed before 1800 s (line 0 in Figure 36a). At 1800 s of phase B, thermal stratification begins to develop in the layer above the pipe outlet. In phase C at 3250 s (line 1), the temperature of the layer below the pipe remains steady at a constant value. In phase D at about 4200 s (line 2), the injected steam flow rate has been rapidly increased to about 210 g/s. Complete mixing is achieved around 4900 s when the pool is considered isothermal around 41 °C. The pool remains isothermal with increasing averaged temperature in phase E and finally in phase F, the pool starts to develop thermal stratification again. For the validation of EHS/EMS models, we consider the build-up of thermal stratification (phase C) and mixing (phase D).

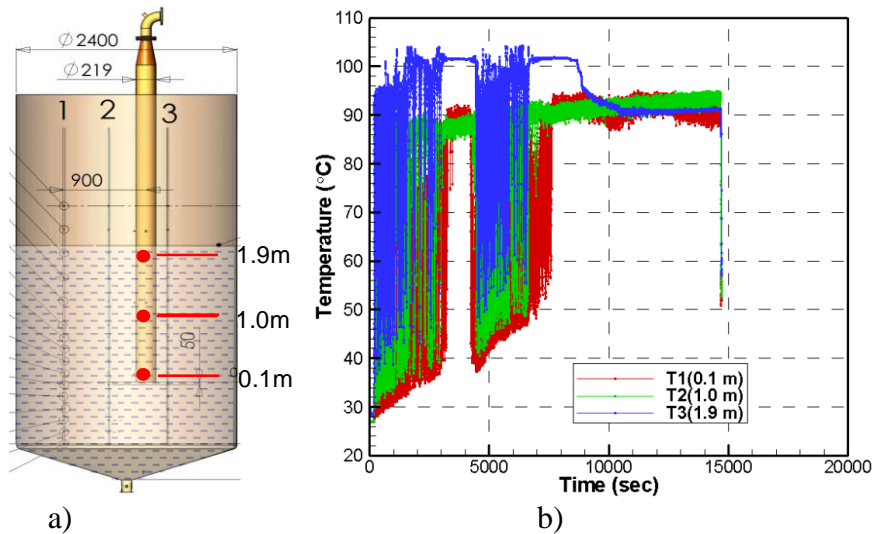


Figure 35: a) Location of thermocouples T1 (at 0.1 m), T2 (at 1.0 m), and T3 (at 1.9 m) installed in the blowdown pipe in POOLEX facility and b) temperature readings in STB-21 test [11].

Figure 36c shows part of the data simulated with EHS-EMS models while Figure 36d shows the corresponding heat rates used in the EHS implementation. The main reason behind this heat flux that changes from imposing it on the pipe's submerged surface to the pipe's exit is the limited wall condensation at high steam flow rates and most of the energy release is expected at the pipe's exit where direct contact condensation occurs. In the succeeding section, we also investigate the effect of heat flux distribution on the case with uniform heat fluxes on the pipe's submerged surface.

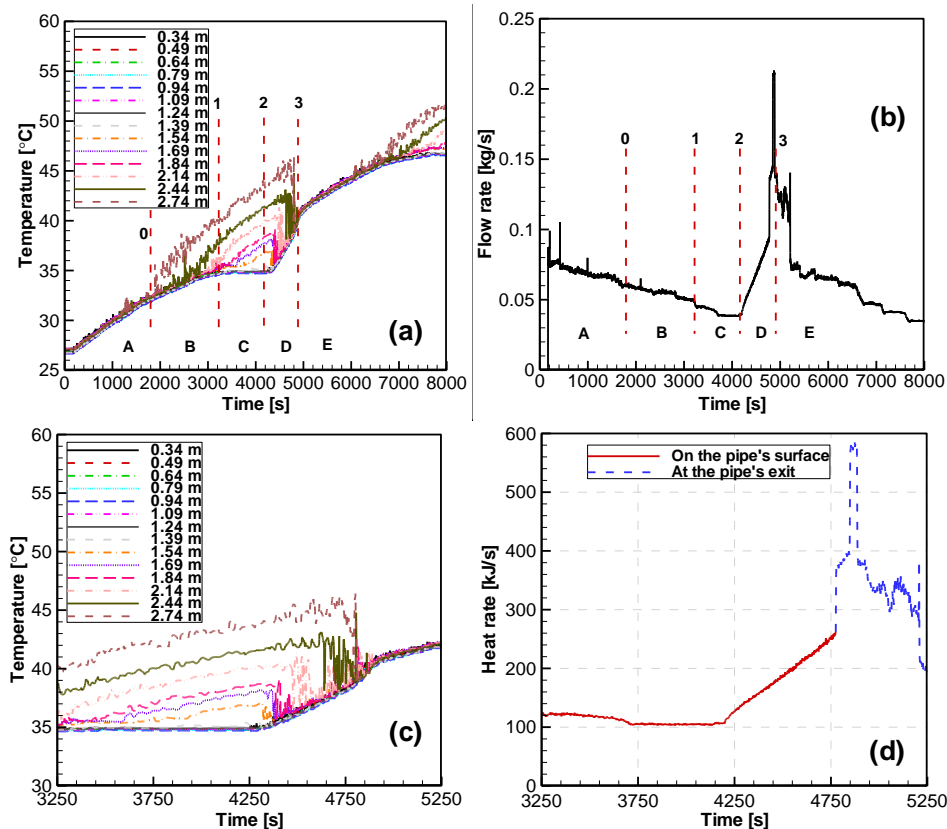


Figure 36: (a) Vertical temperature distribution in STB-21 test [11], (b) measured steam flow rate [11], (c) part of data that is simulated with EHS-EMS models [11], and (d) corresponding imposed heat fluxes that change from the pipe's submerged surface to the pipe's exit. Phase A: First mixing. Phase B: Onset of stratification. Phase C: Stratification. Phase D: Onset of second mixing. Phase E: second mixing. Phase F: Stratification.

4.2.1 Estimation of Effective Momentum

The effective momentum can be calculated based on the synthetic jet theory which relates the thrust velocity to the frequency and amplitude of water-level oscillation inside the blowdown pipe. In the POOLEX facility, only three thermocouples are installed inside the blowdown pipe which can be used to determine the water level during a test.

Figure 37 shows thermocouple measurements inside the blowdown pipe in the STB-21 test at representative time periods. The oscillation patterns are different in each time period due to varying pool temperature and steam mass flow rates. In Figure 37a, TC measurements between 4300 s and 4400 s is shown where changes happen mostly at the 0.1 m level which makes the estimation of amplitude and frequency of water level oscillation highly uncertain. Although it can be discerned from the figure that the water level (with obviously the water having much lower temperature than the steam) is oscillating inside the blowdown pipe. Roughly, the amplitude and frequency of oscillation is estimated to be between 0.3-0.4 Hz and 0.1-1.0 m, respectively. Clearly, more thermocouples installed inside the blowdown pipe are necessary in order to provide more accurate assessment of the amplitude and frequency of oscillation. Such

improvement is implemented in the PPOOLEX MIX-01 test and an example is shown in Figure 38.

In Figure 37b, TC measurements from time $t = 4600$ s to $t = 4700$ s are shown. Temperature at the 1.9 m level also reaches lower temperature implying that the water level oscillates with peaks reaching that level. In addition, the frequency is lower in this time period than in the previous period and is roughly estimated to be between 0.18-0.25 Hz while the amplitude is estimated to be between 1.0-1.9 m. Similarly, frequency and amplitude of oscillations have been estimated for the time periods 4800-4850 s (Figure 37c) and 4860-4880 s (Figure 37d) and summarized in Table 1. Given the frequency f and amplitude L of water level oscillation in the blowdown pipe, we can calculate the effective momentum based on the synthetic jet theory as discussed in detail above. But briefly, the centerline velocity U of the resulting jet induced by oscillation of the water level inside the blowdown pipe is equal to $\sqrt{2}fL$. The corresponding effective momentum rate is then equal to $\frac{\pi}{4}\rho U^2 d^2$ where ρ is the liquid density and d is the diameter of the pipe. Due to uncertainty in the estimated values from TC measurements, different cases were parametrically studied (to be discussed in the next section). They correspond to the minimum, maximum, and somewhere in-between values and are also summarized in Table 1.

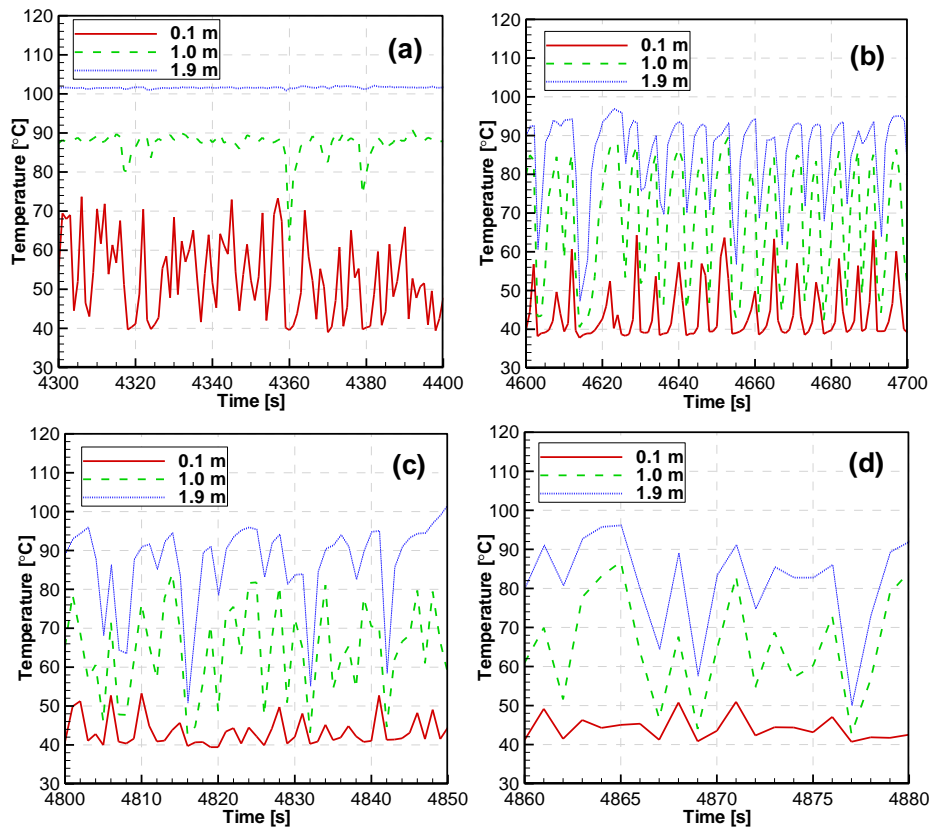


Figure 37: Thermocouple measurements inside the blowdown pipe during STB-21 test at representative time periods taken with 3 TCs at 0.1 m, 1.0 m, and 1.9 m distances from the pipe outlet [11].

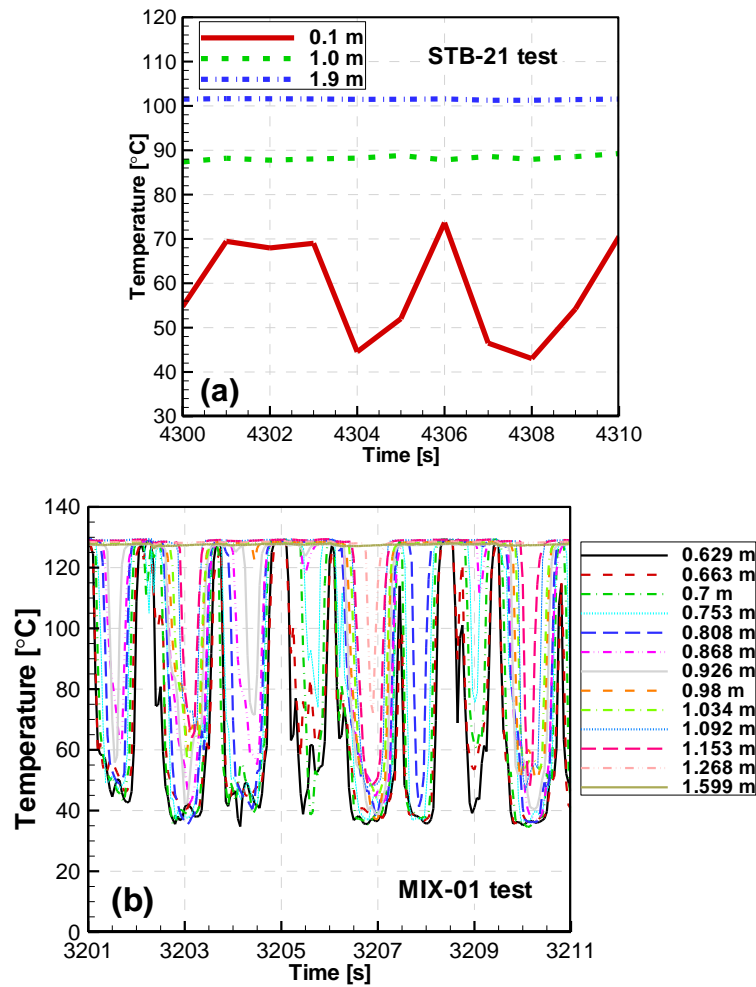


Figure 38: Improvement in space and time resolution of temperature measurements inside the blowdown pipe during the chugging regime in MIX-01 test as compared to STB-21 test [11, 14].

Table 1: Estimation of effective momentum given the frequency and amplitude of water level oscillations inside the blowdown pipe in STB-21 test.

Estimated frequency and amplitude of oscillations based on TC measurements in STB-21				Velocity based on synthetic jet theory and chosen momentum rates within the estimated range of velocity			
Time [s]	Period [s]	Frequency [Hz]	Amplitude [m]	Velocity [m/s]	Momentum rate [kg·m/s ²]		
					Case 1	Cases 2a, 2b	Case 3
4300-4400	2.5-3.3	0.303-0.4	0.1-1.0	0.043-0.57	0.066	10.32	11.5
4600-4700	4-5.6	0.18-0.25	1.9-3.8	0.48-1.36	8.43	54.4	67
4800-4850	2.5-3.3	0.3-0.4	1.9-3.8	0.81-2.18	23.4	151	171.5
4860-4880	2-3.1	0.33-0.5	1.9-3.8	0.88-2.73	27.55	177.7	268

4.2.2 EHS-EMS models validation and parametric studies

The scheme for modeling of POOLEX with EMS is shown in Figure 39a. The grid for pool tank is 48×114 and the vapor space is also modeled. The pumps are used to connect two vertically adjacent cells in the pool and impose the momentum. Since the outlet of the blowdown pipe is resolved with 4 cells, four pumps are needed on the corresponding cell surfaces as shown in Figure 39b. The heat loss through the bottom and side wall is modeled by two conductors. Effective Heat Source (EHS) model is involved by using thermal conductors on the submerged pipe surface. One 3D connector is used to model the open orifice on the top of tank.

As mentioned in the previous section, different momentum rates are chosen as momentum sources for the validation of EMS against the STB-21 test. Pump component is used to impose the effective momentum rates with actual input values of volumetric flow rates as shown in Figure 40 for the cases.

Figure 41 shows the comparison of different cases of EHS/EMS simulations against the STB-21 test (see Figure 36c). Case 1 (Figure 41a) corresponds to the minimum momentum rate with uniform heat flux on the pipe's submerged surface. Case 2a (Figure 41b) corresponds to a chosen momentum rate between the minimum and maximum values (as shown in Table 1) with also uniform heat flux on the pipe's submerged surface. Case 2b (Figure 41c) is the same as Case 2a except that the heat flux shifts from the pipe's submerged surface to the pipe's exit (as shown in Figure 36d). Lastly, Case 3 (Figure 41d) corresponds to the maximum momentum rate with uniform heat flux as in the other cases.

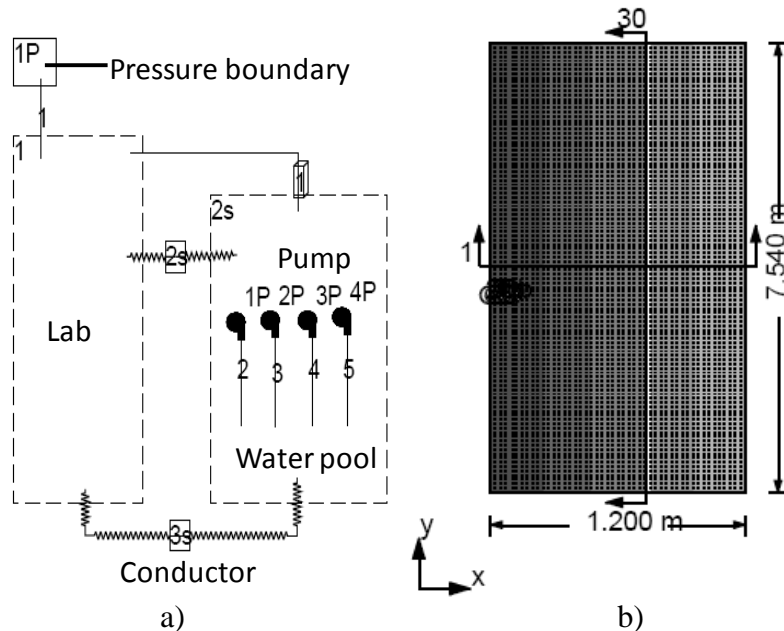


Figure 39: GOTHIC code model used for simulations with effective momentum simulated by pump. a) GOTHIC schematic diagram, b) grid resolution on XY plane.

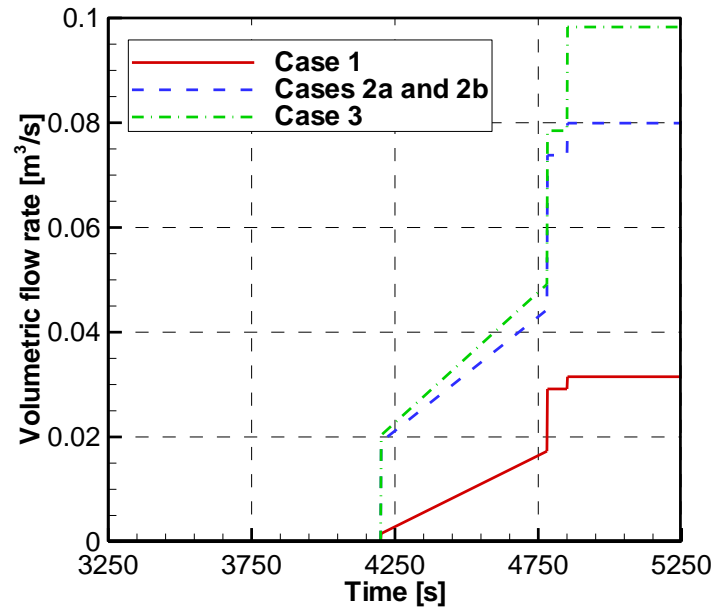


Figure 40: Input volumetric flow rates for the pump corresponding to different effective momentum rates as shown in Table 1.

In Case 1, a build-up of thermal stratification is also observed similar to the stratification phase in the experiment but in this case the stratification prolongs for another 500 s and the upper layer remains stratified with increasing temperature until the end. In Case 2a, a similar behavior to Case 1 is observed with the main difference of having a thinner layer at the top that remains stratified with increasing temperature. In these two cases, the temperature at the top layer increases significantly and does not mix with the pool which means that the heat source dominates over the momentum source. In Case 2b, however, when the heat flux at high flow rates is shifted from the pipe's submerged surface to the pipe's exit (where most heat releases occur due to significant contact condensation), the clockwise flow circulation in the pool due to buoyant plume directed upwards is counter-balanced by the momentum source causing a counter-clockwise flow circulation in the pool. Although the momentum source is the same as in Case 2a, complete mixing is observed in Case 2b as opposed to Case 2a. The time scale of mixing for Case 2b is about 600 s compared to about 550 s in the STB-21 experiment. With the maximum momentum rate and uniform heat flux, complete mixing is observed a bit later at about 950 s. This is mostly due to apparent higher resistance to mixing in the top of the stratified layer. However, mixing of the bottom layer occurs faster than in Case 2b with lesser momentum rate.

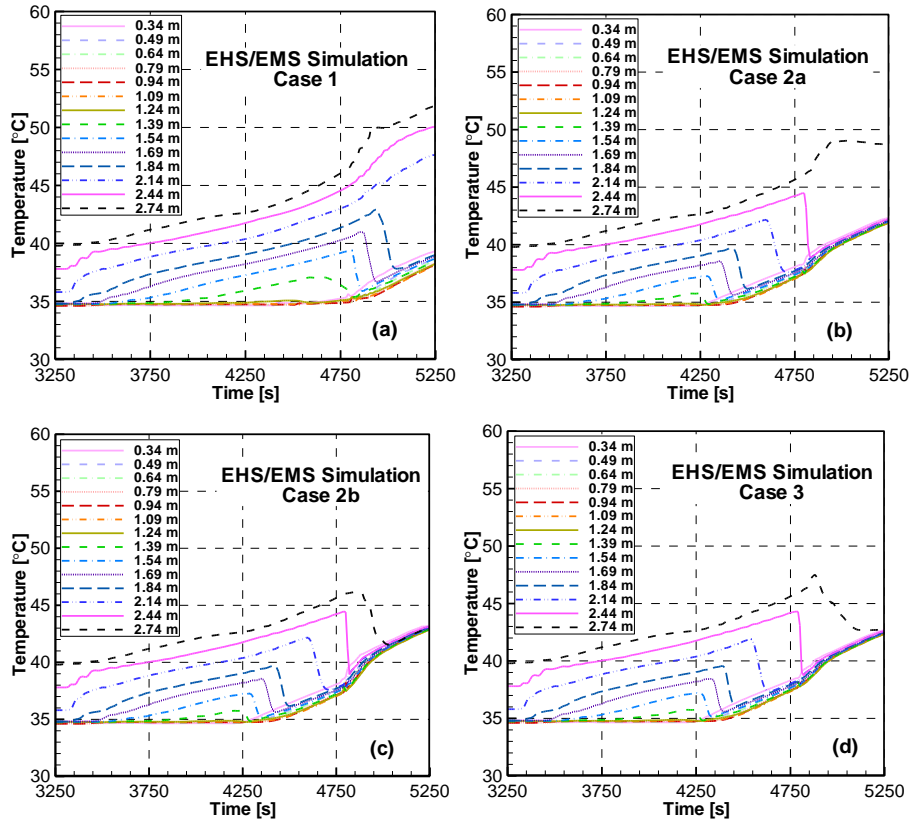


Figure 41: Comparison of different cases of EHS/EMS simulations, (a) Case 1 corresponds to the minimum momentum rate with uniform heat flux on the pipe's submerged surface, (b) Case 2a corresponds to a chosen momentum rate between the minimum and maximum values with also uniform heat flux on the pipe's submerged surface, (c) Case 2b is the same as Case 2a except that the heat flux shifts from the pipe's submerged surface to the pipe's exit, and (d) Case 3 corresponds to the maximum momentum rate with also uniform heat flux on the pipe's submerged surface.

Given the uncertainties in the input conditions, the above discussion demonstrates the robustness of the EHS and EMS models which captures interplay of competing effects, heat and momentum sources, and allows to get reasonable agreement with the experimental data. All results obtained with EHS/EMS are in fact not far off from reality. In the next section we discuss application of EHS-EMS models which yield even better predictions when experimental measurement uncertainties are significantly reduced.

4.2.3 Validation of EMS model based on analytical estimation of amplitude and frequency

Aya and Nariai have proposed an analytical model for the prediction of frequency and amplitude of oscillation in the blowdown pipe during steam injection [51]. The specific analytical model for chugging is included in their models. The velocity and momentum calculated based on the Aya and Nariai model and comparison to the momentum estimated by experimental data are summarized in Table 2.

Table 2: Comparison of amplitude and frequency calculated by the analytical model and estimated from the experimental measurements

Time (s)	Calculated Frequency and Amplitude with analytical Model for STB-21			Estimated Frequency and Amplitude from TC measurements in STB-21		
	Period (s)	Frequency (Hz)	Amplitude L (m)	Period (s)	Frequency (Hz)	Amplitude L (m)
4300-4400	0.152-0.34	6.6-2.9	0.1-0.99	2.5-3.3	0.303-0.4	0.1-1.0
4600-4700	1.05-1.414	0.95-0.71	1.94-3.79	4-5.6	0.18-0.25	1.9-3.8
4800-4850	0.403-0.56	2.48-1.79	1.97-3.78	2.5-3.3	0.3-0.4	1.9-3.8
4860-4880	0.381-0.55	2.62-1.82	1.91-3.79	2-3.1	0.33-0.5	1.9-3.8

In the analytical model, the parameter C is determined by the experiment and it depends on the steam injection conditions and pool condition. For STB-21, the parameter C is adjusted to match the maximum and minimum amplitude estimated by the experimental data.

As shown in the table, the difference of momentum between analytical value and experimental value is rather large. It is instructive to note that the analytical model is derived based on the experimental data from small scale facility with adiabatic drywell above the blowdown pipe. Further development of the analytical model for prediction of oscillation at larger scales (e.g. POOLEX facility and plant blowdown pipes) is necessary.

5 Validation of effective models against PPOOLEX tests

5.1 Validation of Effective Heat Source (EHS) model against PPOOLEX STR-03 test

Based on the measured steam mass flow rate in the inlet plenum and the pool bulk temperature, the condensation regime in STR-03 changed from region 1 (steam completely condensed inside the blowdown pipe) to region 5 (transition region), as shown in Figure 42. Although it passes through the chugging regime, the water level oscillations in the blowdown pipe were not apparent in the temperature measurements, as shown in Figure 43. A possible reason is that the oscillation amplitude is so small and the water-level is always below the thermocouples that are installed. Another possible reason is that only the hot condensates are involved in the chugging and this chugging cannot be detected by thermocouples. In any case, it is reasonable to assume that the momentum from the pipe outlet is negligible and only the effective heat source model can be used for simulation.

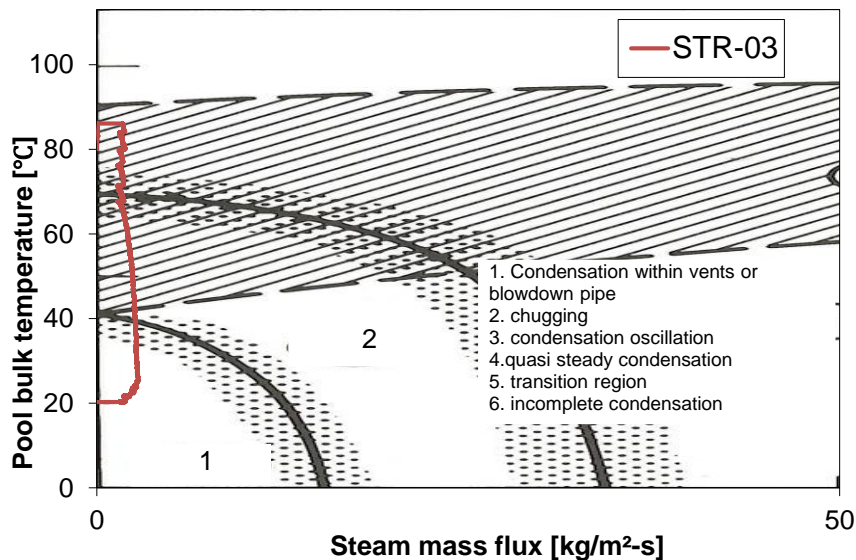


Figure 42: Condensation regime in STR-03 test.

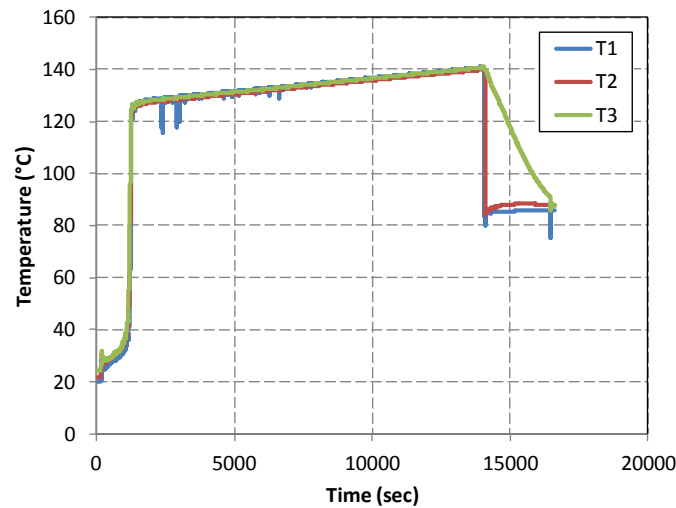


Figure 43: Temperature measured in the blowdown pipe [12].

As shown in Figure 15b, the first mixing was obtained during the first 1500 s that is attributed to the air clearing from the drywell to the wetwell. Then thermal stratification developed until about 14000 s in the upper part of the water pool in the wetwell. It can be seen that the upper part of the water pool was almost completely isothermal during the stratification development. This behavior is different to STB-20 where significant temperature gradients were observed in the pool. The temperature at T507 in STR-03 (below the level of the pipe's outlet) has also increased during the stratification development before 9000 seconds, while it is relatively constant at the beginning of stratification development in STB-20. The possible reason for such differences is that in STR-03, a higher steam mass flow rate, about 0.1 kg/s, is used from 3000 seconds. Most of the steam condensation with such injection flow rate occurs rather at the exit of the pipe, than on the surface of the pipe wall. If most of the heat is provided at the pipe exit, then the layer above the steam injection point will be isothermal. The layer below the pipe exit is heated due to the stronger convection at higher steam flow rate.

5.1.1 *GOTHIC modeling and assumptions*

In PPOOLEX tests, the steam mass flow rate is measured in the steam line, but not in the blowdown pipe. Before the steam is injected into the wetwell pool in PPOOLEX facility, part of the steam is condensed in the drywell. Thus, the actual steam mass flow rate through the blowdown pipe is unknown. This quantity is important for the EHS model since the effective heat source is calculated based on it. Since GOTHIC has models to simulate the steam condensation on the walls, it is possible to use GOTHIC lumped models to calculate the steam condensation rate in the drywell and the steam mass flow rate through the blowdown pipe. Therefore, a lumped simulation is performed first to obtain the needed boundary conditions for 2D simulation with the EHS model.

GOTHIC lumped model is shown in Figure 44. The drywell, wetwell, blowdown pipe and lab are all modeled with lumped volumes. The flow boundary, 1F, supplies the steam for injection into the drywell. The pressure, temperature, and steam mass flow rate measured in the experiment are input parameters in the corresponding flow boundaries. One pressure boundary, 2P, is used to keep a constant condition in the lab.

The lab temperature is not measured during the experiment, but here it is assumed to be 20 °C in all the STR tests.

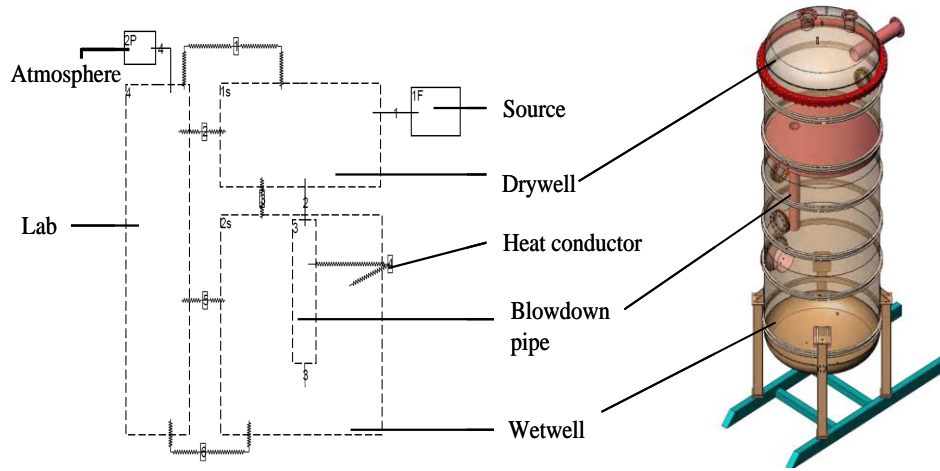


Figure 44: GOthic Lumped modeling (left) for PPOOLEX facility (right) [12].

The heat transfer through all the solid structures, for example, the intermediate floor between the drywell and wetwell, and the tank walls, are all modeled by thermal conductors. The initial temperatures for these conductors are taken from the experimental data.

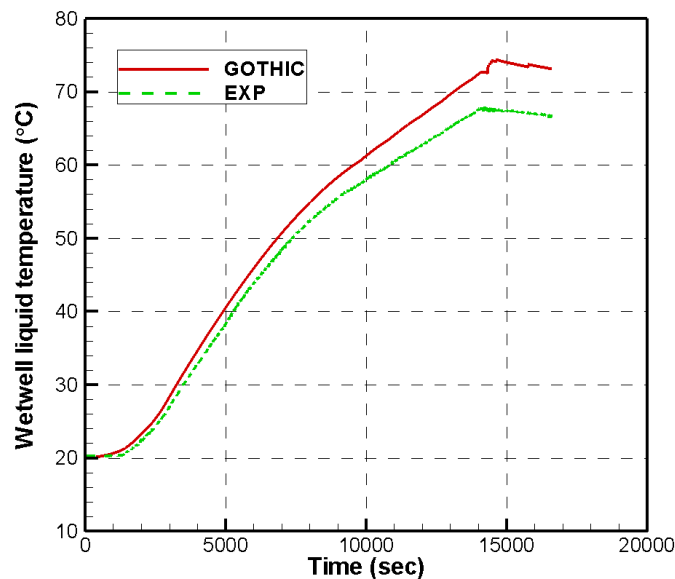


Figure 45: Comparison of predicted pool liquid temperature to averaged liquid temperature in the experiment.

The pool liquid temperature predicted by GOthic lumped model is compared to the averaged liquid temperature in the experiment. As shown in Figure 45, the pool temperature is over-predicted in the simulation, which can imply that more steam is injected into the wetwell through the blowdown pipe in the simulation than in the experiment. A possible reason is that the condensation rate in the drywell is under-predicted. Another possible reason is that the lumped model cannot predict thermal stratification. Further study will be performed to investigate this discrepancy.

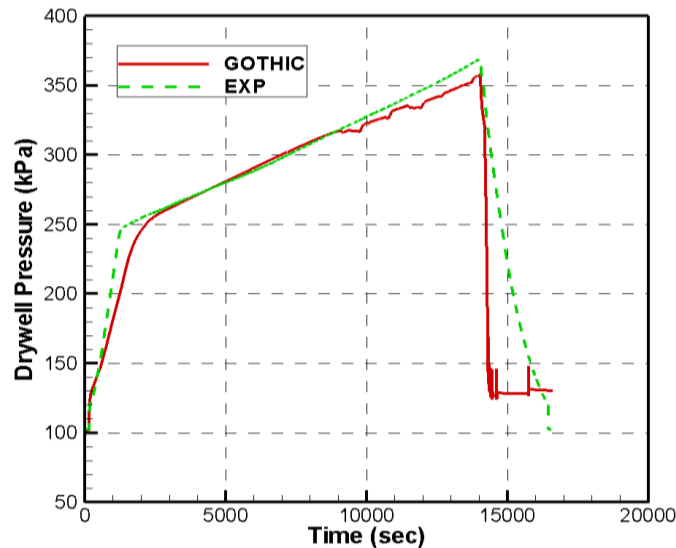


Figure 46: Comparison of drywell pressure predicted by GOTHIC simulation against experiment.

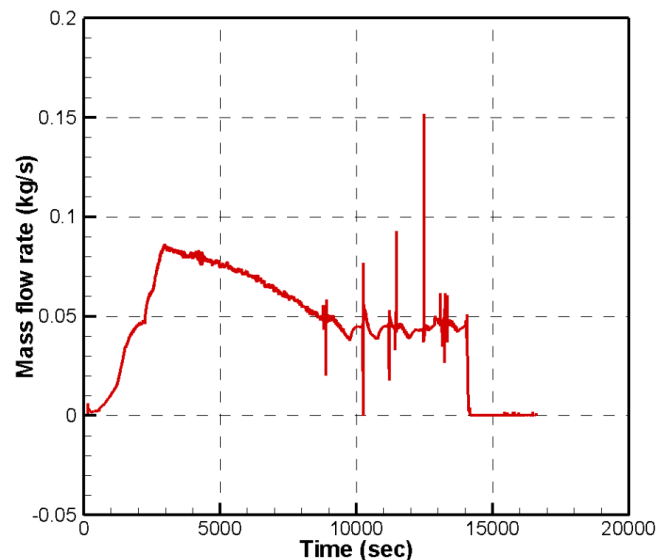


Figure 47: Calculated steam mass flow rate through the blowdown pipe from the GOTHIC lumped model.

The comparison of the predicted drywell pressure to the measured value in the experiment is shown in Figure 46. The first 1500 s in the experiment is the clearing phase, that is, when the air in the drywell is pushed into the wetwell. In the simulation, the clearing phase corresponds to the first 2500 s, during which the drywell pressure has increased from around 1 bar to 2.6 bars. The reason for this delay in the simulation is attributed to the deficiency of lumped modeling. With the lumped model, it is always assumed that the steam injected into the drywell is well-mixed with air remaining in the drywell. In reality, the air from the drywell is not completely mixed, especially at the beginning, and large portion of it is pushed by steam like a piston into the wetwell. This behavior can be resolved by using a 3D volume for the drywell. The part after 9000 seconds in the experiment has lower pressure than that in the simulation, because the temperature of pool surface with thermal stratification in the experiment is higher than in the simulation.

The steam mass flow rate through the blowdown pipe in the simulation is shown in Figure 47. Compared to the measured injected steam mass flow rate shown in Figure 15a, the calculated flow rate through the pipe is lower and has some jumps which are attributed to numerical instabilities. However, the averaged mass flow rate through the pipe is reasonable compared to the injected steam mass flow rate. In the 2D simulation with EHS model, it is assumed that all steam which flows into the blowdown pipe is completely condensed inside the pipe and only the hot condensates flows out. The momentum introduced by jumps of condensate flow rate in the calculation is assumed to have negligible effect on the thermal behavior in the pool. The effective heat source, $Q_{in} = G_s H_{latent}$, is calculated which is based on steam mass flow rate through the blowdown pipe. The value of heat source is shown in Figure 48. This effective heat source is used as an input in the 2D simulation discussed in the next section.

The GOTHIC 2D modeling is shown in Figure 49a while the grid resolution is shown in Figure 49b with grids 48×70 for the liquid part and 48×5 for the vapor part. Only the wetwell is modeled with a 2D volume and the rest is lumped. Four flow boundaries are used to supply the water source out of the blowdown pipe, since the diameter of the pipe is occupied by four cells. The lab is modeled with a large lumped volume connected to a pressure boundary with atmospheric conditions. Two thermal conductors are used to model the heat loss through the side wall and bottom of the wetwell. The heat transfer through the plate separating the wetwell and the drywell is obtained from the lumped simulation.

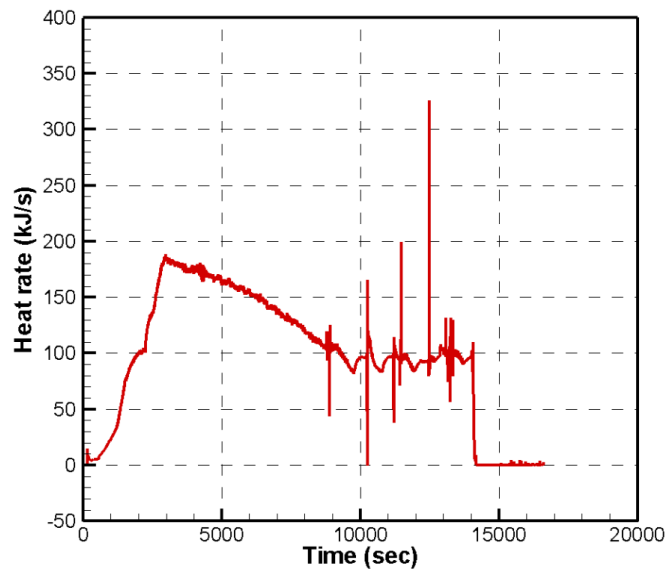


Figure 48: The effective heat source based on steam flow rate through the blowdown pipe.

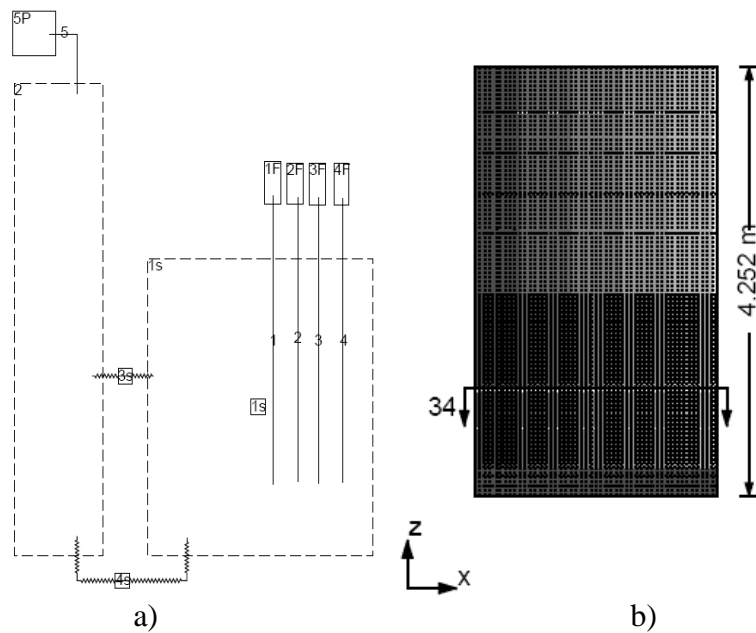


Figure 49: GOTHIC 2D modeling and grid resolution for wetwell.

The effective heat source calculated in lumped simulations is imposed on the thermal conductors in the blowdown pipe. Two distribution schemes are used in the simulation. In case 1, the heat source is uniformly distributed on the surface of submerged pipe part. It is assumed that all steam is condensed on the pipe walls. For case 2, the heat source is located at the end of the pipe. In this case, we assume that the steam is condensed near the end of the pipe on the free steam-water interface. For both cases, the bounded second order upwind difference scheme is used in the GOTHIC calculation.

5.1.2 Analysis of results

The predicted temperature of the pool in case 1 with uniformly distributed heat source on the surface of blowdown pipe is shown in Figure 50a. It can be seen that the thermal stratification is predicted in the simulation. Only the temperature in the part above the pipe outlet has increased during the transient while the remaining lower part is constant. Compared to the experimental data shown in Figure 50c, the temperature difference in the upper part of case 1 is higher and the top surface has a higher temperature at any given time. For example at 14000 s, the temperature difference in the upper layer is about 25 °C in case 1 with a peak temperature of about 106 °C while is about 5 °C in the experiment with a peak temperature of about 90 °C.

With case 2 where the heat source is located at the end of pipe, the temperature profile agrees better with the experimental data, as shown in Figure 50b. The predicted temperature of the upper part is almost mixed in the simulation. The temperature at the location of T507 has also increased in the simulation, which is similar to that in the experiment.

The comparison demonstrates that in STR-03, most of the steam has condensed close to the end of the blowdown pipe. It also implies that for different regimes, such as chugging and condensation oscillation, the heat source distribution on the pipe side and

bottom are different. In addition to the simple limiting cases we need more mechanistic approaches which would provide heat source distribution based on the distribution of steam condensation in the pipe.

It is noted that the mixing phase at the first hundreds of seconds is not well predicted because the momentum created by air injection in the clearing phase is not considered in the simulation. Generally, the air injection will cause a strong buoyancy force and will enhance mixing in the pool.

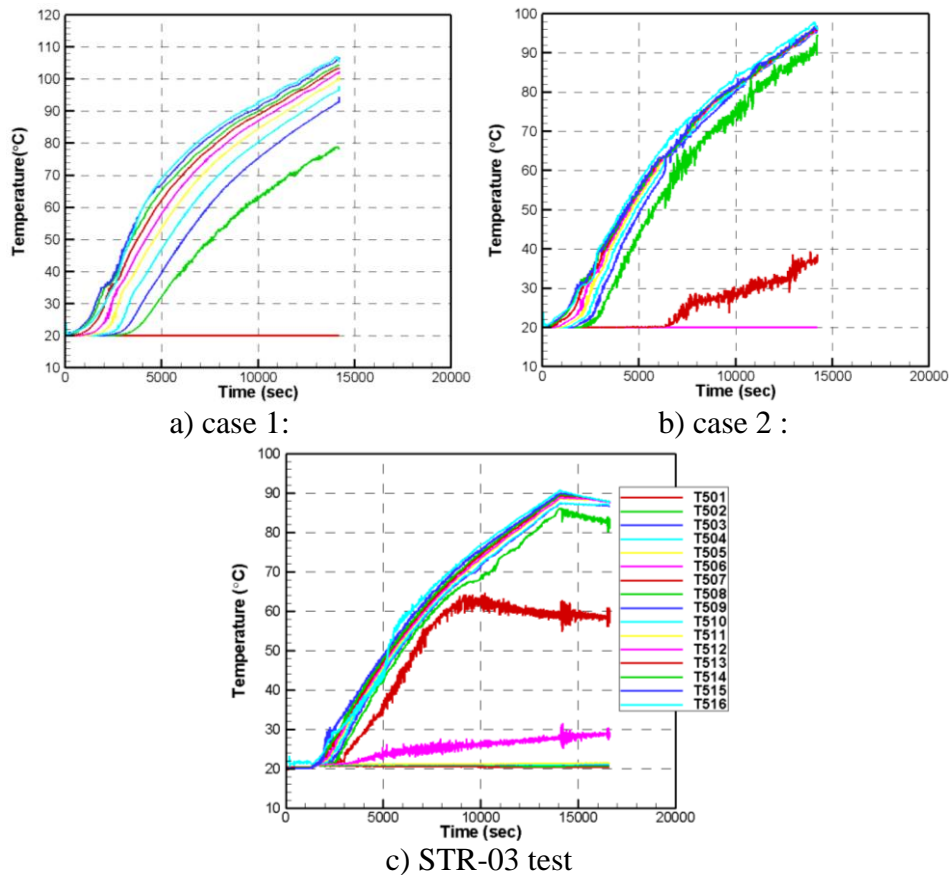


Figure 50: Pool temperature in a) case 1 with uniform heat source on the pipe surface, b) case 2 with heat source at the end of the pipe, c) measured data in test STR-03 [12].

5.2 Validation of EHS and EMS models against PPOOLEX MIX-01 to MIX-06 tests

The tests from MIX-01 to MIX-06 have a blowdown pipe with 214 mm in diameter. They consists mainly of three phases, namely, the clearing phase, stratification phase, and finally the mixing phase which are related to the steam flow rates. During the test, the steam mass flow rates are measured in the steam line and not in the inlet of the blowdown pipe. Thus, the measured steam flow rate is not necessarily the same as the steam flow rate from the drywell to the wetwell through the blowdown pipe. This is especially true during the clearing phase as the drywell is initially cold (about 14 - 28 °C) and filled with non-condensable gases. During the clearing phase, steam pushes all the non-condensable gases from the drywell to the wetwell first while steam condenses on the drywell walls and heats up the drywell compartment. For example, at ~200 g/s steam mass flow rate, a transient time of ~500 s (which is the time period that is set for

the clearing phase) is more than enough to push all the gas to the wetwell. After the clearing phase, it is expected that the steam flow rate in the steam line is almost the same as the steam flow rate to the wetwell and this is found in GOTHIC lumped simulations taking into account the insulated drywell.

For MIX-05 and MIX-06, there is a fourth phase, that is, re-development of thermal stratification, after a complete mixing phase. It is interesting to note that a redevelopment of thermal stratification happened even if the steam mass flow rate was kept the same. As the pool temperature is increasing, the condensation regime changes from chugging to the transition region where the oscillations are much weaker than in the chugging regime and thus unable to generate enough momentum to continuously mix the pool.

The GOTHIC model schematic for test MIX-01 to MIX-06 is similar, and shown in Figure 51a while the 48×75 mesh of the wetwell is shown in Figure 51b. The floor surface temperature of the drywell is measured during the experiment and this is used as boundary condition at the top of the wetwell. The thermal conductor is spanned on the pipe submerged surface to supply the heat source for thermal stratification phase. The heaters are used to supply the heat source when a large steam flow is used for injection. Flow boundaries inject the liquid for mass conservation and pumps are used to impose the momentum. Depending on the different test conditions during the MIX tests, the location of thermal conductors, heaters, flow path for boundaries and pumps are adjusted.

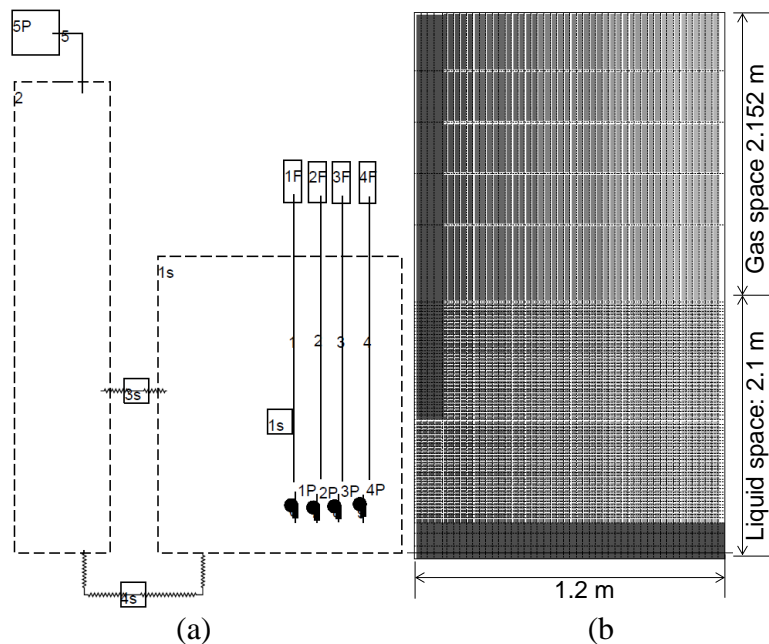


Figure 51: (a) GOTHIC model schematic of MIX-01, (b) corresponding 2D mesh with 48×75 for the wetwell.

In the MIX tests, more thermocouples are installed inside the blowdown pipe to monitor the water level change during the oscillation in the mixing phase. The measurement frequency is much higher (20 Hz) than before. Compared to the STB-21 test, the oscillation pattern inside the blowdown pipe can be well captured. Thus the estimation of the water level position inside the pipe is more accurate in MIX tests than in test STB-21 and STR tests

5.2.1 EHS/EMS validation against MIX-01 test

The steam mass flow rate from the inlet plenum measured in the experiment and estimated by the water level is shown in Figure 52. It should be noted from this point forward that the initial time $t = 0$ s in the simulations (as evident in succeeding figures) correspond to time 1100 s in Figure 52. The start of the mixing phase in the simulation is at time $t = 1573$ s. Figure 53 shows the effective momentum rates based on the water level oscillations in the pipe during the mixing phase in MIX-01 test. But briefly, the TC measurements are converted to water level positions then velocities can be calculated by taking time derivatives. Effective (jet) velocities are calculated based on the synthetic jet theory. Finally, effective momentum rates can be directly calculated. As shown in Figure 53, the non-constant momentum rates are between 12-21 kg·m/s² which are based on effective jet velocities between 0.59-0.77 m/s.

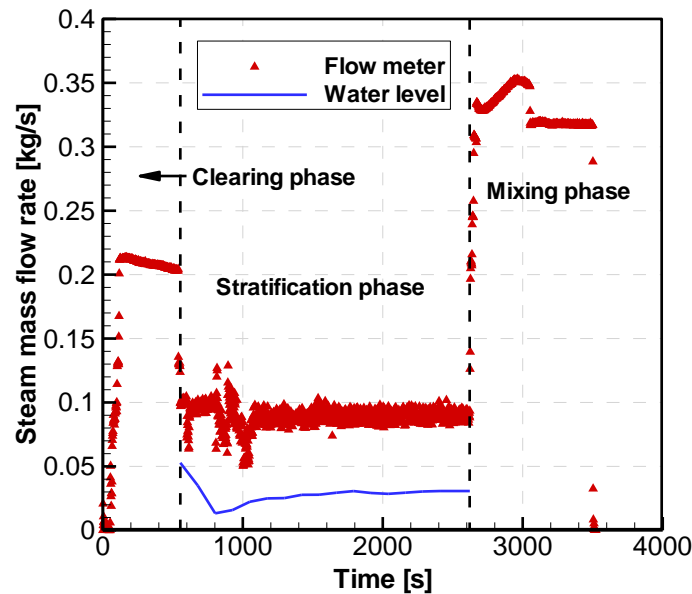


Figure 52: Measured steam mass flow rates with (i) flow meter and (ii) water level in the pool, during the MIX-01 experiment.

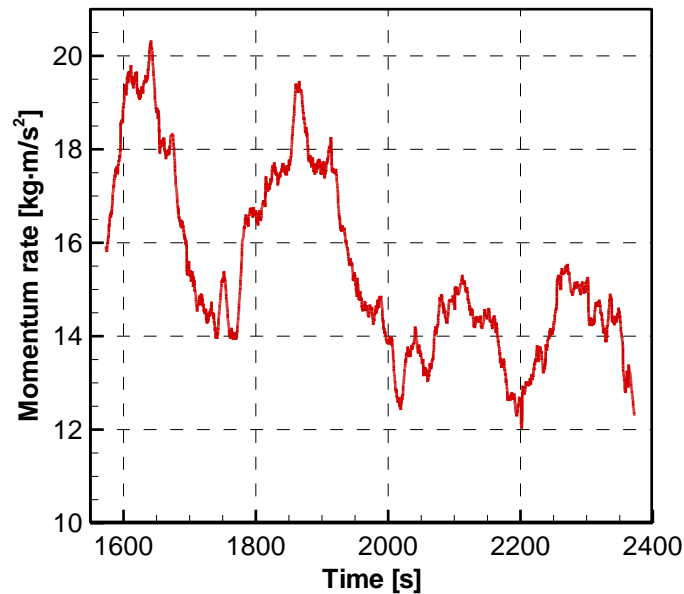


Figure 53: Effective momentum rates based on the water level oscillations in the pipe during the chugging (mixing) phase in MIX-01 test.

In the modeling of MIX-01, one thermal conductor is spanned on the pipe submerged surface from ~ 0.113 m above the pipe exit (see Figure 54) to supply the uniform-distributed heat source for the first thermal stratification phase, since it is observed in the test that the water level inside the pipe is around that level. Two heaters supply the heat source after the first stratification, since then all of the steam condensed out of the pipe in the test. One is located in the cell just below the pipe outlet (the first layer below the pipe outlet), and 0.1095 m from the pipe axial. Another one is just in another cell above it (as shown by red dots in Figure 54). There are four pumps located on four flow paths to impose the momentum from the cells right below the pipe outlet (represented by green dots in Figure 54). Four flow boundaries are used to impose the condensate and conserve the mass (blue dots in Figure 54). The clearing phase has resulted in complete mixing in the pool and has also generated a strong circulation flow that took time to stagnate, about ~ 600 s after the steam flow rate has been decreased. The EHS-EMS calculation only includes part of the thermal stratification and mixing phases and excludes the clearing phase as mentioned above. The calculation time is about 3 hours on 4 processors of an i7 3.4 GHz desktop.

In Figure 55a, the averaged liquid temperature in the pool predicted by the EHS-EMS simulation shows an excellent match against the MIX-01 data. At time $t = 0$ s, the averaged liquid temperature is about 16 °C and it increases to 19.5 °C during the stratification phase compared to 19.2 °C in the simulation. The increase in temperature is more pronounced during the mixing phase where it reaches 39.5 °C while the predicted temperature is 39 °C. Even the predicted increase in water level in the pool (see Figure 55b) shows an excellent match. The initial water level is at 2.11 m and during the stratification phase increases to only 2.12 m while the predicted water level is also at 2.12 m. And during the mixing phase, the water level shows an abrupt increase to 2.2 m while the predicted water level is 2.19 m. This also confirms that the heat losses through the wetwell walls are modeled properly.

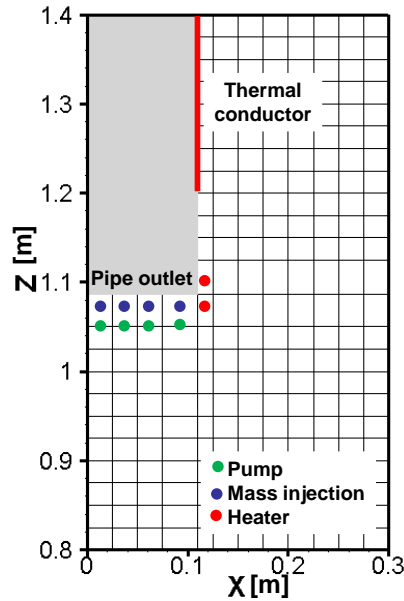


Figure 54: Configurations of components for EHS/EMS model for MIX-01.

Figure 56 shows the comparison in pool temperature between the MIX-01 measured data and EHS-EMS simulation. In general, the predicted pool temperature agrees very well with the measured data, except for the small fluctuations in the TC measurements. The development of thermal stratification in different layers is well captured in the simulation except for the small region in the vicinity of the pipe outlet (from heights of 1.16 m to 1.43 m) which is attributed to the uniform heat flux distribution assumed in the simulation. A non-uniform heat flux distribution due to non-uniform condensation inside the pipe is a subject for further study. In addition, the temperature behavior at the top layer of the wetwell pool (which is an important quantity in plant safety that can affect operator actions) is quite well predicted in the simulation. At the end of the stratification phase, the predicted temperature at the top layer is about 27 °C while the measured temperature is about 28 °C. As a result of higher steam flow rates and transition of the condensation regime to chugging, there is a strong circulation flow in the pool which leads to complete mixing. In the simulation, the time scale for mixing is about 200 s while in the MIX-01 experiment it is about 250 s. Part of the reason is the slight (~1 degree) under-prediction of temperature difference between the top and bottom layers at the end of the stratification phase. Another possible reason is the small overestimation of the momentum rate during the mixing phase.

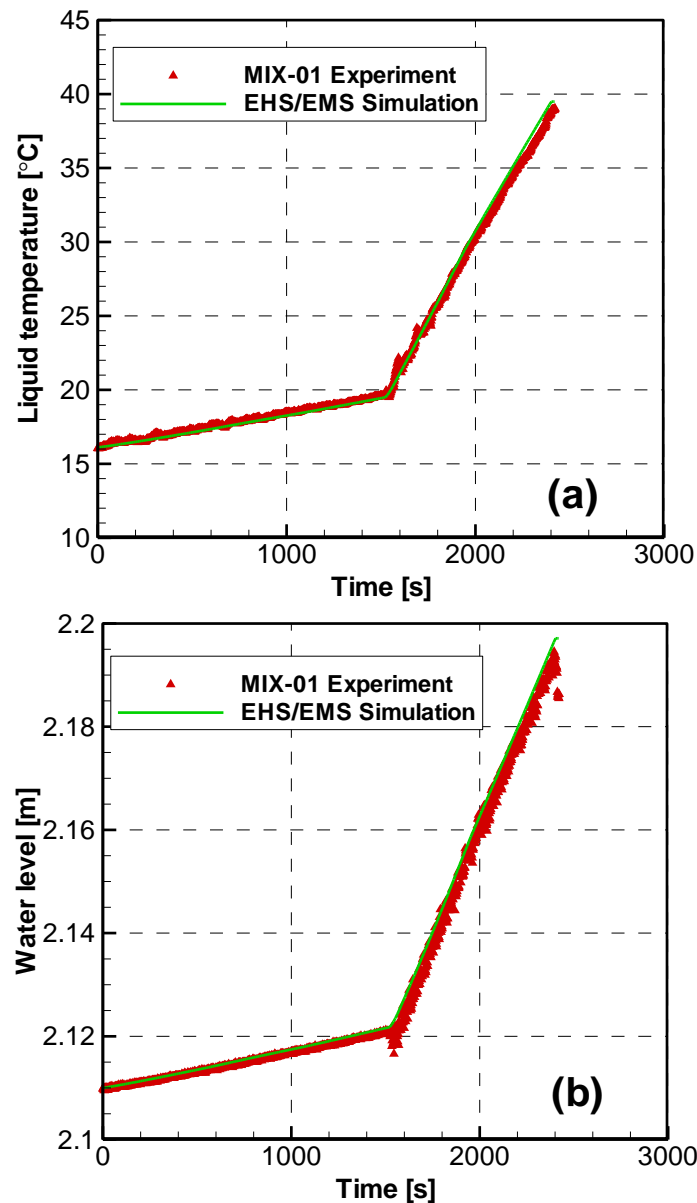


Figure 55: Comparison between EHS-EMS simulation results and MIX-01 test on (a) averaged liquid temperature and (b) water level in the wetwell pool.

A more detailed comparison of the temperature behavior in the pool is shown in Figure 57. In Figure 57a, the temperature profiles of the middle (about 0.48 m from the bottom) and bottom layers both in the EHS-EMS simulation and MIX-01 experiment are shown. In the simulation, the bottom of the tank is modeled as a flat plate to simplify implementation given that GOETHIC only supports Cartesian coordinate system. For the comparison, the corresponding locations of the bottom and middle layers are then adjusted accordingly. As can be seen in the figure, the bottom layers both in the simulation and experiment are higher than the middle layers. This is caused by the downward flow of heated water right from the blowdown pipe outlet (and can be clearly seen in Figure 58c). The temperature at the bottom layer though is 2-3 degrees higher in the simulation than in the experiment.

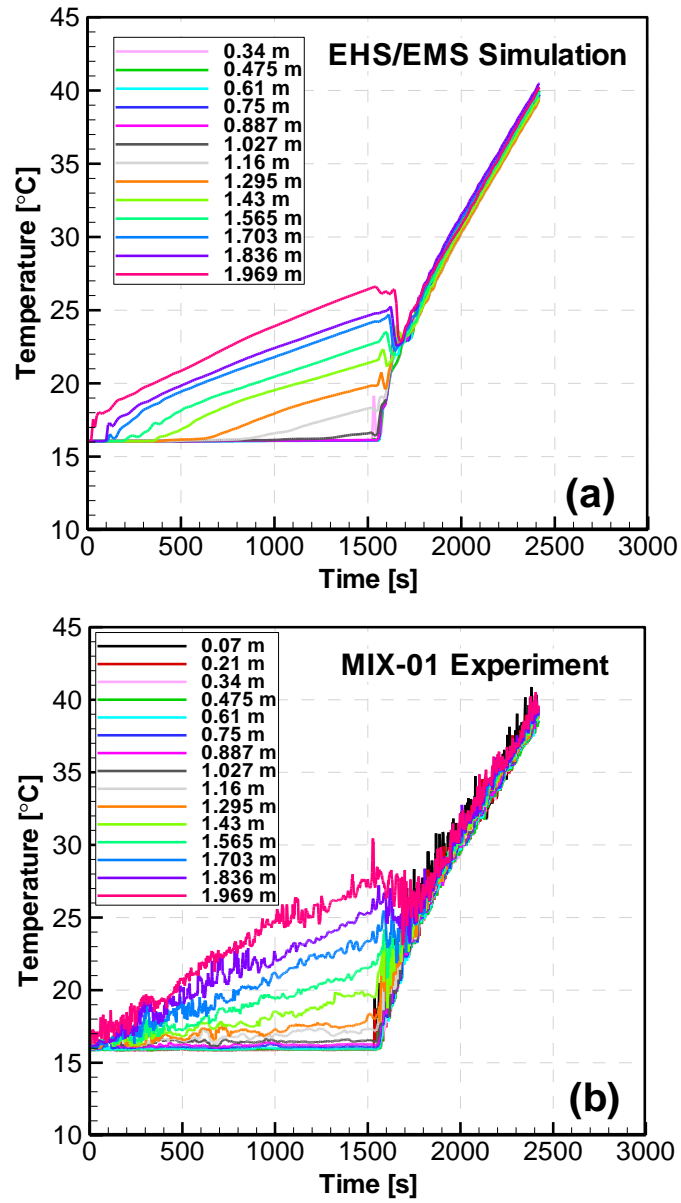


Figure 56: Comparison of pool temperature between (a) EHS-EMS simulation and (b) MIX-01 measured data. The level of the pipe outlet is at 1.045 m.

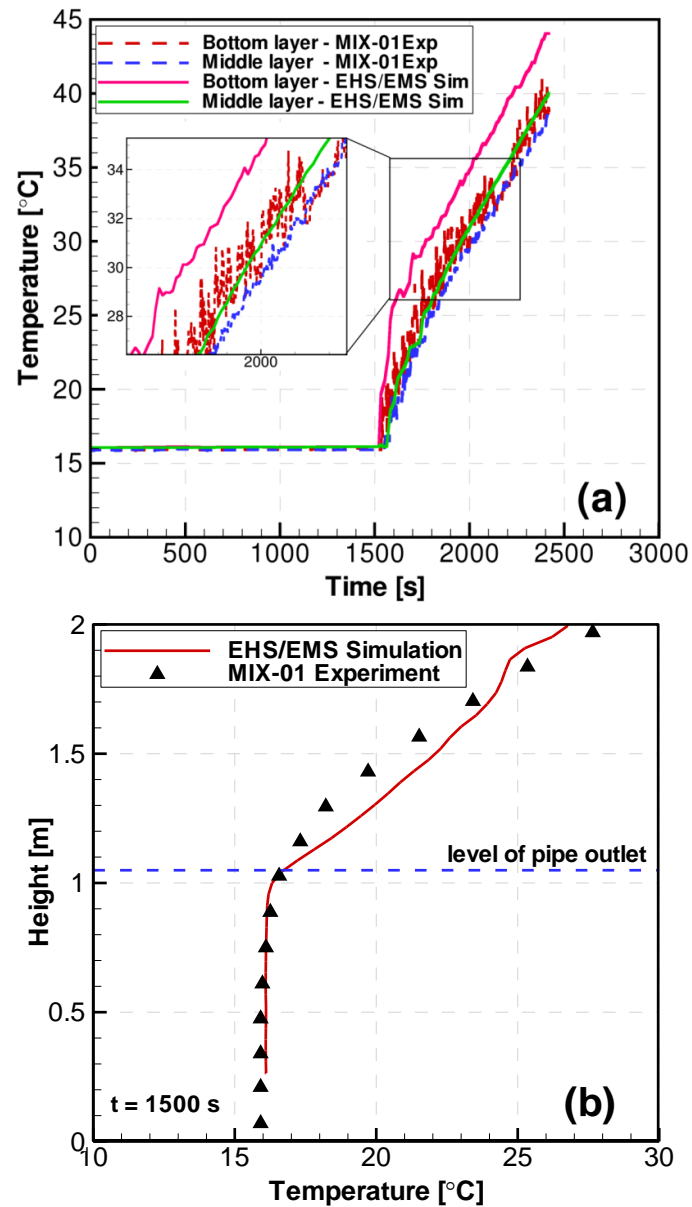


Figure 57: Comparison of pool temperature (a) at selected levels in the pool and (b) snapshot of vertical temperature profile at time $t = 1500$ s.

In Figure 57b, a snapshot of the vertical temperature profile near the end of the thermal stratification phase (at time $t = 1500$ s) is shown. Both the experiment and simulation shows that the layer below the pipe outlet remains cold (about 16 °C, same as initial) while the upper layer develops thermal stratification.

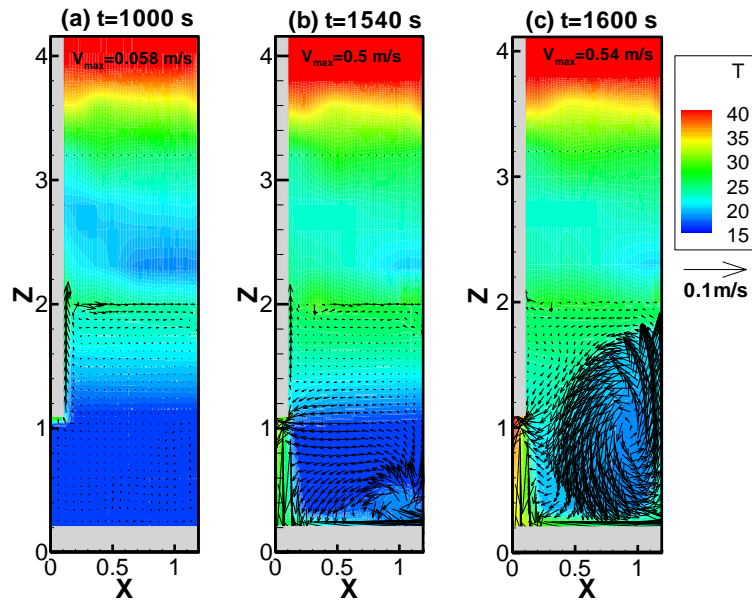


Figure 58: EHS-EMS simulation snapshots of temperature profiles with superimposed velocity fields at different times (a) $t = 1000$ s, during stratification phase, (b) $t = 1540$ s, early stage of mixing phase, and (c) $t = 1600$ s, during mixing phase.

Figure 58 shows snapshots of the predicted temperature and velocity profiles at different times $t = 1000$ s (stratification phase), $t = 1540$ s (early mixing phase), and $t = 1600$ s (mixing phase). At $t = 1000$ s, the upper layer develops a thermally stratified layer mainly due to the heating of the water surrounding the pipe creating a buoyant plume of hot water circulating in a clockwise manner, while the lower layer remains cold as mentioned earlier. The magnitude of the maximum velocity at this time is just 0.06 m/s. At $t = 1540$ s, the development of thermal stratification can still be observed but a jet directed downwards is clearly visible and the magnitude of the maximum velocity at this time has increased to about 0.46 m/s. During the mixing phase at $t = 1600$ s, the flow circulation changes to counter-clockwise manner due to the dominant effect of the jet from the pipe outlet. The magnitude of the maximum velocity at this time is also about 0.45 m/s. As mentioned earlier, the jet directed downwards transports hot water to the bottom layer which is also observed in the experiment.

5.2.2 EHS/EMS validation against MIX-02 test

As in MIX-01 test, the MIX-02 test also consists mainly of the clearing phase, stratification phase, and finally the mixing phase. The steam mass flow rate from the inlet plenum measured in the experiment and estimated by the water level is shown in Figure 59. The estimated flow rates during the stratification phase and the measured steam flow rates after this phase are then used as input for the EHS-EMS simulation.

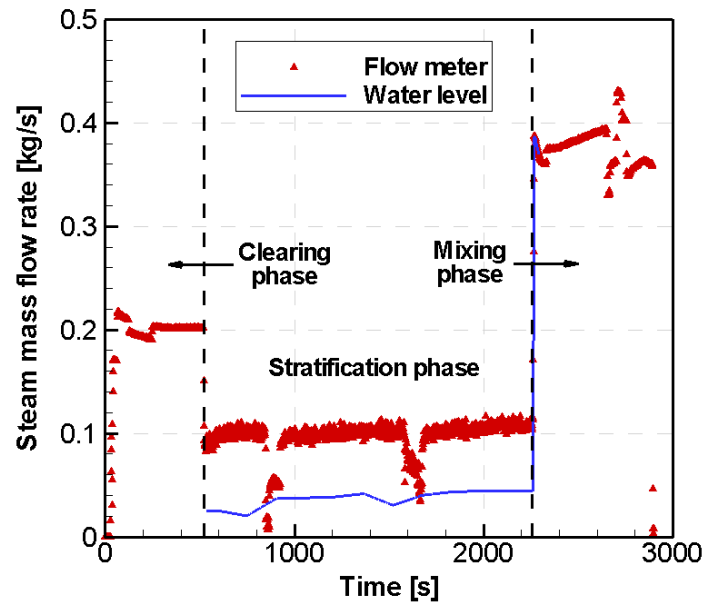


Figure 59: Measured steam mass flow rates with (i) flow meter and (ii) water level in the pool, during the MIX-02 experiment.

The clearing phase has resulted in complete mixing in the pool and has also generated a strong circulation flow that took about ~ 450 s to stagnate from the time the steam flow rate has been decreased. Thus, the initial time $t = 0$ s in the simulation corresponds to time 1000 s in Figure 59. The EHS-EMS calculation only includes part of the thermal stratification and mixing phases. The mixing phase starts at time $t = 1264$ s in the simulation. The effective momentum rates during the mixing phase in MIX-02 test is shown in Figure 60. The non-constant momentum rates are between 15 - 20 $\text{kg}\cdot\text{m}/\text{s}^2$ which are based on effective jet velocities between 0.66 - 0.8 m/s.

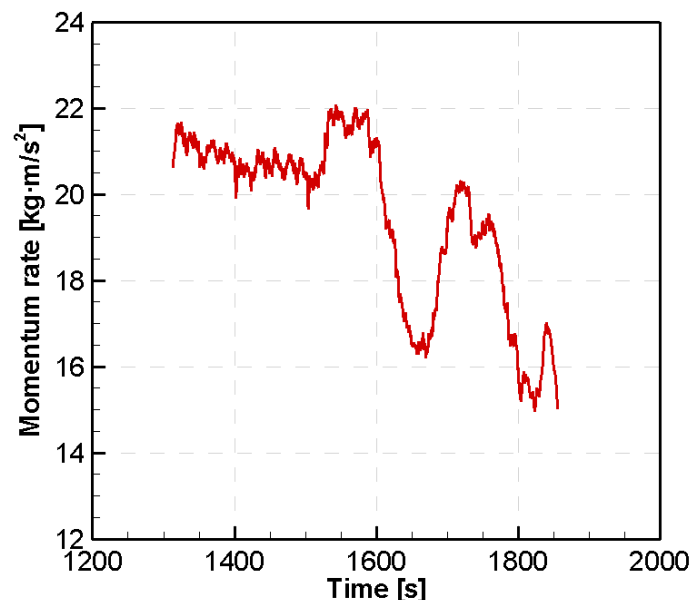


Figure 60: Effective momentum rates based on the water level oscillations in the pipe during the chugging (mixing) phase in MIX-02 test.

The configuration of thermal conductor, heaters, flow boundaries and pumps in the modeling of MIX-02, are the same as in MIX-01. The details are shown in Figure 61.

The heat rate on the thermal conductor and heaters, and pump speed is based on the steam latent heat and the momentum in MIX-02.

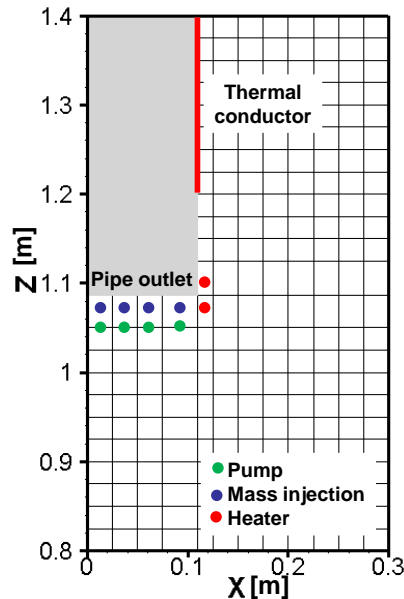


Figure 61: Configurations of components for EHS/EMS model for MIX-02.

The averaged liquid temperature in the pool predicted by the EHS-EMS simulation shows an excellent match against the MIX-02 data, which can be seen in Figure 62a. The averaged liquid temperature is about 16 °C at time $t = 0$ s, and it increases to 19 °C during the stratification phase compared to 19.5 °C in the simulation. At the end of the mixing phase, it reaches 34.9 °C in the test while the predicted temperature is 35 °C. The predicted increase in water level in the pool (see Figure 62b) also shows an excellent match. The initial water level is at 2.108 m and during the stratification phase increases to 2.121 m while the predicted water level is about at 2.119 m. And during the mixing phase, the water level shows an abrupt increase to 2.18 m while the predicted water level is also 2.18 m.

The comparison in pool temperature between the MIX-02 measured data and EHS-EMS simulation is shown in Figure 63. In general, the predicted pool temperature agrees very well with the measured data. The development of thermal stratification in different layers is well captured in the simulation except for the small region in the vicinity of the pipe outlet which may be attributed to the uniform heat flux distribution assumed in the simulation. There is a strong circulation flow in the pool during the chugging with high steam flow rate, and it leads to complete mixing. In the simulation, the time scale for mixing is about 100 s while in the MIX-02 experiment it is about 150 s. The experimental data shows unstable temperature in the free surface of the pool, which is not predicted in the simulation.

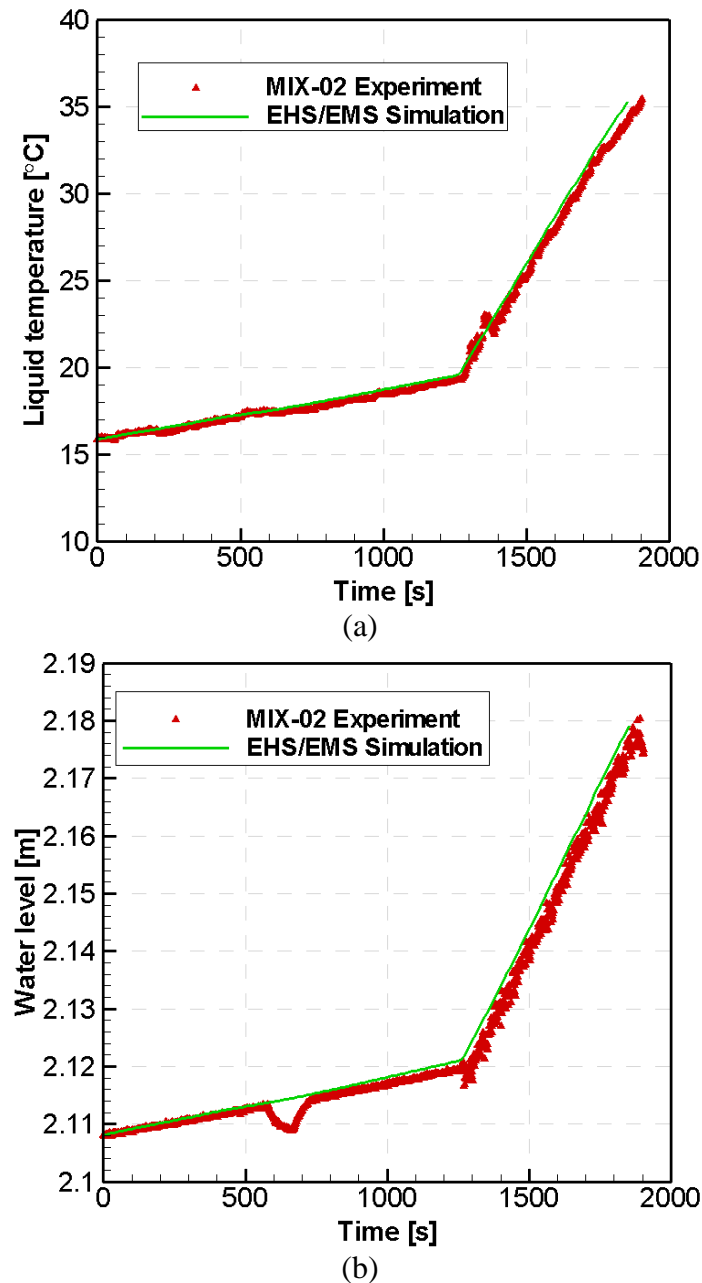
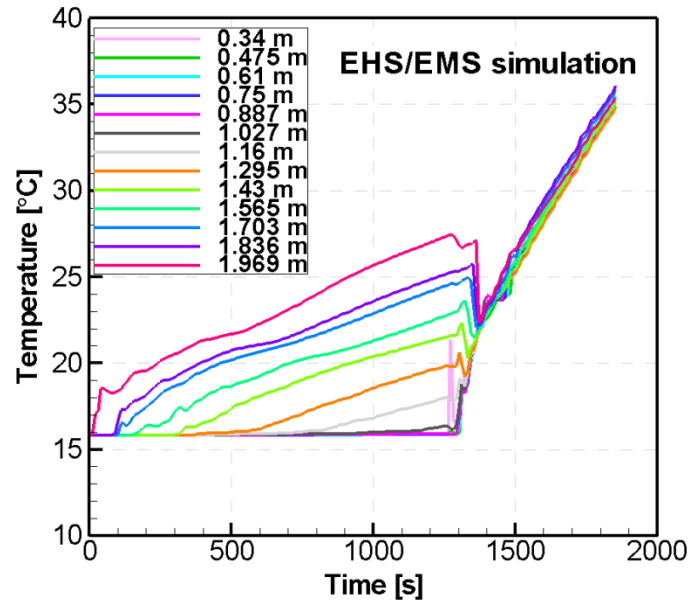
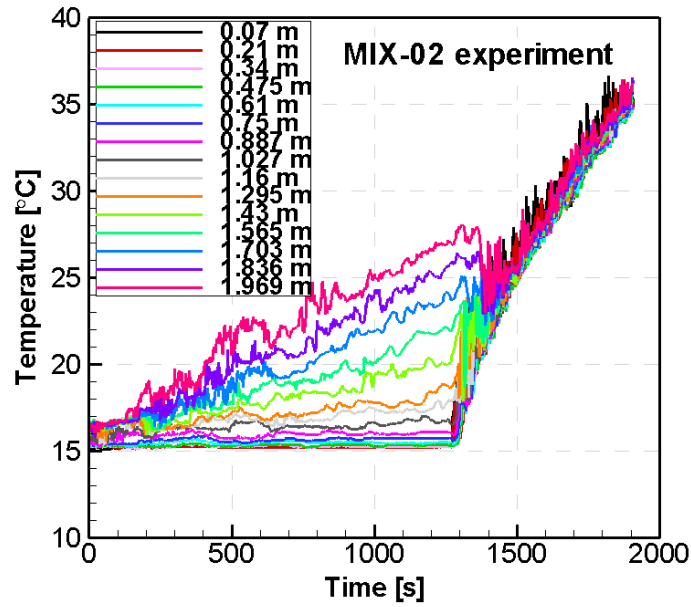


Figure 62: Comparison between EHS-EMS simulation results and MIX-02 test on (a) averaged liquid temperature and (b) water level in the wetwell pool.

Figure 64 shows a more detailed comparison of the temperature behavior in the pool. In Figure 65, a snapshot of the vertical temperature profile near the end of the thermal stratification phase (at time $t = 1200$ s) is shown. Both the experiment and simulation shows that the layer below the pipe outlet remains cold (about 15 °C, same as initial) while the upper layer develops thermal stratification. In the mixing phase, the temperature at the bottom layer both in the simulation and experiment are higher than the middle layers. This is caused by the downward flow of heated water right from the blowdown pipe outlet (and can be clearly seen in Figure 66 and Figure 67). The temperature at the bottom layer though is about 2-3 degrees higher in the simulation than in the experiment.



(a)



(b)

Figure 63: Comparison of pool temperature between (a) EHS-EMS simulation and (b) MIX-02 measured data. The level of the pipe outlet is at 1.045 m.

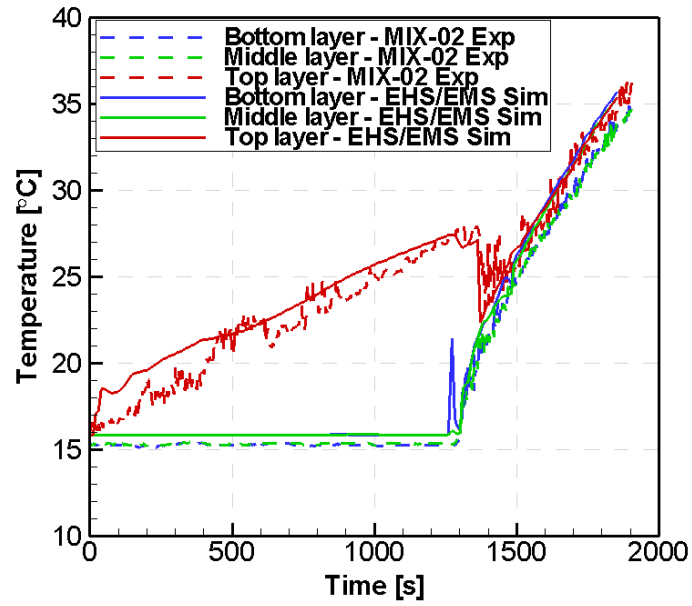


Figure 64: Comparison of pool temperature at selected levels in the pool.

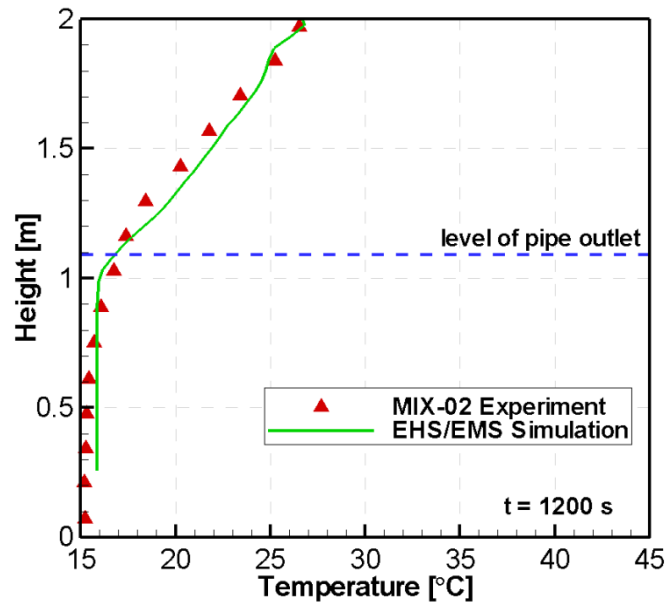


Figure 65: Comparison of vertical temperature profile at time t = 1200 s.

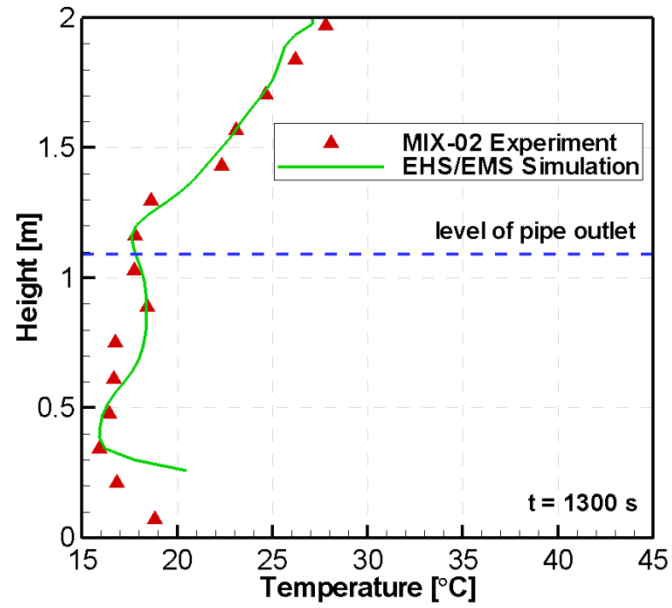


Figure 66: Comparison of vertical temperature profile at time $t = 1300$ s.

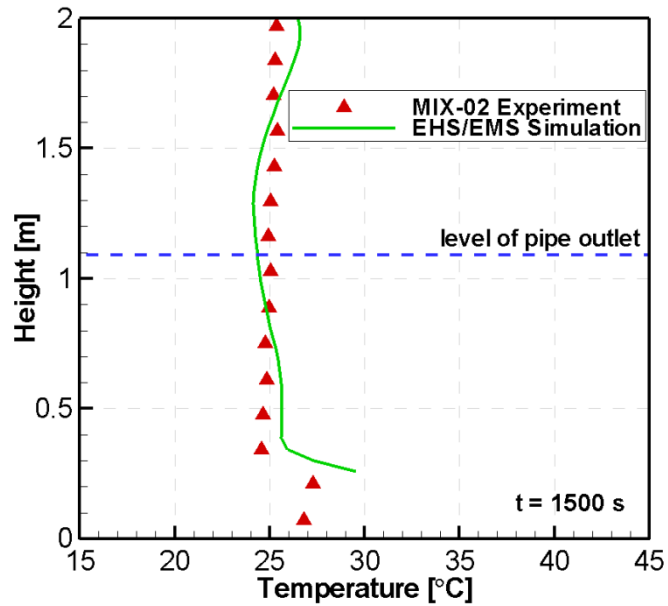


Figure 67: Comparison of vertical temperature profile at time $t = 1500$ s.

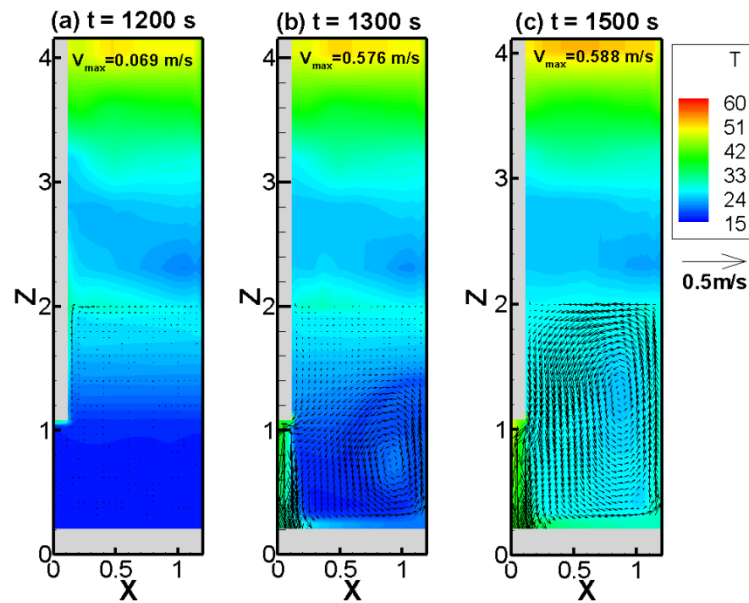


Figure 68: EHS-EMS simulation snapshots of temperature profiles with superimposed velocity fields at different times (a) $t = 1200$ s, during stratification phase, (b) $t = 1300$ s, early stage of mixing phase, and (c) $t = 1500$ s, during mixing phase.

The snapshots of the predicted temperature and velocity profiles at different times $t = 1200$ s (stratification phase), $t = 1300$ s (early mixing phase), and $t = 1500$ s (mixing phase) is shown in Figure 68. At $t = 1200$ s, the thermal stratification develops on the upper layers mainly due to the heating of the water surrounding the pipe creating a buoyant plume of hot water circulating in a clockwise manner, while the lower layer remains cold. The magnitude of the maximum velocity at this time is 0.069 m/s. At $t = 1300$ s, a jet directed downwards due to big momentum is clearly visible and the magnitude of the maximum velocity has increased to about 0.576 m/s. At $t = 1500$ s, the flow circulation changes to counter-clockwise manner due to the dominant effect of the jet from the pipe outlet. The magnitude of the maximum velocity is also about 0.588 m/s.

5.2.3 EHS/EMS validation against MIX-03 test

The steam mass flow rate from the inlet plenum measured in the test MIX-03 and estimated by the water level is shown in Figure 69. Compared to MIX-01 and MIX-02, the steam mass flow rate for both thermal stratification and mixing phase are relatively stable.

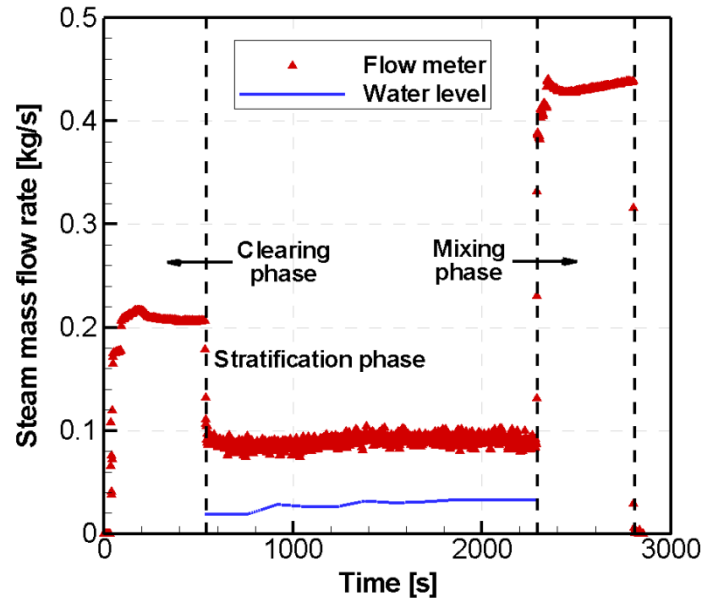


Figure 69: Measured steam mass flow rates with (i) flow meter and (ii) water level in the pool, during the MIX-03 experiment.

The initial time $t = 0$ s in the simulation corresponds to time 1000 s in Figure 69. The start of the mixing phase in the simulation is at time $t = 1288$ s. Figure 70 shows the effective momentum rates during the mixing phase in MIX-03 test. The momentum rates are between 16.5 - 25 $\text{kg}\cdot\text{m}/\text{s}^2$, and the effective jet velocities are between 0.71 - 0.85 m/s.

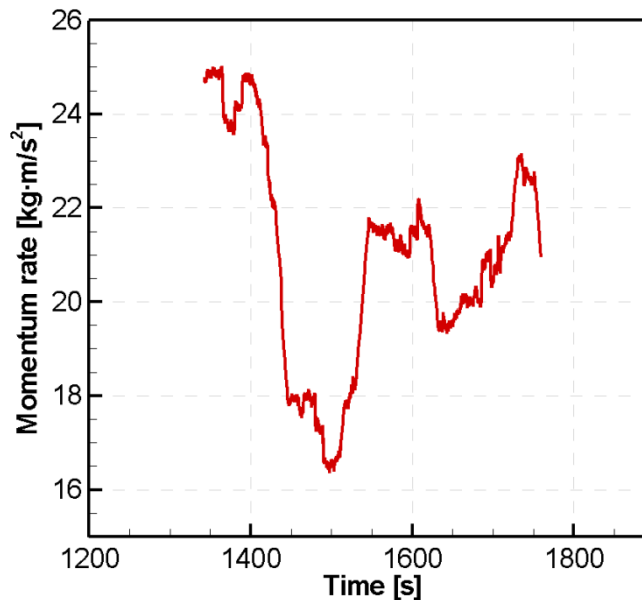


Figure 70: Effective momentum rates based on the water level oscillations in the pipe during the chugging (mixing) phase in MIX-03 test.

The details of configuration of thermal conductor, heaters, flow boundaries and pumps in the modeling of MIX-03 are shown in Figure 71. It is the same as in MIX-01 and MIX-02 tests.

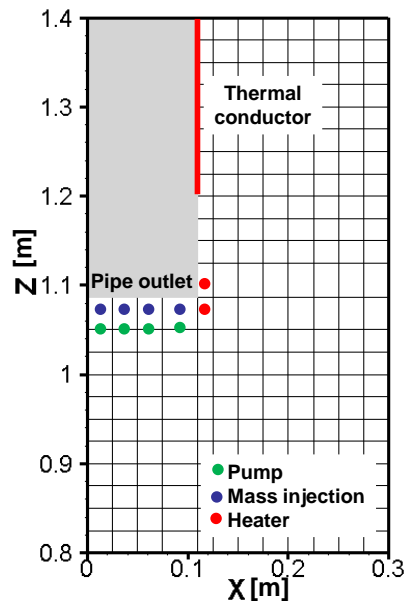


Figure 71: Configurations of components for EHS/EMS model for MIX-03.

In Figure 72a, the averaged liquid temperature in the pool predicted by the EHS-EMS simulation shows an excellent agreement with the MIX-03 data. At time $t = 0$ s, the averaged liquid temperature is about $16\text{ }^{\circ}\text{C}$. At the end of the development of stratification, it increases to $17\text{ }^{\circ}\text{C}$ in the test, and $17.5\text{ }^{\circ}\text{C}$ in the simulation. It reaches $34\text{ }^{\circ}\text{C}$ at the end of the mixing in the test, while the predicted temperature is $33\text{ }^{\circ}\text{C}$ at the end of the simulation earlier than the transient end. A good agreement in the water level in the pool between the test and simulation is shown in Figure 72b. The water level increases from 2.112 m to only 2.12 m for stratification phase. And during the mixing phase, the water level increase to 2.175 m .

Figure 73 also shows the good agreement in pool temperature between the MIX-03 measured data and EHS-EMS simulation. The uniform heat flux distribution assumed in the simulation may cause the difference on the temperature at the top layer of the wetwell pool. At the end of the stratification phase, the predicted temperature at the top layer is about $25.5\text{ }^{\circ}\text{C}$ while the measured temperature is about $27\text{ }^{\circ}\text{C}$. For mixing phase with high steam flow rate, the time scale for mixing is about 80 s in the simulation while in the MIX-03 experiment it is about 130 s . Part of the reason is the slight (~ 1.5 degree) under-prediction of temperature difference between the top and bottom layers at the end of the stratification phase.

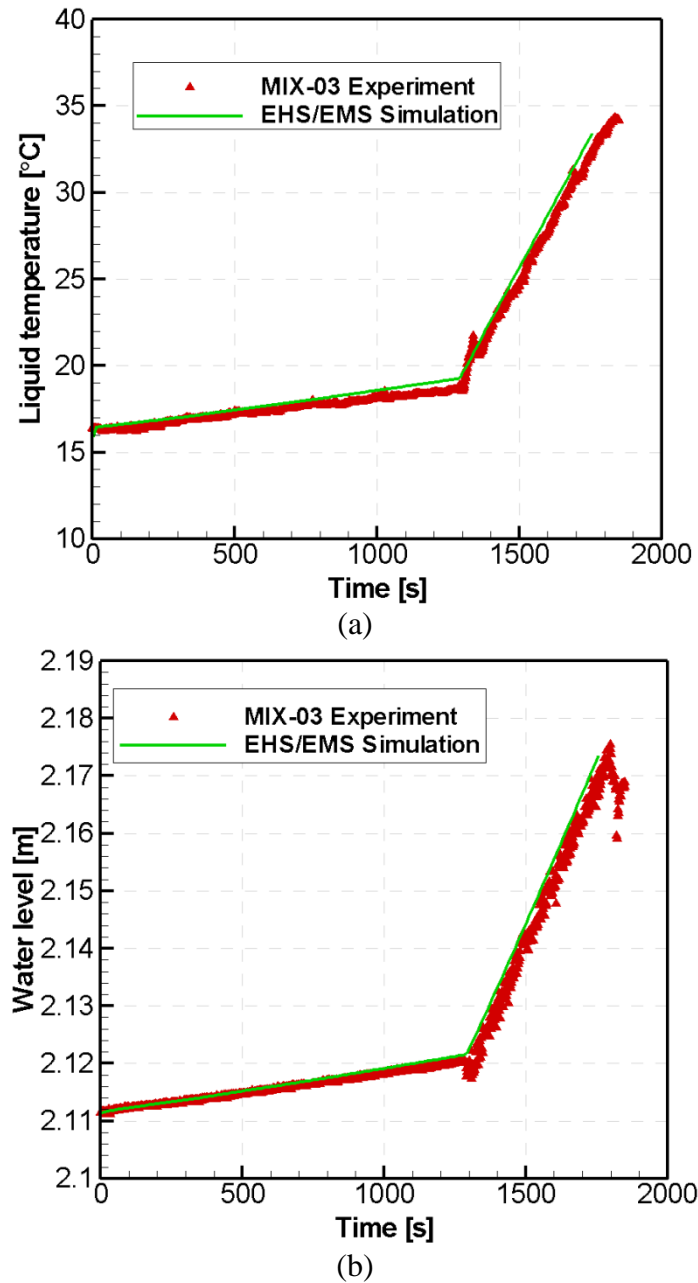
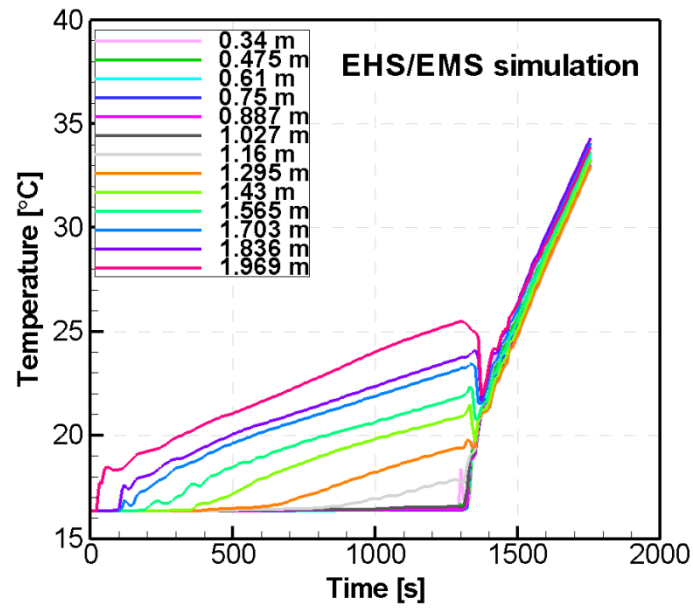
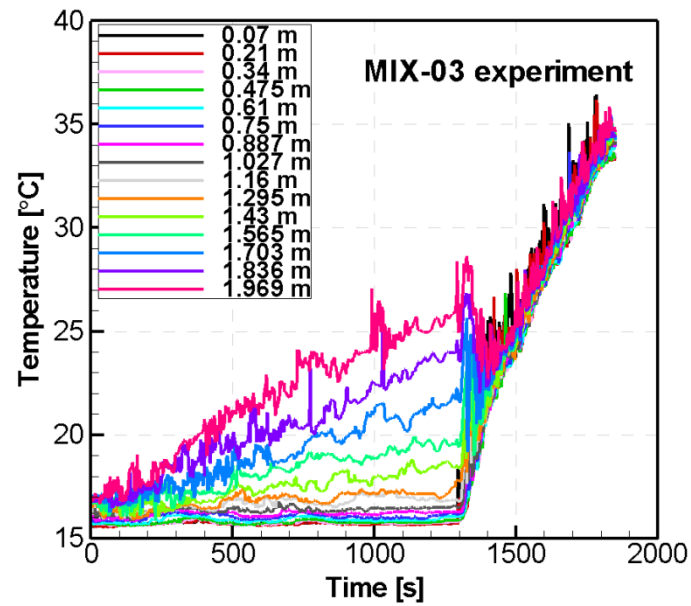


Figure 72: Comparison between EHS-EMS simulation results and MIX-03 test on (a) averaged liquid temperature and (b) water level in the wetwell pool.

A more detailed comparison of the temperature behavior in the pool is shown in Figure 74. As can be seen in the figure, the bottom layer in the simulation is initially higher than experiment. In Figure 75, a snapshot of the vertical temperature profile near the end of the thermal stratification phase (at time $t = 1200$ s) is shown. Both the experiment and simulation shows that the layer below the pipe outlet remains cold at about 16 °C while the upper layer develops thermal stratification. In the mixing phase as shown in Figure 76 and Figure 77, the temperature at the bottom layer both in the simulation and experiment are higher than the middle layers. This is caused by the downward flow of heated water right from the blowdown pipe outlet.



(a)



(b)

Figure 73: Comparison of pool temperature between (a) EHS-EMS simulation and (b) MIX-03 measured data. The level of the pipe outlet is at 1.045 m.

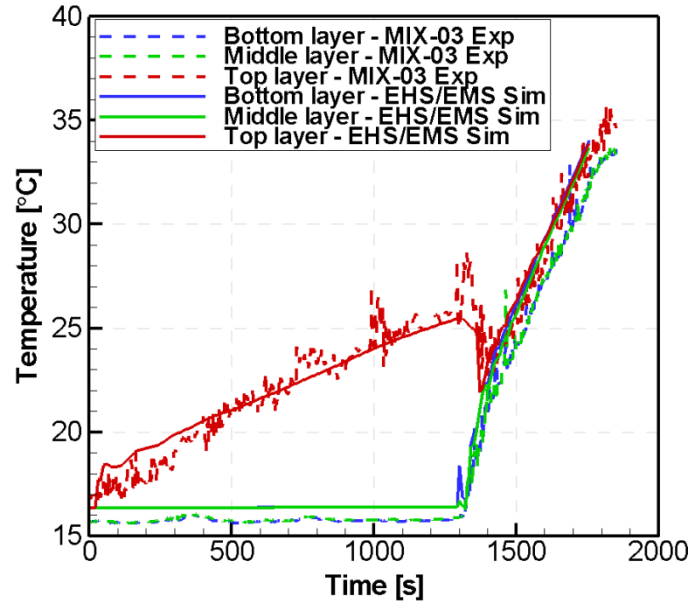


Figure 74: Comparison of pool temperature at selected levels in the pool.

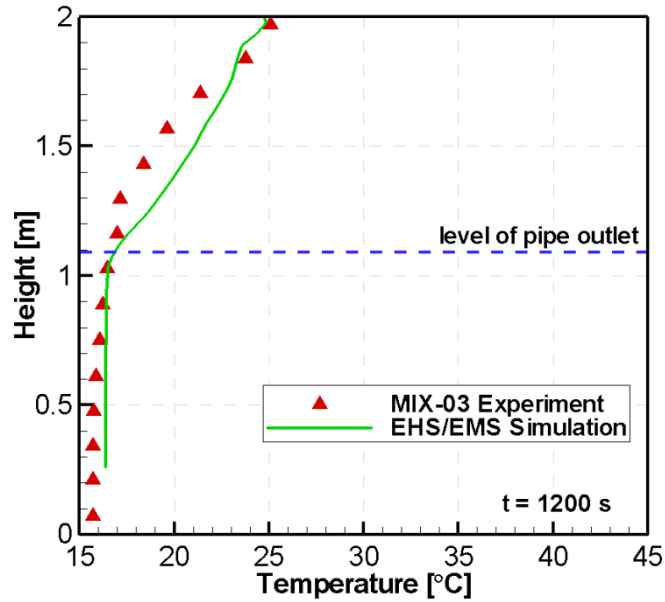
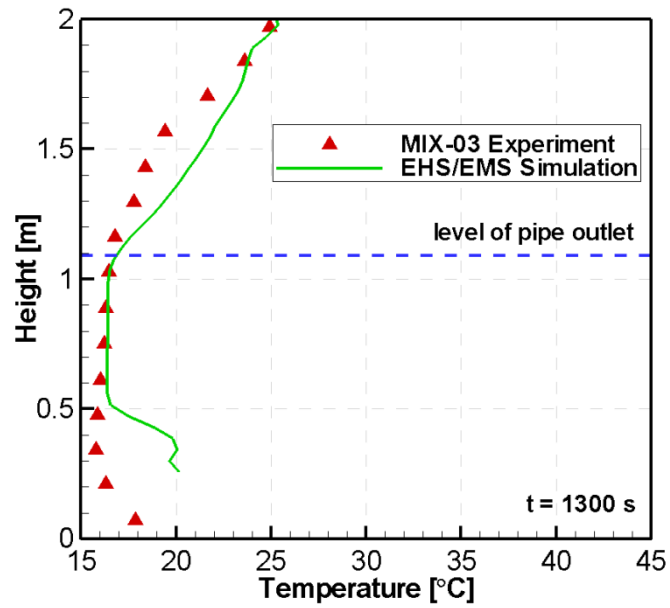
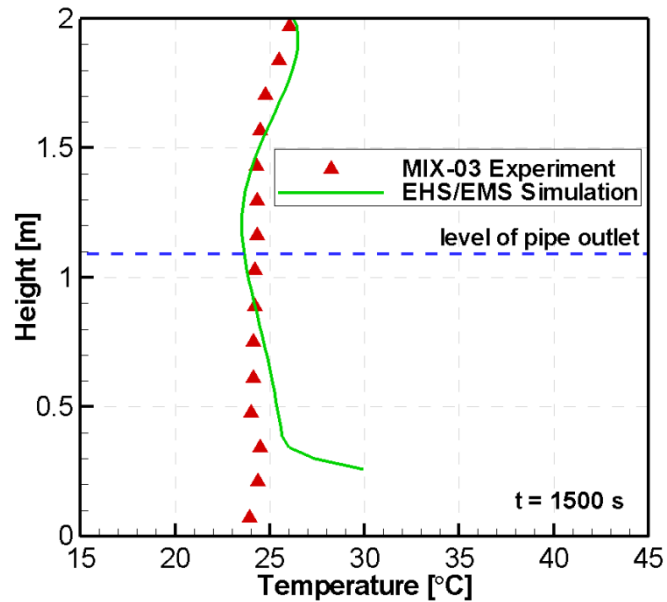


Figure 75: Comparison of vertical temperature profile at time $t = 1200$ s.

Figure 76: Comparison of vertical temperature profile at time $t = 1300$ s.Figure 77: Comparison of vertical temperature profile at time $t = 1500$ s.

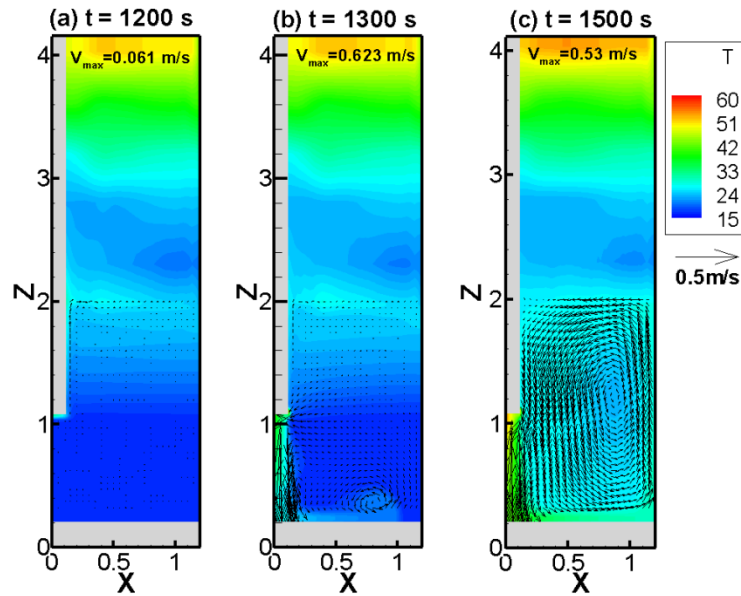


Figure 78: EHS-EMS simulation snapshots of temperature profiles with superimposed velocity fields at different times (a) $t = 1200$ s, during stratification phase, (b) $t = 1300$ s, early stage of mixing phase, and (c) $t = 1500$ s, during mixing phase.

The thermal behavior and velocity profiles at different times $t = 1200$ s (stratification phase), $t = 1300$ s (early mixing phase), and $t = 1500$ s (mixing phase) is shown in Figure 78. Similar to MIX-01 and MIX-02 tests, the upper layer develops a thermally stratified layer mainly due to a buoyant plume of hot water, while the lower layer remains cold. At $t = 1300$ s, the flow circulation changes to counter-clockwise manner and starts to break the stratification, due to the dominant effect of the jet from the pipe outlet. The magnitude of the maximum velocity is just 0.061 m/s at $t = 1200$ s, but 0.623 m/s at $t = 1300$ s and 0.53 m/s at $t = 1500$ s.

5.2.4 EHS/EMS validation against MIX-04 test

The MIX-04 test has similar procedure as in previous MIX tests. The steam mass flow rate from the inlet plenum is shown in Figure 79. The steam mass flow rate for mixing is around 325 g/s. The estimated flow rates during the stratification and mixing phases are then used for the EHS-EMS simulation.

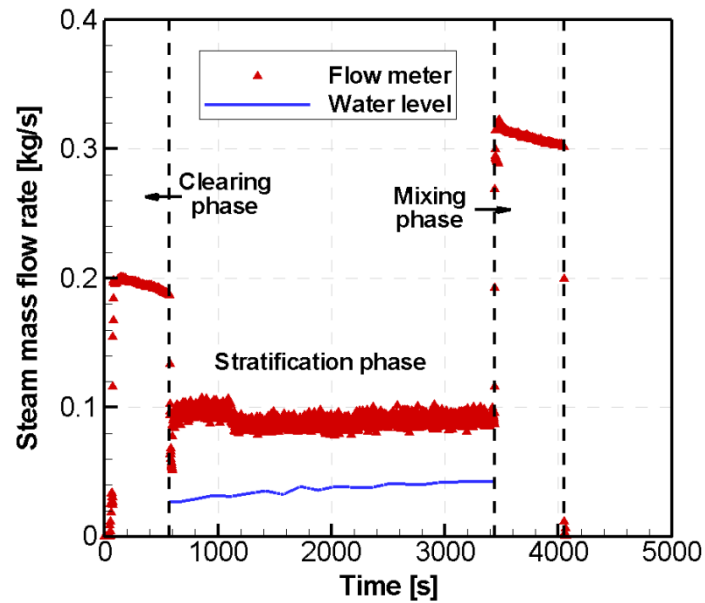


Figure 79: Measured steam mass flow rates with (i) flow meter and (ii) water level in the pool, during the MIX-04 experiment.

The initial time $t = 0$ s in the simulation of MIX-04 corresponds to time 1000 s in Figure 79. The mixing phase starts at time $t = 2441$ s in the simulation. Effective momentum rates during the mixing phase are between 10.5 - 17.2 $\text{kg}\cdot\text{m}/\text{s}^2$, as shown in Figure 80.

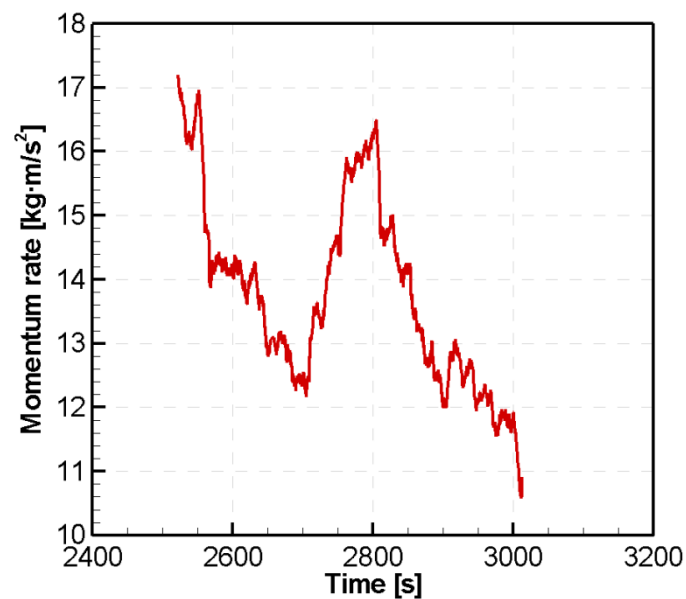


Figure 80: Effective momentum rates based on the water level oscillations in the pipe during the chugging (mixing) phase in MIX-04 test.

The location of thermal conductor, heaters, flow boundaries and pumps are shown in Figure 81, which is the same as in MIX-01 to MIX-03.

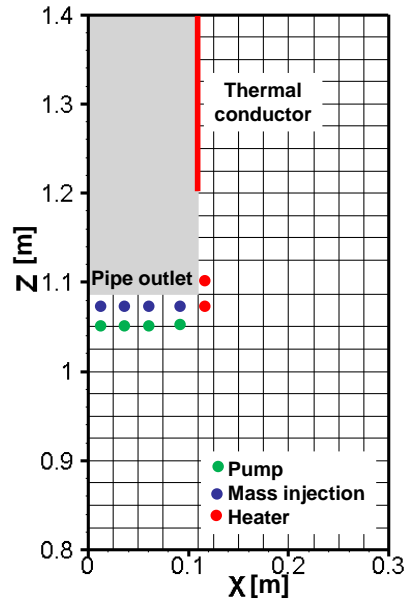


Figure 81: Configurations of components for EHS/EMS model in MIX-04.

The averaged liquid temperature and water level in the pool predicted by the EHS-EMS simulation shows an excellent match against the MIX-04 data, as shown in Figure 82. The averaged liquid temperature increases from 18 °C to about 37.5 °C both in the experiment and simulation. The initial water level is at 2.114 m and during the stratification phase increases to only 2.135 m while the predicted water level is about at 2.137 m. And during the mixing phase, the water level shows an abrupt increase to 2.185 m while the predicted water level is 2.18 m.

The comparison in pool temperature between the MIX-04 measured data and EHS-EMS simulation is shown in Figure 83. The development of thermal stratification in different layers is well captured in the simulation. At the end of the stratification phase, the predicted temperature at the top layer is about 35 °C while the measured temperature is about 36.5 °C. It is due to the uniform heat flux distribution assumed in the simulation. In the simulation, the time scale for mixing is about 250 s while in the MIX-04 experiment it is about 300 s, which is similar to other MIX tests.

A more detailed comparison of the temperature behavior in the pool is shown in Figure 84. There is a slight difference between the experimental data and simulation results. The time scale for the mixing phase is so close in the simulation and experiment.

In Figure 85, Figure 86, and Figure 87, a snapshot of the vertical temperature profile at different phase ($t = 2000$ s, $t = 2500$ s, $t = 3000$ s) are shown. The quantitative comparison between the experimental data and simulation results can be seen clearly. The reason for temperature profile at $t = 2500$ s is currently being investigated.

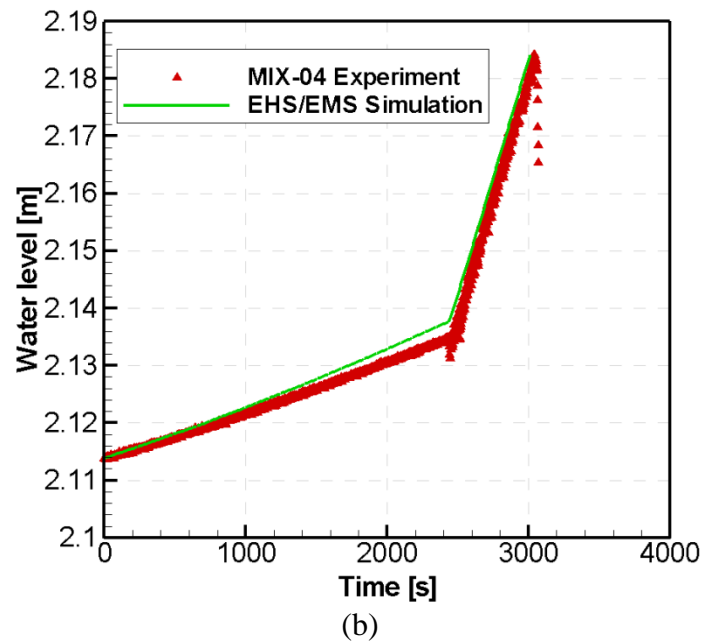
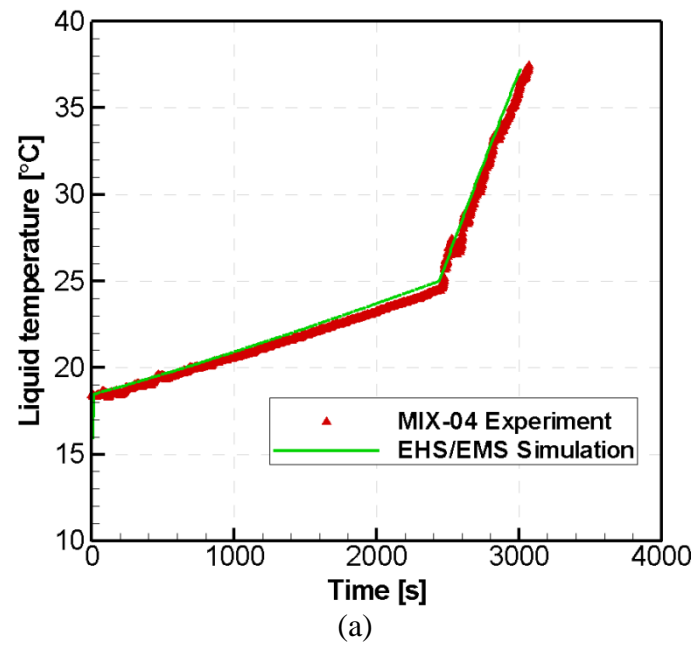
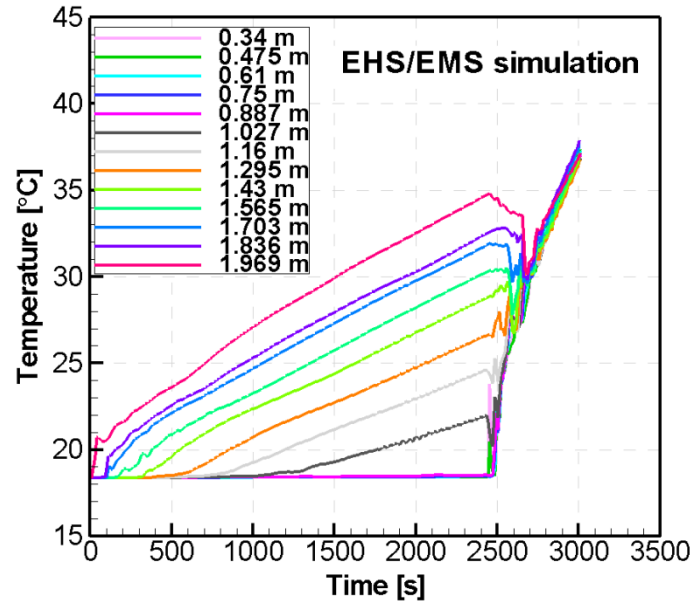
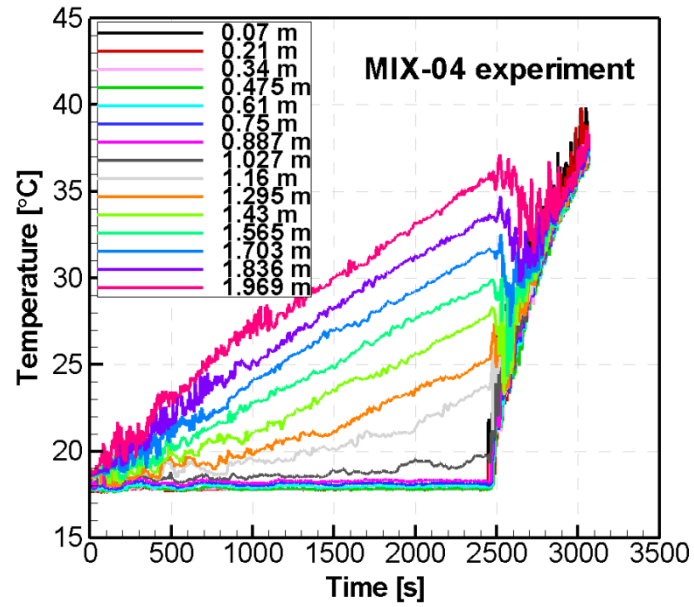


Figure 82: Comparison between EHS-EMS simulation results and MIX-04 test on (a) averaged liquid temperature and (b) water level in the wetwell pool.



(a)



(b)

Figure 83: Comparison of pool temperature between (a) EHS-EMS simulation and (b) MIX-04 measured data. The level of the pipe outlet is at 1.045 m.

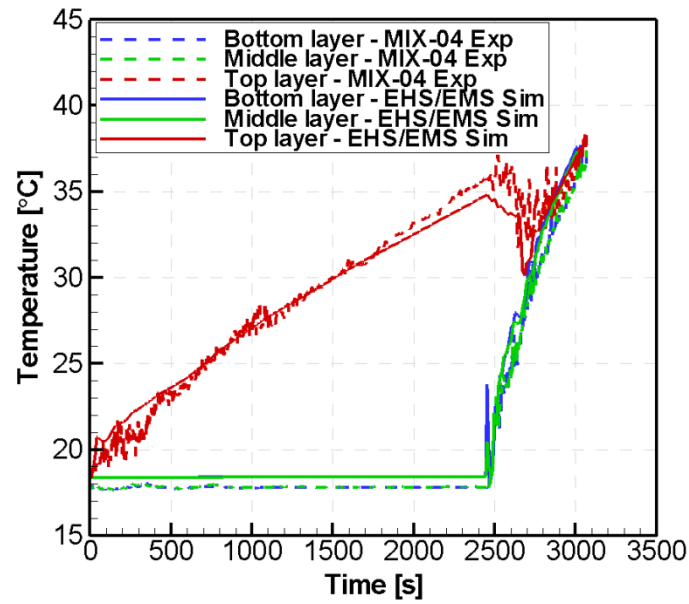


Figure 84: Comparison of pool temperature at selected levels in the pool.

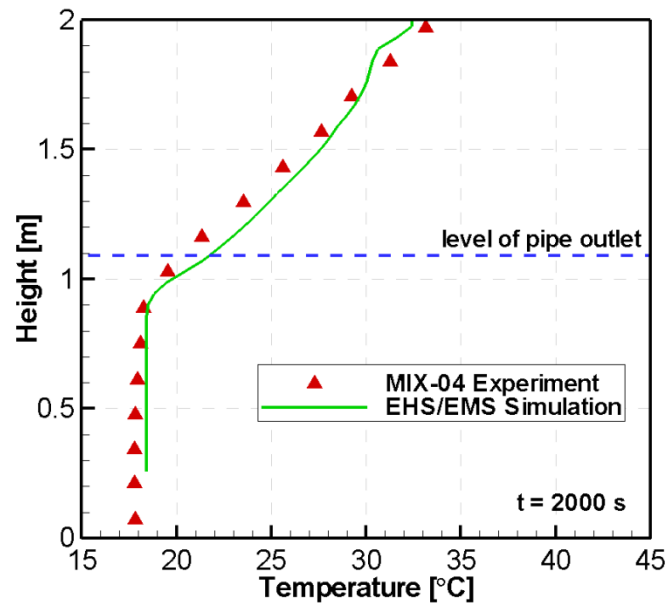


Figure 85: Comparison of vertical temperature profile at time t = 2000 s.

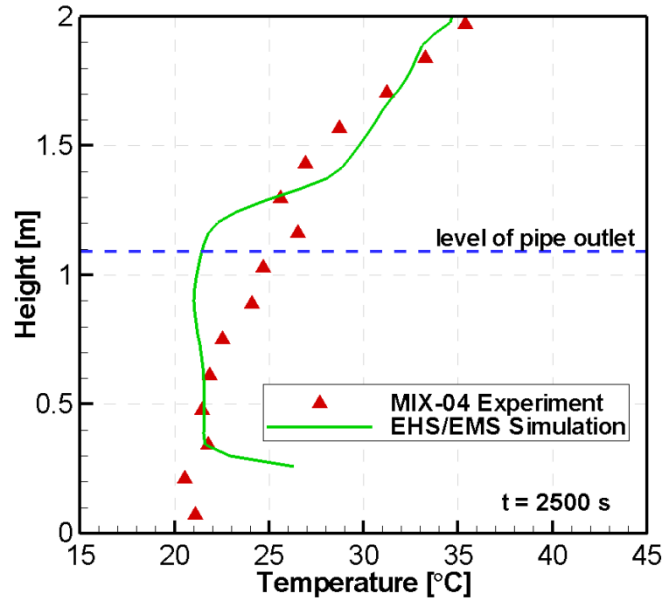


Figure 86: Comparison of vertical temperature profile at time $t = 2500$ s.

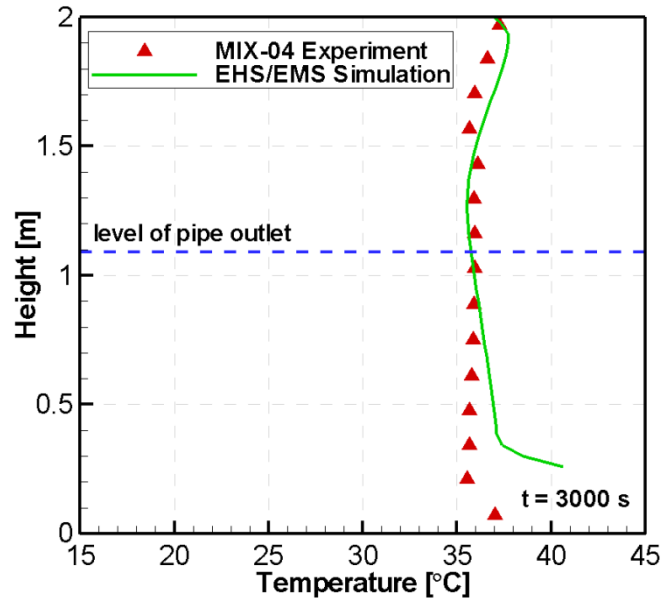


Figure 87: Comparison of vertical temperature profile at time $t = 3000$ s.

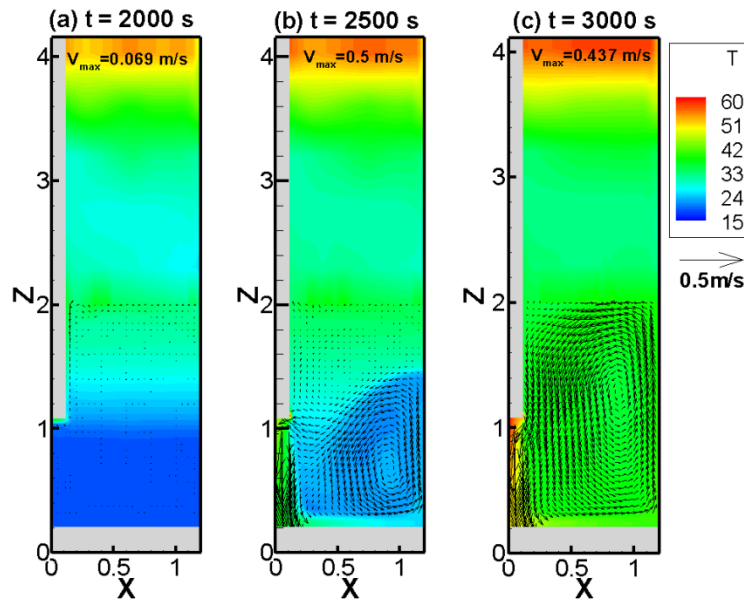


Figure 88: EHS-EMS simulation snapshots of temperature profiles with superimposed velocity fields at different times (a) $t = 2000$ s, during stratification phase, (b) $t = 2500$ s, early stage of mixing phase, and (c) $t = 3000$ s, during mixing phase.

Figure 88 shows snapshots of the predicted temperature and velocity profiles at different times $t = 2000$ s (stratification phase), $t = 2500$ s (early mixing phase), and $t = 3000$ s (mixing phase). It shows the process of the development of thermal stratification due to the buoyance force, and mixing due to the downward momentum injection. The magnitude of the maximum velocity at time of $t = 2000$ s in the stratification phase is just 0.069 m/s. At $t = 2500$ s and $t = 3000$ s, the magnitude of the maximum velocity is about 0.5 m/s and 0.437 m/s, respectively.

5.2.5 EHS/EMS validation against MIX-05 test

Compared to MIX-01 to MIX-04, MIX-05 test has four phases; a clearing phase, a thermal stratification phase, a mixing phase, and then redevelopment of thermal stratification phase (see Figure 89). It is noted that a redevelopment of thermal stratification happened even if the steam mass flow rate was kept the same. As the pool temperature is increasing, the condensation regime changes from chugging to the transition region where the oscillations are much weaker than in the chugging regime and thus unable to generate enough momentum (see Figure 90) to continuously mix the pool.

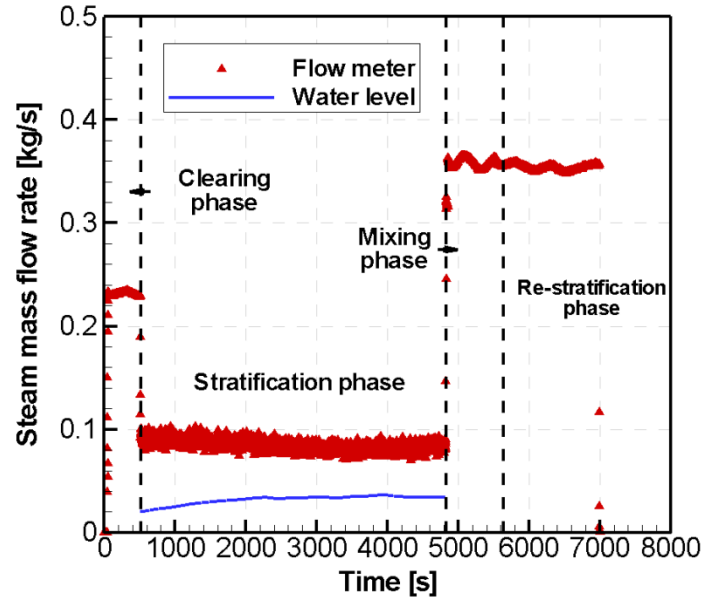


Figure 89: Measured steam mass flow rates with (i) flow meter and (ii) water level in the pool, during the MIX-05 experiment.

Similar to the MIX-01 test, the steam mass flow rates are estimated based on the collapsed water level in the pool. The initial time $t = 0$ s in the simulation corresponds to time 1000 s in Figure 89. The start of the mixing phase in the simulation is at time $t = 3881$ s. The effective momentum rates calculated based on the reading of thermocouples inside the blowdown pipe is shown in Figure 90.

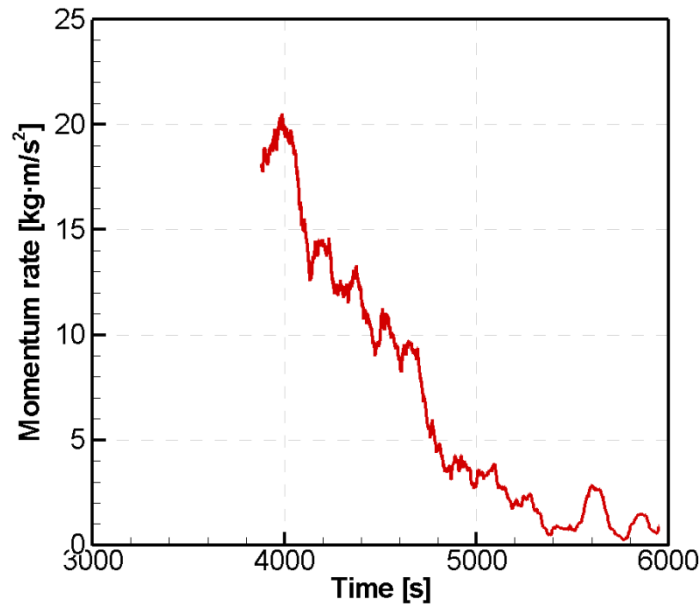


Figure 90: Effective momentum rates based on the water level oscillations in the pipe during the chugging (mixing) phase in MIX-05 test.

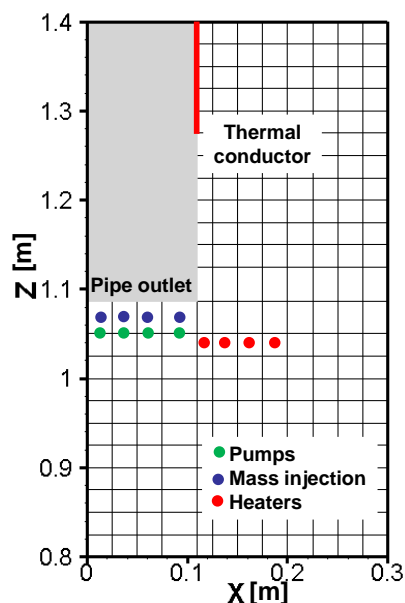


Figure 91: Configurations of heaters and pumps in MIX-06.

In the modeling of MIX-05, one thermal conductor is spanned on the pipe submerged surface, from around 0.188 m above the pipe exit, to supply the uniform-distributed heat source for the first thermal stratification phase. It is based on the experimental observation that the temperature of TC04 is always lower than the steam temperature in the stratification phase. Four heaters are located side by side in the cells about 0.037 m lower than the pipe outlet (the second layer below the pipe outlet), and 0.1095 m, 0.125 m, 0.15 m, 0.175 m from the pipe axial respectively (as shown by red dots in Figure 91). The heaters supply the heat source after the first stratification, since then all of the steam condensed out of the pipe in the test. There are four pumps located on four flow paths to impose the momentum from the cells right below the pipe outlet (represented by green dots in Figure 91). The condensates with temperature measured by TC01 are injected right below the pipe exit through 4 flow boundaries (represented by blue dots in Figure 91) or make total mass conserved in the simulation.

In Figure 92, the averaged liquid temperature and water level in the pool predicted by the EHS-EMS simulation shows a good agreement with the MIX-05 data. At time $t = 0$ s, the averaged liquid temperature is about 18 °C and it increases to 26 °C during the stratification phase, matching both experiment and simulation. Then it reaches 73 °C while the predicted temperature is 75 °C, since large steam mass flow rate is used for injection. The initial water level is at 2.12 m and during the stratification phase increases to 2.15 m, and during the mixing phase, the water level shows an abrupt increase to 2.37 m both in the experiment and simulation.

Figure 93 shows the comparison in pool temperature. The development of the first thermal stratification in different layers is captured in the simulation except for the small region in the vicinity of the pipe outlet. A fine grid resolution around the pipe exit can be used to improve the accuracy. In the simulation, the time scale for mixing is about 250 s while in the MIX-05 experiment it is about 400 s. Since in the experiment the temperature measured on the top layer is not stable during this transition and such instability is not predicted by the simulation. It can be seen from Figure 94. The continuous mixing and escalation of temperature in the pool is also well captured except that the re-stratification starts earlier in the simulation than in the experiment. This early

re-stratification leads to different top and bottom layer temperatures, although the general behavior of the re-stratification is captured in the simulation. The main possible reason is that with increasing pool bulk temperature the condensation region goes from chugging regime to transition regime. The steam out of the pipe would also take longer distance and time to be condensed in the pool, and also the momentum due to entrainment should be considered in this regime.

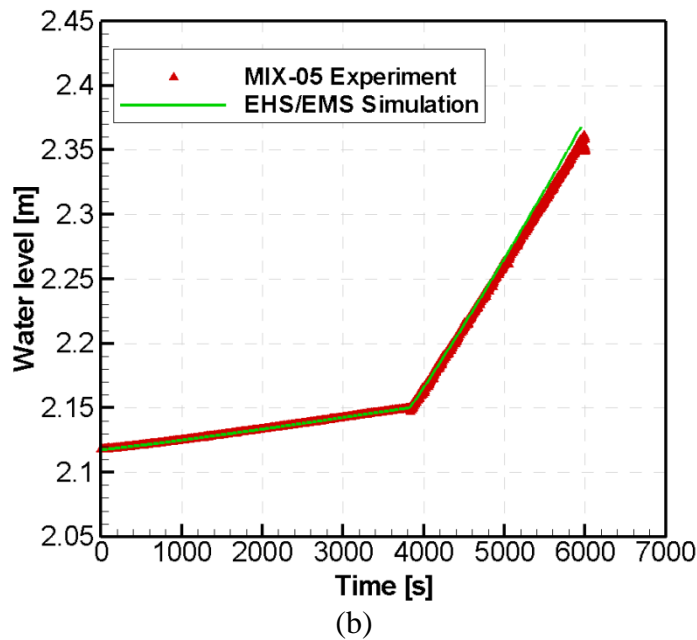
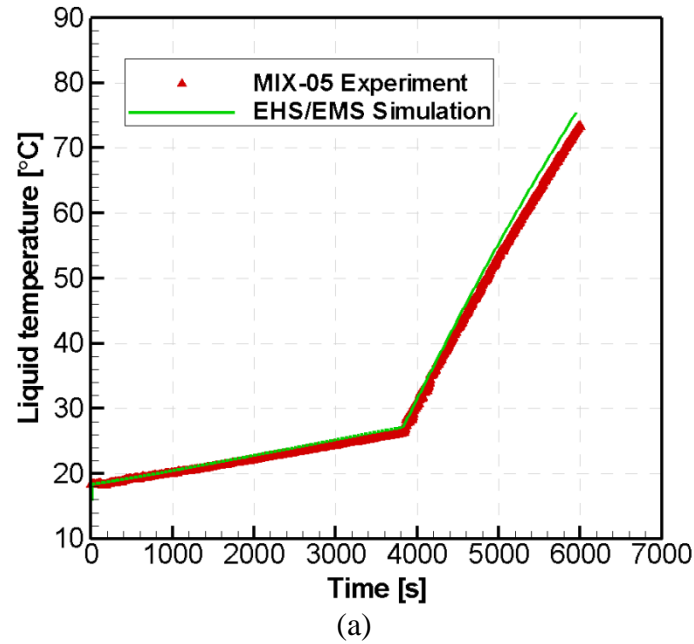


Figure 92: Comparison between EHS-EMS simulation results and MIX-05 test on (a) averaged liquid temperature and (b) water level in the wetwell pool.

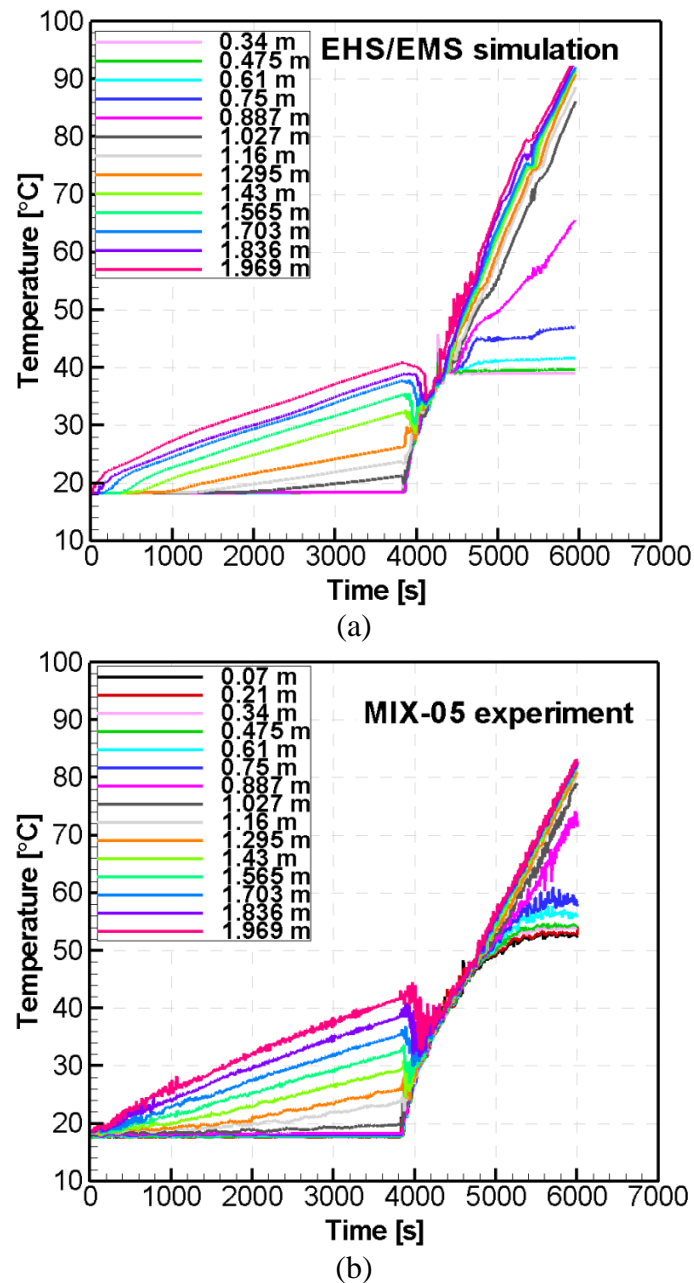


Figure 93: Comparison of pool temperature between (a) EHS-EMS simulation and (b) MIX-05 measured data. The level of the pipe outlet is at 1.045 m.

Figure 95 - Figure 97 show the comparison of vertical temperature profiles in the pool at different times. At time $t = 3000$ s (end of stratification phase) in Figure 95, the simulation can predict the colder bottom layer around 18 °C while the upper layer is thermally stratified. Also in Figure 96 at $t = 4000$ s during the mixing phase, the vertical temperature of the generally mixed pool is also captured in the simulation. At $t = 5000$ s during the re-stratification phase (see Figure 97), the thermocline trend is captured in the simulation but the temperature difference at the same time is higher in simulation. It is due to an early start of the re-stratification phase in the simulation. The EHS/EMS model, which was mainly developed and validated for condensation inside the pipe and chugging regimes, needs further improvement for the transition condensation regime.

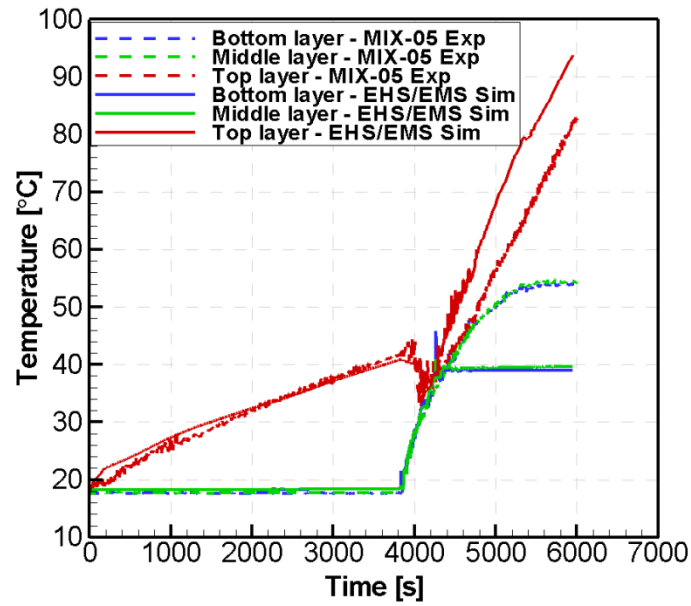


Figure 94: Comparison of pool temperature between EHS-EMS simulation and MIX-05 measured data at same layers.

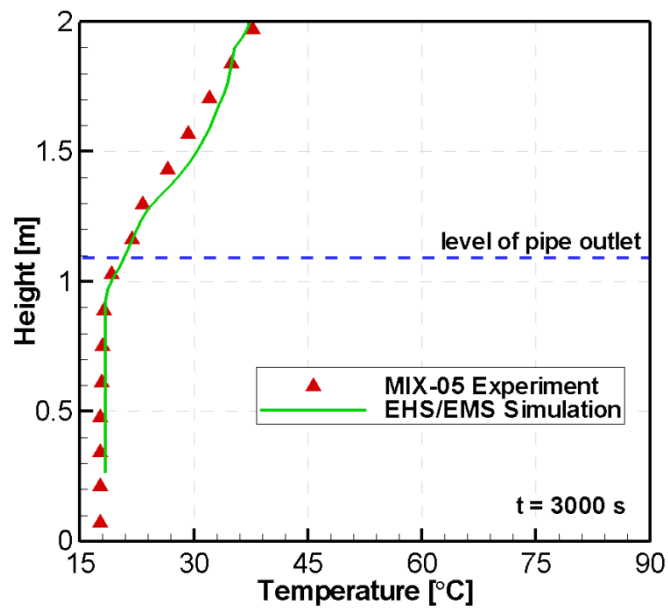


Figure 95: Comparison of vertical temperature profiles in the pool between MIX-05 test and EHS-EMS simulation at time $t = 3000$ s (end of stratification phase).

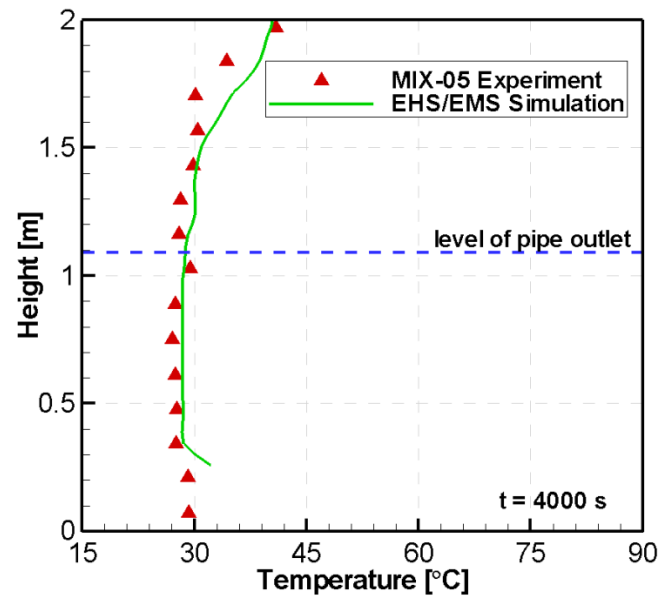


Figure 96: Comparison of vertical temperature profiles in the pool between MIX-05 test and EHS-EMS simulation at time $t = 4000$ s (during the mixing phase).

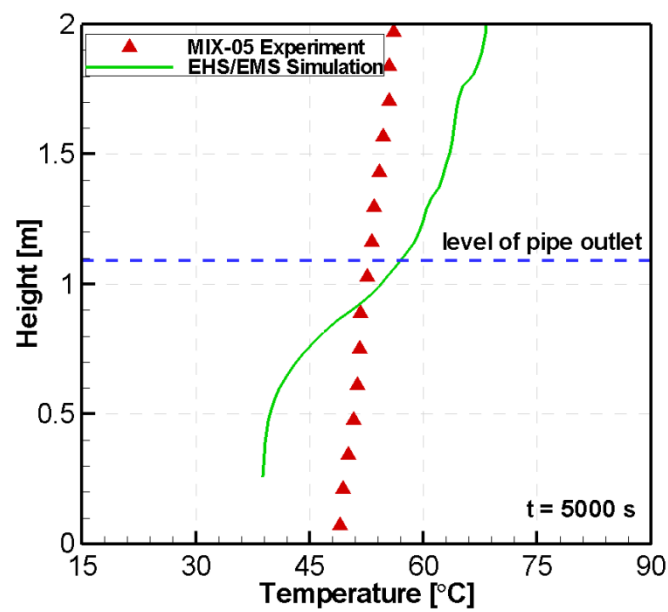


Figure 97: Comparison of vertical temperature profiles in the pool between MIX-05 test and EHS-EMS simulation at time $t = 5000$ s (during the re-stratification phase).

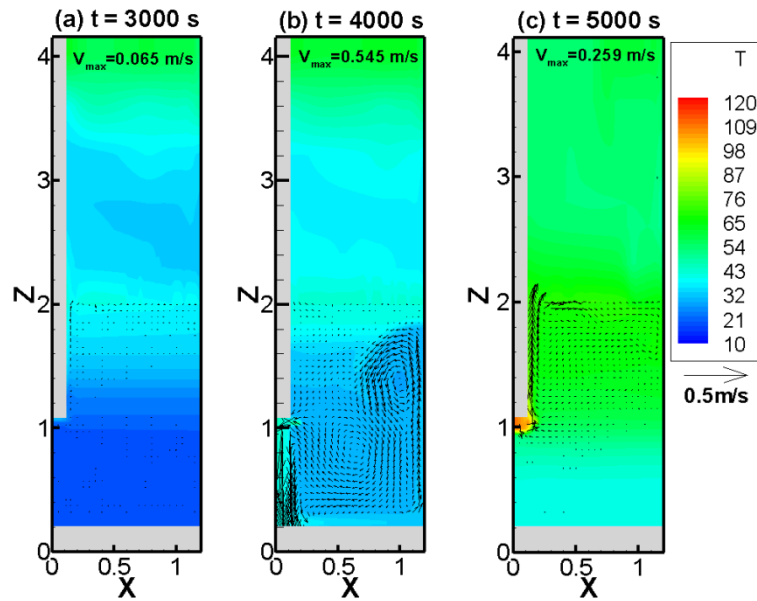


Figure 98: EHS-EMS simulation snapshots of temperature profiles with superimposed velocity fields at different times (a) $t = 3000$ s, during first stratification phase, (b) $t = 4000$ s, during mixing phase, and (c) $t = 5000$ s, during the re-stratification phase.

The snapshots of the predicted temperature and velocity profiles at different times $t = 3000$ s (stratification phase), $t = 4000$ s (mixing phase), and $t = 5000$ s (re-stratification phase) are shown in Figure 98. The magnitude of the maximum velocity at the time in the stratification phase is just 0.065 m/s. During the mixing phase at $t = 3000$ s, the magnitude of the maximum velocity is about 0.545 m/s. During the re-stratification phase at $t = 5000$ s, the flow circulation changes to clockwise manner again due to weak momentum downward and a significant buoyant plume near the pipe outlet. The magnitude of the maximum velocity is about 0.259 m/s.

5.2.6 EHS/EMS validation against MIX-06 test

MIX-06 test is similar to MIX-05 and it has four phases; a clearing phase, a thermal stratification phase, a mixing phase, and then redevelopment of thermal stratification phase.

The steam mass flow rate is shown in Figure 99. The estimated flow rates during the stratification phase and the measured steam flow rates after this phase are then used as input for the EHS-EMS simulation. The initial time $t = 0$ s in the simulation corresponds to time 600 s in Figure 99. The start of the mixing phase in the simulation is at time $t = 2045$ s. The effective momentum rates calculated based on the reading of thermocouples inside the blowdown pipe is shown in Figure 100. The maximum momentum rates in the mixing phase is around $24 \text{ kg}\cdot\text{m}/\text{s}^2$, while the momentum rate during the redevelopment is nearly 0.

The configuration of components in the modeling for MIX-06 is similar to MIX-05, except on the thermal conductor that is spanned on the pipe submerged surface. As shown in Figure 101, the thermal conductor is spanned on the whole pipe submerged surface, to supply the uniform-distributed heat source for the first thermal stratification

phase. The thermocouple inside the pipe closest to the exit (TC01) fluctuates during the thermal stratification, which means the water level inside the pipe is close to the pipe exit.

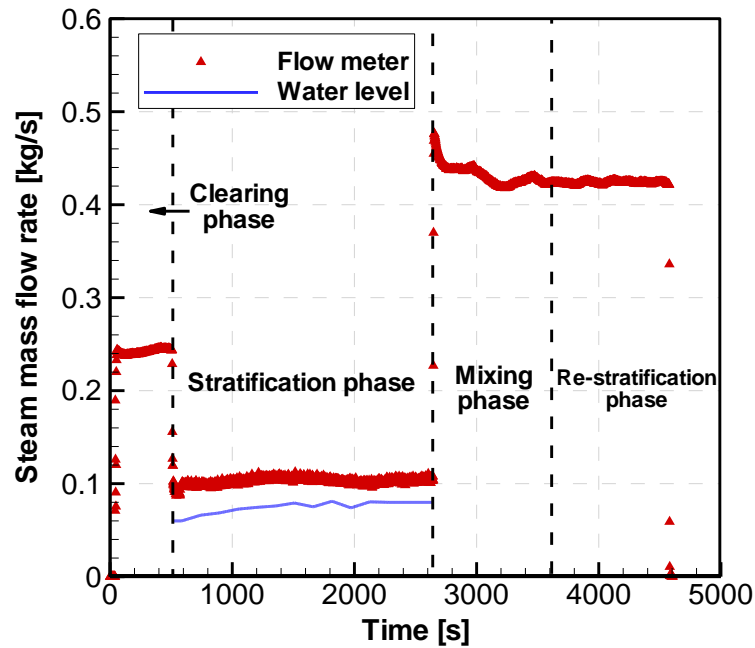


Figure 99: Measured steam mass flow rates with (i) flow meter and (ii) water level in the pool, during the MIX-06 experiment.

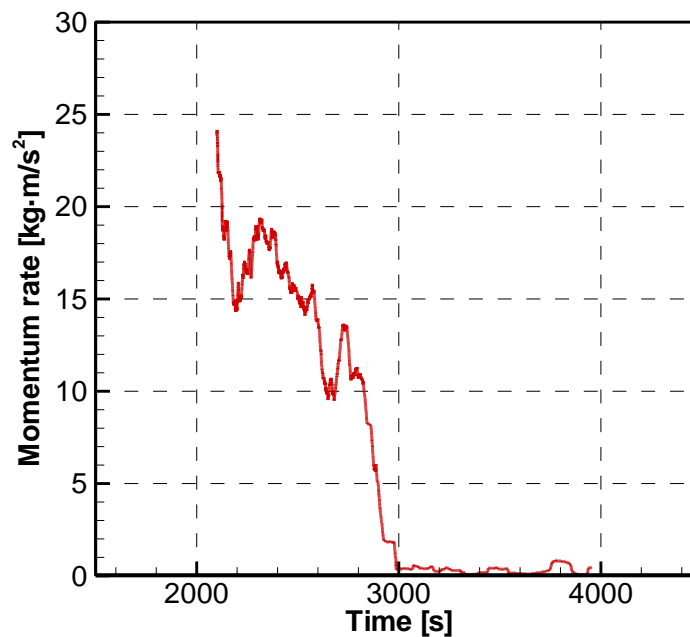


Figure 100: Effective momentum rates based on the water level oscillations in the pipe during the chugging (mixing) phase in MIX-06 test.

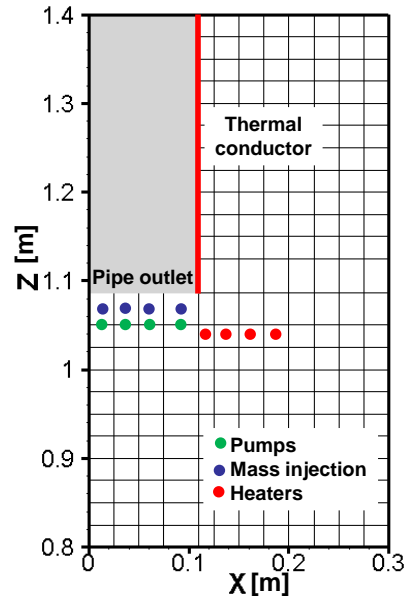
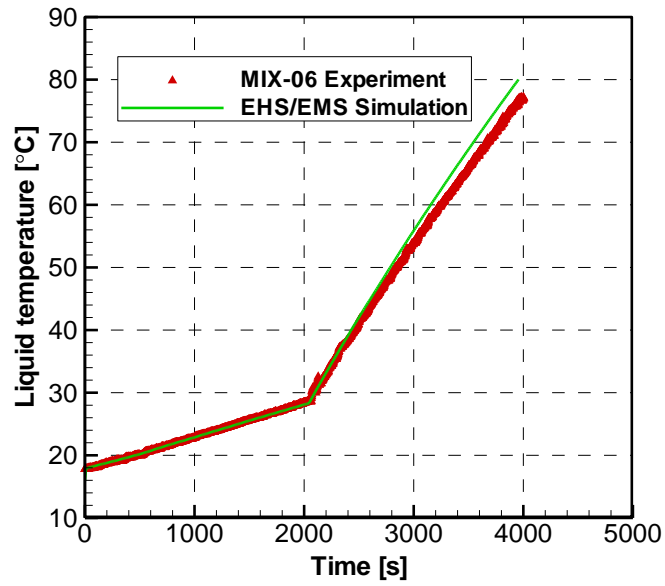


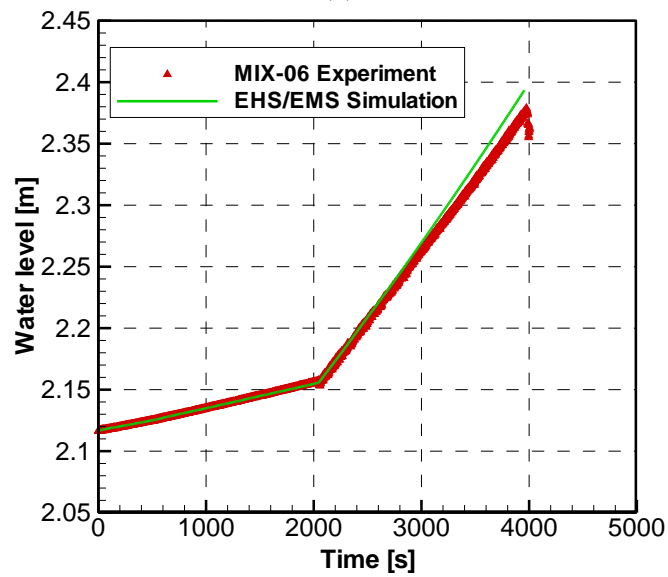
Figure 101: Configurations of heaters and pumps in MIX-06.

Figure 102 shows the agreement in the averaged liquid temperature and water level in the pool predicted by the EHS-EMS simulation and measured in the experiment. At time $t = 0$ s, the averaged liquid temperature is about $18\text{ }^{\circ}\text{C}$ and it increases to $28\text{ }^{\circ}\text{C}$ during the stratification phase matching both experiment and simulation. The increase in temperature is more pronounced at the end of transient as it reaches $76\text{ }^{\circ}\text{C}$ while the predicted temperature is $80\text{ }^{\circ}\text{C}$, since large steam mass flow rate is used for injection. The predicted increase in water level in the pool (see Figure 102b) shows an excellent match before 2800 s. The initial water level is at 2.12 m and during the stratification phase increases to 2.15 m while the predicted water level is also at 2.15 m. And during the mixing phase, the water level shows an abrupt increase to 2.25 m while the predicted water level is 2.23 m. The noticeable difference between the measured and predicted water level can be seen after about 2800 s, when thermal stratification starts to develop again.

The comparison in pool temperature is shown in Figure 103. The development of the first thermal stratification in different layers predicted is well captured. The time scale for mixing predicted is about 200 s while in the MIX-06 experiment it is about 250 s. The redevelopment of thermal stratification starts earlier in the simulation than in the experiment. This early re-stratification leads to different top and bottom layer temperatures, although the general behavior of the re-stratification is captured in the simulation.

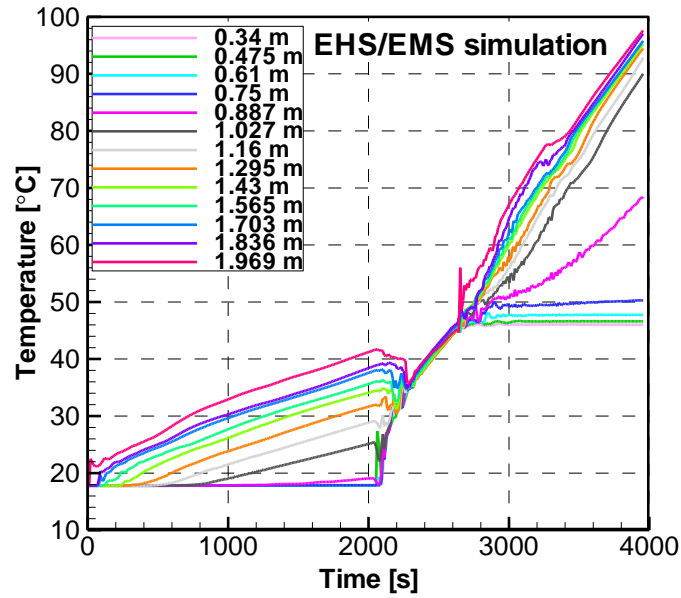


(a)

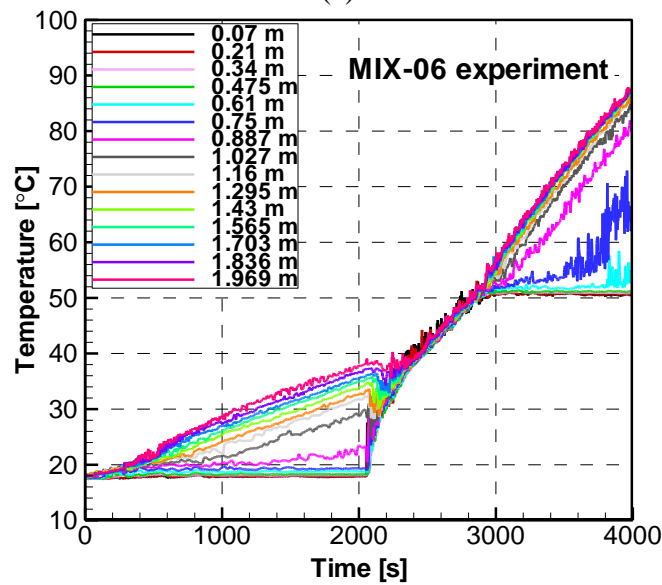


(b)

Figure 102: Comparison between EHS-EMS simulation results and MIX-06 test on (a) averaged liquid temperature and (b) water level in the wetwell pool.



(a)



(b)

Figure 103: Comparison of pool temperature between (a) EHS-EMS simulation and (b) MIX-06 measured data. The level of the pipe outlet is at 1.045 m.

Figure 104 - Figure 106 show the comparison of vertical temperature profiles in the pool at different times. A good agreement can be seen from figure at time $t = 2000$ s (end of stratification phase) in Figure 104, and in Figure 105 at $t = 2500$ s. At $t = 3500$ s during the re-stratification phase (see Figure 106), the thermocline trend is captured in the simulation with the reason similar to MIX-05.

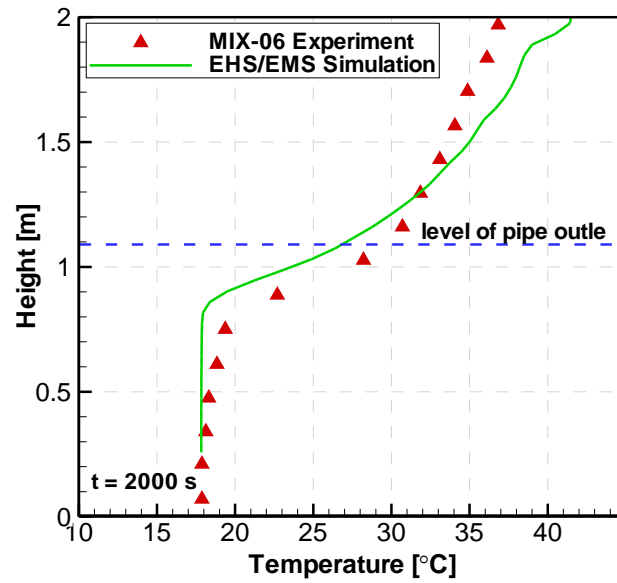


Figure 104: Comparison of vertical temperature profiles in the pool between MIX-06 test and EHS-EMS simulation at time $t = 2000$ s (end of stratification phase).

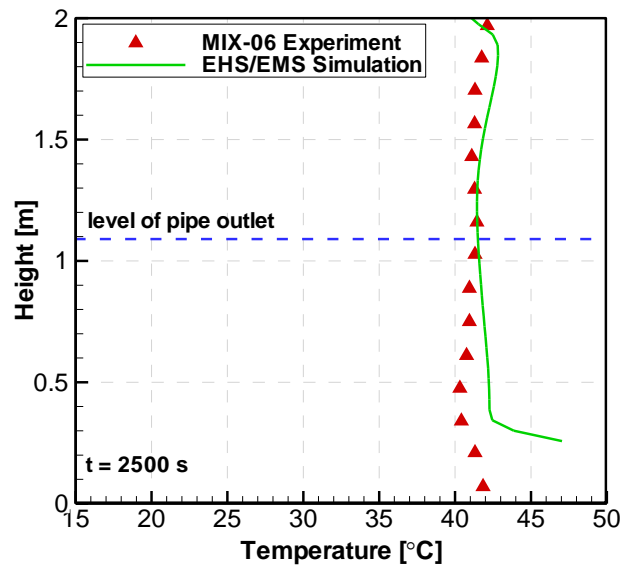


Figure 105: Comparison of vertical temperature profiles in the pool between MIX-06 test and EHS-EMS simulation at time $t = 2500$ s (during the mixing phase).

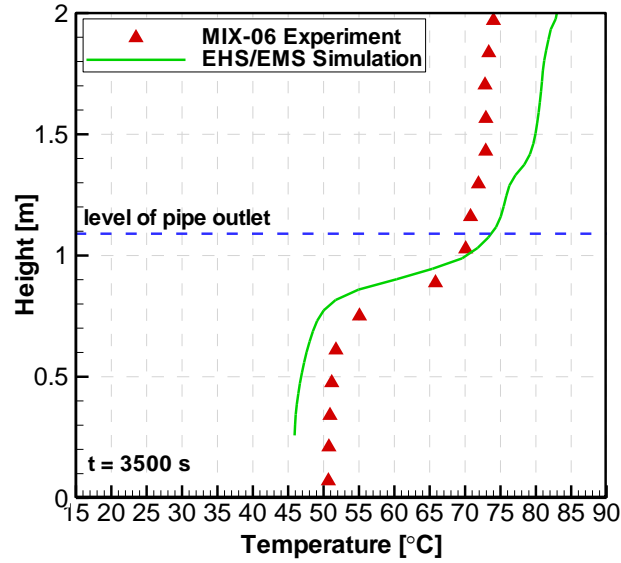


Figure 106: Comparison of vertical temperature profiles in the pool between MIX-06 test and EHS-EMS simulation at time $t = 3500$ s (during the re-stratification phase).

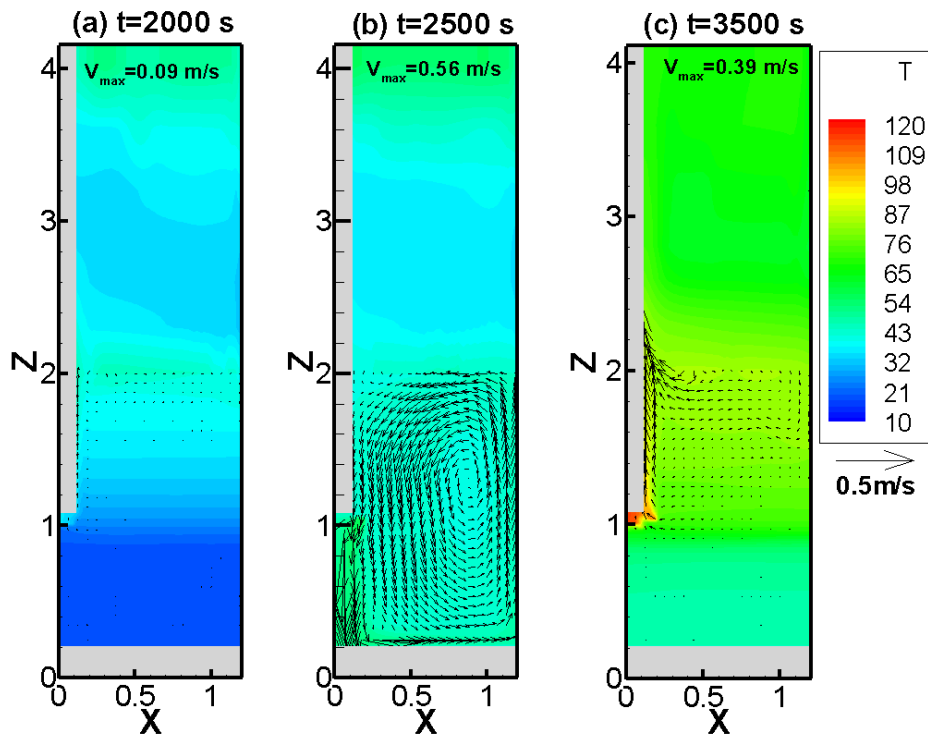


Figure 107: EHS-EMS simulation snapshots of temperature profiles with superimposed velocity fields at different times (a) $t = 2000$ s, during first stratification phase, (b) $t = 2500$ s, during mixing phase, and (c) $t = 3500$ s, during second stratification phase.

Figure 107 shows snapshots of the predicted temperature and velocity profiles at different times $t = 2000$ s (stratification phase), $t = 2500$ s (mixing phase), and $t = 3500$ s (re-stratification phase). At $t = 2000$ s, a thermally stratified layer develops at the top while the lower layer remains cold. The magnitude of the maximum velocity at this time is just 0.09 m/s. During the mixing phase at $t = 2500$ s, the flow circulation changes to counter-clockwise manner due to the dominant effect of the jet from the pipe

outlet. The magnitude of the maximum velocity at this time is about 0.56 m/s. During the re-stratification phase at $t = 3500$ s, the flow circulation changes to clockwise manner again due to weak momentum downward and high buoyancy force produced by heat fluxes from the pipe.

5.3 Validation of EHS and EMS models against PPOOLEX MIX-07 to MIX-12 tests

The tests from MIX-07 to MIX-12 have a blowdown pipe with 114.3 mm in diameter and a thickness of 2.5 mm. This pipe diameter is smaller compared to the previous MIX-01 to 06 tests (with diameter of 214 mm), but higher steam fluxes can be attained which can then cover a wider range in the chugging regime of the condensation map. The blowdown pipe is also about 312 mm shorter than the previous one. In order to have the same submergence depth as in the previous tests, a higher initial water level of the pool is set during the tests.

The experimental procedure of the test is similar to MIX-05 and MIX-06 test, that is, a clearing phase using high steam flow rate, followed by the thermal stratification with low steam flow rate, and then the high steam flow rate is used to mix the pool and heat up the pool until close to the limit of the tank pressure.

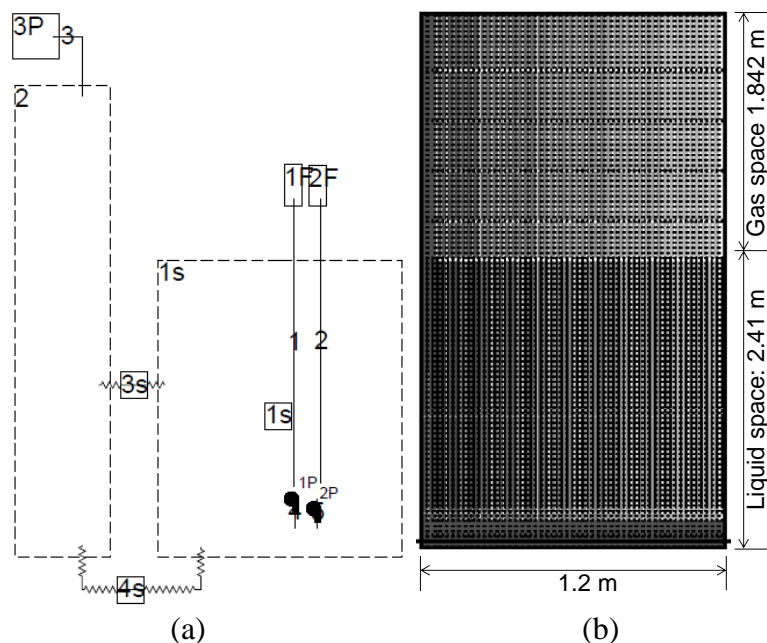


Figure 108: (a) GOTHIC model schematic of MIX-07 and (b) corresponding 2D mesh with 48×87 for the wetwell.

Given the pipe diameter and initial water level in the wetwell, the GOTHIC model schematic and grid configuration of the wetwell is shown in Figure 108. Only two flow boundaries and two pumps are used for liquid injection and momentum injection, due to the small size of the blowdown pipe. A 48×87 mesh is used for the wetwell because the water level is higher than in the previous tests. The configuration of thermal conductor, heaters, flow boundaries and pumps considers the test conditions in each test.

5.3.1 EHS/EMS validation against MIX-07 test

In MIX-07 test, the steam mass flow estimated is shown in Figure 109, which is based on the collapsed water level. It should be noted that during the thermal stratification phase, there are two steam mass flow rates used. The circulation motion after the clearing phase decreases during the time with a small flow rate with about 15 g/s. Taking this into account, the initial time $t = 0$ s in the simulation corresponds to time 1804 s in Figure 109. In the simulation, the start of the phase with high steam flow rate for mixing is at time $t = 4551$ s. It is observed that incomplete mixing is achieved in the experiment during this phase. This can be explained from Figure 110 with calculated effective momentum rates. The maximum momentum rates with high steam mass flow rate is only around $0.4 \text{ kg}\cdot\text{m}/\text{s}^2$, and the momentum rate decreases to nearly $0.03 \text{ kg}\cdot\text{m}/\text{s}^2$ at the end of the transient. It is also observed that the oscillation amplitude during chugging is lower with a smaller diameter pipe compared to a larger pipe as in the previous tests (more details is provided in the next section on scaling approach).

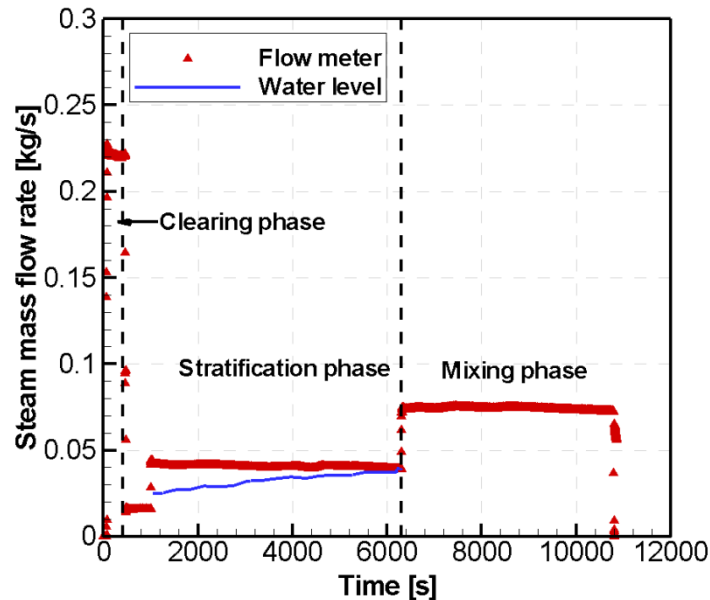


Figure 109: Measured steam mass flow rates with (i) flow meter and (ii) water level in the pool, during the MIX-07 experiment.

Figure 111 shows the configuration of thermal conductor, heaters, boundaries and pumps used for simulation. In the modeling, one thermal conductor is spanned on the pipe's submerged surface, to supply the uniform-distributed heat source for the thermal stratification phase. Eight heaters supply the heat source after the stratification. Four heaters are located in the cell below the pipe outlet (the first to fourth layer below the pipe outlet), and 0.0571 m from the pipe axial. The other four are just in another cell beside (as shown by red dots in Figure 111). There are two pumps located on two flow paths to impose the momentum from the cells right below the pipe outlet (represented by green dots in Figure 111). Two flow boundaries are used to release the condensate and conserve mass (blue dots in Figure 111).

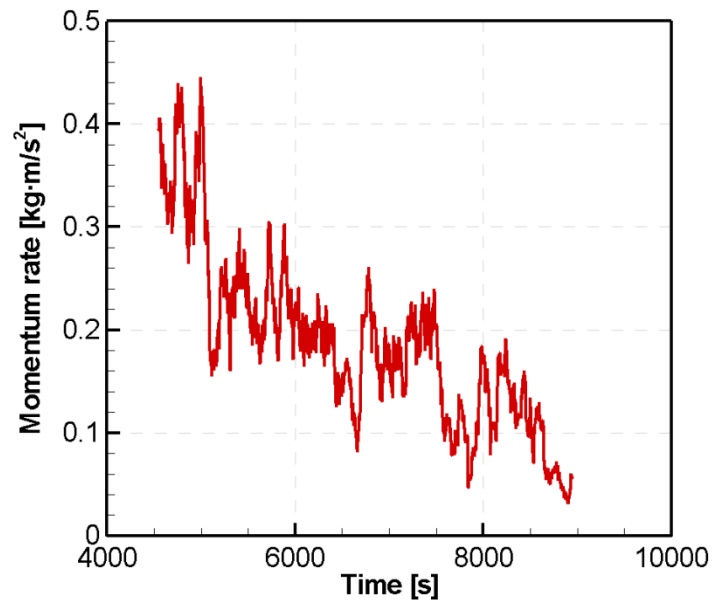


Figure 110: Effective momentum rates based on the water level oscillations in the pipe during the chugging (mixing) phase in MIX-07 test.

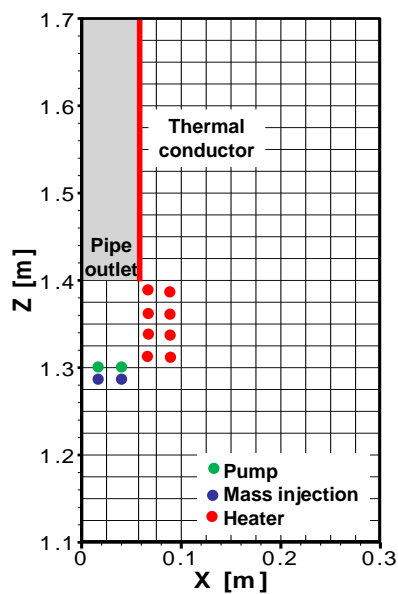
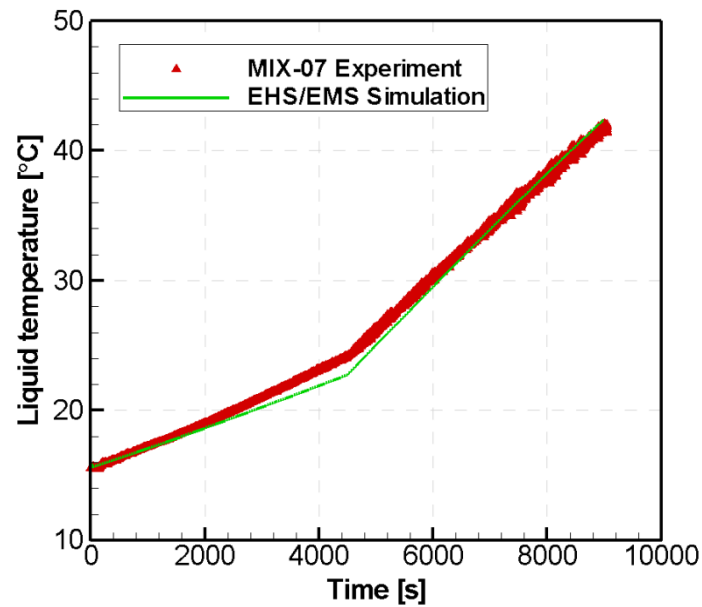
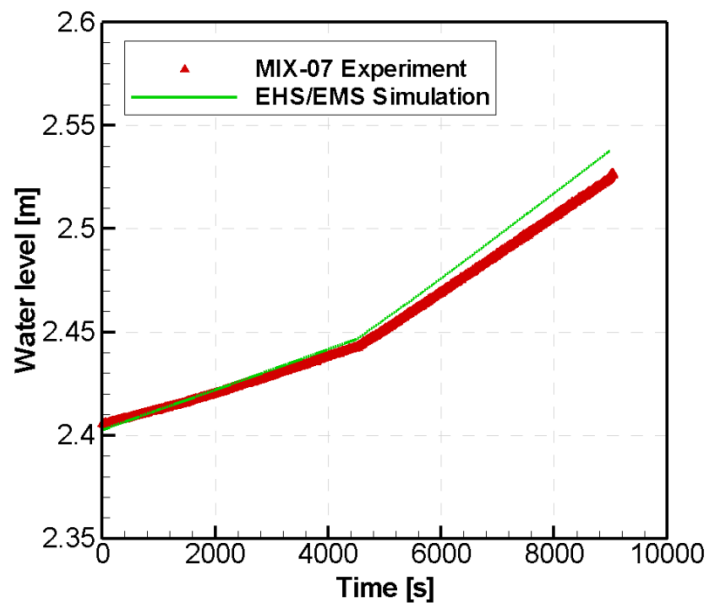


Figure 111: Configurations of components for EHS/EMS model for MIX-07.

The averaged liquid temperature and the water level in the pool predicted by the EHS-EMS simulation are compared to the measured data, as shown in Figure 112. The behavior of the average temperature and the water level is well predicted. There are some slight differences between the simulation results and measured data, possibly due to some uncertainties in the measurement for water level and temperature. At time $t = 0$ s, the averaged liquid temperature is about $16\text{ }^{\circ}\text{C}$ and it increases to $24\text{ }^{\circ}\text{C}$ during the stratification phase compared to $22\text{ }^{\circ}\text{C}$ in the simulation. During the phase with high steam flow rate, the water level shows an abrupt increase to 2.525 m while the predicted water level is 2.54 m . A significant difference on the measured and predicted water level can be seen in the period after about 4600 s , in which one possible reason is the over-measurement of the steam mass flow during that period.



(a)



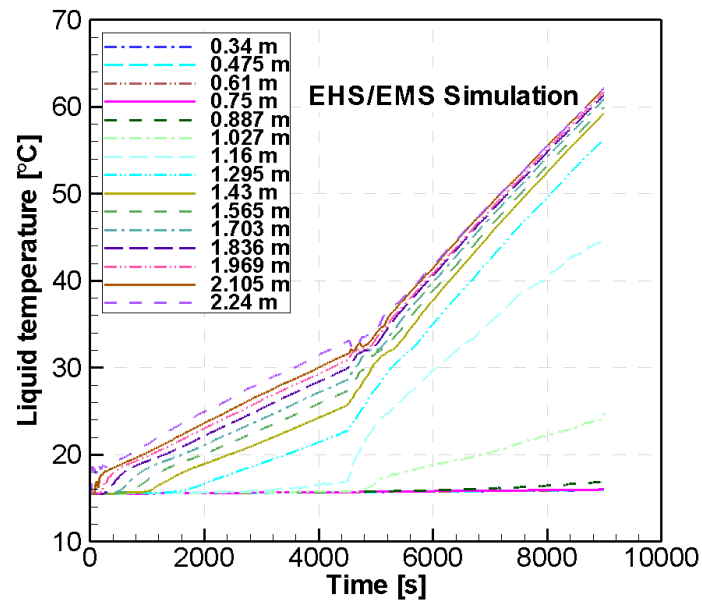
(b)

Figure 112: Comparison between EHS-EMS simulation results and MIX-07 test on (a) averaged liquid temperature and (b) water level in the wetwell pool.

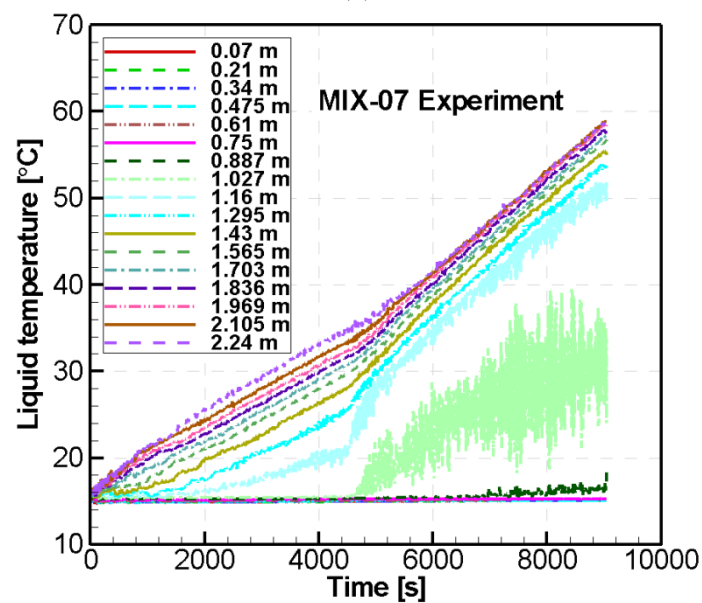
Figure 113 shows the comparison in pool temperature between the MIX-07 measured data and EHS-EMS simulation. The development of the first thermal stratification in different layers is well captured in the simulation. At the end of the stratification phase, the predicted temperature at the top layer is about 33 °C while the measured temperature is about 35 °C. As a result of higher steam flow rates and transition of the condensation regime to chugging, downward momentum produces a circulation flow in the pool. Since the momentum produced by chugging is quite small and the downward jet cannot reach the bottom of the pool, a weak circulation leads to incomplete mixing. In the simulation, such incomplete mixing is also well captured.

A more detailed comparison of the temperature behavior in the pool is shown in Figure 114. The temperature profiles in the middle (about 1.295 m from the bottom) and

bottom layers both in the EHS-EMS simulation and MIX-07 experiment are shown. The temperature behavior on all three layers in the experiment and simulation are well matched.



(a)



(b)

Figure 113: Comparison of pool temperature between (a) EHS-EMS simulation and (b) MIX-07 measured data. The level of the pipe outlet is at 1.4 m.

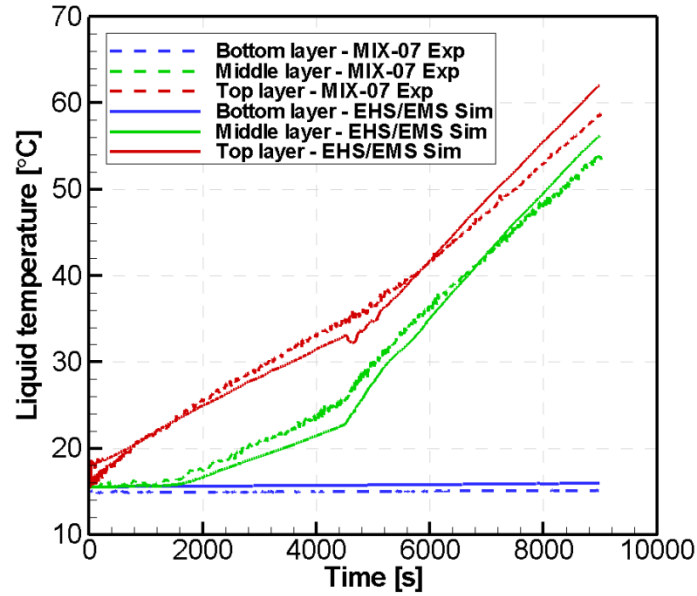
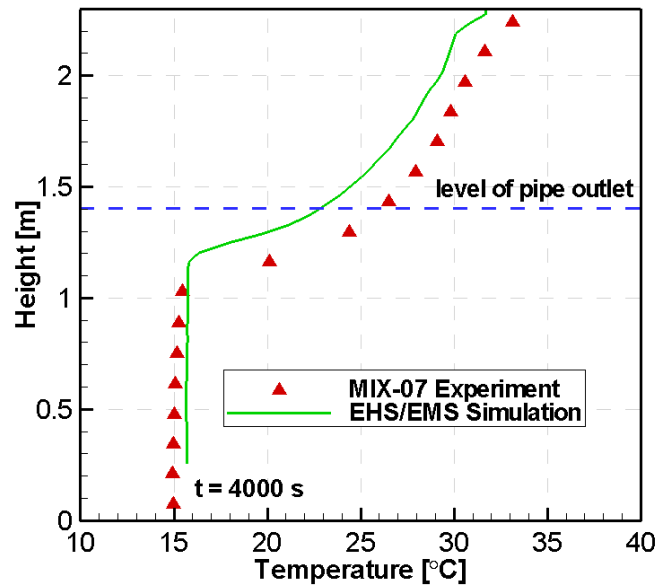


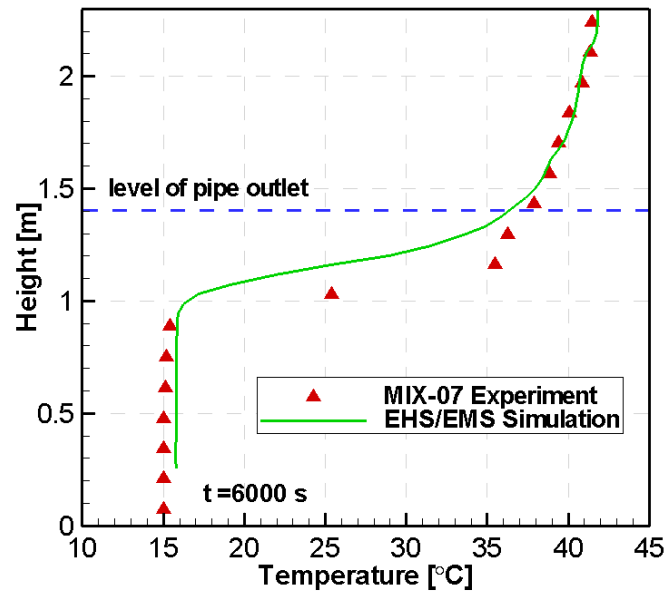
Figure 114: Comparison of pool temperature at selected levels in the pool

In Figure 115a, a snapshot of the vertical temperature profile near the end of the thermal stratification phase (at time $t = 4000$ s) is shown. Both the experiment and simulation shows that the layer below the pipe outlet remains cold while the upper layer develops thermal stratification.

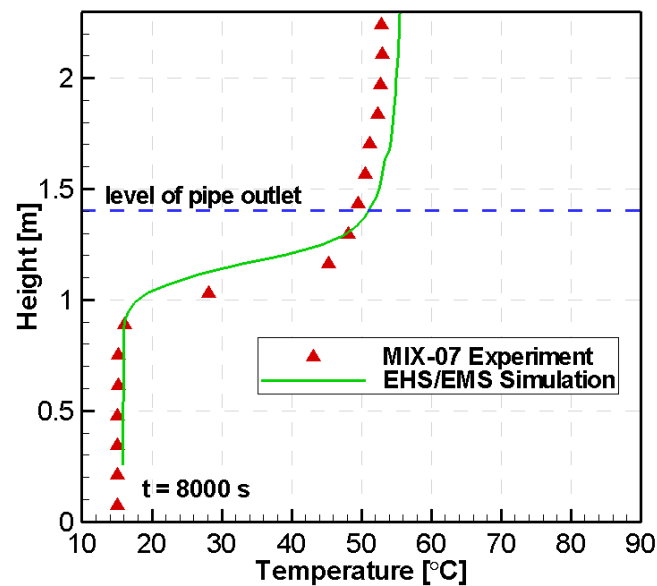
The temperature behavior in the phase with high steam flow rate is also well captured, as seen in Figure 115b and Figure 115c. The temperature at the bottom layer remains cold while the middle part starts to mix with upper part. A finer mesh is needed in the simulation in order to capture well the behavior around the pipe exit.



(a)



(b)



(c)

Figure 115: Comparison of pool temperature (a) snapshot of vertical temperature profile at time $t = 4000$ s, (b) snapshot of vertical temperature profile at time $t = 6000$ s, (c) snapshot of vertical temperature profile at time $t = 8000$ s.

Figure 116 shows snapshots of the predicted temperature and velocity profiles at different times $t = 4000$ s (first stratification phase), $t = 6000$ s and $t = 8000$ s (the phase with high steam flow rate). At $t = 4000$ s, the heating of the water surrounding the pipe creates a buoyant plume of hot water circulating in a clockwise manner. The magnitude of the maximum velocity at this time is just 0.074 m/s. At $t = 6000$ s with high steam mass flow, the buoyant force becomes more dominant than inertial force since the downward momentum is small due to weak chugging. The magnitude of the maximum velocity at this time is about 0.168 m/s. At $t = 8000$ s, the magnitude of the maximum velocity is higher, at 0.205 m/s, than the previous snapshot but with the same clockwise circulation in the upper part.

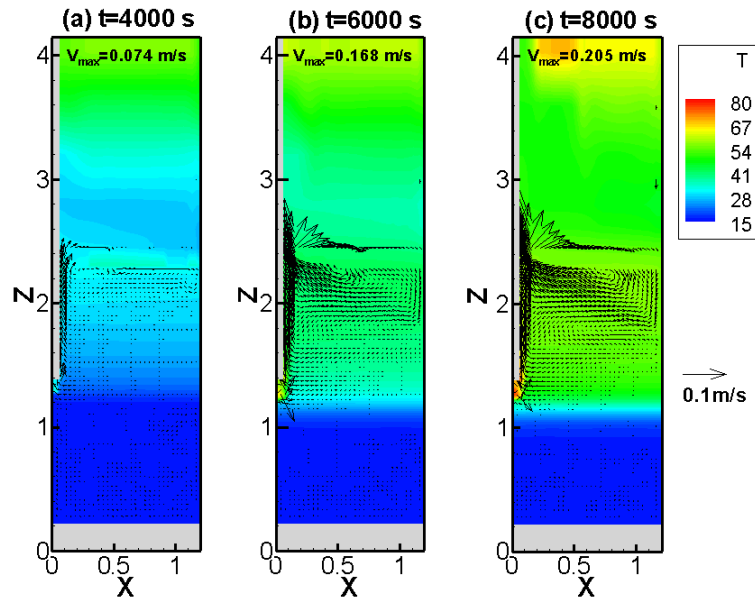


Figure 116. EHS-EMS simulation snapshots of temperature profiles with superimposed velocity fields at different times (a) $t = 4000$ s, during first stratification phase, (b) $t = 6000$ s, and (c) $t = 8000$ s.

5.3.2 EHS/EMS validation against MIX-08 test

In MIX-08 test, the steam mass flow used during the test is shown in Figure 117. The estimated flow rates during the stratification phase and the measured steam flow rates after this phase are then used as input for the EHS-EMS simulation.

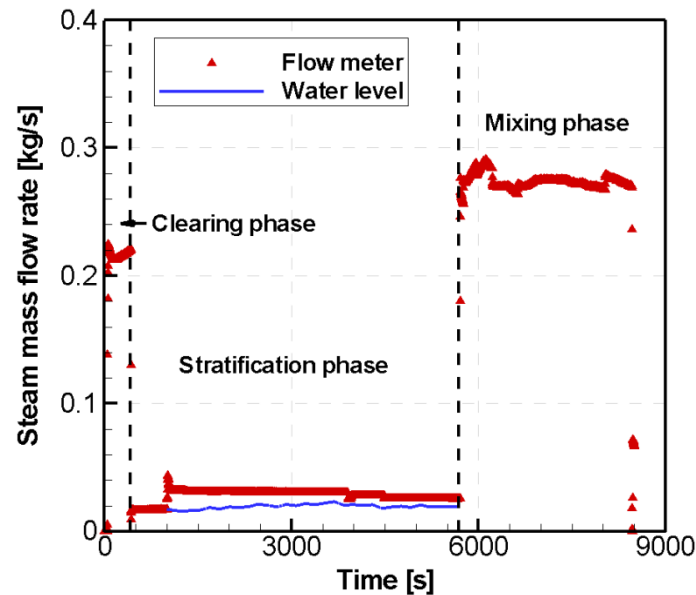


Figure 117: Measured steam mass flow rates with (i) flow meter and (ii) water level in the pool, during the MIX-08 experiment.

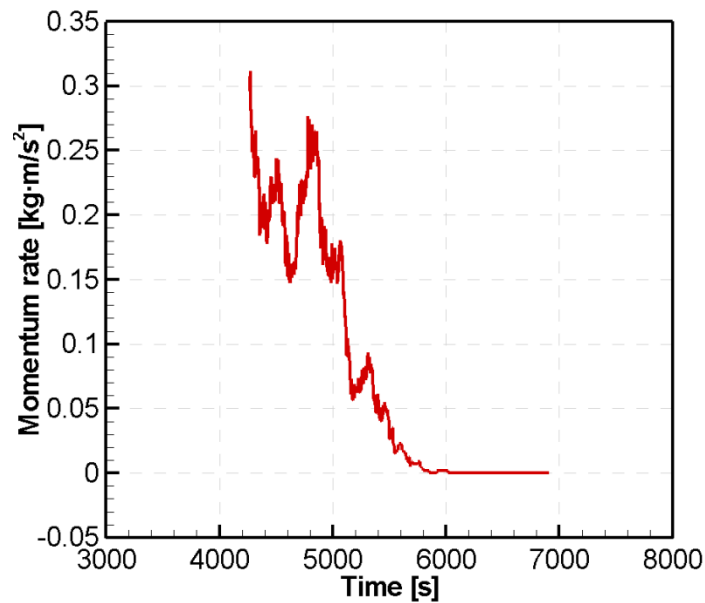


Figure 118: Effective momentum rates based on the water level oscillations in the pipe during the chugging phase in MIX-08 test.

The initial time $t = 0$ s in the simulation corresponds to time 1500 s in Figure 117. The start of the phase with high steam flow rate in the simulation is at time $t = 4209$ s. The effective momentum rates calculated based on the thermocouple readings inside the blowdown pipe is shown in Figure 118.

In the modeling for MIX-08, as shown in Figure 119, one thermal conductor is spanned on the pipe submerged surface from 0.1 m above the pipe exit, to supply the uniform-distributed heat source for the thermal stratification phase. Other components' positions are the same as in MIX-07 test.

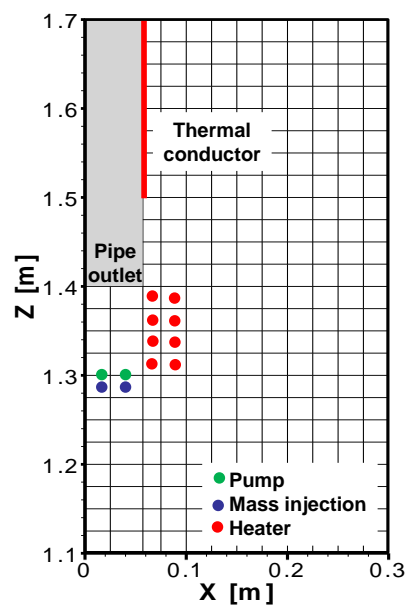


Figure 119: Configurations of components for EHS/EMS model for MIX-08.

Figure 120 shows a good agreement on the averaged liquid temperature and the water level in the pool between the EHS-EMS simulation and experiment. The largest

difference (although insignificant) on the measured and predicted water level is in the period after ~6000 s, in which one possible reason is over-measurement of the steam flow.

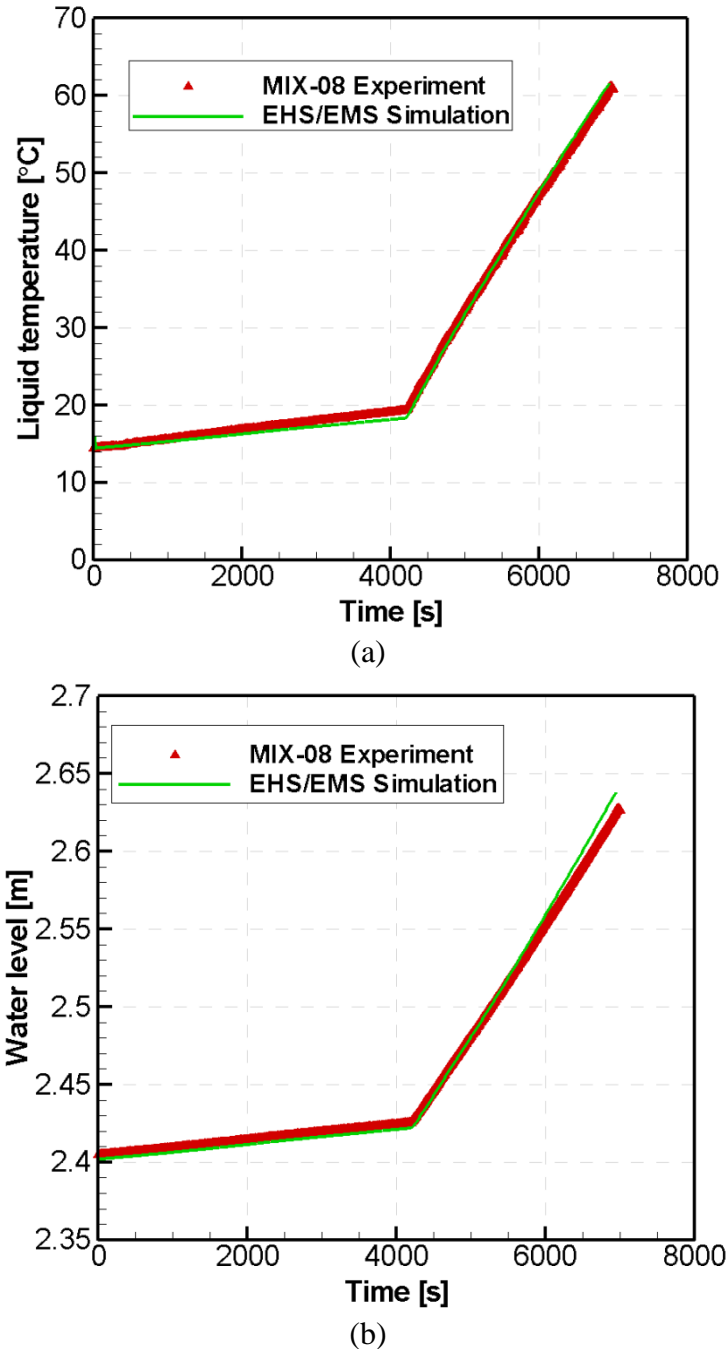
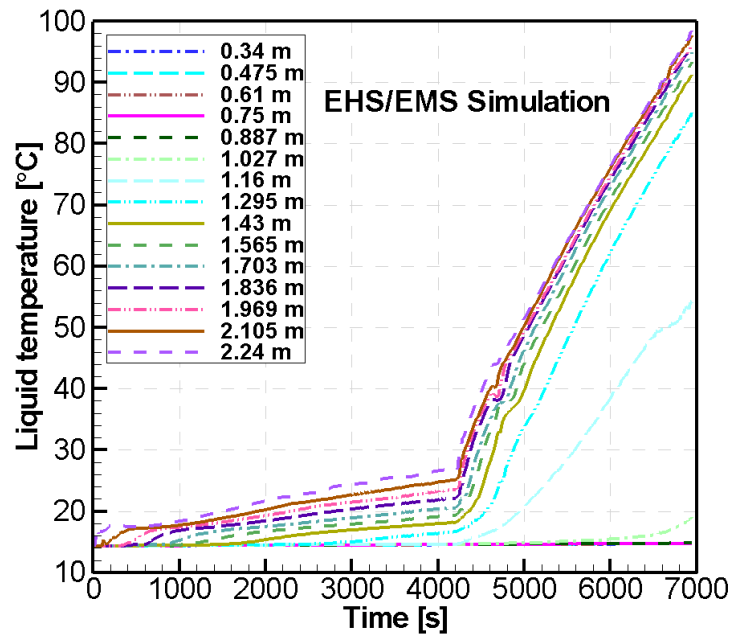


Figure 120: Comparison between EHS-EMS simulation results and MIX-08 test on (a) averaged liquid temperature and (b) water level in the wetwell pool.

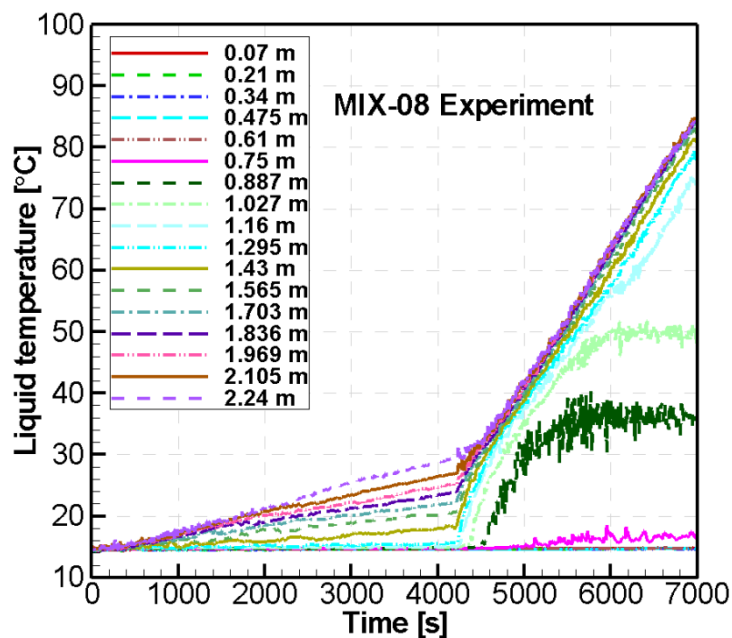
The comparison in pool temperature between the MIX-08 measured data and EHS-EMS simulation is shown in Figure 121. The development of the first thermal stratification in different layers is well captured in the simulation. For the phase with high steam flow rate, the downward momentum produced by chugging oscillation is not large enough to mix the entire pool. In the simulation, such incomplete mixing is also captured. The difference is that in the experiment the jet reaches a deeper layer

than in the simulation which implies that the momentum used in the simulation is underestimated.

A more detailed comparison of the temperature behavior in the pool is shown in Figure 122a. As mentioned above, in the experiment more layers below the pipe outlet is heated up, therefore the temperature on the upper layers are over-predicted.

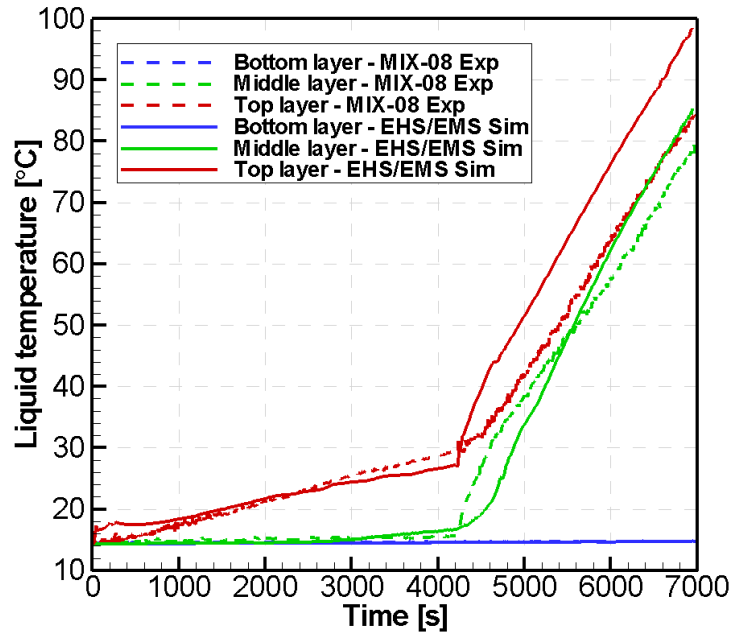


(a)

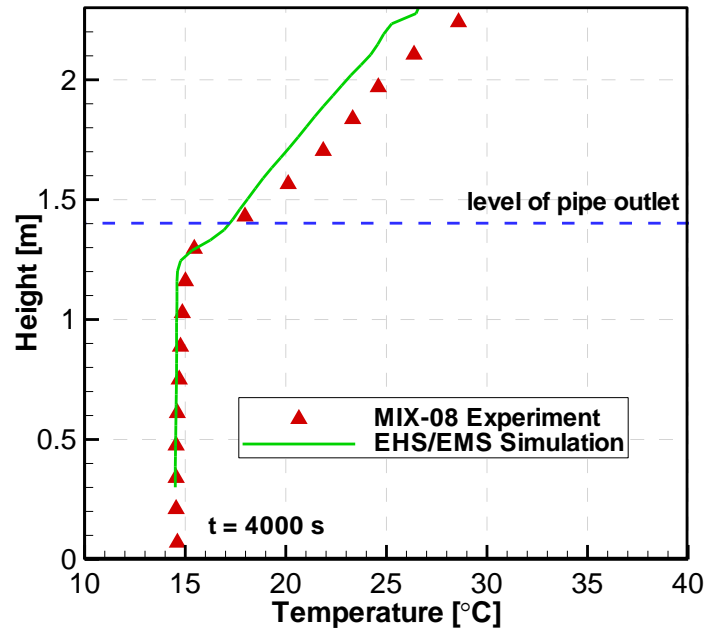


(b)

Figure 121: Comparison of pool temperature between (a) EHS-EMS simulation and (b) MIX-08 measured data. The level of the pipe outlet is at 1.4 m.



(a)



(b)

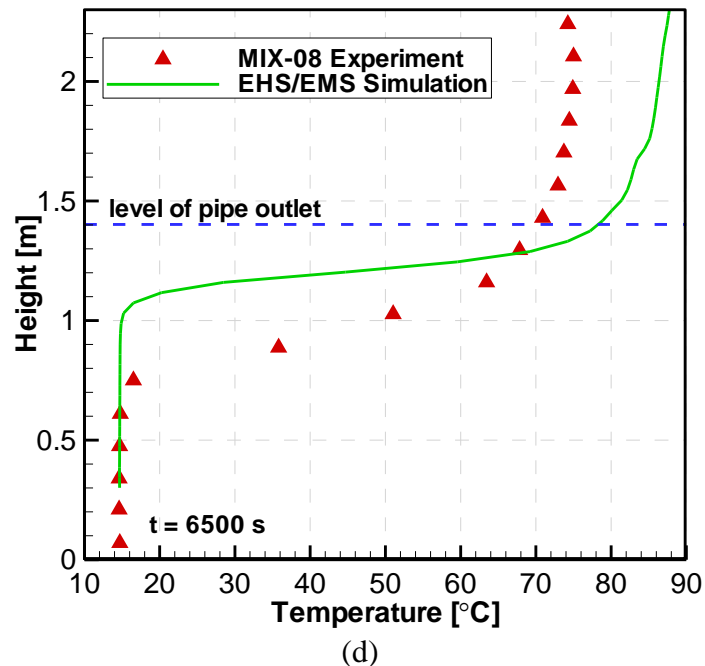
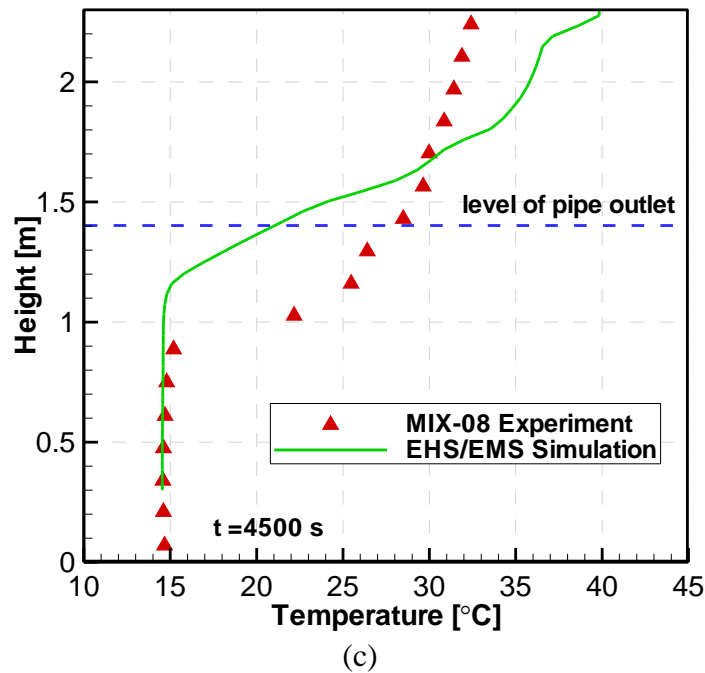


Figure 122: Comparison of pool temperature (a) at selected levels in the pool, (b) snapshot of vertical temperature profile at time $t = 4000$ s, (c) snapshot of vertical temperature profile at time $t = 4500$ s, (d) snapshot of vertical temperature profile at time $t = 6500$ s.

In Figure 122b, Figure 122c, and Figure 122d, a snapshot of the vertical temperature profile at time $t = 4000$ s, $t = 4500$ s, and $t = 6500$ s are shown. The simulation predicts the first thermal stratification well, but some differences are seen in the part with high steam flow rate. One possible solution is to use finer mesh for the layer close to the pipe exit. The behavior of the pipe during the transition condensation regime needs further investigation.

Figure 123 shows snapshots of the predicted temperature and velocity profiles at different times $t = 4000$ s (first stratification phase), $t = 4500$ s and $t = 6500$ s (the phase with high steam flow rate). At $t = 4000$ s, a buoyant plume along the pipe surface can be clearly seen. The magnitude of the maximum velocity at this time is 0.076 m/s. At $t = 4500$ s, the buoyant force becomes stronger. The magnitude of the maximum velocity at this time is about 0.25 m/s, which is located along the pipe surface. At $t = 6500$ s, the maximum velocity is larger than the previous time but the circulation behavior is the same.

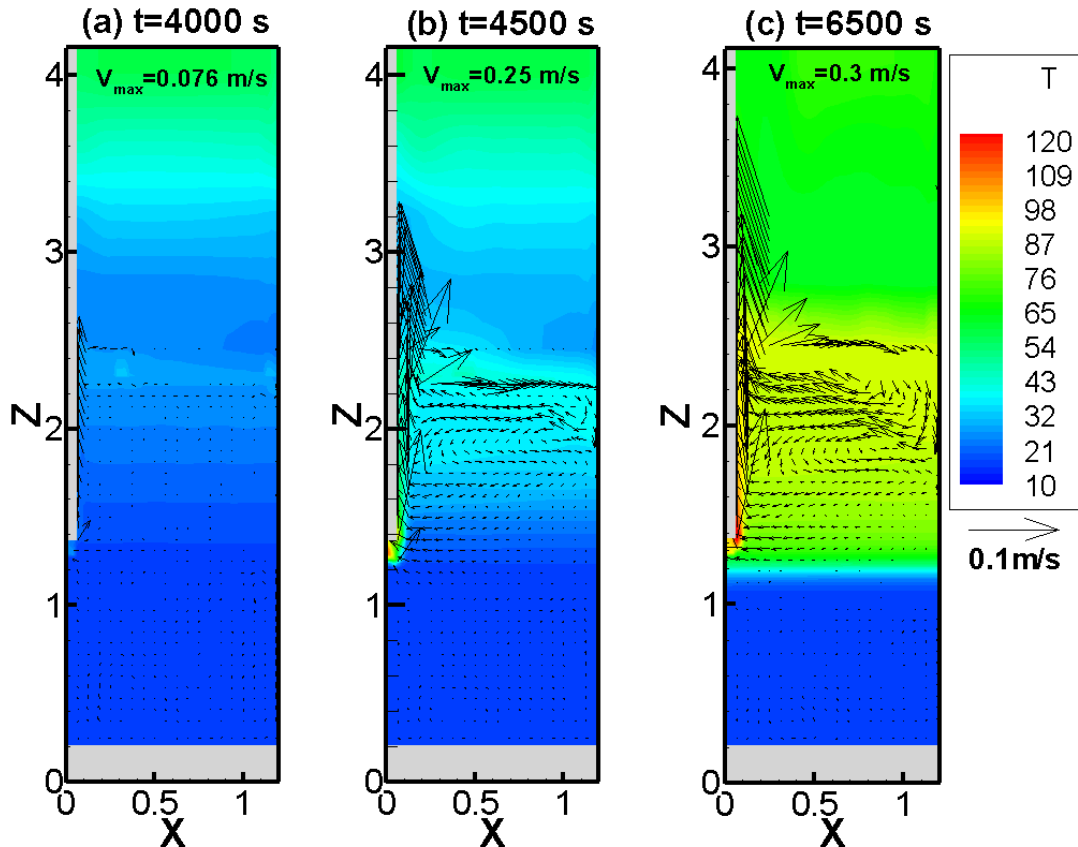


Figure 123. EHS-EMS simulation snapshots of temperature profiles with superimposed velocity fields at different times (a) $t = 4000$ s, during first stratification phase, (b) $t = 4500$ s, and (c) $t = 6500$ s.

5.3.3 EHS/EMS validation against MIX-09 test

The steam mass flow used in the test is shown in Figure 124. A smaller steam flow compared to the previous tests is used during the mixing phase. The effective momentum rates calculated based on the TC readings inside the blowdown pipe is shown in Figure 125.

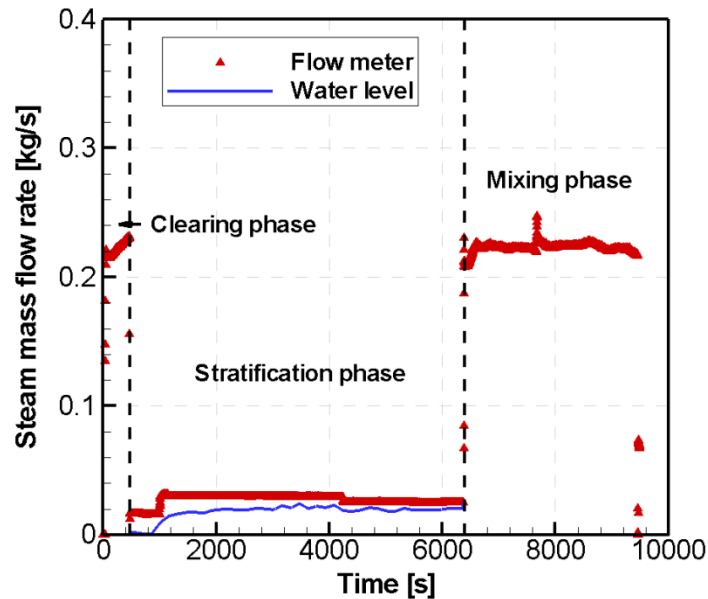


Figure 124: Measured steam mass flow rates with (i) flow meter and (ii) water level in the pool, during the MIX-09 experiment.

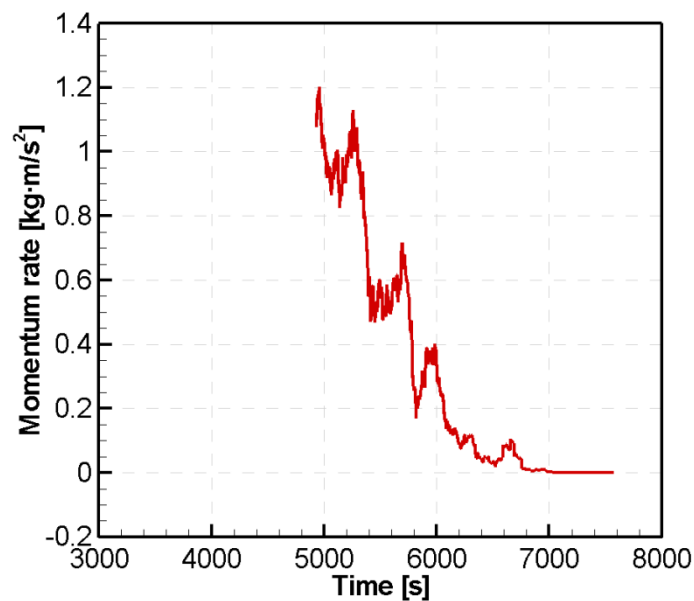


Figure 125: Effective momentum rates based on the water level oscillations in the pipe during the chugging (mixing) phase in MIX-09 test.

The simulation starts ($t = 0$ s) from time 1500 s in Figure 124. The phase with high steam flow rate in the simulation is at time $t = 4877$ s. As seen in Figure 125, the maximum momentum rate is only around $1.2 \text{ kg}\cdot\text{m}/\text{s}^2$ and this rate decreases to 0 at the end of the transient.

The configuration of components used in the modeling is the same as in MIX-07, and is shown in Figure 126. One thermal conductor is spanned on the pipe's submerged surface from the pipe exit.

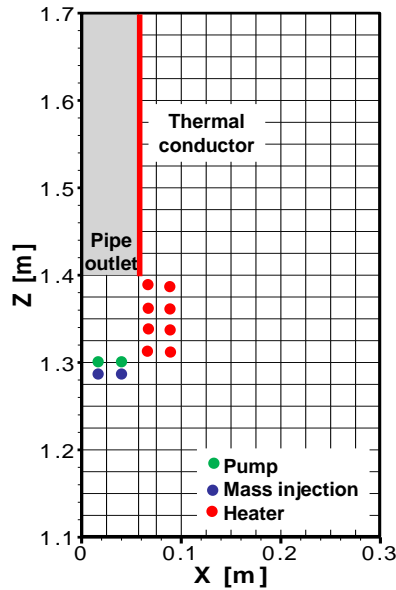


Figure 126: Configurations of components for EHS/EMS model for MIX-09.

Figure 127 shows an excellent agreement on the averaged liquid temperature and the water level in the pool between the EHS-EMS simulation and experiment. At time $t = 0$ s, the averaged liquid temperature is about $15\text{ }^{\circ}\text{C}$ and it increases to $20\text{ }^{\circ}\text{C}$ during the stratification phase. At the end of transient it reaches $58\text{ }^{\circ}\text{C}$ since large steam mass flow rate is used for injection. The initial water level is at 2.405 m and during the stratification phase increases to 2.42 m . And during the phase with high steam flow rate, the water level shows an abrupt increase to 2.62 m .

Figure 128 shows the comparison in pool temperature between the MIX-09 measured data and EHS-EMS simulation. The development of the first thermal stratification in different layers is well captured in the simulation. At the end of the stratification phase, the predicted temperature at the top layer is about $27\text{ }^{\circ}\text{C}$ while the measured temperature is about $32\text{ }^{\circ}\text{C}$ which is attributed to the uniform heat flux imposed on the pipe's submerged surface. For the phase with high steam flow rate, the general behavior is also captured in the simulation. In the experiment, the temperature at the height of 0.75 m increases, while it remains cold in the simulation. This difference is attributed to the under-estimation of the momentum where the jet does not penetrate as deep as in the experiment.

The temperature profiles in the middle (about 1.295 m from the bottom) and bottom layers both in the EHS-EMS simulation and MIX-09 experiment are shown in Figure 129. It shows similar simulation results as in MIX-08, that is, the temperature on the upper part is over-predicted.

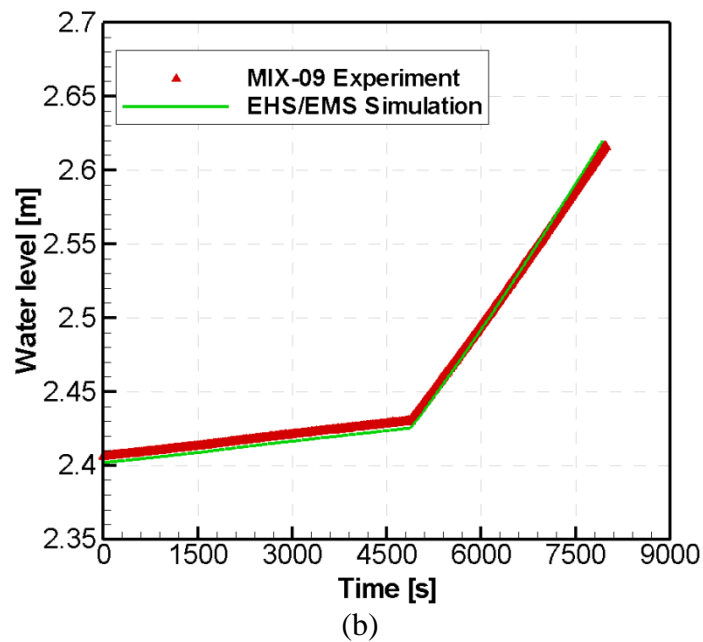
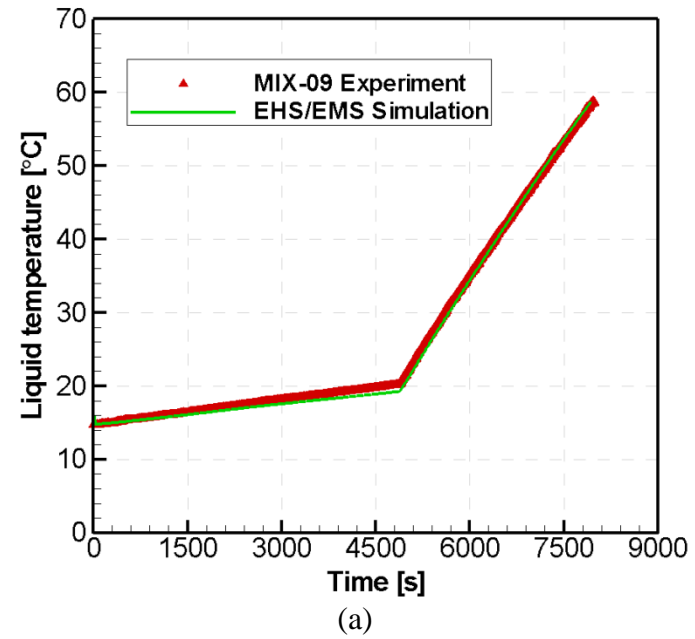
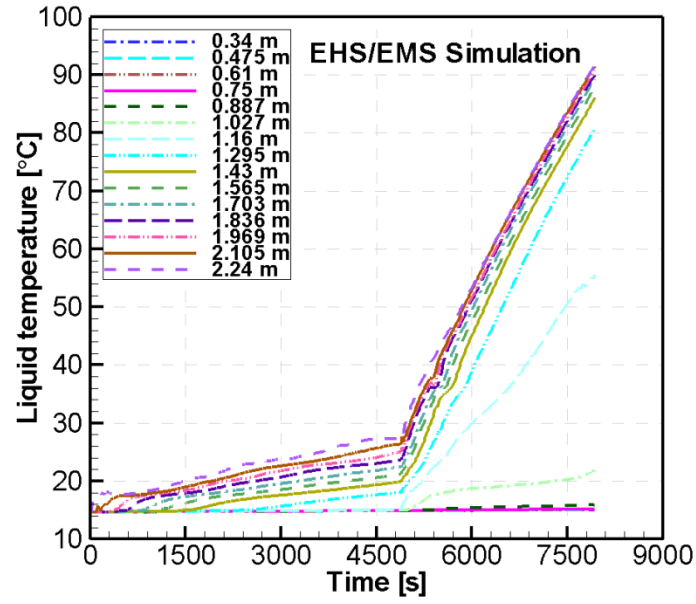
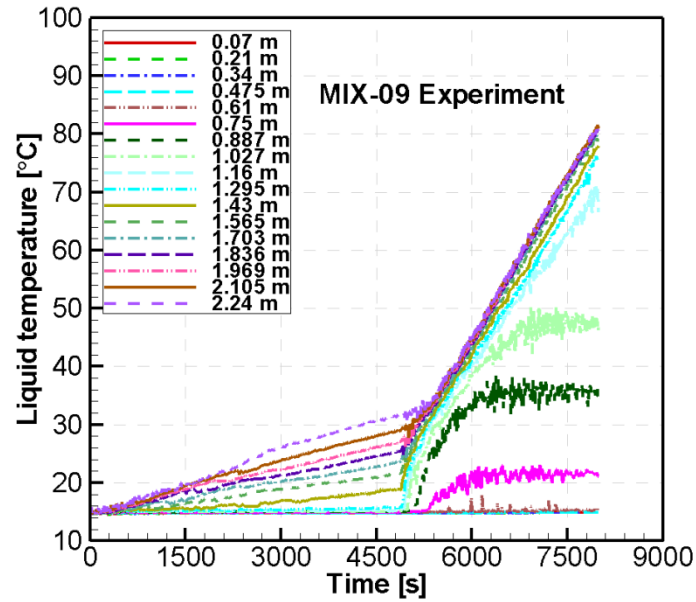


Figure 127: Comparison between EHS-EMS simulation results and MIX-09 test on (a) averaged liquid temperature and (b) water level in the wetwell pool.



(a)



(b)

Figure 128: Comparison of pool temperature between (a) EHS-EMS simulation and (b) MIX-09 measured data. The level of the pipe outlet is at 1.4 m.

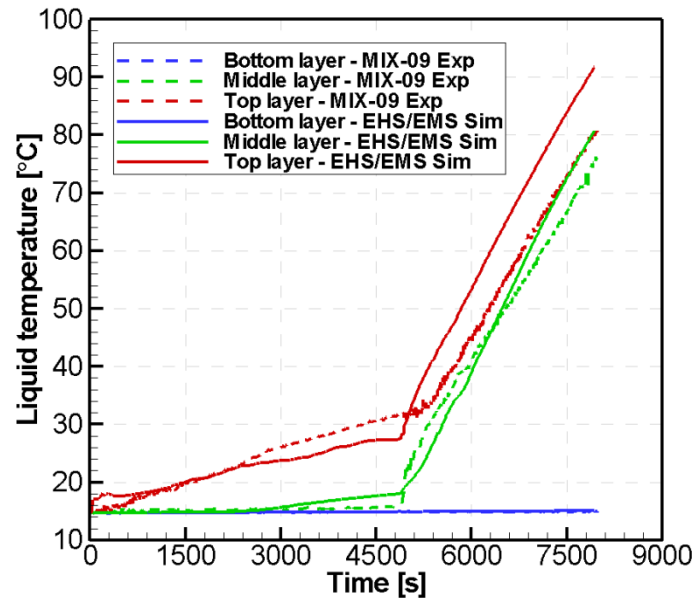
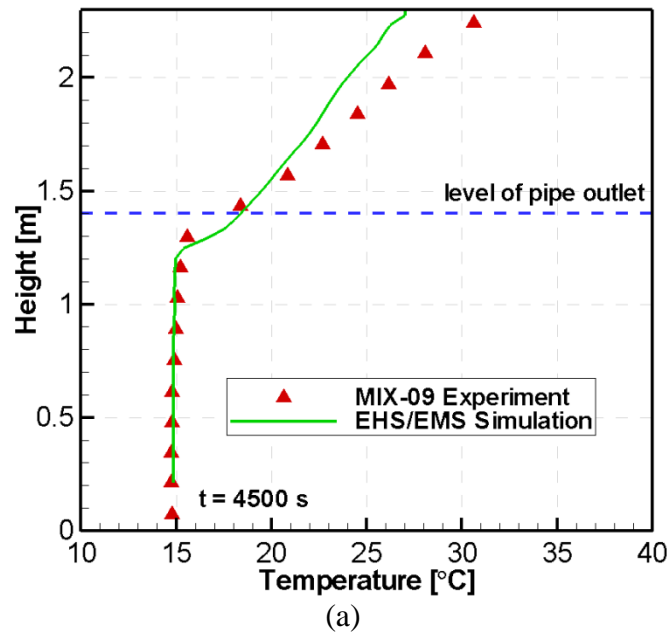
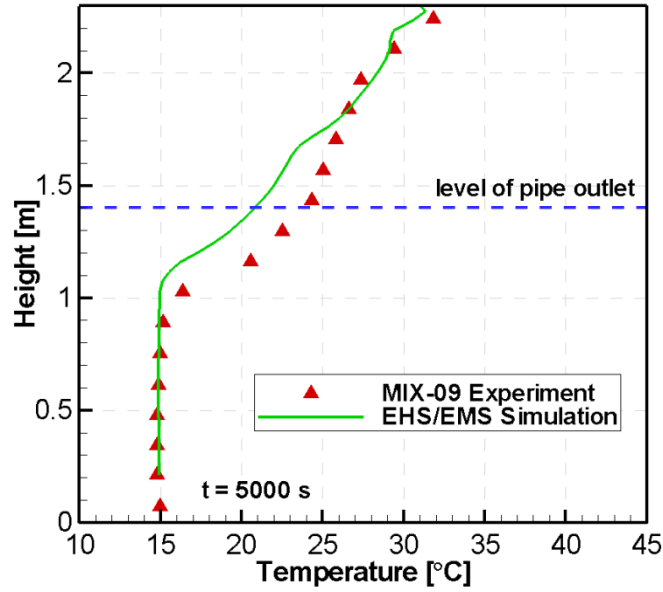


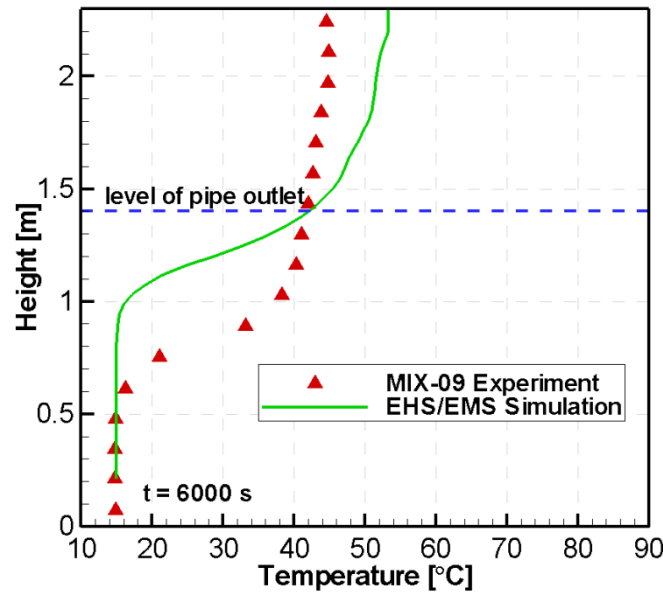
Figure 129: Comparison of pool temperature at selected levels in the pool

In Figure 130a, both the experiment and simulation shows that the layer below the pipe outlet remains cold (about 15 °C, same as initially), while the upper layer develops thermal stratification, near the end of the thermal stratification phase (at time $t = 4500$ s). The temperature behavior in the phase with high steam flow rate is also well captured at time $t = 5000$ s, as seen in Figure 130b. The temperature at the bottom layer remains cold while the middle part starts to mix with upper part. For the condensation regime with transition at time $t = 6000$ s in Figure 130c, the experimental data shows that deeper layers are heated. It implies that the steam jet length should be considered in the simulation for transition condensation regime.





(b)



(c)

Figure 130: Comparison of pool temperature (a) snapshot of vertical temperature profile at time $t = 4500$ s, (b) snapshot of vertical temperature profile at time $t = 5000$ s, (c) snapshot of vertical temperature profile at time $t = 6000$ s.

The predicted temperature and velocity profiles at different times $t = 4500$ s (first stratification phase), $t = 5000$ s and $t = 6000$ s (the phase with high steam flow rate) is shown in Figure 131. A buoyant plume of hot water can be seen in Figure 131a during the stratification phase. At $t = 5000$ s, the buoyant force becomes stronger while the downward momentum remains small. At a later time $t = 6000$ s, the magnitude of the maximum velocity is ~ 0.278 m/s similar to the previous snapshot.

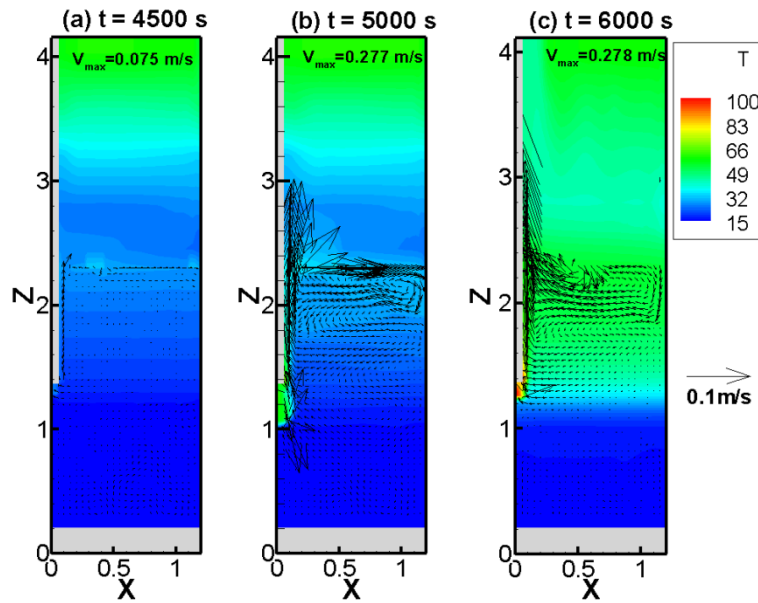


Figure 131. EHS-EMS simulation snapshots of temperature profiles with superimposed velocity fields at different times (a) $t = 4500$ s, during first stratification phase, (b) $t = 5000$ s, and (c) $t = 6000$ s.

5.3.4 EHS/EMS validation against MIX-10 test

The steam mass flow used in the test is shown in Figure 132. The steam flow is around 150 g/s during the ‘mixing’ (chugging) phase. The effective momentum rates calculated based on TC readings inside the blowdown pipe is shown in Figure 133.

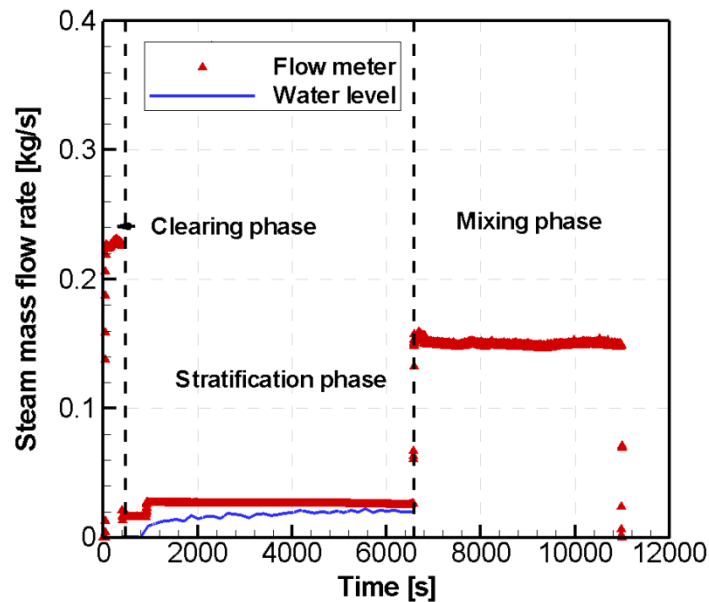


Figure 132: Measured steam mass flow rates with (i) flow meter and (ii) water level in the pool, during the MIX-10 experiment.

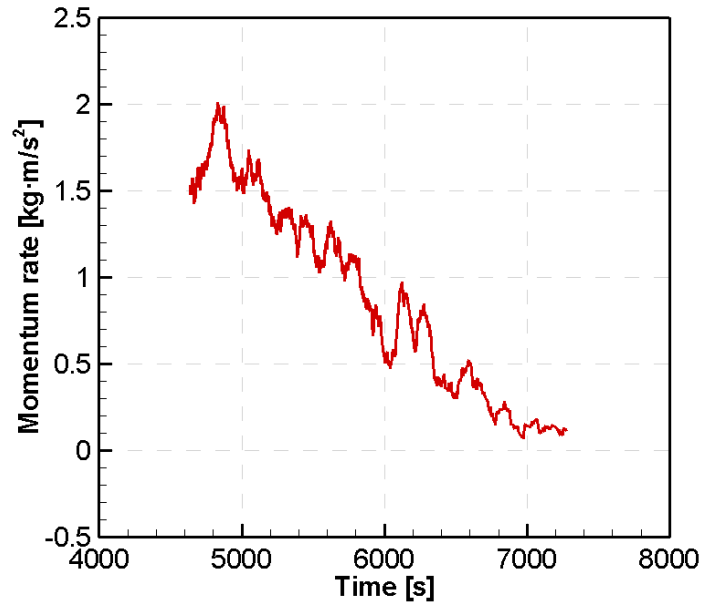


Figure 133: Effective momentum rates based on the water level oscillations in the pipe during the chugging (mixing) phase in MIX-10 test.

The initial time $t = 0$ s in the simulations correspond to time 2000 s in Figure 132. The phase with high steam flow rate in the simulation is at time $t = 4580$ s. The maximum momentum rates with high steam mass flow rate is only around $2 \text{ kg}\cdot\text{m}/\text{s}^2$, slightly higher than in MIX-09 test.

The configuration of components used in the modeling is shown in Figure 134, which is the same as in MIX-09.

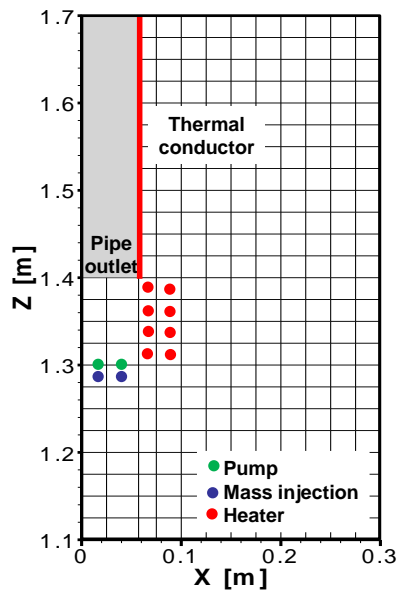
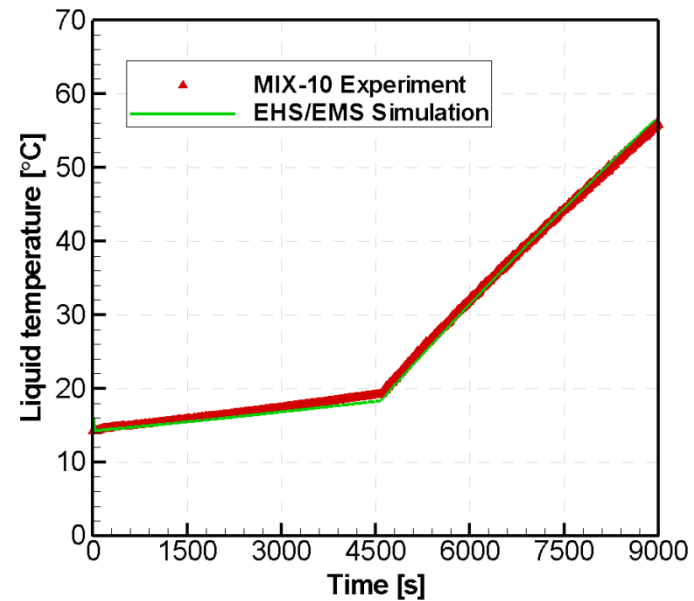


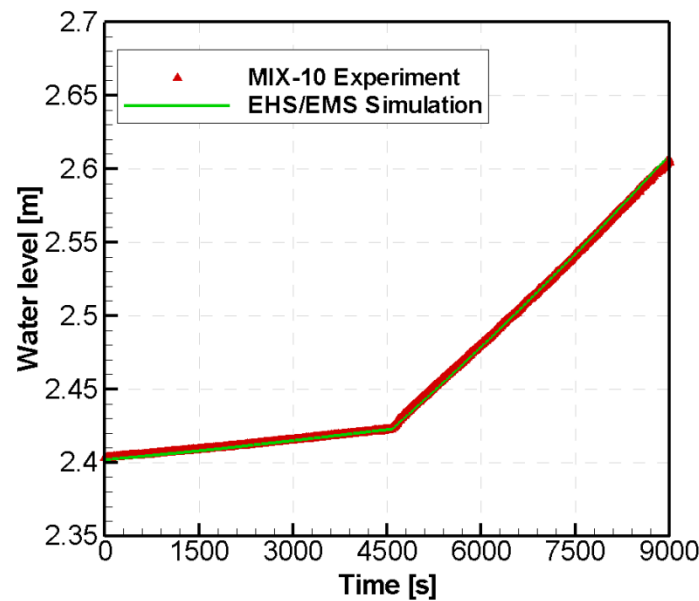
Figure 134: Configurations of components for EHS/EMS model for MIX-10.

Figure 135 shows an excellent agreement on the averaged liquid temperature and the water level in the pool between the EHS-EMS simulation and experiment. At time $t = 0$ s, the averaged liquid temperature is about $14 \text{ }^\circ\text{C}$ and it increases to $19 \text{ }^\circ\text{C}$ during the stratification phase. At the end of transient it reaches $56 \text{ }^\circ\text{C}$. The initial water level

is at 2.4 m and during the stratification phase increases to 2.42 m. And during the phase with high steam flow rate, the water level shows an abrupt increase to 2.6 m.



(a)

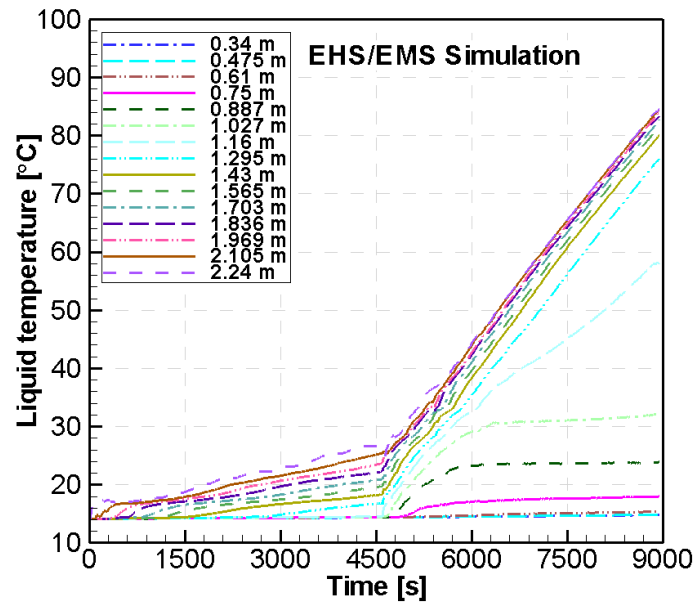


(b)

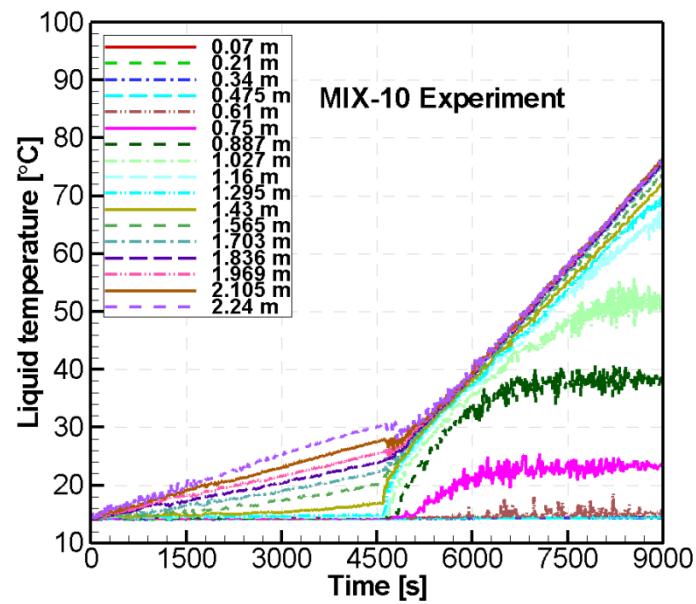
Figure 135: Comparison between EHS-EMS simulation results and MIX-10 test on (a) averaged liquid temperature and (b) water level in the wetwell pool.

The comparison in pool temperature between the MIX-10 measured data and EHS-EMS simulation is shown in Figure 136. The general behavior is captured. However, at the end of the stratification phase, the predicted temperature at the top layer is about ~ 26 °C and under-predicts the experimental value of ~ 30 °C which is attributed to the uniform heat flux distribution as mentioned in MIX-09 test. The further development of thermal stratification at high steam flow rates is also captured, although some of the lower layers has under-predicted temperature.

A more detailed comparison of the temperature behavior in the pool is shown in Figure 137. It can be seen that the temperature at the top layer is over-predicted, since less heat goes directly to the lower part.



(a)



(b)

Figure 136: Comparison of pool temperature between (a) EHS-EMS simulation and (b) MIX-10 measured data. The level of the pipe outlet is at 1.4 m.

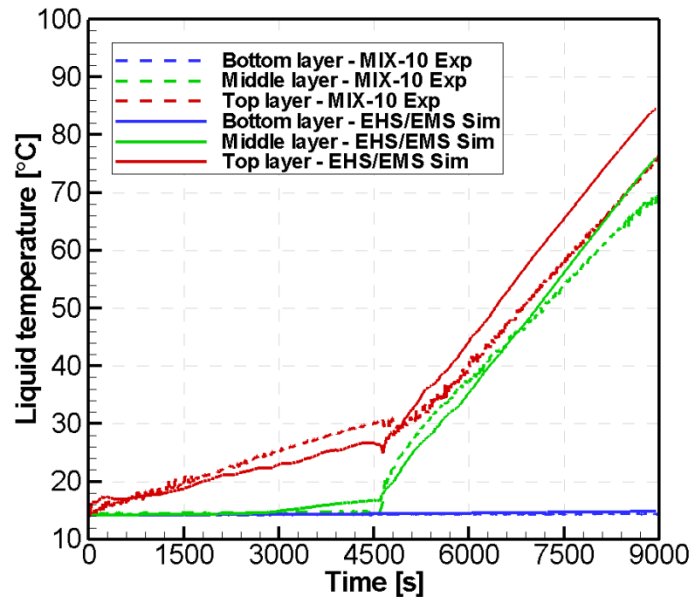
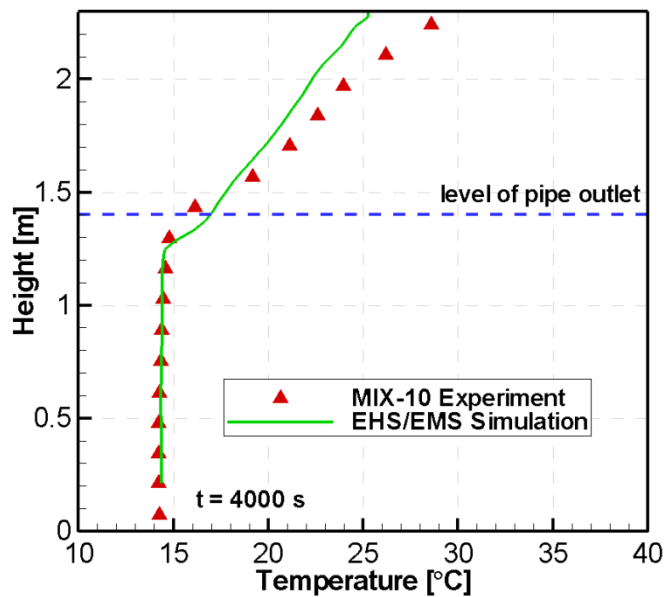
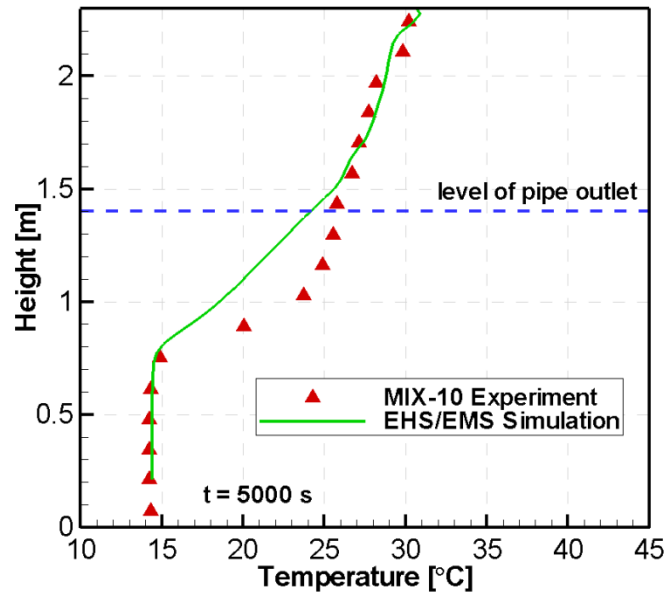


Figure 137: Comparison of pool temperature at selected levels in the pool

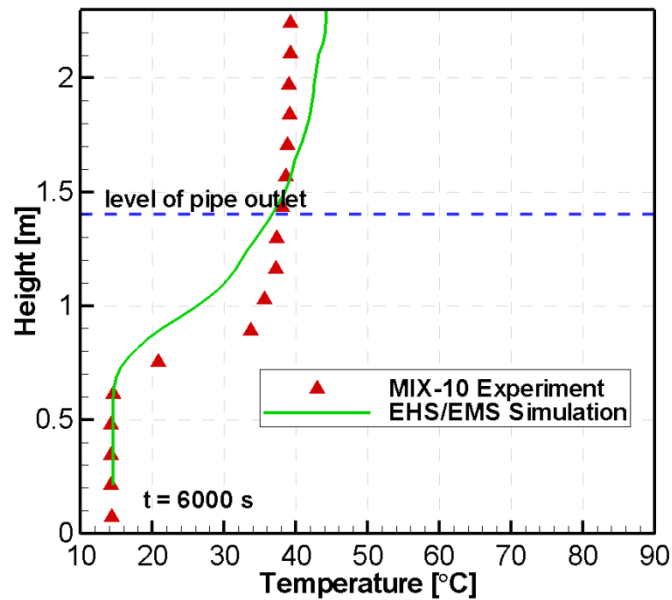
Figure 138a shows a snapshot of the vertical temperature profile near the end of the thermal stratification phase (at time $t = 4000$ s). In general, the simulation captures well the behavior of the stratification. The temperature behavior in the phase with high steam flow rate is also well captured at time $t = 5000$ s, as seen in Figure 138b. For the condensation regime with transition at time $t = 6000$ s in Figure 138c, the experimental data shows that the more layers at the low part are heated up. It implies that the jet reaches deeper layers in the experiment.



(a)



(b)



(c)

Figure 138: Comparison of pool temperature (a) snapshot of vertical temperature profile at time $t = 4000$ s, (b) snapshot of vertical temperature profile at time $t = 5000$ s, (c) snapshot of vertical temperature profile at time $t = 6000$ s.

Figure 139 shows snapshots of the predicted temperature and velocity profiles at different times $t = 4000$ s (first stratification phase), $t = 5000$ s and $t = 6000$ s (the phase with high steam flow rate). At $t = 4000$ s, the magnitude of the maximum velocity at this time is just 0.087 m/s. At $t = 5000$ s, the downward momentum due to chugging is small that it cannot reach the bottom. The magnitude of the maximum velocity at this time is only about 0.361 m/s. At $t = 6000$ s, the downward momentum even decreases.

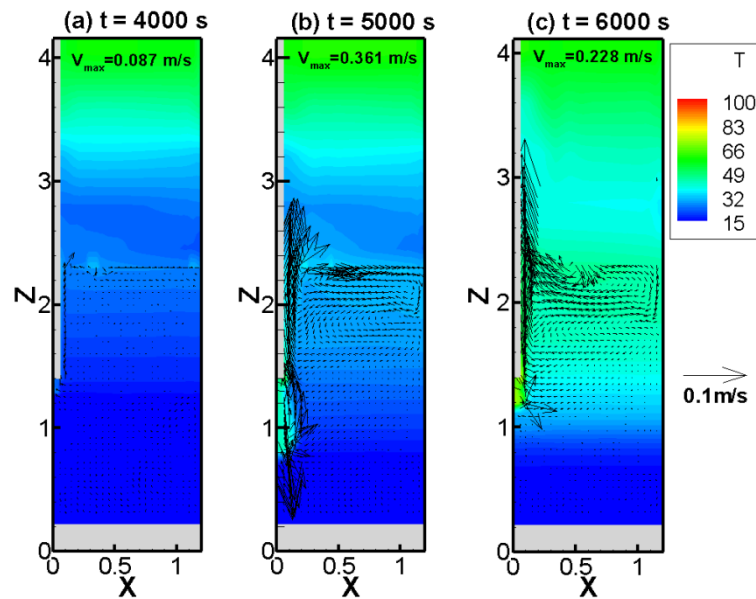


Figure 139. EHS-EMS simulation snapshots of temperature profiles with superimposed velocity fields at different times (a) $t = 4000$ s, during first stratification phase, (b) $t = 5000$ s, and (c) $t = 6000$ s.

5.3.5 EHS/EMS validation against MIX-11 test

In MIX-11, the steam mass flow is shown in Figure 140. Compared to the previous MIX-10 test, only the steam flow rate for mixing phase is different. The effective momentum rates calculated based on TC readings inside the blowdown pipe is shown in Figure 141. The initial time $t = 0$ s in the simulation corresponds to time 2000 s in Figure 140. The start of the phase with high steam flow rate in the simulation is at time $t = 4600$ s.

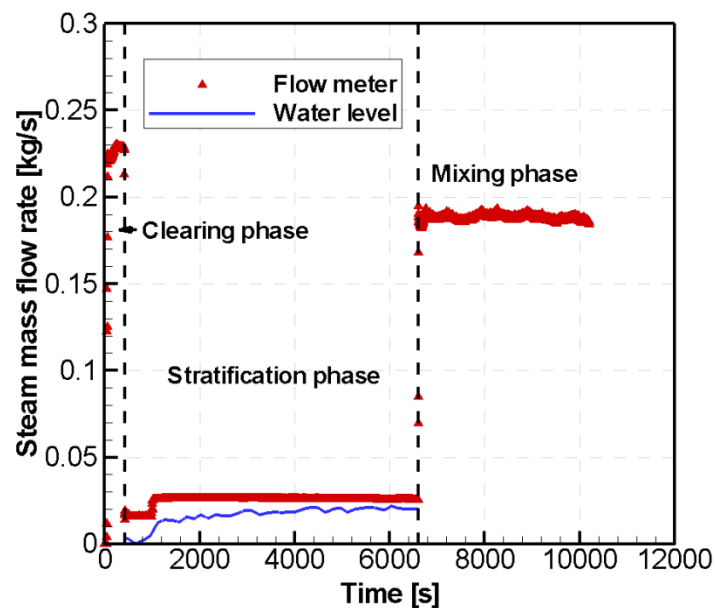


Figure 140: Measured steam mass flow rates with (i) flow meter and (ii) water level in the pool, during the MIX-11 experiment.

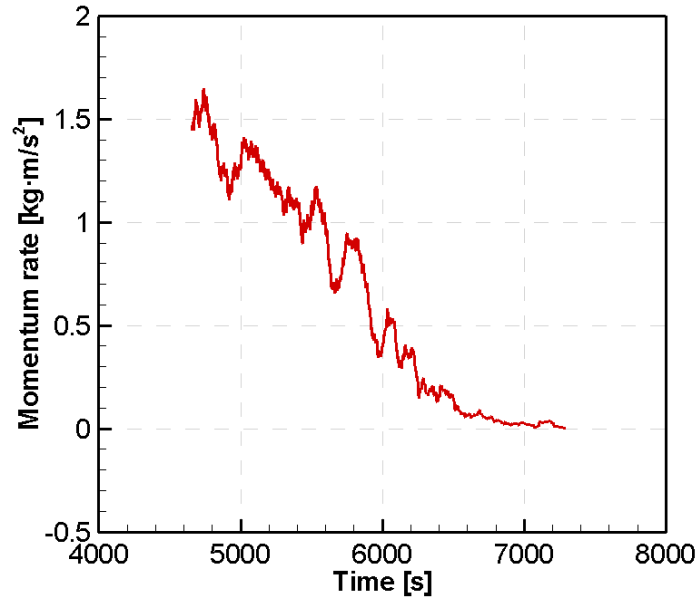


Figure 141: Effective momentum rates based on the water level oscillations in the pipe during the chugging (mixing) phase in MIX-11 test.

The configuration of components used in the modeling is the same as in MIX-07, which can be seen from Figure 142. One thermal conductor is spanned on the pipe's submerged surface from the pipe exit.

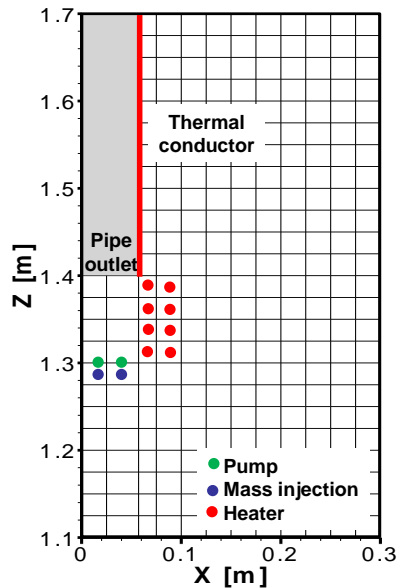
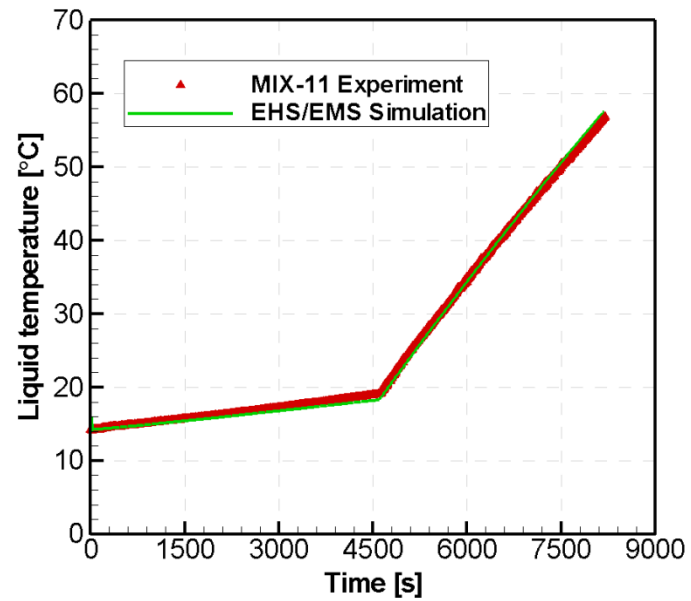
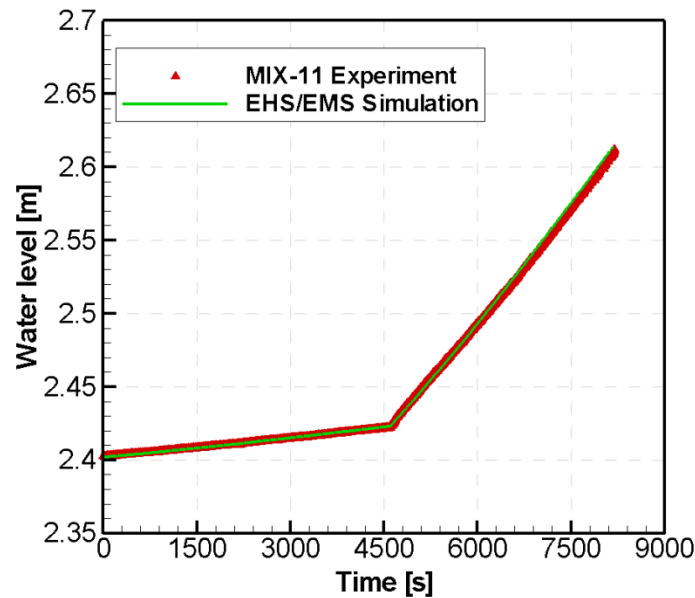


Figure 142: Configurations of components for EHS/EMS model for MIX-11.

An excellent agreement on the averaged liquid temperature and the water level in the pool between the EHS-EMS simulation and experiment is shown in Figure 143. The averaged liquid temperature increases from about 14 °C to 19 °C during the stratification phase. The increase in temperature is more pronounced at the end of transient as it reaches 57 °C. The initial water level is at 2.4 m and during the phase with high steam flow, the water level shows an abrupt increase to 2.61 m both in the simulation and experiment.



(a)

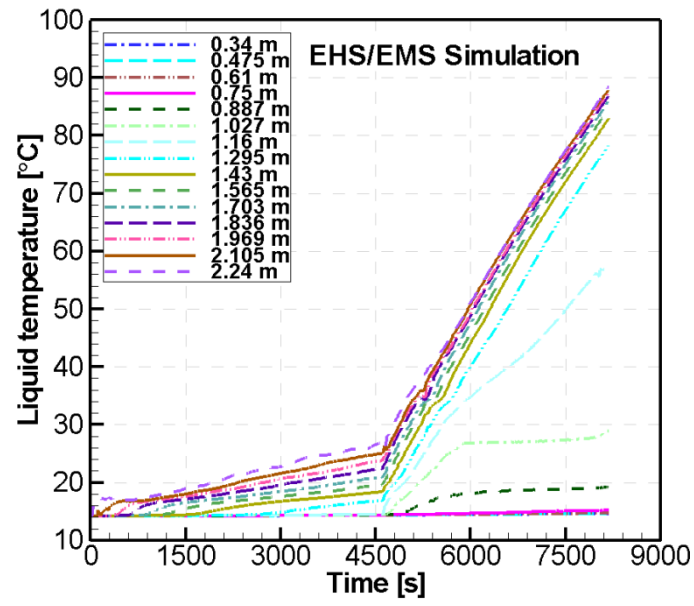


(b)

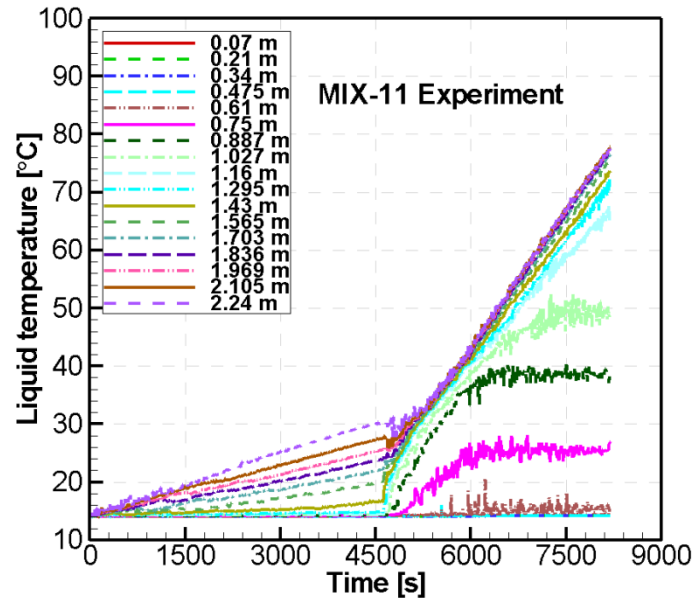
Figure 143: Comparison between EHS-EMS simulation results and MIX-11 test on (a) averaged liquid temperature and (b) water level in the wetwell pool.

Figure 144 shows the comparison in pool temperature. At the end of the stratification phase, the predicted temperature at the top layer is about 26 °C while the measured temperature is about 30 °C. It is shown in the experiment that the temperature at the height of 0.75 m increases at high steam flow. However in the simulation the temperature at the same height of 0.75 m remains cold. The under-estimation of the momentum is the likely the reason, as is also mentioned in previous MIX tests.

A more detailed comparison of the temperature behavior in the pool is shown in Figure 145. The temperature profiles in the middle (about 1.295 m from the bottom) and bottom layers both in the EHS-EMS simulation and MIX-11 experiment shows better agreement than temperatures in the top layer in which the simulation over-predicts the experiment significantly.



(a)



(b)

Figure 144: Comparison of pool temperature between (a) EHS-EMS simulation and (b) MIX-11 measured data. The level of the pipe outlet is at 1.4 m.

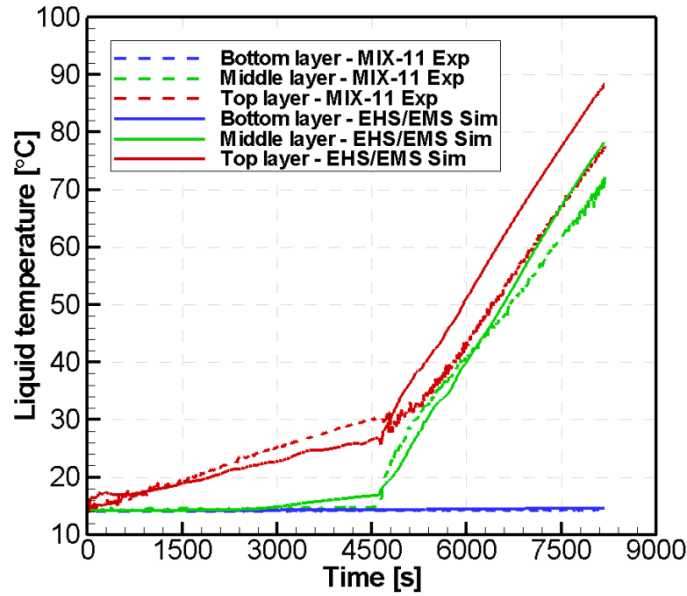
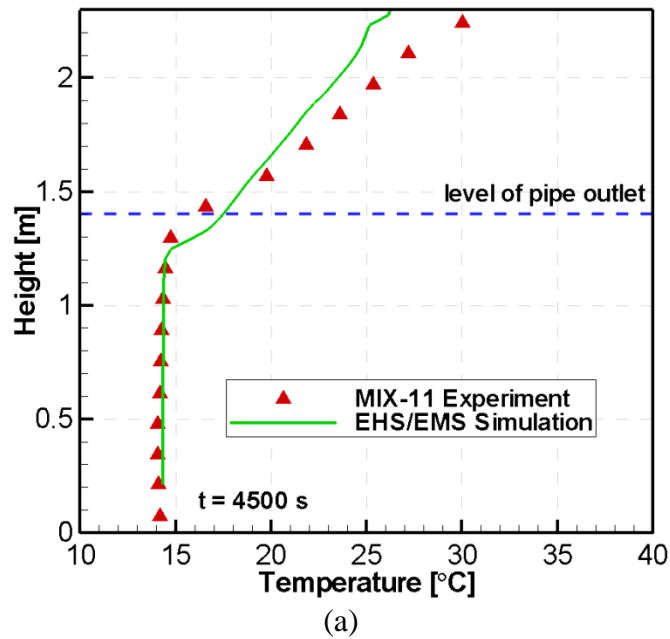
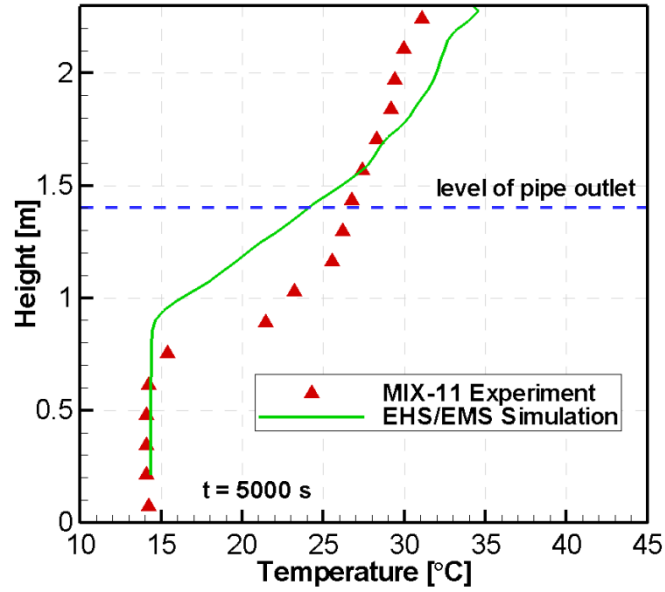


Figure 145: Comparison of pool temperature at selected levels in the pool

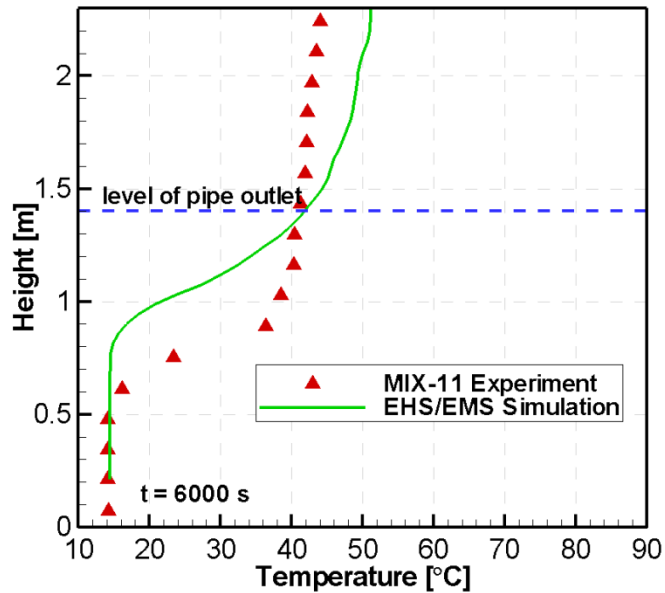
Snapshots of the vertical temperature profile near the end of the thermal stratification phase (at time $t = 4500$ s), and at time $t = 5000$ s, at time $t = 6000$ s with high steam flow rate are shown in Figure 146. The thermal stratification is generally predicted in the simulation. However, differences can be seen in the layers below the pipe outlet which is attributed to the estimation of the jet momentum and in the upper layer which is attributed to the uniform distribution of heat fluxes.



(a)



(b)



(c)

Figure 146: Comparison of pool temperature (a) snapshot of vertical temperature profile at time $t = 4500$ s, (b) snapshot of vertical temperature profile at time $t = 5000$ s, (c) snapshot of vertical temperature profile at time $t = 6000$ s.

Figure 147 shows snapshots of the predicted temperature and velocity profiles at different times $t = 4500$ s (first stratification phase), $t = 5000$ s and $t = 6000$ s (the phase with high steam flow rate). At $t = 4500$ s, the upper layer develops a thermally stratified layer mainly due to a buoyant plume near the pipe surface. At $t = 5000$ s, the buoyant force becomes stronger while the downward momentum remains weak. At a later time $t = 6000$ s, the behavior is more pronounced than in the previous time, that is, stronger buoyancy and weaker downward momentum from the jet.

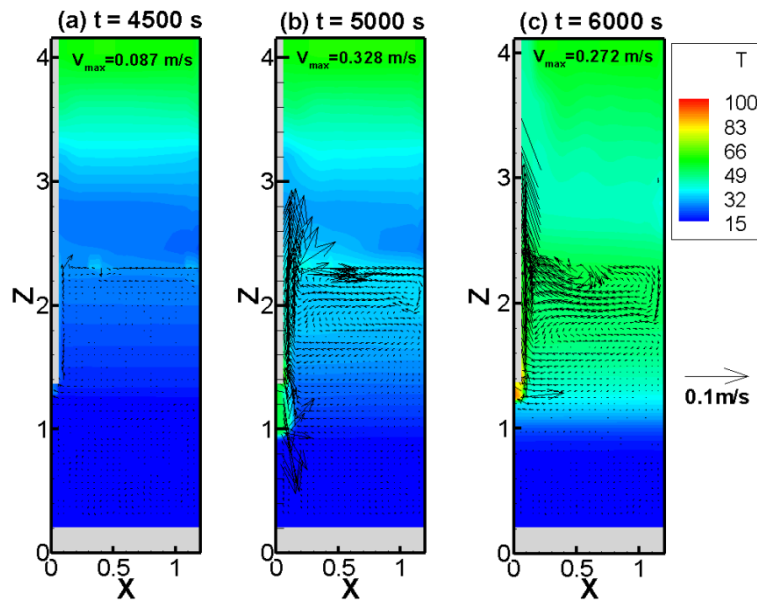


Figure 147. EHS-EMS simulation snapshots of temperature profiles with superimposed velocity fields at different times (a) $t = 4500$ s, during first stratification phase, (b) $t = 5000$ s, and (c) $t = 6000$ s.

5.3.6 EHS/EMS validation against MIX-12 test

Figure 148 shows the steam mass flow rates in MIX-12 test. Only the steam flow rate during the ‘mixing’ (chugging) phase is different compared to the previous MIX-11 test. Figure 149 shows the decreasing effective momentum rates calculated based on TC readings inside the blowdown pipe. The simulation starts from time 1500 s in Figure 148. The start of the phase with high steam flow rate in the simulation is at time $t = 5106$ s. The configuration of components used in the modeling is shown Figure 150. One thermal conductor is spanned on the pipe’s submerged surface from the pipe exit.

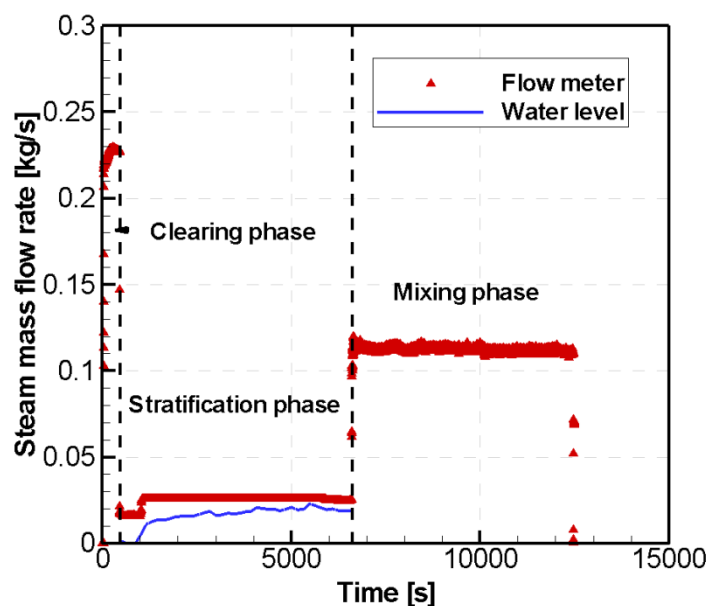


Figure 148: Measured steam mass flow rates with (i) flow meter and (ii) water level in the pool, during the MIX-12 experiment.

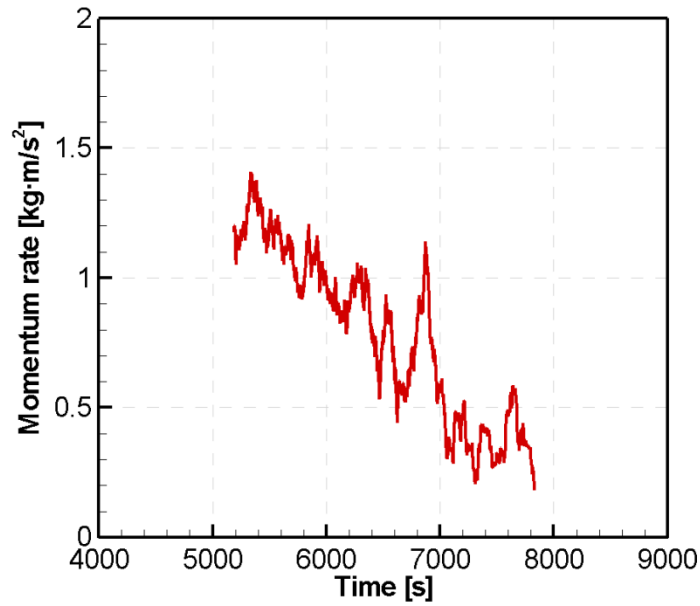


Figure 149: Effective momentum rates based on the water level oscillations in the pipe during the chugging (mixing) phase in MIX-12 test.

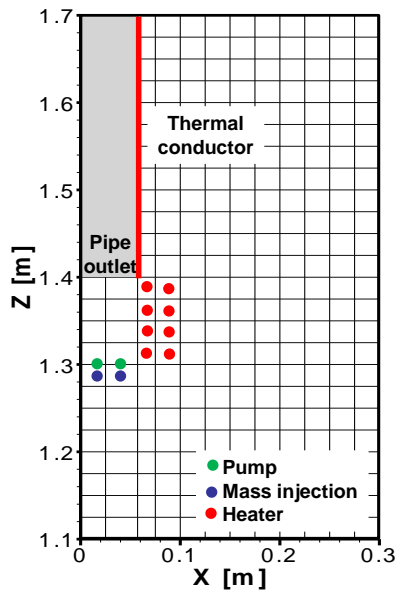
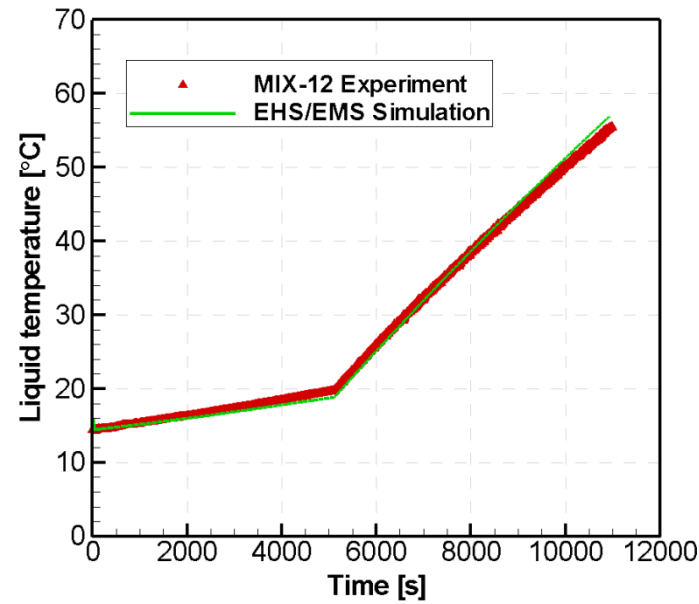
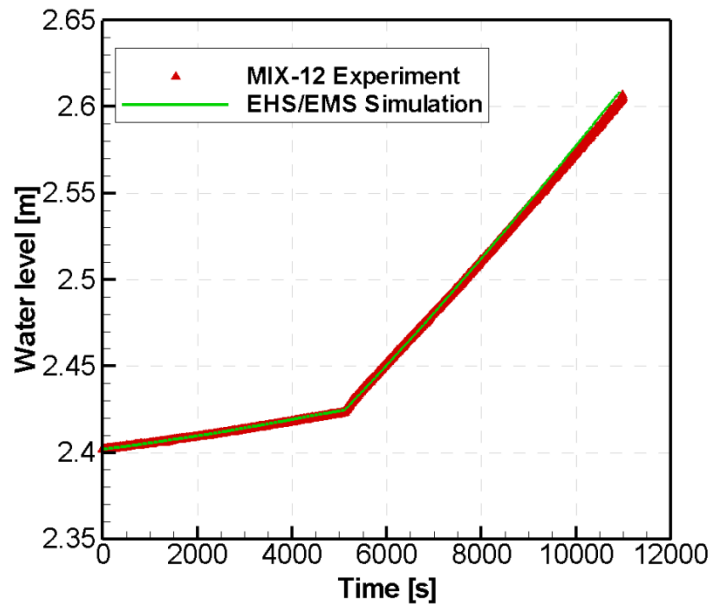


Figure 150: Configurations of components for EHS/EMS model for MIX-12.

An excellent agreement on the averaged liquid temperature and the water level in the pool between the EHS-EMS simulation and the experiment is shown in Figure 151. At time $t = 0$ s, the averaged liquid temperature is about $14.5\text{ }^{\circ}\text{C}$ and it increases to $20\text{ }^{\circ}\text{C}$. At the end of transient it reaches $56\text{ }^{\circ}\text{C}$ while the predicted temperature is $55\text{ }^{\circ}\text{C}$. The initial water level is at 2.4 m and during the stratification phase increases to 2.42 m . And during the phase with high steam flow, the water level shows an abrupt increase to 2.61 m both in the simulation and experiment.



(a)

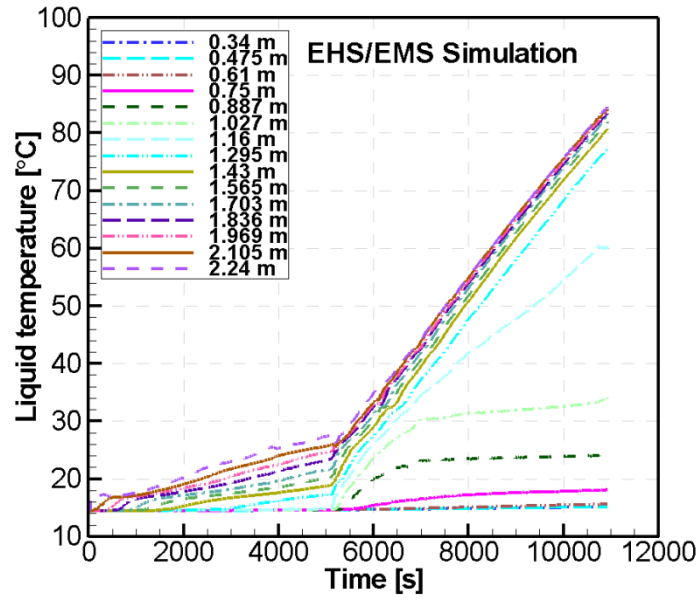


(b)

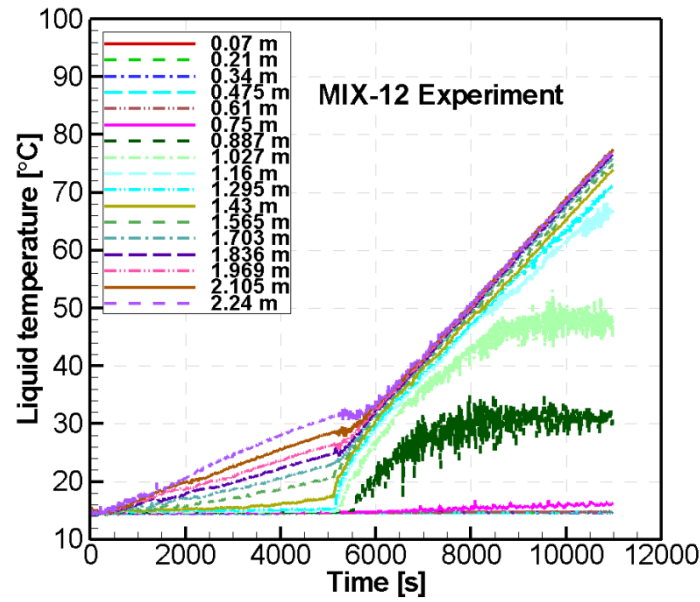
Figure 151: Comparison between EHS-EMS simulation results and MIX-12 test on (a) averaged liquid temperature and (b) water level in the wetwell pool.

The development of the first thermal stratification in different layers is well captured in the simulation, as shown in Figure 152. Although at the end of the stratification phase, the predicted temperature at the top layer is about 27 °C while the measured temperature is about 32 °C. Incomplete mixing is observed in the experiment and is also captured in the simulation.

A more detailed comparison of the temperature behavior in the pool is shown in Figure 153. The temperature profiles of the middle (about 1.295 m from the bottom) and bottom layers both in the EHS-EMS simulation and MIX-12 experiment are shown and they generally agree well. Differences at the top layers, as also observed previously, is due to the uniform heat distribution on the pipe's submerged surface.



(a)



(b)

Figure 152: Comparison of pool temperature between (a) EHS-EMS simulation and (b) MIX-12 measured data. The level of the pipe outlet is at 1.4 m.

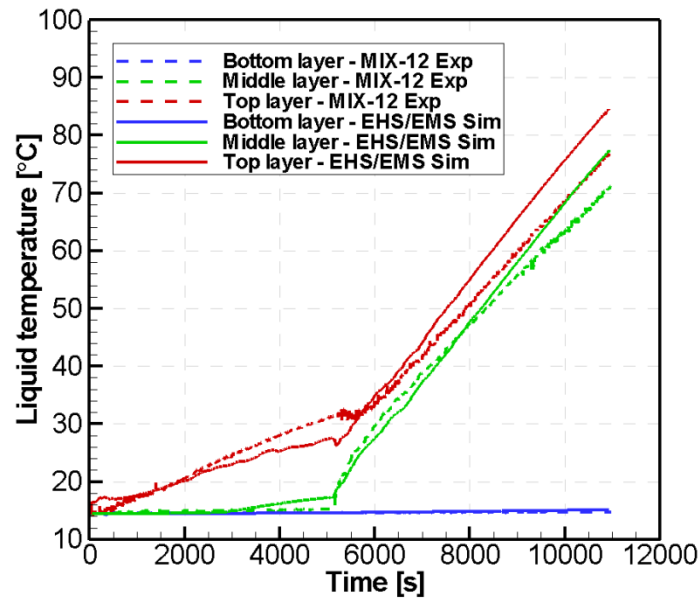
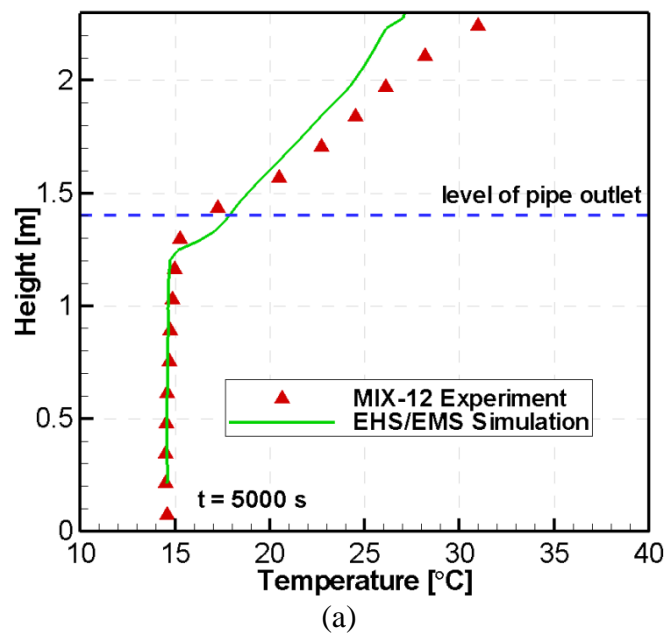
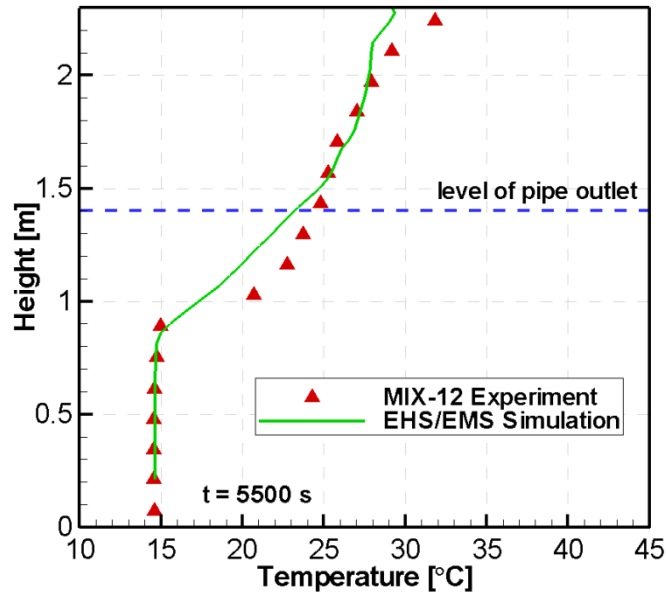


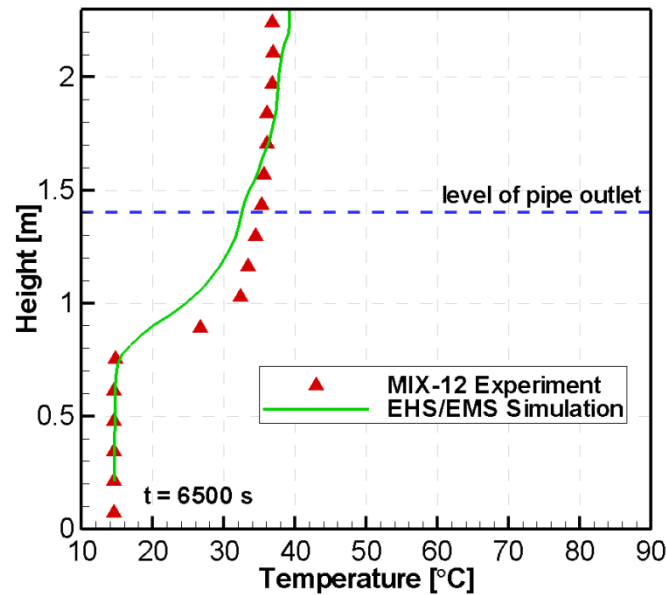
Figure 153: Comparison of pool temperature at selected levels in the pool

In Figure 154, snapshots of the vertical temperature profile at different times are shown. The comparison generally shows good agreement. Finer mesh around the pipe exit could improve the simulation results and expected to decrease the differences with the experiment.





(b)



(c)

Figure 154: Comparison of pool temperature (a) snapshot of vertical temperature profile at time $t = 5000$ s, (b) snapshot of vertical temperature profile at time $t = 5500$ s, (c) snapshot of vertical temperature profile at time $t = 6500$ s.

Figure 155 shows snapshots of the predicted temperature and velocity profiles at different times $t = 5000$ s (first stratification phase), $t = 5500$ s and $t = 6500$ s (the phase with high steam flow rate). At $t = 5000$ s, the heating of the water surrounding the pipe creates a buoyant plume of hot water. The magnitude of the maximum velocity at this time is just 0.076 m/s. At $t = 5500$ s, the buoyant force is much stronger due to the high steam mass flow rate at the pipe exit. The downward momentum can be seen and the jet does not reach the bottom. The magnitude of the maximum velocity at this time is about 0.322 m/s. At $t = 6500$ s, the downward momentum decreases and the flow behavior in the pool is still dominated by buoyancy.

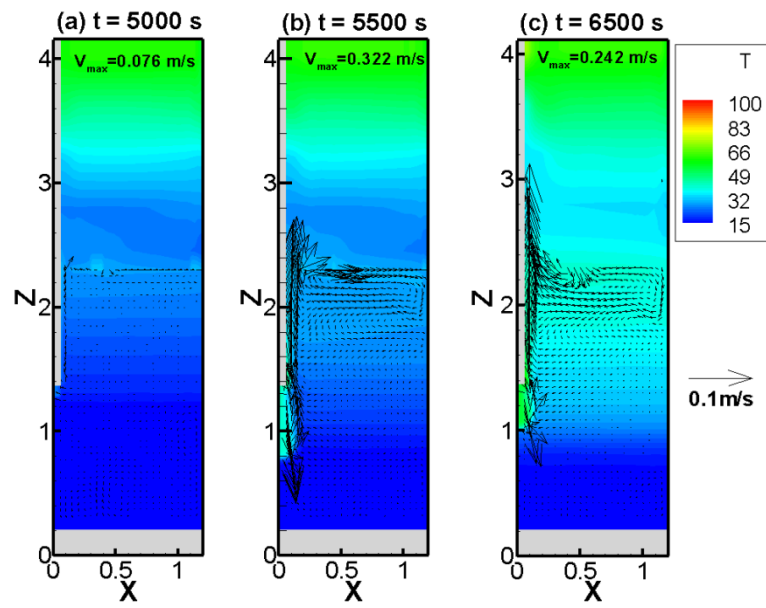


Figure 155. EHS-EMS simulation snapshots of temperature profiles with superimposed velocity fields at different times (a) $t = 4500$ s, during first stratification phase, (b) $t = 5000$ s, and (c) $t = 6000$ s.

6 Scaling approach for generalization of experimental data on amplitude and frequency of oscillations

6.1 Available experimental data and relevant scaling parameters

We present two sets of available experimental data, first, the PPOOLEX-MIX tests [14] performed at the Lappeenranta University of Technology (LUT) in Finland, and second, the experiments performed by Aya and Nariai [9, 10, 51].

The PPOOLEX facility is a closed cylindrical stainless steel tank with an outer diameter of 2.4 m, a water pool depth of 2.14 m, and a pipe submergence depth of 1.05 m. The schematic diagram of the PPOOLEX MIX experimental tests is shown in Figure 156. Steam is injected with a mass flux G through the drywell part of the containment having a volume V and pressure P_D . At first, steam pushes non-condensable gases through a blowdown pipe with diameter d to the wetwell part of the containment. Depending on the condensation regime, the steam-water interface can oscillate inside the blowdown pipe with an amplitude z and frequency f , such as in chugging regime.

There are 12 experimental tests performed in PPOOLEX-MIX series. The first subseries, MIX-01 to 06, was done with a 0.209 m diameter of the blowdown pipe while the second, MIX-07 to 12, was done with a smaller 0.109 m diameter of the blowdown pipe. The MIX tests cover three regimes in the condensation regime map [2] as shown in Figure 157; condensation within the blowdown pipe (regime 1), chugging (regime 2), and transition (regime 5). All tests start from regime 1 followed by regime 2 and then go to regime 5. The second subseries covers a wider region in the chugging regime than the first subseries.

Aya and Nariai [9, 10, 51] have performed similar experiments earlier (see schematic in Figure 165), but in a smaller scale (more details later). The cylindrical pool is open with a diameter of 0.5 m and a pipe submergence depth of 0.25 m.

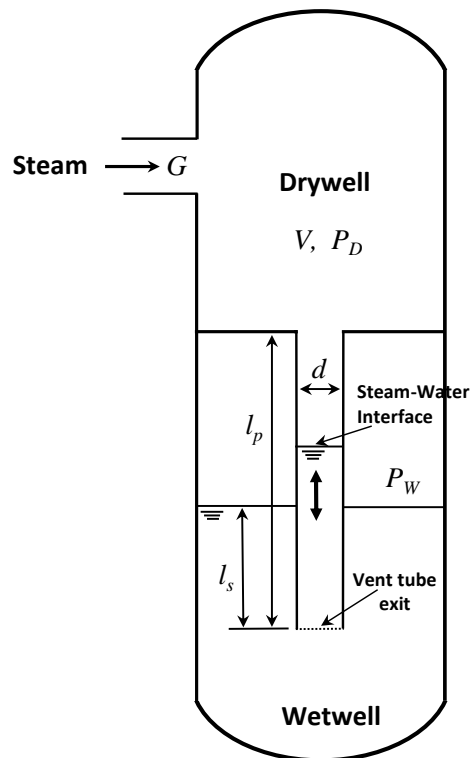


Figure 156: Schematic of the PPOOLEX MIX tests [14]

Table 3 summarizes the relevant dimensional parameters and measured or calculated quantities in the MIX tests and Aya and Nariai experiments. The MIX test set-up is much larger than the Aya and Nariai experimental set-up as mentioned earlier. The volume of the header (V) in the PPOOLEX MIX facility is 13.3 m^3 and in Aya and Nariai set-up it is only 0.02 m^3 . More importantly, the diameters of the blowdown pipe (d) in MIX tests are 0.209 m and 0.109 m while in Aya and Nariai experiments it is only 0.018 m . The length of the blowdown pipe (l_p) in MIX-01 to 06 is 3.14 m while in MIX-07 to 12, it is 2.83 m , and they are about 3 times compared to Aya and Nariai experiments where $l_p = 1 \text{ m}$. The measured steam mass fluxes (G) in the MIX tests range from $7.81\text{-}30.98 \text{ kg/m}^2\text{s}$ and the range in the Aya and Nariai experiments is from $0.65\text{-}20.65 \text{ kg/m}^2\text{s}$. Also in MIX tests, the pressure in the header/drywell ranges from $2.45\text{-}3.34 \text{ bars}$ and is comparable to the pressure in the wetwell that ranges from $2.40\text{-}3.28 \text{ bars}$. But in the Aya and Nariai experiments, the pressure in the header and wetwell is just a bit above 1 bar . The steam vapor temperature in the header is between $126.8\text{-}137.3 \text{ }^\circ\text{C}$ in MIX tests, higher than in the Aya and Nariai experiment at $100.5 \text{ }^\circ\text{C}$. The pool ‘bulk’ temperature in MIX tests, denoted by T_p (which is the temperature measured in the same horizontal layer as the pipe outlet but located about 0.8 m away from the axis of the pipe), is between $16.4\text{-}44.9 \text{ }^\circ\text{C}$. In the Aya and Nariai experiment, the pool temperature is kept nearly constant during short transient tests, e.g., $20 \text{ }^\circ\text{C}$. Similarly, the pool saturation temperature in the Aya and Nariai tests is at $100 \text{ }^\circ\text{C}$, lower than in the MIX tests that is within the range $126.1\text{-}136.5 \text{ }^\circ\text{C}$. Other relevant dimensional parameters in both experiments are given in Table 3.

Table 4 summarizes the corresponding non-dimensional parameters associated with the dimensional parameters in Table 3. The aspect ratio (\tilde{l}) of pipe length to the submergence depth is from $2.56\text{-}3.04$ in MIX tests compared to 4.0 in the Aya and Nariai experiments. The ratio (\tilde{V}) of header/drywell volume to initial volume occupied

by liquid inside the pipe is orders of magnitude different between the experiments. The ratio is from 342.2-375.8 in MIX 01-06 tests, 1281.2-1385.4 in MIX 07-08, and 63.0 in Aya and Nariai experiments. The scaled pool temperature (\tilde{T}) with respect to the saturation temperature is comparable between experiments, around 0.8.

The Euler number (Eu), which is the ratio of pressure forces to inertial forces, is from 0.03-0.52 in MIX tests, compared to a wider range of 0.02-18.99 in the Aya and Nariai experiments. The Froude number (Fr), which is the ratio of inertial forces to gravitational forces, is from 4.15-17.73 in the MIX tests, which is narrower than the range 2.44-80.80 in the Aya and Nariai experiments. The Reynolds number based on the steam injection (Re_s), which is defined as the ratio of inertial forces to viscous forces, is from 6.33×10^4 - 2.05×10^5 in the MIX tests, compared to a lower range of 9.16×10^2 - 3.03×10^4 in the Aya and Nariai experiments. The Grashof number (Gr_l), which is the ratio of buoyancy to viscous forces, is from 3.57×10^9 - 6.43×10^{10} in the MIX tests compared to 1.31×10^7 in the Aya and Nariai. Values of the Jakob number (Ja), which is the ratio of sensible heat to latent heat, is also determined; 96.28-149.90 in the MIX tests and 243.43 in the Aya and Nariai. Lastly, the Richardson number (Ri) which is defined as the ratio of Grashof number to the square of the Reynolds number, relating the natural to forced convection is also calculated; a range of 0.07-2.64 in the MIX tests and a range of 0.01-15.66 in the Aya and Nariai experiments. During the chugging phenomena, the dimensionless numbers indicate an inertial flow dominating over pressure and viscous forces but competing against buoyancy forces.

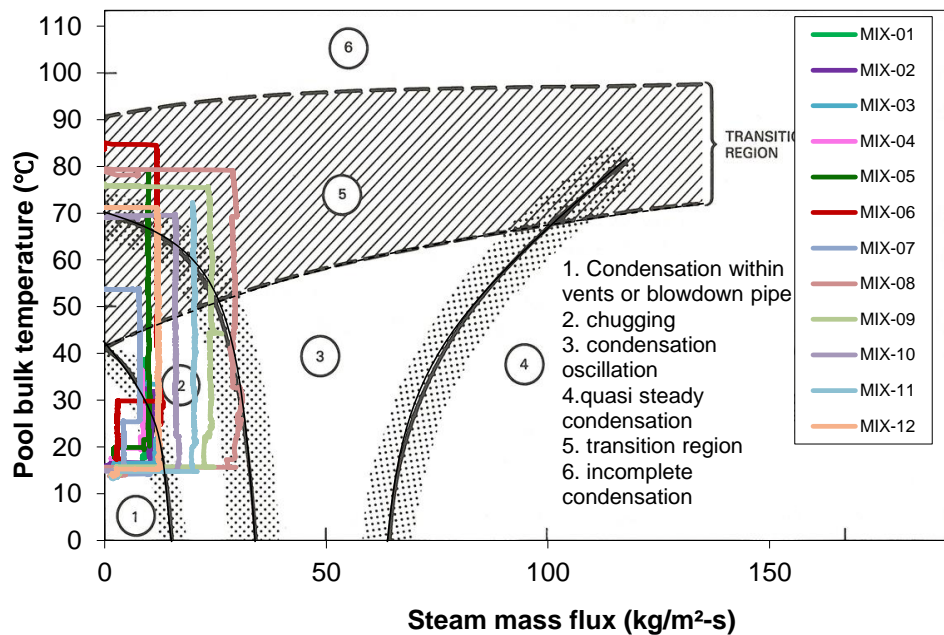


Figure 157: Condensation regimes of the MIX tests [2, 14].

Table 3: Relevant dimensional parameters and measured/calculated quantities in MIX tests and Aya and Nariai experiment.

	Header Volume V [m ³]	Pipe diameter d [m]	Pipe length l_p [m]	Submergence depth l_s [m]	Steam Mass Flux G [kg/m ² s]	Header pressure P_D [bar]	Wetwell pressure P_w [bar]	Header vapor temperature $T_s(P_D)$ [°C]	Pool temperature* T_p [°C]	Pool sat. temperature $T_{sat}(P_w)$ [°C]	Steam viscosity $\mu_s(P_D)$ [Pa·s]	Liquid viscosity $\mu_l(P_w, T_p)$ [Pa·s]	Specific heat capacity $C_{p,l}(P_w, T_p)$ [kJ/(kg·°C)]	Latent heat $h_{fg}(P_D)$ [kJ/kg]	Pool liquid density $\rho_l(P_w, T_p)$ [kg/m ³]	Header vapor density $\rho_s(P_D)$ [kg/m ³]
MIX-01	13.3	0.209	3.139	1.03-1.10	9.22-10.29	2.45-2.57	2.40-2.47	126.8-128.3	18.2-37.7	126.1-127.0	1.32e-5	6.82e-4-1.05e-3	4.18-4.19	2179-2183	993.1-998.6	1.37-1.43
MIX-02	13.3	0.209	3.139	1.07-1.09	10.13-12.53	2.56-2.64	2.49-2.53	128.2-129.2	30.8-34.1	127.3-127.9	1.32e-5	7.33e-4-7.83e-4	4.18-4.18	2176-2179	994.4-995.5	1.42-1.46
MIX-03	13.3	0.209	3.139	1.03-1.08	12.44-12.84	2.53-2.62	2.47-2.53	127.8-129.0	18.0-32.2	127.0-127.8	1.32e-5	7.61e-4-1.05e-3	4.18-4.19	2177-2180	995.0-998.7	1.41-1.46
MIX-04	13.3	0.209	3.139	1.05-1.09	8.82-9.20	2.82-2.95	2.73-2.82	131.5-133.0	23.1-36.4	130.3-131.4	1.34e-5	7.00e-4-9.29e-4	4.18-4.18	2165-2169	993.6-997.6	1.56-1.63
MIX-05	13.3	0.209	3.139	1.06-1.13	10.21-10.65	3.01-3.25	2.93-3.13	133.7-136.2	22.7-44.7	132.8-135.0	1.34e-5	5.99e-4-9.39e-4	4.18-4.18	2155-2163	990.4-997.7	1.66-1.78
MIX-06	13.3	0.209	3.139	1.07-1.13	12.18-13.13	2.87-3.06	2.80-2.93	132.1-134.2	26.7-44.9	131.1-132.7	1.34e-5	5.97e-4-8.56e-4	4.18-4.18	2162-2168	990.3-996.7	1.59-1.68
MIX-07	13.3	0.1093	2.827	1.04-1.09	7.81-8.03	3.12-3.34	3.06-3.28	134.9-137.3	25.9-45.0	134.2-136.5	1.35e-5	5.96e-4-8.72e-4	4.18-4.18	2152-2159	990.3-996.9	1.72-1.83
MIX-08	13.3	0.1093	2.827	1.02-1.10	28.09-30.98	3.02-3.23	2.92-3.14	133.7-136.1	18.4-45.0	132.7-135.1	1.34e-5	5.96e-4-1.04e-3	4.18-4.19	2156-2163	990.3-998.6	1.66-1.77
MIX-09	13.3	0.1093	2.827	1.03-1.10	22.17-26.32	3.13-3.34	3.06-3.27	134.9-137.2	18.0-45.0	134.2-136.5	1.35e-5	5.96e-4-1.05e-3	4.18-4.19	2152-2159	990.3-998.7	1.72-1.83
MIX-10	13.3	0.1093	2.827	1.02-1.10	15.72-16.95	3.07-3.31	3.00-3.23	134.3-136.9	16.2-45.0	133.6-136.1	1.35e-5	5.97e-4-1.10e-3	4.18-4.19	2154-2161	990.3-999.0	1.69-1.81
MIX-11	13.3	0.1093	2.827	1.02-1.11	19.39-20.60	3.08-3.31	3.00-3.23	134.4-136.9	16.4-44.9	133.5-136.0	1.35e-5	5.97e-4-1.10e-3	4.18-4.19	2153-2161	990.4-999.0	1.69-1.81
MIX-12	13.3	0.1093	2.827	1.02-1.10	11.70-12.52	3.07-3.29	3.00-3.22	134.3-136.7	17.9-44.9	133.5-135.9	1.34e-5	5.97e-4-1.06e-3	4.18-4.19	2154-2161	990.4-998.7	1.69-1.80
Aya and Nariai exp.	0.02	0.018	1.000	0.25	0.65-20.65	1.033	1.013	100.5	20.0	100.0	1.23e-5	1.00e-3	4.18	2255	998.2	0.61

*The pool 'bulk' temperature T_p in MIX tests is the temperature measured in the same horizontal layer as the pipe outlet but located about 0.8 m away from the axis of the pipe.

Table 4: Relevant non-dimensional parameters in MIX tests and Aya and Nariai experiment.

	$\tilde{l} = \frac{l_p}{l_s}$	$\tilde{V} = \frac{V/n}{l_s \pi d^2 / 4}$	$\tilde{T} = \frac{T_{sat} - T_p}{T_{sat}}$	$Eu = \frac{(P_D - P_W)}{\rho_L \left(\frac{G}{\rho_s}\right)^2}$	$Fr = \frac{G/\rho_s}{\sqrt{dg}}$	$Re_s = \frac{Gd}{\mu_s}$	$Gr_l = \frac{g\beta(T_s - T_p)d^3}{(\mu_l/\rho_l)^2}$	$Ja = \frac{\rho_l}{\rho_s} c_{p,l} \frac{T_{sat} - T_p}{h_{fg}}$	$Ri = \frac{Gr_l}{Re_s^2}$
MIX-01	2.85-3.04	351.8-375.8	0.71-0.86	0.06-0.30	4.53-5.24	1.46e5-1.63e5	2.54e10-4.94e10	118.76-149.90	1.11-2.32
MIX-02	2.89-2.93	356.7-362.0	0.74-0.76	0.07-0.25	4.89-6.12	1.60e5-1.98e5	4.06e10-4.50e10	122.09-128.97	1.04-1.67
MIX-03	2.91-3.04	359.0-375.7	0.75-0.86	0.04-0.16	6.01-6.35	1.96e5-2.03e5	2.56e10-4.24e10	125.53-147.71	0.62-1.05
MIX-04	2.87-3.00	355.0-370.4	0.73-0.82	0.22-0.52	3.80-4.10	1.38e5-1.44e5	3.22e10-5.00e10	112.04-131.11	1.58-2.64
MIX-05	2.77-2.97	342.2-366.2	0.67-0.83	0.09-0.39	4.06-4.44	1.58e5-1.65e5	3.22e10-6.43e10	97.52-128.27	1.25-2.51
MIX-06	2.78-2.94	343.0-363.7	0.67-0.80	0.10-0.25	5.06-5.76	1.89e5-2.05e5	3.67e10-6.31e10	100.08-126.65	0.88-1.75
MIX-07	2.58-2.72	1295.3-1364.8	0.67-0.81	0.29-0.38	4.15-4.46	6.33e4-6.50e4	5.24e9-9.36e9	96.32-121.91	1.28-2.33
MIX-08	2.56-2.76	1285.9-1383.9	0.67-0.86	0.03-0.04	15.57-17.73	2.28e5-2.52e5	3.89e9-9.24e9	97.56-133.10	0.07-0.17
MIX-09	2.56-2.75	1283.6-1379.4	0.67-0.87	0.03-0.05	12.37-13.95	1.80e5-2.12e5	3.87e9-9.36e9	96.28-131.13	0.12-0.26
MIX-10	2.56-2.76	1283.3-1384.5	0.67-0.88	0.07-0.10	8.41-9.69	1.27e5-1.38e5	3.57e9-9.31e9	96.83-134.51	0.20-0.57
MIX-11	2.56-2.76	1281.2-1385.4	0.67-0.88	0.05-0.07	10.80-11.70	1.58e5-1.67e5	3.60e9-9.31e9	96.65-134.11	0.14-0.35
MIX-12	2.57-2.76	1288.2-1384.1	0.67-0.87	0.12-0.18	6.36-7.15	9.48e4-1.02e5	3.83e9-9.28e9	97.10-132.69	0.38-1.00
Aya and Nariai exp.	4.00	63.0	0.80	0.02-18.99	2.44-80.80	9.16e2-3.03e4	1.31e7	243.43	0.01-15.66

Notes: (i) The parameter n is the number of blowdown pipes: $n = 1$ in MIX tests and $n = 5$ in the Aya and Nariai experiment. (ii) The constant coefficient β is set to $2.87e-3 \text{ C}^{-1}$.

6.2 Oscillations characteristics in chugging phenomena

In this section, we present a scaling approach to provide universal description for amplitude and frequency as a function of scaling parameters.

6.2.1 Amplitude of oscillations

Figure 158 shows the amplitude of oscillations in the blowdown pipe during chugging plotted with respect to the steam mass flux. The data includes the PPOOLEX MIX series (100 mm and 200 mm blowdown pipe diameters) and the experiments performed by Aya and Nariai with a blowdown pipe diameter of ~18 mm. There is no clear pattern or trend in the plot as a whole. Although the subgroups are spread out in certain ranges and situated in certain regions of the plot. The range in amplitude for the Aya and Nariai experiment is from nearly zero to 0.3 m. The range in amplitude of the first MIX subseries is between 0.23-0.48 m while the range in the second subseries is between 0.04-0.1 m.

As mentioned previously, the experimental set-ups between the PPOOLEX MIX and Aya and Nariai's experiments are quite similar (except for the geometrical scales and absolute values of some parameters) and so are the competing effects in the phenomena. As indicated in the previous section, we choose the diameter of the blowdown pipe as the characteristic length. Then scale the steam mass flux (representing the inertial force) with the gravitational force, which is essentially the Froude number, defined as

$$Fr = \frac{G/\rho_s}{\sqrt{gd}} \quad \text{Eq. 8}$$

where G is the steam mass flux, ρ_s is the density of steam, d is the diameter of the blowdown pipe, and g is the gravitational constant. The amplitude A is scaled with the pipe diameter d and multiplied by the volume ratio \tilde{V} and aspect ratio \tilde{l} ,

$$\tilde{A} = \frac{A}{d} \cdot \frac{V/n}{l_s \pi d^2/4} \cdot \frac{l_p}{l_s}. \quad \text{Eq. 9}$$

Figure 159 shows the scaled amplitude of all available data plotted against Froude number. Now we can observe a trend in the data. There are two regimes in the plot: an increasing trend in amplitude is observed when $Fr < 10$ while there is a decreasing trend in amplitude when $Fr > 10$. The vertical spread in the data is attributed to dependence on temperature.

Figure 160 shows the MIX data plotted in amplitude versus Fr but grouped into different 'bulk' temperature (T_p) ranges to show the dependence in temperature. The available Aya and Nariai data on amplitude which is performed at bulk temperature of 20 °C is also given. Generally, the lower the bulk temperature is the higher the scaled amplitude of oscillations in the pipe, especially in the high Fr range.

It is important to note that the scaled amplitude is also plotted (but not shown) with respect to the Euler number, Reynolds number, Grashof number, Jakob number, and Richardson number (see Table 4) but no clear trends or patterns have been observed.

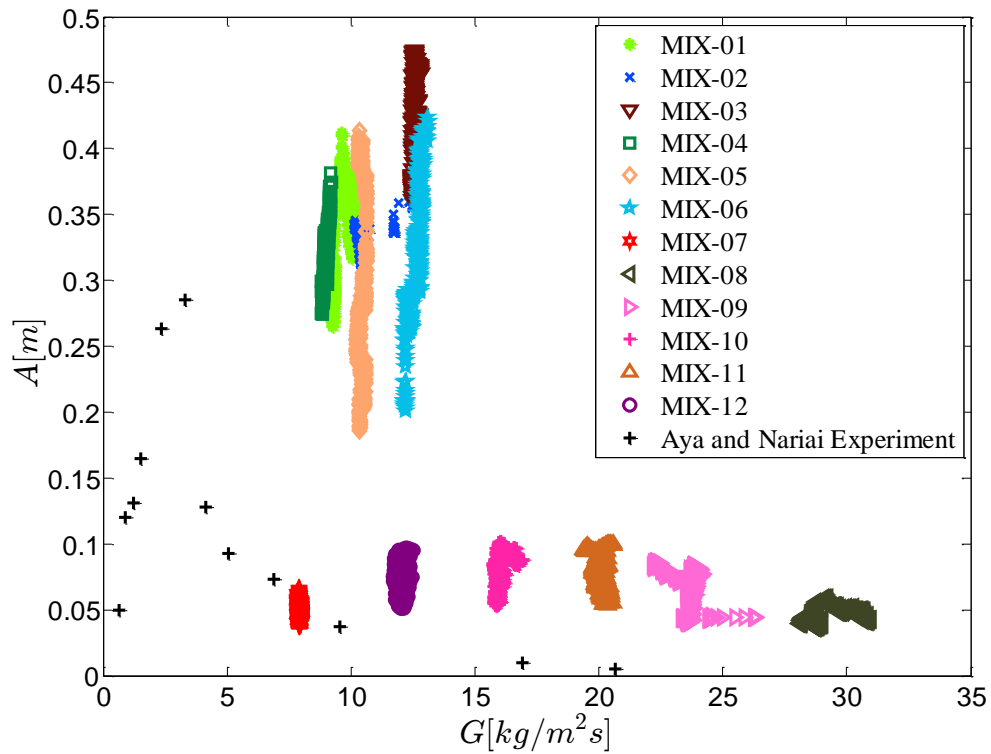


Figure 158: Amplitude of oscillations in the blowdown pipe with respect to steam mass flux in experiments with different pipe diameters. The Aya and Nariai experimental data [9] corresponds to 20 °C bulk temperature and $V/A_p=15.7$ m where V and A_p are the volume of the header and flow area of the pipe, respectively.

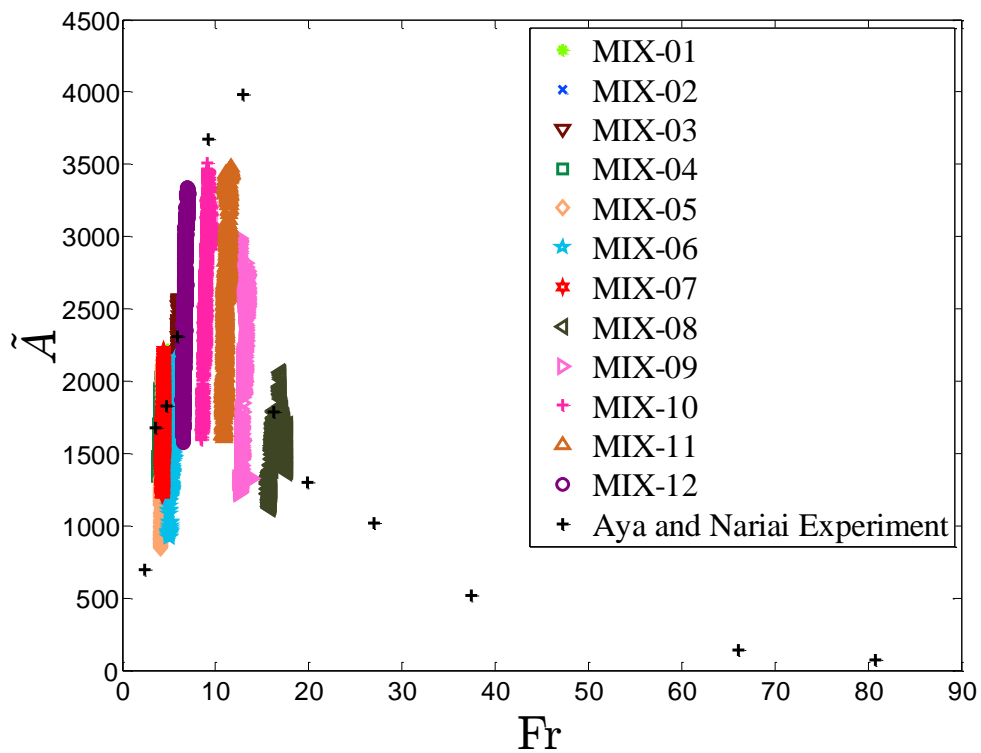


Figure 159: Dimensionless amplitude (Eq. 9) with respect to the Froude number (Eq. 8).

Figure 161 shows the comparison of scaled amplitude vs Fr between the experimental data and prediction of Aya and Nariai analytical theory (see appendix for the dimensional analytical model). For the plot, we have non-dimensionalized the 1D Aya and Nariai model (Eq. 11) by choosing characteristic scales. The Aya and Nariai analytical model was able to capture the decreasing trend in amplitude in the $Fr > 10$ range. This is expected since it is also shown in the comparison (in dimensional amplitude vs steam mass flux) of Aya and Nariai experiment against their analytical model [9]. However, the strong dependence of amplitude on temperature has not been captured by the analytical model as shown in Figure 161, since terms involving temperature such as condensation were neglected in their analysis, except density liquid dependence on the temperature. The analytical model is monotonically decreasing; hence it is obvious that it cannot capture the increasing trend in amplitude for the range of Fr below ~ 10 . Finally, an exponential fit for the data with bulk temperature T_p around 20°C is also plotted.

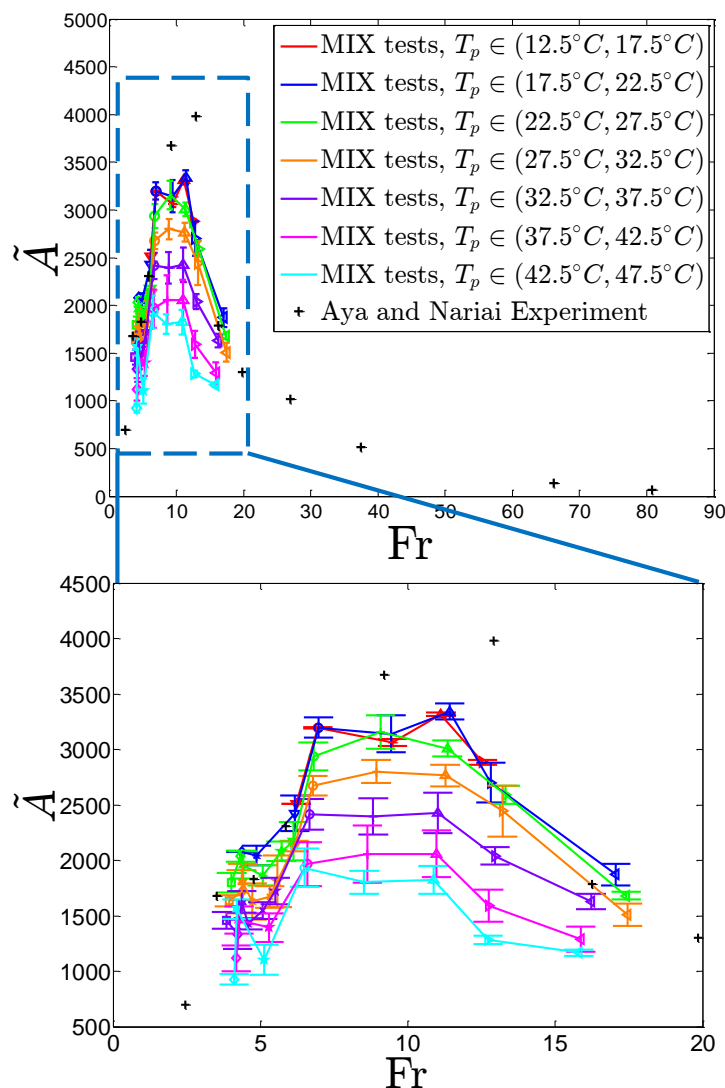


Figure 160: Dependence in temperature of the amplitude of oscillations in MIX tests where T_p is the temperature measured in the same horizontal layer as the pipe outlet but located about 0.8 m away from the axis of the pipe. The MIX data are grouped according to T_p and the plot points and error bars correspond to the mean and variance, respectively.

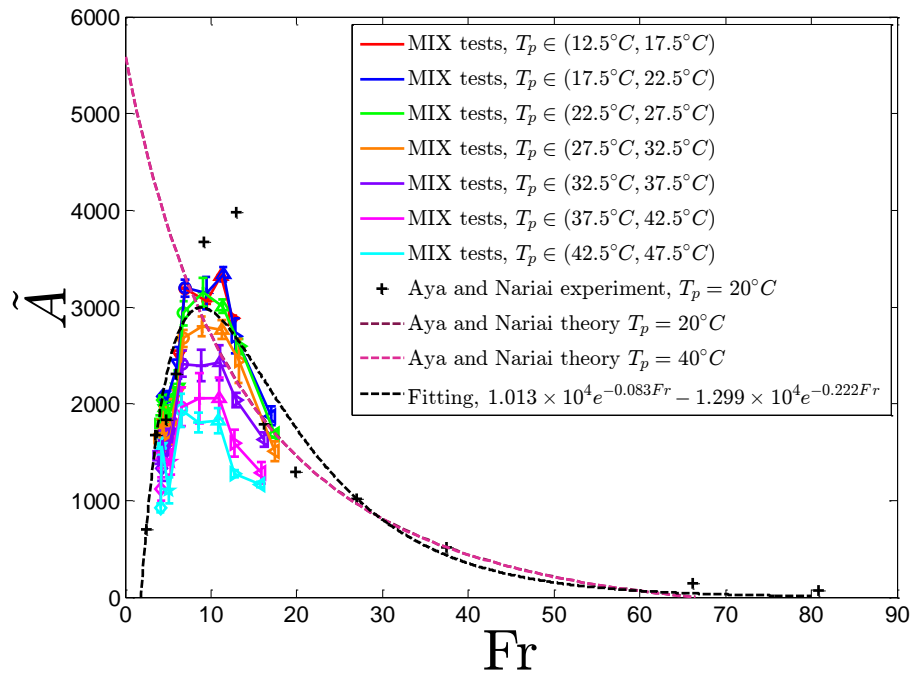


Figure 161: Comparison of scaled amplitude as a function of Fr between experimental data and prediction of Aya and Nariai analytical theory. The predictions of Aya and Nariai theory at $T_p = 20^\circ\text{C}$ and $T_p = 40^\circ\text{C}$ are almost identical since the temperature dependence in the theory only appears through the density of the liquid. An exponential fit for the data with T_p around 20°C is also plotted.

6.2.2 Frequency of oscillations

Similarly, Figure 162 shows the frequency of oscillations in the blowdown pipe with respect to the steam mass flux from available experimental data with different pipe diameters. The steam mass flux is between 4-37 kg/(m²s) while the frequency is between nearly zero to ~75 Hz. The high frequency range is from the experimental data of Aya and Nariai with small pipe diameters. Similar to the amplitude plot, there is no clear trend of the frequency as a function of steam mass flux.

Figure 163 shows a scaled plot of the frequency with respect to Froude number. The frequency f is scaled with the time scale $\rho_s d / G$, that is,

$$\tilde{f} = f \cdot \frac{d}{G/\rho_s}. \quad \text{Eq. 10}$$

We can observe a decreasing trend in frequency for $Fr < 20$. All of the MIX tests data are in this $Fr < 20$ range while most of the Aya and Nariai data are in the $Fr > 20$ range which is in an increasing trend but quite spread out. This spread, however, is due to the dependence in temperature where lower bulk temperature leads to higher scaled frequency of oscillations.

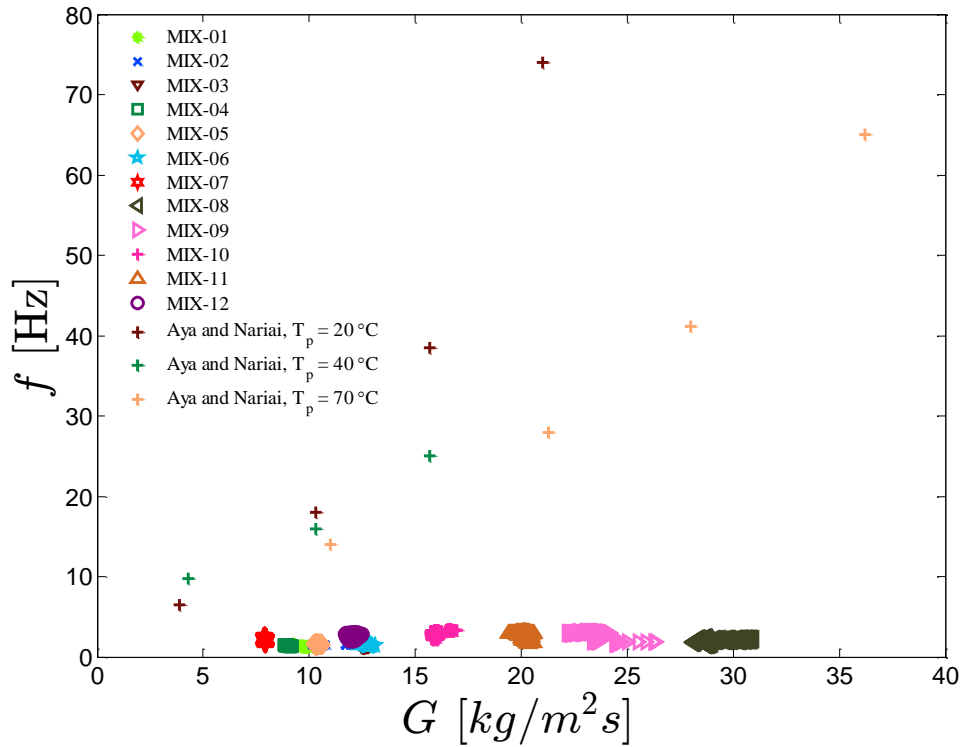


Figure 162: Frequency of oscillations in the blowdown pipe with respect to steam mass flux in experiments with different pipe diameters. The Aya and Nariai data [9] corresponds to $V/A_p=20$ m.

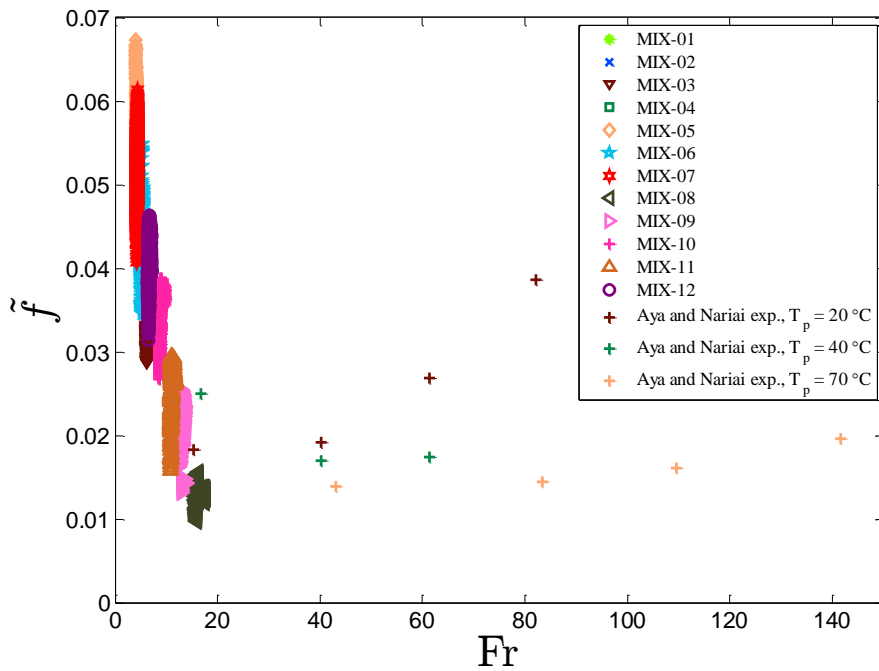


Figure 163: Dimensionless frequency (Eq. 10) with respect to the Froude number (Eq. 8).

It should also be noted that the scaled frequency is plotted (but not shown) with respect to the Euler number, Reynolds number, Grashof number, Jakob number, and Richardson number (see Table 4) but no clear trends or patterns have been observed.

Figure 164 shows the comparison of scaled frequency vs Fr between the experimental data and prediction of Aya and Nariai analytical theory. Similar to the trend in the experimental data, the scaled frequency predicted by the analytical model has a decreasing trend at low Fr and an increasing trend at higher Fr. However, a satisfactory agreement is only observed between the analytical model and the Aya and Nariai data at $T_p = 20^\circ\text{C}$. Similar to the amplitude, the strong dependence of frequency on temperature has not been captured by the analytical model. Thus, further analysis to predict the amplitude and frequency with dependence on temperature is warranted.

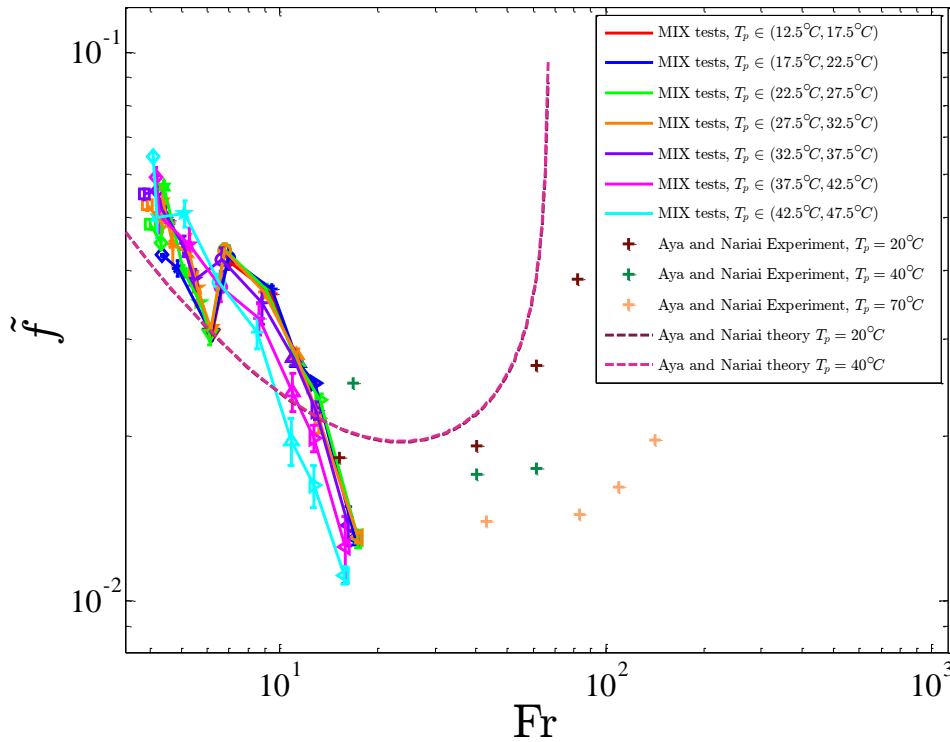


Figure 164: Comparison of scaled frequency as a function of Fr between experimental data and prediction of Aya and Nariai analytical theory. The predictions of Aya and Nariai theory at $T_p = 20^\circ\text{C}$ and $T_p = 40^\circ\text{C}$ are almost identical since the temperature dependence in the theory only appears through the density of the liquid.

7 Conclusions

Steam venting and condensation in a large pool of water creates both a source of heat and a source of momentum. It is important to resolve the interplay between them in order to predict development of thermal stratification or mixing in the pool. This problem is especially important for safety assessment of pressure suppression pool (PSP) in a boiling water reactor (BWR), and also relevant to the new designs of advanced light water reactors (LWR) with in-containment refueling water storage tanks (IRWST).

In order to enable sufficiently accurate and computationally affordable simulations of thermal stratification and mixing during a steam injection into a large pool of water, the concepts of Effective Heat Source (EHS) and Effective Momentum Source (EMS) models are proposed in this work. Specifically, the EHS/EMS models are developed for steam injection through a vertical pipe submerged into a pool under two condensation regimes: complete condensation inside the pipe and chugging. These models are computationally efficient since small time and space scale behaviors are not resolved directly but their integral effect on the large scale flow structure in the pool is taken into account.

The EHS model provides integral heat source caused by steam injection. Its purpose is to conserve mass and thermal energy of injected steam and to provide thermal boundary conditions for prediction of stratification development in the pool.

The EMS model is based on the synthetic jet model which predicts momentum source induced by the oscillation of the steam water surface in the process of steam injection and condensation. The data about amplitude and frequency of the condensation oscillations in different flow regimes is necessary as an input to the model. The purpose of the model is to enable prediction of the pool mixing.

The EHS and EMS models are implemented in GOTHIC which is used as a computational vehicle for resolving 3D flow structures and temperature distributions in the pool with boundary conditions and source terms provided by the EHS and EMS. In principle other computational fluid dynamic (CFD) codes also can be used instead of GOTHIC in combination with EHS and EMS.

Previously, the EHS/EMS models and GOTHIC code have been extensively validated against POOLEX STB and PPOOLEX STR experiments on thermal stratification and mixing induced by steam injection into a large pool of water. For completeness, a more organized parametric sensitivity analysis and updated discussion of some of the STB and STR tests have been included. However, the focus of this work is on the recent PPOOLEX MIX tests.

First, the EHS/EMS models are validated against the PPOOLEX MIX tests in which space and time resolution of temperature measurements inside the blowdown pipe were significantly improved. In MIX-01 to MIX-06, the blowdown pipe diameter is 214 mm, while in MIX-07 to MIX-12 the diameter of pipe is about 109 mm. All of MIX tests are used for model validation and excellent agreement in averaged pool temperature and

water level in the pool between the experiment and simulation has been achieved. The development of thermal stratification in the pool is well captured in the simulation as well as the mixing phase. Moreover, the heating up of the bottom layer due to the impinging jet of hot water is also observed both in the simulation and experiment. The re-stratification phase in some of MIX tests after mixing phase is also captured and it implies that the EHS/EMS model also works for transition condensation regime.

Secondly, a scaling approach is proposed to generalize available data on amplitude and frequency of oscillations induced by steam injection into a subcooled pool. Proper scaling of the amplitude plotted against the Froude number Fr (which relates the inertial forces to gravitational forces) has provided general trend for the amplitude obtained experimentally at different scales. The amplitude is increasing when $Fr < 10$ and decreasing when $Fr > 10$. In addition, there is strong dependence of amplitude on temperature; the lower the bulk temperature is the higher the scaled amplitude. The analytical theory of Aya and Nariai can only capture the decreasing trend in amplitude and fails to capture the increasing trend and the temperature dependence. Similarly, proper scaling of the frequency plotted against Fr has revealed a general trend for the frequency, that is, decreasing frequency when $Fr < 20$ and increasing trend when $Fr > 20$. A strong dependence on temperature is also observed, specifically, the lower the bulk temperature is the higher the scaled frequency. The Aya and Nariai analytical theory is able to capture qualitatively the general trend in frequency. Moreover, the strong dependence of frequency on temperature has not been captured as expected.

In the future work, the EHS-EMS models for blowdown pipes should be improved further in order to reduce uncertainties and enhance accuracy in predictions. Specifically, modifications of the EHS model for non-uniform condensation inside the blowdown pipe should be addressed. For the EMS model, an extension of existing models for prediction of frequency and amplitude of oscillations (given only the condensation regime and design specific parameters) is needed. It should be pointed out that experimental data is limited for validation of such models. So far, the only available and sufficiently detailed experimental data are the POOLEX/PPOOLEX experiments. Further extension of the EHS and EMS models to other elements of the PSP such as spargers, nozzles of the residual heat removal system, and strainers will be necessary for comprehensive safety analysis of realistic transients in a BWR containment.

Acknowledgement

Financial support from the NORTHNET RM3 and Nordic Nuclear Safety Program (NKS) is greatly acknowledged. Authors are grateful to Markku Puustinen (LUT) and co-workers for very fruitful discussions and unique experimental data which helped a lot in understanding, development and validation of the models.

GOTHIC is developed and maintained by the Numerical Applications Division of Zachry Nuclear Engineering under EPRI sponsorship. We would like to acknowledge NAI for providing access to the program for educational and research purposes.

NKS conveys its gratitude to all organizations and persons who by means of financial support or contributions in kind have made the work presented in this report possible.

Disclaimer

The views expressed in this document remain the responsibility of the author(s) and do not necessarily reflect those of NKS. In particular, neither NKS nor any other organisation or body supporting NKS activities can be held responsible for the material presented in this report.

Appendix

Analytical model of Aya and Nariai for prediction of amplitude and frequency of oscillations during chugging

Prediction of the amplitude and frequency of the free surface oscillations in the pipe for specific steam condensation regime is necessary if such characteristics are not known from an experiment. Aya and Nariai [9, 10, 51] have studied experimentally and analytically the frequency and amplitude of fluid oscillations in different condensation regimes. In particular, Figure 165 shows a sketch of their analytical model for chugging [51]. A 1D model of the water level oscillation in the blowdown pipe has been derived from conservation laws neglecting the condensation in the continuity equation and given as,

$$\frac{d^3z}{dt^3} + \omega_c^2 \frac{dz}{dt} + D = 0 \quad \text{Eq. 11}$$

where the frequency ω_c and coefficient D are

$$\omega_c^2 = \frac{g}{\bar{z} + l_m} \left(1 + \frac{\pi \kappa P_{s0} d^2}{4 \rho_L g V_s} \right), \quad \text{Eq. 12}$$

$$D = \frac{\pi \kappa G_0 P_{s0} d^2}{4 \rho_L \rho_{s0} (\bar{z} + l_m) V_s} \quad \text{Eq. 13}$$

and \bar{z} is the averaged water level taken as $\bar{z} = 0.5z_{max}$. The density of liquid and steam are denoted by ρ_L and ρ_s , respectively. Also, G_0 , d , V_s , P , κ , and l_m , are the steam mass flow rate, diameter of the pipe, volume of header, pressure, ratio for specific heat for steam, and inertia length of pool water, respectively. The particular solution when $z = 0$ at $t = 0$ is given as,

$$z(t) = C \cdot \sin(\omega_c t) - \frac{D}{\omega_c^2} t \quad \text{Eq. 14}$$

where C is the maximum elevation of the interface.

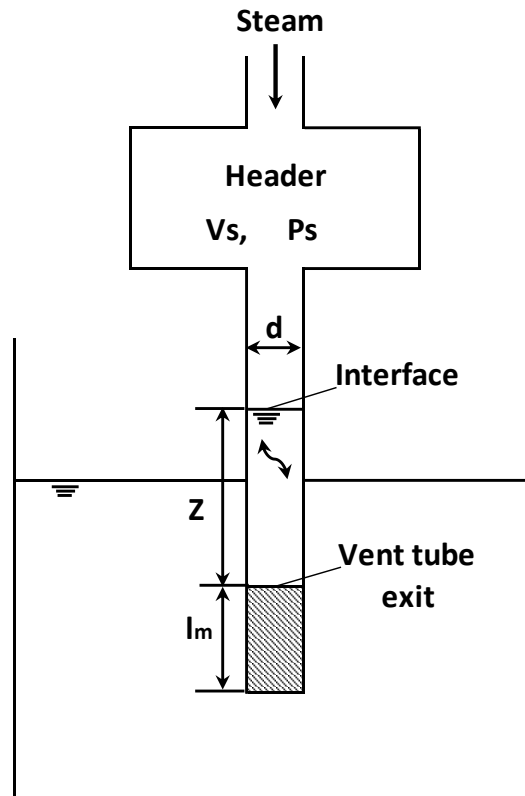


Figure 165: Analytical model for large chugging [51].

References

1. R. E. Gamble, T. T. Nguyen, P. F. Peterson, "Pressure suppression pool mixing in passive advanced BWR plants," *Nuclear Engineering and Design*, 204, 321-336, 2000.
2. R. T. Lahey, F. J. Moody, "The Thermal Hydraulics of a Boiling Water Reactor, second ed.," American Nuclear Society, Illinois, 582 p., 1993.
3. C. K. Chan, C. K. B. Lee, "A regime map for direct contact condensation," *International Journal of Multiphase Flow*, 8 (1), 11-20, 1982.
4. K. S. Liang, P. Griffith, "Experimental and analytical study of direct contact condensation of steam in water," *Nuclear Engineering and Design* 147, 425-435, 1994.
5. S. Cho, C. H. Song, C. K. Park, S. K. Yang, M. K. Chung, "Experimental study on dynamic pressure pulse in direct contact condensation of steam Jets Discharging into Subcooled Water," *NTHAS98*, 291, 1997.
6. D. H. Youn, K. B. Ko, Y. Y. Lee, M. H. Kim, Y. Y. Bae, J. K. Park, "The direct contact condensation of steam in a pool at low mass flux," *Journal of Nuclear Science and Technology*, 40 (10), 881-885, 2003.
7. A. Petrovic-de With, R. K. Calay, G. de With, "Three dimensional regime map for direct contact condensation of steam injected into water," *International Journal of Heat and Mass Transfer*, 50, 1762-1770, 2007.
8. G. W. Fitzsimmons, D. L. Galyard, R. B. Nixon, M. J. Mann, K. P. Yu, "Mark I Containment Program, Full Scale Test Program Final Report," General Electric Report, NEDE-24539, August 1979.
9. I. Aya, H. Nariai, "Chugging Phenomenon Induced by Steam condensation into pool water (amplitude and frequency of fluid oscillation)," *Heat transfer Japanese Research*, 14, 26-43, 1985.
10. I. Aya, H. Nariai, M. Kobayashi, "Pressure and fluid oscillations in vent system due to steam condensation (I), experimental results and analysis model for chugging," *Nuclear Science and Technology*, 17, 499-515, 1980.
11. J. Laine, M. Puustinen, "Thermal stratification experiments with the condensation pool test rig," *NKS-117*, 2006.
12. M. Puustinen, J. Laine, A. Räsänen, "PPOOLEX experiments on thermal stratification and mixing". Research report CONDEX 1/2008, NKS-198, 2009.
13. J. Laine, M. Puustinen, A. Räsänen V. Tanskanen, "PPOOLEX experiments on stratification and mixing in the wet well pool," *NKS-240*, 2011.
14. J. Laine, M. Puustinen, A. Räsänen, "PPOOLEX experiments on dynamics of free water surface in the blowdown pipe," Research report EXCOP 2/2012, NKS-281, 2013.
15. P. F. Peterson, I. J. Rao, V. E. Schrock, "Transient thermal stratification in pools with shallow buoyant jets," In: Hassan, Y.A., Hochreiter, L.E. (Eds.), *Nuclear Reactor Thermal Hydraulics*, HTD-Vol. 190, ASME, New York, 55-62, 1991.
16. Y. Kataoka, T. Fukui, S. Hatamiya, "Experimental study on convection heat transfer along a vertical flat plate between different temperature pools," *ANS National Heat Transfer Conference*, Minneapolis, 28-31 July, 1991.
17. R. J. Fox, "Temperature distribution in pools with shallow buoyant jets," *Fifth International Topical Meeting on Nuclear Reactor Thermal Hydraulics (NURETH-5)*, September 21-24, Salt Lake City, Utah. 1227-1234, 1992.

18. B. L. Smith, T. V. Dury, M. Huggenberger, N. Nöthiger, "Analysis of single-phase mixing experiments in open pools," In: Cheung, F.B., Peterson, P.F. (Eds.), *Thermal Hydraulics of Advanced and Special Purpose Reactors*, ASME HTD, vol. 209. ASME, New York, 91-100, 1992.
19. L. Cheng, K. S. Woo, M. Ishii, J. Lim, J. Han, "Suppression pool mixing and condensation tests in PUMA facility," *International Conference on Nuclear Engineering, ICONE*, 2006.
20. T. L. Norman, H. S. Park, S. T. Revankar, M. Ishii, J. M. Kelly, "Thermal stratification and mixing in an open water pool by submerged mixtures of steam and air," *ASME International Mechanical Engineering Congress and Exposition, IMECE2006 - Nuclear Engineering*, 2006.
21. A. Timperi, T. Pättikangas, J. Niemi, "Analysis of Loads and Fluid-Structure Interactions in a Condensation Pool," NKS-154, 2007.
22. T. Pättikangas, J. Niemi, A. Timperi, "CFD and FEM modeling of PPOOLEX experiments," NKS-236. 2011.
23. T. Pättikangas, J. Niemi, A. Timperi, "Numerical modelling of pressure suppression pools with CFD and FEM codes," NKS-249. 2011
24. P. F. Peterson, "Scaling and analysis of mixing in large stratified volumes," *International Journal of Heat and Mass Transfer*, 37, 97-106, 1994.
25. P. F. Peterson, R. Gamble, "Scaling for forced-convection augmentation of heat and mass transfer in large enclosures by injected jets," *Trans. Am. Nucl. Soc.*, 78, 265-266, 1998.
26. S. Z. Kuhn, H. K. Kang, P. F. Peterson, "Study of Mixing and Augmentation of Natural Convection Heat Transfer by a Forced Jet in a Large Enclosure," *Journal of Heat Transfer*, Volume 124, Issue 4, 660-666, 2002.
27. H. Zhao, "Computation of mixing in large stably stratified enclosures," Ph.D. Dissertation. University of California, Berkeley, 2003.
28. F. Niu, H. Zhao, P. F. Peterson, J. Woodcock, R. E. Henry, "Investigation of mixed convection in a large rectangular enclosure," *Nuclear Engineering and Design*, 237(10), 1025-1032, May 2007.
29. H. Zhao, P. F. Peterson, "One-dimensional analysis of thermal stratification in AHTR and SFR coolant pools," *Proceedings - 12th International Topical Meeting on Nuclear Reactor Thermal Hydraulics, NURETH-12*, 2007.
30. C. H. Song, W. P. Baek, M. K. Chung, J. K. Park, "Multi-dimensional thermal-hydraulic phenomena in advanced nuclear reactor systems: current status and perspectives of the R&D program at KAERI," *Proceedings International Conference on Nuclear Reactor Thermal Hydraulics (NURETH-10)*, Seoul, Korea, October 5-9, Paper I00121, 2003.
31. H. S. Kang, C. H. Song, "CFD Analysis for Thermal Mixing in a Subcooled Water Tank under a High Steam Mass Flux Discharge Condition," *Nuclear Engineering and Design*, 238 (3), 492-501, 2008.
32. Y. T. Moon, H. D. Lee, G. C. Park, "CFD simulation of steam jet-induced thermal mixing in subcooled water pool," *Nuclear Engineering and Design*, 239, 2849-2863, 2009.
33. S. Austin, D. Baisley, *System 80+ Summary of Program to Evaluate DCRT Issues Related to the Safety Depressurization System and IRWST - Task 12*, ABB-CE Documentation, 1992.
34. R. R. Nourgaliev, T. N. Dinh, "The investigation of turbulence characteristics in an internally-heated unstably-stratified fluid layer," *Nuclear engineering and design*, 178, 235-258, 1997.

35. V. Tanskanen, D. Lakehal, M. Puustinen, "Validation of direct contact condensation CFD models against condensation pool experiment," XCFD4NRS OECD Conf., Grenoble, Sep. 12-15, 2008.
36. H. Li, P. Kudinov, "GOTHIC code simulation of thermal stratification in POOLEX facility," NKS-196, 2009
37. H. Li, P. Kudinov, W. Villanueva, "Modeling of Condensation, Stratification, and Mixing Phenomena in a Pool of Water," NKS-225, 2010.
38. H. Li, P. Kudinov, W. Villanueva, "Development and Validation of Effective Models for Simulation of Stratification and Mixing Phenomena in a Pool of Water," NKS-248, 2011.
39. H. Li, W. Villanueva, P. Kudinov, "Effective Momentum and Heat Flux Models for Simulation of Stratification and Mixing in a Large Pool of Water," NKS-266, 2012.
40. H. Li, P. Kudinov, "An approach toward simulation and analysis of thermal stratification and mixing in a pressure suppression pool," NUTHOS-7, Seoul, Korea, October 5-9, Paper 243, 2008.
41. H. Li, P. Kudinov, "An Approach for Simulation of Mixing in a Stratified Pool with the GOTHIC code," ANS Transactions, 2009.
42. "GOTHIC containment analysis package qualification report," Version 8.0 (beta 1), NAI 8907-09 Rev 12, May 2010.
43. M. Andreani, "Pretest calculations of phase A of ISP-42 (PANDA) using the GOTHIC containment code and comparison with the experimental results," Nuclear Technology, 148, 35-47, 2004.
44. M. Andreani, F. Putz, "Simulation of gas mixing and inter-compartment transport using the GOTHIC code," 11th International Conference on Nuclear Engineering (ICONE-11), Tokyo, Japan, April20-23, 2003.
45. B. L. Smith, G. S. Swift, "A comparison between synthetic jets and continuous jets," Experiments in Fluids, 34, 467-472, 2003.
46. Y. Utturkar, R. Holman, R. Mittal, R. Carroll, B. Sheplak, L. Cattafesta, "A Jet Formation Criterion for Synthetic Jet Actuators," 41st Aerospace Sciences Meeting and Exhibit, AIAA Paper 2003-0636, Reno, NV, 2003.
47. Q. Gallas, R. Holman, T. Nishida, B. Carroll, M. Sheplak, L. Cattafesta, "Lumped Element Modeling of Piezoelectric-Driven Synthetic Jet Actuators," AIAA Journal, Vol. 41, No. 2, pp. 240-247, 2003
48. B. L. Smith, A. Glezer, "The formation and evolution of synthetic jets," Physics of Fluids, Volume 10, Number 9, 2281-2297, 1998.
49. S. Mallinson, G. Hong, J. Reizes, "Some Characteristics of Synthetic Jets," 30th AIAA Fluid Dynamics Conference, AIAA Paper 1999-3651, Norfolk, VA, 1999.
50. B. Smith, G. Swift, "Synthetic Jets at Larger Reynolds Number and comparison with Continuous Jets," 31st AIAA Fluid Dynamics Conference and Exhibit, AIAA Paper 2001-3030, Anaheim, CA, 2001.
51. H. Nariai, I. Aya, "Fluid and pressure oscillations occurring at direct contact condensation of steam flow with cold water," Nuclear Engineering Design, 95, 35-45, 1986.
52. "GOTHIC containment analysis package user manual," Version 8.0 (beta 1), NAI 8907-09 Rev 12, May 2010.

Title	Effective Models for Simulation of Thermal Stratification and Mixing Induced by Steam Injection into a Large Pool of Water
Author(s)	Hua Li, Walter Villanueva, Pavel Kudinov
Affiliation(s)	Division of Nuclear Power Safety, Royal Institute of Technology (KTH), Stockholm, Sweden
ISBN	978-87-7893-395-9
Date	October 2014
Project	NKS-R / ENPOOL
No. of pages	165
No. of tables	4
No. of illustrations	165
No. of references	52
Abstract	<p>Steam condensation in a large pool of water creates both a source of heat and a source of momentum. Complex interplay between these two sources leads to either thermal stratification or mixing. Development of thermal stratification in a pressure suppression pool (PSP) of a boiling water reactor (BWR), increases temperature of the free surface reducing the steam condensation capacity of the pool and increasing containment pressure. It is important to know how fast a stratified pool can be mixed. Modelling of direct contact condensation on the steam-water interface remains a computational challenge. Therefore Effective Heat Source (EHS) and Effective Momentum Source (EMS) models have been proposed to model thermal stratification and mixing in case of steam injection through a vertical pipe submerged in a pool under two condensation regimes: complete condensation inside the pipe and chugging. Computational efficiency and sufficiently accuracy of the models are achieved by resolving only integral effect of small scale steam condensation phenomena on the large scale flow structures and temperature distributions in the pool. The models are implemented in GOTHIC® software. In previous NKS reports, validation of EHS and EMS models against POOLEX STB and PPOOLEX STR tests have been presented.</p> <p>In this report, we focus on the validation of the EHS/EMS models against recent PPOOLEX MIX tests. Excellent agreement in the development of thermal stratification and mixing in the pool between the experiment and simulation has been achieved. For completeness, an updated discussion of some of the previous STB and STR tests have been included with parametric sensitivity analysis. Improvement of EHS/EMS models are discussed. Effective momentum can be determined based on the frequency and amplitude of oscillations in the blowdown pipe. We demonstrate that existing analytical models (e.g. by Nariai) that can be used for prediction of the frequency and amplitude were developed using data from small scale experiments and have rather large uncertainty when applied to large scale PPOOLEX tests. A scaling approach is proposed to generalize available data on amplitude and frequency of oscillations during chugging at different scales.</p>
Key words	Thermal Stratification, Mixing, Pressure Suppression Pool, Containment, Thermal Hydraulic, GOTHIC, Light Water Reactor